DEVELOPMENT OF A SOLID ROCKET PROPELLANT NONLINEAR CONSTITUTIVE THEORY

Richard J. Farris, et al

Aerojet Solid Propulsion Company

Prepared for:

Air Force Rocket Propulsion Laboratory

May 1975

AFRPL-TR-75-20

DEVELOPMENT OF A SOLID ROCKET PROPELLANT NONLINEAR VISCOELASTIC CONSTITUTIVE THEORY

FINAL REPORT

Richard J. Farris
Aerojet Solid Propulsion Company
P. O. Box 13400
Sacramento, California, 95813

Leonard R. Herrmann and James R. Hutchinson
University of California
Davis, California

Richard A. Schapery
Texas A&M University
College Station, Texas

May 1975

Approved for Public Release; Distribution Unlimited

Prepared for

Air Force Rocket Propulsion Laboratory
Director of Science and Technology
Air Force Systems Command
Edwards, California, 93523

NOTICES

When U. S. Government drawings, specifications, or other data are used for any purpose other than a definitely related Government procurement operation, the Government thereby incurs no responsibility nor any obligation whatsoever, and the fact that the Government may have formulated, furnished, or in any way supplied the said drawings, specifications, or other data, is not to be regarded by implication or otherwise, or in any manner licensing the holder or any other person or corporation, or conveying any rights or permission to manufacture, use or sell any patented invention that may in any way be related thereto.

FOREWORD

The technical effort reported herein was accomplished under Contract No. F04611-73-C-0060, Job Order No. 305910WF with the Air Force Rocket Propulsion Laboratory, Edwards, Calif., 93523, and covered the period from May 1973 through July 1974. Dr. Randall L. Peeters was the Air Force materials engineer. This report has been reviewed and is suitable for public release.

The program was successful in meeting its objectives. The success of the program was due to the combined efforts of key personnel at three facilities; the Aerojet Solid Propulsion Company, consultants from the University of California, Davis, and the Texas A&M Research Foundation. The Aerojet team performed an extensive experimental effort, developed the computerized characterization codes, and performed theoretical work in developing constitutive and failure equations which model the multiaxial response of solid propellants. The consultants from the University of California, Davis, were responsible for the two dimensional nonlinear viscoelastic finite element stress analysis codes developed under this contract. The Texas A&M Research Foundation provided theoretical backup and independently pursued the modeling of propellant response and failure behavior based on fracture mechanics of viscoelastic materials having microstructural damage.

The key technical personnel on this program were: Dr. Richard J. Farris, who directed the Aerojet effort and coordinated the overall effort as the Program Technical Manager, Dr. Leonard R. Herrmann and Dr. James R. Hutchinson of the University of California, Davis, who were responsible for the finite element code development, and Dr. Richard A. Schapery of Texas A&M University who provided technical backup through the Texas A&M Research Foundation. Mr. Dennis F. Vronay was primarily responsible for the computer characterization coding. Mr. Frederick H. Davidson and Mr. David A. Hare performed all of the experimental work. The propellants characterized on this program were supplied by the Hercules Powder Company, the Thiokol Corporation, and the Aerojet Solid Propulsion Company.

This report has been reviewed by the Information Office/DOZ and is releasable to the National Technical Information Service (NTIS). At NTIS it will be available to the general public, including foreign nations.

RANDALL L. PEETERS
Project Engineer

CHARLES E. PAYNE, Major, USAF
Chief, Surveillance and
Mechanical Behavior Section

FOR THE COMMANDER

CHARLES R. COOKE, Chief
Solid Rocket Division

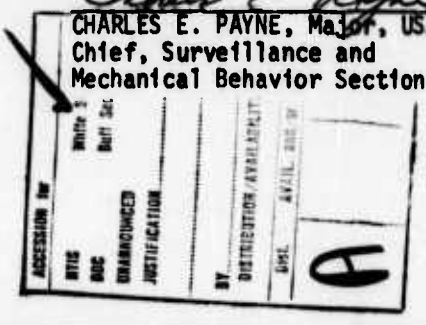

SECURITY CLASSIFICATION OF THIS PAGE (When Data Entered)

REPORT DOCUMENTATION PAGE

READ INSTRUCTIONS BEFORE COMPLETING FORM

1. REPORT NUMBER: AFRPL-TR-75-20	2. GOVT ACCESSION NO.
3. RECIPIENT'S CATALOG NUMBER	
4. TITLE (and Subtitle): Development of a Solid Rocket Propellant Nonlinear Constitutive Theory	5. TYPE OF REPORT & PERIOD COVERED: Final Report, May 1973 to July 1974
	6. PERFORMING ORG. REPORT NUMBER: 1074-26F
7. AUTHOR(s): Richard J. Farris, Richard A. Schapery, Leonard R. Herrmann, James R. Hutchinson,	8. CONTRACT OR GRANT NUMBER(s): F04611-73-C-0060
9. PERFORMING ORGANIZATION NAME AND ADDRESS: Aerojet Solid Propulsion Company, P. O. Box 13400, Sacramento, California 95813	10. PROGRAM ELEMENT, PROJECT, TASK AREA & WORK UNIT NUMBERS: AFSC Project 3059, Task 10
11. CONTROLLING OFFICE NAME AND ADDRESS: Air Force Rocket Propulsion Laboratory, Edwards, California 93523	12. REPORT DATE: May 1975
	13. NUMBER OF PAGES: 361 ~~264~~
14. MONITORING AGENCY NAME & ADDRESS(if different from Controlling Office)	15. SECURITY CLASS. (of this report): Unclassified
	15a. DECLASSIFICATION/DOWNGRADING SCHEDULE

16. DISTRIBUTION STATEMENT (of this Report)

Approved for Public Release; Distribution Unlimited

17. DISTRIBUTION STATEMENT (of the abstract entered in Block 20, if different from Report)

18. SUPPLEMENTARY NOTES

19. KEY WORDS (Continue on reverse side if necessary and identify by block number)

Nonlinear Viscoelasticity
Constitutive Theory
Thermoviscoelasticity
Solid Propellants
Computer Codes
Response Characterization
Failure Characterization
Cumulative Damage
Data Library
Structural Analyses

20. ABSTRACT (Continue on reverse side if necessary and identify by block number)

The objective of this program was to develop a nonlinear viscoelastic constitutive theory which could accurately model solid propellant response and to include this theory into a finite element structural analyses procedure. To accomplish these goals the program was divided into four tasks.

During Task I the constitutive theory and computerized characterization codes developed on previous Navy and Air Force contracts were modified extensively

DD FORM 1 JAN 73 1473 EDITION OF 1 NOV 65 IS OBSOLETE

UNCLASSIFIED

SECURITY CLASSIFICATION OF THIS PAGE (When Data Entered)

19. Key Words (Continued)

One-dimensional
Two-dimensional

20. Abstract (Continued)

to provide a user oriented characterization procedure which could obtain an accurate distortional, dilatational and failure characterization of propellant response. These computer codes use a linearized expansion of nonlinear functional relations in an iterative procedure to converge on the best set of parameters in the nonlinear viscoelastic relations, including the time-temperature equivalence relations. A separate code was also developed for linear viscoelastic characterization. In this procedure up to 1000 data points from as many as 100 experiments having arbitrary fields can be used as input.

In Task II the accuracy of these codes was then successfully demonstrated using three propellants: ANB-3124, a fast burning Aerojet HTPB formulation using large amounts of ultra-fine oxidizer; VMO, a Hercules cross-linked double base (XLDB) propellant and, TPH-1135, a high solids Thiokol HTPB propellant containing mostly coarse oxidizer.

Task III resulted in the development of a finite element computer code that utilizes the same nonlinear viscoelastic relations for material property descriptors as determined in the characterization codes. This code performs two dimensional stress analyses for transient thermal and/or pressurization loading histories in typical propellant geometries. Code options include the ability to handle orthotropic case properties, multi-layered structures, mass conservation with finite deformations, and automatic grid generation. This code was designed to perform linear elastic, linear viscoelastic or nonlinear viscoelastic stress analyses.

In Task IV the applicability of the mathematical representations of the characterization and finite element codes were to be demonstrated by comparing observed force-deformation and volume dilatation-deformation with predictions using two dimensional plane stress samples which had high strain gradients and were subjected to complex deformation histories. Instabilities in the plane stress portions of the finite element codes made such comparisons impossible. These difficulties were isolated as being due to the numerical formulation of the plane stress solution and were not attributed to the constitutive representations.

Overall, the program was successful in meeting its objectives. There are no doubt refinements that could be included in the constitutive representations and the codes, however, just what improvements can be made will best be determined by usage.

TABLE OF CONTENTS

TABLE OF CONTENTS (Cont.)

TABLE OF CONTENTS (Cont.)

TABLE OF CONTENTS (Cont.)

LIST OF FIGURES

LIST OF FIGURES (CONT.)

LIST OF FIGURES (CONT.)

LIST OF FIGURES (CONT.)

LIST OF TABLES

SECTION 1

INTRODUCTION

A. NATURE OF REPORT

This is the final technical report submitted in fulfillment of the requirements of Contract F04611-73-0060, "Development of a Solid Rocket Propellant Nonlinear Viscoelastic Constitutive Theory".

The technical discussion covers the four tasks of the original contract work statement. Briefly described, they are: Task I - To develop user-oriented computer characterization codes that fit multi-axial mechanical properties test data to constitutive theories developed on a previous AFRPL contract. These codes were to have the capability of optimizing all of the nonlinear as well as linear parameters entering into these constitutive relations, including the time-temperature equivalence relations which appear in the thermoviscoelastic nonlinear integral equations. In addition to the above, computerized failure characterization codes were to be developed using a cumulative damage measure theory. The accuracy of the analytical models and the characterization codes were to be demonstrated in Task II on three propellants that reflected current and future applications in Air Force weapon systems. To obtain as wide a range in properties as possible and to promote industry's confidence in this study, the propellants selected were: (1) TPH-1135, a Thiokol high solids PBAN formulation containing large amounts of coarse oxidizer, (2) VMO, a Hercules crosslinked double base (XLDB) propellant, a high energy propellant containing high solids and high energy plasticizers, and (3) ANB-3124, an Aerojet high burning rate propellant, containing large amounts of UFAP (ultrafine ammonium perchlorate). All testing was performed

at Aerojet and the propellants were characterized using the codes developed in Task I. In Task III the constitutive theory was to be incorporated into a two-dimensional finite element code capable of handling transient thermal, time-varying pressure (within quasistatic inertial restrictions) and gravitational loads. The code was to be compatible with the characterization code and include damage measures at key locations. In Task IV, an experimental effort was to be conducted to verify the validity of the Task III effort. Originally, tests were to be run on instrumented subscale motors subjected to transient thermal and pressure loads. These results were to be compared with analyses. Because of difficulties encountered during the program (fully described in the text of this report), this work was abandoned and instead experimental and analytical results were to be compared on specimens having large strain and stress gradients subjected to complex loading histories.

Together these four tasks were designed to demonstrate that nonlinear viscoelastic characterization of propellant materials and nonlinear viscoelastic analyses of propellant structures are in many cases necessary and that, with the proper tools, they can be performed in a semi-routine fashion. In the opinion of the research team, this work forms a strong base from which the structural analysis of advanced solid propellant systems can be placed on a sound engineering basis; namely, good material response modeling, good structural modeling, and the capability of handling realistic loads such as time-varying pressure and transient thermal loads. The wealth of experimental data, the computerized response characterization and failure codes, and the finite element

codes should make it relatively easy for others to test the validity of this work or should it prove necessary, to modify and improve upon this work. Recalling it has taken many years to develop polished codes capable of two-dimensional linear elastic analyses, and that there is still considerable research going on to develop improved linear codes, the progress made during th ogram over a relatively brief period of time indicates that polished, refined nonlinear viscoelastic analysis techniques required for accurate structural analyses of advanced propellant systems may soon be available.

The Texas A&M University's sub-contract pursued an alternative approach to characterizing the effect of microstructural damage on the overall mechanical response of solid propellants. This approach unites a viscoelastic theory of crack growth, statistical properties of the microstructure, and a model that accounts for the effects of microcracks on the softening of the bulk composite to develop an alternative constitutive representation. The technique was used to predict the effect of stress and temperature histories on the statistical distribution of failure times for specimens. Their investigations also included some studies on the effects of superimposed pressure and the healing of microcracks on the constitutive relations. The final report provided by Texas A&M University is included here as Appendix A.

B. PROGRAM OBJECTIVE

The objective of this program was to develop and demonstrate the accuracy of totally computerized response and failure characterizations and finite element stress and deformation analyses of propellant systems. These analyses were to be based on the nonlinear viscoelastic constitutive theory developed on earlier Air Force and Navy contracts (1,2). To meet these objectives, the work to be accomplished was divided into four distinct tasks which were defined in the original Air Force contract. Tasks I and III were development tasks wherein the computerized characterization and finite element programs were defined, coded and assembled.

Tasks II and IV were demonstration tasks wherein the developments of Tasks I and III were evaluated in realistic situtations. The technical discussion of this report provides a detailed description of the work performed to meet the objectives of this program. Also included under separate headings are the descriptions of each computer code, its function, and sample problems.

C. BACKGROUND

Work on propellant nonlinear viscoelastic theory started in 1968 at the University of Utah on AFOSR Project Themis (3 and 4). It was shown that current viscoelastic theories could not describe propellant response at small strains when time and history effects dominated the response. This led to a new type of nonlinear constitutive theory based on the effects of time dependent microstructural degradation as well as internal viscosity as they contributed to the stress state. This work was immediately followed by a Navy contract to ASPC (NOSC N00017-70-C-4441, 1970-1971) which successfully applied the theory developed at Utah to propellant behavior over a broad range of test conditions prior to vacuole dilatational effects (2). This work in turn led to two AFRPL contracts (F04611-71-C-0046, 1971-1973 and its follow-on F04611-73-C-0060, 1973-1974) to ASPC to further extend this work. The first AFRPL contract (1) was devoted to extending and demonstrating the applicability of the theory to include large strains, multiaxial conditions and vacuole dilatation. The second AFRPL contract, of which this is the final report, had as its purpose two main goals: 1) to develop and demonstrate user-oriented computerized response and failure characterization techniques so that those unfamiliar with the complex mathematical methods could successfully apply this theory to their materials; and 2) to develop and demonstrate the applicability of finite element analyses of propellant structures using this nonlinear viscoelastic theory. The previous contracts had clearly demonstrated the need for nonlinear viscoelastic characterization

and analyses of propellant systems when time and history effects dominated their response. The referenced reports give detailed explanations of the causes of the nonlinearities and how these effects were accounted for in the resulting constitutive theory, hence those reportings are not repeated here. Readers unfamiliar with the representations and methods being used are referred to these earlier reports (1-4) which contain all of the necessary background information which led to work accomplished under the present contract.

SECTION 2

SUMMARY AND CONCLUSIONS

The objectives of this program were to develop a nonlinear viscoelastic constitutive theory which could accurately model the stress-strain response of solid propellants and to incorporate this theory into a finite element structural analysis code. To accomplish these goals the program was divided into two development and two demonstration tasks.

In Task I the constitutive theory and characterization techniques developed in previous Navy and Air Force contracts were modified extensively to provide a user-oriented, computerized, characterization code which can obtain an accurate distortional, dilatational and failure characterization of propellant response. These computer codes use a linearized expansion of the nonlinear viscoelastic functional relations as an iterative procedure to converge on the best set of parameters in the nonlinear viscoelastic relations. A separate code was also developed for linear viscoelastic characterization. In this procedure up to 1000 data points from as many as 100 experiments having arbitrary deformation histories and uniaxial and/or biaxial stress fields can be used as input. These codes are extremely versatile and determine all of the constitutive parameters including the time-temperature equivalence relations. In addition, any of the parameters in the constitutive equation can be fixed at the users discretion. To complement the characterization codes two additional codes were developed. One code converts raw experimental data into meaningful stress-strain data, assigns an identification sequence to each experiment and transfers the data to a permanent magnetic tape library which in turn is used as input to the characterization codes. The second code is a library catalog code which provides a history of experimental information by sequence number to aid the user in selecting experiments for a characterization.

In Task II the characterization codes were demonstrated using three propellants: ANB-3124, a fast-burning Aerojet HTPB formulation using large amounts of ultra-fine oxidizer; VMO, a Hercules cross-linked double base propellant; and TPH-1135, a high solids Thiokol propellant using mostly coarse oxidizer. This task required a thorough experimental evaluation of each propellant's response. All data was obtained using uniaxial and biaxial gas dilatometric measurements to provide the 3-dimensional strain information required for 3-dimensional constitutive characterizations. Data from these three propellants, as well as two additional Aerojet propellants, are now included on permanent tape library files and represent a very large collection of propellant stress-strain-dilatational information available to test various constitutive theories against. The experimental conditions covered a broad range of temperatures, deformation histories, and superimposed hydrostatic pressure levels.

Generally speaking, the distortional characterization was excellent out to failure, having a coefficient of variation of less than 15% of the predicted stress values. The dilatational characterization was generally fair with a coefficient of variation near 25%. It should be pointed out that dilatation is much more sensitive to pressure effects than stress and changes from a near zero value to a quite large value. Dilatational measurements are also very difficult to make with high precision compounding the problem. In general, the dilatational predictions show all the proper trends but deviate in magnitude much more than the stress predictions. Failure predictions using a nonlinear cumulative damage theory vary from good to excellent. Considering the variety of test conditions and difficulty in determining failure in biaxial samples the results are very encouraging. Typical run times on the Univac 1108 computer for a large problem vary from three to eight minutes depending upon the number of iterations. The practical significance of these codes is that the user need not be a skilled mathematician highly familiar with the theory; characterizations can be carried out from practically any experiment including variable thermal histories. The code really demonstrates if the constitutive equations are valid or not valid.

In Task III a finite element computer code was developed that utilizes the same nonlinear viscoelastic relations for material properties descriptors as determined in the characterization codes. The code performs 2-dimensional stress analyses for transient thermal and/or pressure loading histories in typical propellant geometries. Code options include the ability to handle orthotropic case properties, multi-layered structures, mass conservation with finite deformations, and automatic grid generation. The code was designed to perform linear elastic, linear viscoelastic and nonlinear viscoelastic stress analyses. It is currently limited to approximately 200 elements, with no external storage, using a computer with 64K storage. The code checks out well in all modes of operation except for nonlinear solutions with plane stress boundary conditions. For this type of problem convergence was generally poor and often times unstable and the problem could not be resolved within the time limitations of the contract. This code is the first code of its type and it has considerable versatility. It should provide a good baseline from which to build and develop improved nonlinear viscoelastic finite element codes as has been done over the years with linear elastic finite element codes.

In Task IV the applicability of the characterization codes and the finite element codes were to be demonstrated on: instrumented, subscale motors using the Aerojet propellant, and on 2-dimensional plane stress specimens having high strain gardients using all three propellants. After preparing the motor cases, installing the normal stress transducers provided by the Air Force, and accomplishing transducer calibrations prior to propellant casting, it was observed that the stress transducers showed strong path dependency and were unsuitable for use in comparing measured versus finite element stress predictions. These observations were the result of comparing calibrations wherein: first, the transducers were cooled to -65°F at atmospheric pressure and then subjected to 50 psig, and second, the transducers were subjected to 50 psig at ambient temperature and cooled to -65°F holding the pressure constant. The transducer

outputs at 50 psig and -65°F for these two situations varied by as much as 15 millivolts with many transducers showing shifts of 6 to 10 millivolts. These variations correspond to errors of 20% to 50%. This portion of the program was subsequently deleted with the Air Force approval. The true source of the variation was never identified although it is reasonable to assume it was caused by the small propellant potting put on the transducers. Considerable difficulties were also encountered in the second portion of Task IV in comparing measured and finite element force and dilatation data on samples having large strain gradients. All of the experimental data was obtained and is included in this report for future comparisons; however, on this contract, instabilities in the plane stress portion of the finite element code prevented any meaningful comparisons from being made. These problems were identified as being due to the plane stress portion of the code and not the material characterization parameters since the code functioned perfectly for axisymmetric analyses using the same constitutive input. Time limitations prevented resolving the problem on this contract.

Overall, the objectives undertook by this program were quite ambitious. The computerized characterization codes were extremely complex to develop; however it is felt that an extremely versatile characterization technique was developed that can be used by the industry. The finite element code also represents a major step forward since it contains many features, even for linear viscoelastic analyses, that are found in no other codes; such as, orthotropic case properties characterization and finite dilatation measures which are important for large strain analyses. The nonlinear code contains all the features required to be a practical analysis tool. Hopefully it will form the basis for the nonlinear analyses required by the industry in the future. The problems in the plane stress portions of the code do not appear to influence any other mode of operation but they should be resolved to bring it up to its full capability. The experimental work performed on this contract also

represents a major step forward since this is the first time an abundance of 3-dimensional data has been obtained on any propellant. This type of data is a necessity when 3-dimensional characterizations are required for analyses. The great wealth of data stored on the tape library files should provide an excellent basis for any future comparisons of theory to actual propellant response.

SECTION 3

TASK I - AUTOMATED CONSTITUTIVE EQUATION CHARACTERIZATION CODE

This and subsequent sections of the report are organized to correspond to the four tasks contained in the work statement. For purposes of clarity the work to be accomplished, as defined in the contract, is summarized at the beginning of each section. The technical discussion following each statement of work describes in detail the work performed by the research team in satisfying the objectives of each task.

A. WORK TO BE ACCOMPLISHED

The contractor shall modify the automated constitutive equation characterization code (developed under Contract F04611-71-C-0046) to obtain an efficient code oriented towards the general user. Modifications to be incorporated into the characterization code fall into two categories: (a) refined coding and numerical analysis procedures, and (b) improved user orientation. These modifications are detailed in the following subparagraphs.

1. The contractor shall review the present numerical integration scheme to determine if a quadrature procedure would result in a problem formulation that is more computer oriented. If an improved computer orientation does result, the characterization code will be modified to include these quadrature techniques. The contractor shall also examine all analytical equations employed in the present code. In addition to these theoretical improvements, the contractor shall refine all coding procedures to optimize the computational process. Repetitive operations that are frequently used will be prime candidates for this optimization. Stored data shall be kept to a minimum by retaining only essential items. Data manipulation operations should also be kept to a minimum.

2. As part of a user's package, the contractor shall incorporate an automatic calculation of the time-temperature shift function into the present code. This capability shall be included as an option to be utilized at the user's discretion. The contractor shall also develop a cumulative damage indicator by utilizing the same damage models and mathematical formulations used in the basic constitutive theory. This technique would simply involve the automatic monitoring of accumulated damage as calculated by the present technique. This capability will again be incorporated into the characterization computer code as an option. Automatic input data generation procedures should also be considered as a means of minimizing the input requirements of the computer code.

3. At the end of this task, the contractor shall completely document the constitutive equation characterization code. This documentation will not only give the standard code operation information, but also some detail on the construction of the code which will yield optimum material characterization processes for solid propellants.

B. GENERAL OVERVIEW OF THE CHARACTERIZATION PROBLEM

1. Types of Experiments Required

In order to develop computerized response and failure characterization techniques for propellant materials, many individual problems had to be resolved. Previous work had demonstrated the importance of how the past history influences the current state of stress or deformation in these materials (1-6). Therefore, to be meaningful, any characterization technique must have the capability to handle complex deformation histories as well as various types of stress fields. The computer codes were therefore written to accept uniaxial, strip biaxial, and shear experimental data having arbitrary deformation and/or temperature-time histories. Multiaxial variations

of these experiments by the inclusion of a superimposed pressure are also acceptable and can provide a great deal of information on the dependence of stress state on dilatation.

One problem that arises when performing three-dimensional material response characterizations is that three-dimensional input data are required. Recall that even for linear elastic or linear viscoelastic materials each of the six components of the stress tensor, σ_{ij}, are functionally related to the six components of the strain tensor, ϵ_{ij}. Therefore, if three-dimensional characterizations are the desired end product, the experimental process becomes significantly more difficult. This problem has been avoided in the past by: assuming the material to be incompressible and, utilizing a distortional characterization; a procedure completely erroneous for large deformations.

The input to the characterization codes must, therefore, be the observed stress state and the measured total state of strain. For the types of experiments run on propellants (uniaxial, biaxial and shear) the total strain state is determinable from the primary strain measurement in each experiment and the volume dilatation. Since dilatational measurement via a gas dilatometer offers a significant increase in accuracy and versatility over lateral strain determinations via gage or optical techniques, the computer codes have been designed to accept primary strain measurement and the dilatation histories as input. The computer then converts this information into three-dimensional strain information to be used in the characterization. To meet the above requirement, Aerojet equipped its laboratory facility with uniaxial and biaxial strip gas dilatometers that are capable of operation from -65°F to +200°F under superimposed pressures to 1000 psi.

Facilities not having dilatational or other techniques of determining the total state of strain must still assume incompressible behavior in which case only a distortional characterization is possible. Needless to say, the experimental data discussed later in this report probably represents the most extensive collection of information gathered on propellants to date and should be useful to other investigators interested in testing the validity of their nonlinear viscoelastic theories.

2. Tape Libraries - Versatility and Simplification of Input

Another major problem encountered in any type of material characterization is that of data storage and retrieval. This problem is greatly amplified when using computers for the characterization process since storage and retrieval processing is compounded by data selection (i.e. what discrete data are to be used in the characterization), and actual physical data input to the computer. Another problem to be resolved was the transmittal of data from facility to facility. It was felt that in order to have efficient user-oriented characterization codes such problems had to be minimized or completely eliminated. After careful consideration of the needs of the analyst and the experimentalist, a list of desired data storage and manipulation features were established. They were:

- The input process should begin with raw experimental data and should be as simple as possible.

- Data reduction conversions to stress and strain should be accomplished by the computer in order to simplify the raw input.

- Design tape files to minimize experimental data storage and in a manner which eliminates the need for redundant calculations.

- Design simple options wherein a data file can be updated as new information becomes available.

- Attempt to eliminate data scrambling (data from two different propellants in the same file) and establish file protection techniques to preclude erasures or overwriting.

- Develop simple identification procedures for labeling of independent experiments so that when used during characterization they can be called by name.

These features and many others were built into a special code, "preprocessor code - SA037," which has as its function to take raw experimental input data and create a master tape file of useful characterization information. Data from each propellant is stored on a single tape and the capability to update each file with additional information as it becomes available has been provided. Data from each independent experiment is assigned an identification code by the user and the data is stored under this heading. Code SA037 also provides at the user's option a library listing of test identifications on each tape along with a brief listing of test conditions; however, no actual stress-strain data is provided in this listing. The magnetic tape libraries created by SA037 also serve as the input for the characterization codes. In this latter situation, the user can restrict his file query to those experiments he wishes to use in the characterization. Thus, the preprocessor code and associated magnetic tape files it generates, eliminates considerable data reduction and provides a simple and yet versatile format for data input to the computerized characterization.

3. Library Cataloging

In order that the user could have available an up-to-date list of the tests stored on a particular propellant's magnetic tape library, two options have been provided. First, as has been mentioned above, the preprocessor code can be used to generate an abbreviated cataloging which provides a brief one line description of each experiment. This includes test ID, number of data points, type of test (i.e. uniaxial, biaxial or shear), test temperature, and hydrostatic pressure. Since there is a requirement to have a more detailed listing of information from which consideration of deformation history and other variables can be used in the selection of tests for a particular characterization, another special code, "post-processor code SA035," was developed. The only function of this code is to provide a detailed listing of three-dimensional stress/strain history information including the strain invariant time histories.

This code provides the user with all of the information necessary to select experiments for characterization. It also provides an acceptable format for purposes of eliminating spurious data that have somehow been coded in error on the original input or experimental errors such as errors in load scale or cross-head speed notations.

4. Types of Viscoelastic Characterization Possible

The computerized viscoelastic characterization package developed on this program consists of two separate codes; SA034 which performs a linear viscoelastic distortional characterization and SA036 which performs a nonlinear viscoelastic distortional and dilatational response characterization and a nonlinear cumulative damage failure characterization. Both codes use the master data tapes as input with the user having the option of selecting specified experiments. Both codes also permit temperature effects in the form of a reduced time. The coding for these characterization programs is quite complex and every effort has been made to employ the most efficient numerical techniques, eliminate all redundant calculations, and minimize the large storage requirements. These codes operate completely in core and are therefore limited by machine size; however, they are extremely versatile and permit characterizations superior to any other technique known to date.

The linear code uses a Prony series representation of the relaxation modulus. Up to eight (8) coefficients can be used to describe the piece-wise linear approximation of the natural logarithm of the time-temperature equivalence as shift function, a_T, versus temperature. Up to twenty-five (25) series terms can be used in the exponential series used to describe the modulus. In any case, the maximum number of unknowns is twenty-five (25). The code is designed to determine the linear coefficients in the exponential terms and the time-temperature shift function coefficients from experiments having

arbitrary deformation histories, including variable temperature histories. The code can currently handle a total of 500 data points from up to 100 experiments. The linear code uses the same iterative nonlinear regression techniques developed for the nonlinear code and has typical run times of ten (10) minutes when run at full capacity using the Univac 1108 computer. It is interesting to note that the run times for a linear viscoelastic characterization generally are considerably longer than those for the nonlinear characterization even with the same number of unknowns. This is because the nonlinear theory describes the history effects as pth order Lebesgue norms rather than in terms of convolution integrals.

The nonlinear viscoelastic response and failure code, SA036, performs a:

Distortional characterization,

Dilatational characterization, and

Failure characterization.

The constitutive representation used is a slight modification of that arrived at on the last contract. The nonlinear iterative regression procedure determines all the unknown parameters in the equation including the time-temperature equivalence equation, and the order of the Lebesgue norms. The limitations of this code are not as severe as those of the linear code. Six (6) segments can be used to describe the time-temperature shift function and up to 1000 data points from as many as 100 experiments can be used in the characterization. The dilatational and failure characterizations are optional and either or both can follow the distortional characterization.

There are many features that the linear and nonlinear codes have in common. Each code is constructed from a number of subroutines, each of which is described later in this section. This building block approach to programing makes this package versatile and easy to modify. It should not be too difficult to modify these codes to handle other types

of nonlinear representations since the basic constitutive representation effects only a few subroutines. Also, the codes were written to permit the user the greatest degree of flexibility. The Air Force work statement indicated that the determination of the time-temperature shift function by the computer was to be optional and available only if the user wanted to include these additional nonlinear parameters. The computer codes were constructed in such a way that any of the parameters entering into the codes could be held fixed simply by not specifying them as variables. Hence,any of the parameters entering into each characterization can be specified as being constant. These features result in program flexibility without compromising program utility. A detailed description of each code and its usage and limitations is provided at the end of this section.

It should be mentioned that the linear code was not a contractual requirement. It was developed because there are a great many users of linear viscoelasticity and it was thought to be a representative first problem that would not be too difficult to solve. As it turned out, it was in many ways more difficult than the nonlinear characterization code. The finite element codes developed on this program are also capable of linear viscoelastic analyses as an option. The reason codes SA036 and SA034 were not combined was because it would further restrict their independent capacities and the nonlinear code contains some features not contained in the linear code. This capability of both linear and nonlinear characterization will hopefully encourage others to test the ability of linear viscoelastic relations to predict general propellant response and determine for themselves the needs for nonlinear analyses.

C. A NUMERICAL APPROACH TO VISCOELASTIC CHARACTERIZATION

There are a great many problems that arise in fitting data to mathematical relations on a digital computer. When the types of mathematical representations are or include convolution integrals, the problems become much more tedious. The actual relations that were programmed during the course of this contract involved integral equations with many nonlinear parameters. As such the codes presented herein as being the characterization package satisfying the Task I work statement represent an evolution resulting

from the evaluation of many different techniques. Along the way many false starts occurred from which a great deal was learned. Many of the techniques that were tried were discarded, not because they would not work but because they were too expensive to use. The only criteria used during the selection process was cost and the ability to converge on a set of parameters that defined the characterization. The information presented below is a brief description of some of the techniques which were tried as well as the method finally arrived upon, which is a combination of several of the different numerical methods.

1. Selecting a Meaningful Error Measure

The general method of approximating data sets by mathematical functions is dependent on the definition of an error measure. In order to be a meaningful measure, the error must be a positive definite quantity. The most common error measure used in numerical analysis is the common "Least Squares" error which is simply the summation of the squares of the deviations between the function approximations and the known values at similar arguments. In the simplest sense the known values of the data set y_i are functions of a single variable x. The data set then consists of N pairs of known values (y_k, x_k). The purpose of the curve fitting is to replace the discrete set of data by a functional approximation defined by

$$y(x) \approx f(x) \tag{1}$$

The Least Squares error is then defined as

$$\text{LSQERROR} = \sum_{i=1}^{N} \left(y_i - f(x_i)\right)^2 \tag{2}$$

where $y_i = y(x_i) \approx f(x_i)$

Nothing has yet been said about the function f(x). In general, it will contain a set of M unknown parameters $B_k(k=1,M)$ which are to be determined in such a manner that the error is minimized. Since observed

values y_i are known for each x_i the variables in the error minimization are not the values of y or x but instead the values of B_k. Since the error will be an absolute minimum when

$$\frac{\partial(\text{LSQERROR})}{\partial B_k} = 0, (k=1,M) \tag{3}$$

differentiating equation (2) with respect to B_k gives

$$\sum_{i=1}^{N}\left(y_i \frac{\partial f(x_i)}{\partial B_k} - f(x_i)\frac{\partial f(x_i)}{\partial B_k}\right) = 0, (k=1,M) \tag{4}$$

Equation (4) simply represents M simultaneous equations in M unknowns $B_1, B_2, \ldots, B_M$. When this system of equations is solved, the resulting values of B_k are those that minimize the error as defined by Equation (2). It is important to note that the solution set obtained, B_k, depends upon the error measured used. The reason the Least Squares error technique is so popular is that when the function $f(x_i)$, which could more properly be noted as $f(x_i, B_k)$, is a linear function of the B_k, then the system of equations reduces to a set of M simultaneous algebraic equations that are linear in B_k, thereby permitting solution via number of efficient numerical techniques. When the function is non-linear in B_k then solution in one step is unlikely. The problem of handling nonlinear functions of the variables B_k and integral rather than algebraic equations is discussed in the next section. The problem at hand thus reduces to one of choosing a meaningful error measure of which the Least Squares is but a single example.

Another error measure can be defined as

$$\text{Error} = \left\{\sum_{i=1}^{N} |y_i - f(x_i)|^P\right\}^{1/P}, \quad P \geq 1 \tag{5}$$

The problem with these types of error measures is that because of the absolute value signs the derivatives and hence the simultaneous equations become quite complex when analytical techniques are used to obtain the "best" set of B_k. Using definitions contained within Equation (5) it is possible to define the function $f(x_i, B_k)$ such that only the maximum deviations are minimized. This is the case with Chebyshev Polynomials which are used to approximate common library functions in computer software. For this latter example the value of P in Equation (5) is infinity. Equation (5) should also be recognizable as an L_p norm similar to those used in the constitutive theory developed on the preceding Air Force and Navy contracts (1,2).

The problem with error measures such as those defined by Equations (2) or (5) above, is that they can lead to anomalous results when they are used to fit constitutive relations to measured response data even though they are doing precisely what was asked, minimizing the error measure. The reason for this lies in the fact that there is always scatter in the mechanical properties data due to: accuracy of measurement, temperature control and material variability to name a few contributing factors. It also is not uncommon to use data obtained at small strains and high temperatures along with data at larger strains and low temperatures. In a large data set of typical propellant data, it is common to encounter stresses ranging from a few pounds per square inch (psi) to about 1000 psi. When numbers of such varying magnitudes are used in the above error measures, wherein the relative precision of the numbers are roughly the same, the result is that the large numbers dominate the analyses since the scatter in the large numbers is often several times greater than the total magnitude of the smaller numbers. When this Least Squares error technique was used on viscoelastic response characterization over a broad range of test conditions, the results almost always were that the large numbers were fit with high relative accuracy while the lower numbers had meaningless predictions.

Since it was known that the relative precision with which any data point was known was essentially constant, the only logical way in which to proceed was to utilize a relative error measure. Relative or weighted error measures are not new to curve fitting routines, but they are rarely used. It should be pointed out that many types of regression analyses could be greatly improved upon if more users were aware of the limitations of commonly used techniques such as the method of Least Squares. It was decided to normalize the error measure in the simplest possible manner to retain the capacity to use analytical techniques to determine the solution set B_k that defined the characterization.

Since the difficulties were caused by the varying magnitudes of the values of y_i, which are known quantities, the simplest normalization turned out to be to weight each data point by the inverse of its magnitude. A new relative error measure could then be defined as

$$\text{RELERROR} = \sum_{i=1}^{N} \left(\frac{y_i - f(x_i)}{y_i} \right)^2 , \quad y_i \neq 0 \tag{6}$$

This Relative Least Squares error seemed to solve all of the problems that previously troubled the numerical characterization techniques. Zero values did not cause any significant problem since those data points could be bypassed using simple logic. This relative type of error measure now gave all numbers equal weight in the analysis regardless of their magnitude. This method of error analysis also still leads to a linear set of equations when the function $f(x_i, B_k)$ is linear in the B_k. It is possible to define other relative error measures by simple modifications of Equation (5), and some of these were used in early work as discussed in the next section; however, the important conclusion is that relative error measures should always be employed in constitutive characterizations of viscoelastic materials.

2. Nonlinear Parameter Optimization Techniques

In order to optimize the nonlinear parameters in the constitutive representations, especially those pertaining to time-temperature equivalence, it was necessary to do considerable experimentation with different numerical nonlinear optimization techniques and different mathematical representations of the time-temperature dependence. Basically nonlinear optimization schemes are,or have the potential to be very unstable and require iterative procedures with forced constraints to insure stability. The most popular nonlinear optimization schemes are centered around two methods, gradient search techniques and the linearized Taylor's series technique. Each of these techniques have their advantages and disadvantages mostly depending upon the quality of the initial estimates of the parameters being optimized and the types of functions and error measures considered. The advantages and disadvantages of each technique are briefly discussed below. Before proceeding however,it should be re-emphasized that the purpose of the Task I effort was a totally computerized characterization of nonlinear viscoelastic materials. Thus, the quality of the initial estimates may be greatly in error since the users of the code will be unfamiliar, at least initially, with the magnitudes and signs of all the parameters entering the nonlinear constitutive equation. Therefore, severe constraints on the optimization schemes must be enforced if convergence is to be expected.

a. Gradient Search Technique

The gradient search technique minimizes the error function by incrementally altering the parameters in the constitutive equation one at a time and re-evaluating the error measure in a systematic fashion. The technique is selective and tries to operate on that parameter having the highest error gradient as measured by numerically or analytically evaluated partial derivatives. There are many gradient search techniques such as the method of steepest descent, the conjugate gradient technique, and even Monte Carlo techniques. The advantages of these techniques are

that they only involve re-evaluation of the error measure, any error measure is permitted, and they do not require constructing and solving matrix equations. These techniques also require a minimum of storage. The difficulty with the gradient search methods is that they usually require hundreds of times as many iterations as the Taylor's series technique. The trade, therefore, is increased iterations for computational simplicity. One nice feature of this technique is that it forces the error to decrease each time the parameters being optimized are changed since paths on the error surface which cause the error to increase are ignored if they are selected. When gradient search techniques are used for nonlinear viscoelastic parameter optimization many additional difficulties are encountered. Each time the stress state is re-evaluated, considerable calculations are necessary thus requiring additional storage and computational time. Since this technique uses many iterations, the run times are usually very large, especially if the initial parameter estimates are poor. Also some degree of sophistication must be added to these codes if they are not to get trapped in local saddles on the error surface. An additional disadvantage of this technique is that many iterations are required even for linear problems.

b. Linearized Taylor's Series Technique

The linearized Taylor's series technique involves expanding the error function in a Taylor series using the unknown parameters as variables. Thus, the expansion is about the initial estimates and is truncated after the linear terms. When this technique is applied to nonlinear parameter optimization it results in a system of linear equation that when solved provides incremental corrections to all of the parameters being optimized, not simply one at a time as in the gradient search. In order to develop this sytem of equations, significantly more calculations are required than in the gradient search techniques since not only must the error function be re-evaluated but in addition the whole set of simultaneous equations must be constructed and solved for each iteration. In principle this process is repeated

using the corrected parameters in subsequent iterations. The advantage of this technique is that for linear problems it gives the correct optimization in one iteration no matter how poor the initial estimates. Also, if the initial estimates are reasonable this technique converges quite rapidly, usually requiring only five to ten iterations to converge or approach convergence on the best family of nonlinear parameters. The difficulty with the technique is that if the initial estimates are poor, then the linearized expansion is a poor estimate of the function being optimized and the incremental corrections obtained usually overshoot and can cause the error to increase without bound from iteration to iteration, or to oscillate in a unstable manner.

c. The Modified Taylor's Series Method of Nonlinear Parameter Estimation

The technique employed in the nonlinear optimization of the constitutive parameters is essentially a combination of the two techniques discussed above. Basically the technique is the Taylor's series method; however, if the resulting incremental corrections cause the error measure to increase the incremental corrections are halved and the error re-evaluated repeatedly until the error measure decreases to a local minimum. Then the next Taylor's series iteration is started. Thus, the technique assumes that the Taylor's series technique provides the correct sign to the incremental corrections while a combined gradient search assigns a scale factor to their magnitudes. When the initial estimates are very poor this method essentially amounts to a gradient search technique since considerable halving of incremental corrections may be required and only those parameters whose estimates were greatly in error are effected. Thus, the first few iterations are spent getting a decent set of initial estimates through a combined technique which when used in the Taylor's series technique results in convergence. This combined approach appears to use the best from both techniques and has been found to converge in approximately ten iterations.

3. Time-Temperature Equivalence Approximations

One important feature in the optimization of the time-temperature shift function is the mathematical representation selected to characterize the function log a_T versus temperature. Over the temperature range commonly used in the study of the behavior of propellants the function a_T can change by roughly twenty orders of magnitude, 10^{20}. If a representation such as the WLF equation (Reference 7) is used,

$$\log a_T = C_1(T-77)/(C_2 + T-77) \qquad (7)$$

a smoothed shift function results that usually is not the best fit to the data. If a simple polynominal in temperature is used,

$$\log a_T = C_1(T-77) + C_2(T-77)^2 + C_3(T-77)^3, \qquad (8)$$

to provide a more accurate function representation considerable numerical difficulties arise since minor corrections in the parameters C_2 or C_3 can cause a_T to exceed the magnitudes permitted for numbers on a particular computer. When this occurs the computational process is stopped and an error message results. To eliminate such possibilities parameters must be routinely tested and if not acceptable reset to acceptable magnitudes which causes additional difficulties. Generally speaking, these procedures result in increased iterations.

In order to obtain the best overall representation for the function a_T versus temperature it was decided to break the function into several piece-wise linear semi-logarithmic representations such that the function log a_T versus temperature is represented by a series of straight lines which approximate a smooth curve. In this way any curve can be approximated and it effectively uncouples the low temperature and high temperature data from influencing each other's value of a_T which is basically impossible when a continuous function is used. It also eliminates

the problem of exceeding allowable number magnitudes in a particular computer. These simplifications are obtained at the expense of using more parameters to describe the function a_T. A more complete description of the technique is illustrated in the following example.

4. A Linear Thermoviscoelastic Example

The stress strain equations for linear viscoelasticity are presented in this example since they can be written compactly and will demonstrate the nonlinear optimization technique used in computer codes SA036 and SA037. These linear equations were originally used to form the basis for the optimization of the time-temperature shift function. The technique presented is that actually used in the linear and nonlinear viscoelastic characterization codes and it obtains all of the parameters in the constitutive representations including the time-temperature equivalence function a_T.

The shear stress-strain equations for linear viscoelasticity can be represented as

$$\tau(t) = \sum_{i=6}^{N} B_i \int_0^t \exp\left[-\beta_i(t'-\xi')\right]\dot{\varepsilon}(\xi)d\xi \qquad (9)$$

$$\text{where } t'-\xi' = \int_{\xi}^{t} d\xi/a_T(\xi) \qquad (10)$$

In the above equation $\tau(t)$ and $\varepsilon(t)$ represent the distortional stress and strain which can be obtained from uniaxial and biaxial data by subtracting principle stress equations. The β_i in this equation represents a family of inverse relaxation times picked by the user, generally one decade apart. A linear elastic term is included in the expansion by selecting $\beta_6 = 0$. The quantities t and ξ and t' and ξ' represent the

current and chronological values of the real time and the temperature reduced time. The Prony series coefficients $B_6, \ldots, B_N$ are to be determined by the computer.

The first five B_i in this example are used to describe the time-temperature equivalence relation as a piece-wise linear semi-logarithmic function of temperature as given by Equation (11)

$$\ln a_T = \begin{cases} B_1(T-77) & \text{if } T > 77 \\ B_2(77-T) & \text{if } 77 > T > T_1 \\ B_3(T_1-T) + B_2(77-T_1) & \text{if } T_1 > T > T_2 \\ B_4(T_2-T) + B_3(T_1-T_2) + B_2(77-T_1) & \text{if } T_2 > T > T_3 \\ B_5(T_3-T) + B_4(T_2-T_3) + B_3(T_1-T_2) + B_2(77-T_1) & \text{if } T_3 > T \end{cases} \quad (11)$$

This equation represents a piece wise, linear and continuous expression for the time-temperature shift function $\ln a_T$ versus the temperature T. The values of T_i are constant and selected by the user and the number of linear intervals is eight. The value of the B_i, $i = 1,5$ are to be determined by the computer. The five values of temperature, T_i, are called pivot points. In the linear viscoelastic code there can be up to twenty-five (25) B_i of which up to eight (8) can be used to describe the function a_T.

Equations (9), (10), and (11) represent the predicted state of stress in terms of the history of the deformation and temperature for each experiment being used as input. The computer actually computes these integral values using piece wise linear approximations of the strain and temperature histories. For data obtained from testers such as an Instron, which is only capable of constant deformation rate, these are exact representations and not approximations. It should also be noted that although the stress state is functionally dependent on deformation history, at each data point these are definite integrals; hence, the stress is only a function of the variables B_i. In order to

optimize this prediction, the values of B_i (i=1,N) must be selected in such a manner as to minimize the error between the observed stress $\bar{\tau}$ and the predicted values τ for all the data. In a linear optimization technique the only selection of error measure available is that of the so called "Least Squares" method. This technique has been modified, as was pointed out above, to a "Relative Least Squares" method by weighting the error measure by the observed stress $\bar{\tau}$. This error measure is defined as

$$\text{Error} = \sum_{k=1}^{K} \sum_{m=1}^{M_k} [1-f_{mk}]^2 \tag{12}$$

$$\text{where } f_{mk} = \tau_{mk}/\bar{\tau}_{mk}$$

In the above equation the subscript mk signifies the mth data point from kth experiment, M_k is the total number of data points in the kth experiment and K is the total number of experiments.

The function f_{mk} is a function of the variables B_i (i=1,N) part of which define the function a_T and part of which define the function τ. The criterion to reduce the error measure to a minimum is obtained mathematically by requiring

$$\frac{\partial \text{ Error}}{\partial B_i} = 0 \qquad (i = 1, N)$$

or (13)

$$\sum_{mk} (1-f_{mk}) \frac{\partial f_{mk}}{\partial B_i} = 0 \qquad (i = 1, N)$$

Now in a nonlinear problem such as the one described above, this approach yields N simultaneous nonlinear equation in N unknowns, $B_1, B_2, \ldots, B_N$. To circumvent this difficulty the problem is linearized by using a truncated Taylor's series expansion. These expansions are normally taken about a stationary point which for the case of nonlinear optimization represents a set of intial guesses of the B_i, termed B_i^0.

Recalling that the Taylor's series expansion can be written as

$$f(x) = f(a) + (x-a)\left.\frac{\partial f}{\partial x}\right|_a + \text{higher order terms} \qquad (14)$$

A similar multi-dimensional expansion can be expressed as

$$f(B_i) \cong f(B_i) + \sum_i (B_i - B_i^0)\left.\frac{\partial f}{\partial B_i}\right|_{B_i} \qquad (i = 1,N) \qquad (15)$$

Substituting the right hand side of Equation (15) into Equation (13) yields a linear system of N equations in N unknowns, $B_i - B_i^0$ or ΔB_i which can be readily solved by various techniques. These incremental values of ΔB_i are then added to the old values using the relation

$$B_i^0 = B_i^0 + \Delta B_i \qquad (i = 1, N) \qquad (16)$$

In a standard Taylor's series method this process is then repeated using the updated estimates of B_i^0 until ΔB_i approaches zero.

In practice, the Taylor's series method has problems, depending mostly on the quality of the initial guesses of the variables B_i^0. One hopes that the total error defined by Equation (12) would decrease with each iteration. Instead one finds that the total error generally oscillates, often times with great irregularity, and is not monotonically decreasing. This problem is caused by overcorrecting the variables. Nevertheless, the general trend is to drive the error downward and the technique does generally converge.

To get around the problem of error oscillation the total error is evaluated after each iteration. If the new error is less than the last value the Taylor's series approach is used. If the new error is greater than the last value the correction to the variables is halved, yielding:

$$B_i^0 = B_i^0 + \Delta B_i/2 \qquad (i=1, N) \qquad (17)$$

The total error is again evaluated. This halving process is repeated so long as the new error is less than the last value, and then the next iteration is undertaken. The rule employed is

$$B_i^0 = B_i^0 + k\Delta B_i \qquad (i=1, N) \qquad (18)$$

$$k = 1, 1/2, 1/4, 1/8 \ldots$$

The value of k used is that value which causes the first minimum in the total error as k is decreased. This method generally reduces the total error by a factor of one-half on each iteration. This technique might be considered as a combined gradient-search and Taylor's series technique where each method is used alternately. This method appears to work very well and no matter how poor the initial guesses for B_i^0, the method appears to converge.

5. Description of Code

The characteriation code that has been developed is quite general and can be modified for use with other functions with ease. The MAIN code does all the statistics and bookkeeping and calls FCODE and PCODE. FCODE is a subroutine which evaluates the function f and PCODE is a subroutine which evaluates the derivatives $\partial f/\partial B_i$. Both numerical and analytical derivatives are used in the linear and nonlinear viscoelastic code. There are also several other subroutines such as ATEMP, which calculates the function a_T, and WHICH, which keeps track of which test is currently being analyzed. Overall the code is built from an assembly of subroutines and will be of general value. The codes have been written in such a manner that any of the parameters B_k can be specified as constant. By specifying the first five as constant in the example just presented, the time-temperature shift function is fixed and

therefore satisfies the option requirement called out in the work statement. For the case of linear viscoelastic characterization with a fixed a_T function, the technique described above will obtain the best set of parameters in one iteration. Using this code will permit direct and rapid characterization of materials from practically any experiment using no approximate methods of characterization.

D. THE PROPELLANT MATERIALS CHARACTERIZATION PACKAGE

The viscoelastic materials characterization package consists of four main computer codes. These are: SA034, the linear characterization code; SA035, a post processor code; SA036, the nonlinear characterization code; and SA037, the preprocessor code. Detailed descriptions of the codes are given in Appendices B, C, D and E.

The preprocessor code, SA037, has three functions. First, it takes the initial batch of raw test data and generates a master data tape which is required as input to the other three codes. Second, SA037 takes additional raw test data as it is generated and appends it to the existing master data tape, allowing a large pool of data to be easily accumulated and handled. Third, the code may be used to print a catalog of the data residing on an existing master data tape. This provides an efficient method of keeping track of the contents of any tape.

The post processor code, SA035, prints a two-page summary of selected calculated and observed data for specified tests. This allows for the generation of a useful reference directory of tests available for a material.

The linear code, SA034, performs a normalized least squares fit to the distortional stress using a Prony series representation for the kernel of the integral. It simultaneously generates the time-temperature shift function consistent with the final representation.

The nonlinear code, SA036, performs a normalized least squares fit to the distortional stress, dilatation, and cumulative damage failure criteria using the theory developed by Farris as discussed in the body of this report.

A general overview and the flow logic of the material characterization package is shown in Figure 1.

In a typical analysis, a series of tests is run on the material being studied. The test conditions, temperature and pressure, and input strain histories are chosen to span the design range of interest. Once a sufficient number of experiments have been conducted to yield an acceptable data base, a master data tape is created using Code SA037, which assembles temperature, strain rate, stress and dilatation time histories from each test. As additional data are accumulated on this material, SA037 is used to append them to the master data tape. Once created, the master data tape is ready for use by any of the other three codes in the package. For example, SA034 uses these data to perform a linear viscoelastic characterization of the distortional stress using either a Prony or power series representation of the kernel function.

This packaged approach to material characterization provides for a realistic determination of material response early in the design phase, as well as great flexibility in refining the analyses as additional experimental data become available. The ability to independently select the tests to be included in a characterization allows for construction of a mathematical model to match either a narrow or a broad response spectrum. The ability to select test data, all at the same

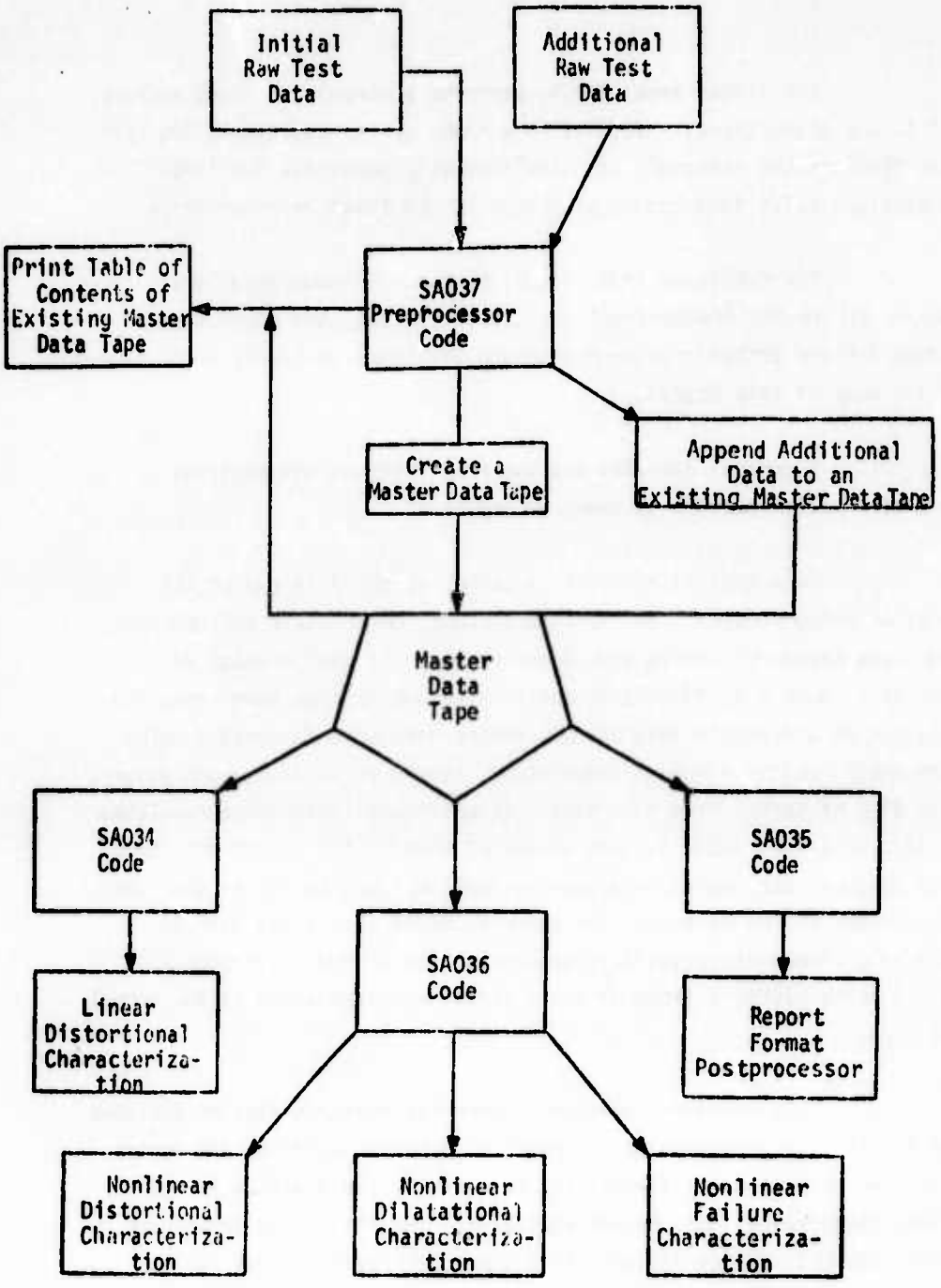

FIGURE 1

OVERVIEW AND FLOW LOGIC OF THE MATERIAL CHARACTERIZATION CODES PACKAGE

temperature and/or pressure, make it especially useful for performing material response sensitivity studies.

Appendices B, C, D and E deal with Codes SA037, SA035, SA034 and SA036, respectively. Each appenidx begins with an overview and general description of the code, followed by a discussion of each of the subroutines required. Following this a "usage" section defines the basic program variables, the input required, and the output received. There then follows a demonstration problem.

Complete source listings, and machine generated flowcharts of the codes may be obtained by request.

SECTION 4

TASK II - CHARACTERIZATION CODE DEMONSTRATION

A. WORK TO BE ACCOMPLISHED

The contractor shall experimentally characterize three propellants utilizing the user's package developed in Task I. The contractor shall establish the accuracy of the analytical model by presenting and discussing the amount of error in all cases. The propellants selected should reflect present and future trends in Air Force weapon systems with as wide a range of mechanical response as possible. Selection of propellants shall be subject to approval of the PCO prior to being utilized in this task.

B. PROPELLANT SELECTION

The three propellants to be characterized in the Task II characterization code demonstration effort were selected early in the program by Aerojet and Air Force personnel. In order to promote industry confidence in the computerized characterization techniques and the constitutive representations being employed it was decided to use propellants made by three different companies. The three companies selected were Aerojet, Hercules and Thiokol. Thiokol provided two large blocks of TPH-1135, a PBAN propellant containing 90 weight percent solids. TPH-1135 is characteristic of the trend in the industry of obtaining higher performance propellants through higher solids loading. This propellant contains conventional oxidizers, mostly coarse in size, aluminum, and has a normal burning rate.

Hercules provided one of their early candidates for the Trident-I Program. The selected formulation, VMO, is one of a series of crosslinked double base propellants (XLDB) with high solids and containing high energy plasticizers. It is representative of the new propellants being developed for the Navy and Air Force for Strategic missiles.

The Aerojet propellant, ANB 3124, is a high solids high burning rate propellant containing large amounts of ultra-fine oxidizer and iron oxide burning rate catalyst. This type of high burning rate propellant is characteristic of the new trends being pursued for tactical missiles.

The researchers of this program would like to thank the Hercules and Thiokol companies for their cooperation with this program.

C. SAMPLE PREPARATION

The sample used in the Task II effort were uniaxial and strip biaxial samples. The uniaxial samples were rectanguloid samples 1/2 x 1/2 x 4 inches in dimension with the exception of the Hercules samples which were truncated JANNAF specimens.

The biaxial strip samples were 1/4 x 1 x 7 inches in dimension. All specimens were end-bonded to metal tabs using epoxy resins and tested in the uniaxial and biaxial dilatometers. With the exception of the Hercules propellant all specimens were prepared at Aerojet using dry cutting techniques. The Hercules samples were prepared by Hercules at Bacchus, Utah and shipped to Aerojet.

The Thiokol propellant arrived early in the program and testing commenced rather quickly. There was considerable delay, several months, in receiving the Hercules material because of mix-ups in paper work and determining who should prepare the samples. Also, the Aerojet propellant was delayed even longer in its preparation because it was to be used in the instrumented subscale work to be performed in Task IV. The delay in this case was caused by several months delay by the Air Force in providing Aerojet with special stress transducers. All of these delays caused problems in getting the sample preparation and testing started and especially affected the Task IV effort.

D. EXPERIMENTAL PHILOSOPHY

The main feature of the computerized characterization codes is that they can characterize a constitutive equation to any experimental stress-strain history. Special deformation histories, such as those required by stress relaxation and constant strain rate experiments, which by mathematical design destroy the integral nature of the constitutive equation, are not required for the characterization code, but are naturally acceptable. These idealized deformation histories generally provide a simple method of obtaining a characterization but because they destroy the integral nature of the constitutive equation they do not test the additivity assumption the integral operator assumes, and thereby do not really test the constitutive equation. The types of experiments which best test a constitutive equation are those which test the integral nature of the equation such as multiple level relaxation experiments and strain reversal experiments. Considerable funds have been spent in the past

to obtain experimental equipment that was capable of providing sudden jumps in the strain to approach the step function input required for a stress relaxation experiment or a true constant strain rate test. If the characterization codes are accepted and used, this type of specialized equipment becomes unnecessary.

Mathematically speaking, a constitutive equation represents a mathematical idealization of a material's response to various input disturbances that influence its current stress and strain state. A true material characterization will not only fit experimental data to the theory but will also test the validity of the constitutive theory and provide some measure of its applicability. To simply determine the kernel function of an integral equation, such as linear viscoelasticity, from experimental data without testing the validity of the constitutive assumptions, such as proportionality of input and output and the integral additivity assumption, is a gross oversimplification of the characterization process. These features and many more are handled by the characterization codes which take a constitutive equation and complex experimental data and fit the theory to the data using the actual constitutive form, not an idealization. In this sense fitting an integral hereditary constitutive equation to experimental data is like fitting a function to some data. Even though the function might be designed to show the proper trends at very small or large arguments of the function, one normally trys to experimentally bracket the range of interest and within this range is willing to accept a function approximation to the data. Error bounds and accuracy of fit are normally obtained in such regression types of analyses to assist in quantitizing just how good the function approximation was to the experimentally determined data. A constitutive

characterization of a materials response should be looked upon with the same degree of complexity. Comparisons of predicted and experimental data in viscoelastic characterizations complete with error bounds are seldom presented. Generally one is provided with a graph of a relaxation function and a time-temperature equivalence function and little else. From such limited information it is impossible to judge how accurately the constitutive equation being employed predicts the actual propellant materials response. Since the constitutive equation is the only ingredient going into a structural analysis that describes the materials response the accuracy of the analysis is directly related to the accuracy of the constitutive equation. Of course, all of this testing and data analysis is of no real value unless they are used in stress analyses codes, and viscoelastic analyses of any type are still the exception rather than the rule in the industry today.

What this all leads up to is the experimental and characterization philosophy employed during this contract. Since the characterization codes have been designed to handle arbitrary inputs the testing should not be restricted to the usual stress relaxation and constant strain rate experiments. Instead the experimental effort should be designed to bracket or span the types of deformation histories, temperatures, times, and stress states expected to be encountered in the structural analyses for which the characterization is being developed. Since the user can build a library file of experiments covering a broad range of conditions, and since the characterization process permits the user to specify which experiments are to be used in a given characterization, only those tests relevant to a given analyses should be employed in that characterization to increase the accuracy of the representation. These features are further aided within the characterization codes format since the user can specify bounds for strain and dilatational values and only those data points from a given experiment having values less than these specified bounds are actually used in the characterization.

Example 1. Thermal Stress Analyses

Suppose that a characterization was wanted for a thermal stress analyses of a propellant grain from the cure temperature of 135°F to 0°F for repetitive cycling wherein the maximum strain to be expected is 0.15. Testing in this situation would best be restricted to uniaxial and biaxial tensile tests at low rates of strain and in the temperature range from 0°F to +135°F. It may be justifiable to go to higher temperatures to provide information at longer times(which is employing the time-temperature equivalence relation), but there is no reason to weigh the characterization analyses with data obtained below 0°F. Similarly, most of the testing should be confined to strain levels below a magnitude of 0.15 and when the characterization code is actually used the strain bound EMAT should be set at 0.15. For transient thermal analyses it is naturally desirable to employ some transient thermal experiments to weigh the additivity assumptions being used in the constitutive equations toward the true conditions. The testing should also include multiple level stress relaxation tests on single samples because this too weights the analyses towards the proper types of histories. Since the analysis is to be for repetitive cycling then the characterization should include strain reversal tests since as much time will probably be spent unloading as will be spent loading. In addition, since the dominant state of mean pressure in the propellant will be hydrostatic tension, the experimental effort should probably contain no experimental work with superimposed pressure; i.e., hydrostatic compression.

Example 2. Pressurization

In the case of simulated ignition pressurization analyses at or near the cure temperature the characterization should be heavily weighted with short time uniaxial and biaxial tensile tests under conditions of

superimposed pressure. Except for attempting to obtain shorter time data by using the time-temperature equivalence relations, it would be wrong to weight the characterization heavily with low temperature data and strain reversal data.

Example 3. Low Temperature Ignition

This situation calls for a complete characterization involving all of the variables and really tests the validity of the constitutive equation. Testing in this situation should cover the range of temperatures, times, histories, and pressure levels required. Since the constitutive equation is nonlinear it should be obvious that superposition of a thermal analysis and a pressurization analysis is not valid and instead the actual simulated history must be approximated in the structural analyses.

Although some restricted characterizations were performed during the course of this program, the characterizations discussed later in this section are general characterizations covering the total response of the material up to and including the failure points. The testing included uniaxial and biaxial experimentation with complex histories over a considerable temperature range and pressures to 1000 psi. The accuracy of these characterizations could no doubt be improved upon considerably by using more restrictive conditions.

E. EXPERIMENTAL EQUIPMENT

All but the transient thermal experiments were conducted on an Instron tester, with an environmental chamber, for the straining mechanism and the gas dilatometers for the stress and volumetric measurements. For the uniaxial and biaxial tests conducted this combination of axial strain and volume dilatation measurements provides a complete measure of the

strain state. Since the purpose of this program was to develop characterization codes for three dimensional stress-strain equations the input required is three dimensional strain and stress histories, hence the degree of sophistication described for monitoring three dimensional strain state, or something equivalent is necessary. Without this degree of experimental sophistication the three dimensional constitutive equations are indeterminate from a characterization point of view. If a facility is not equipped to make three dimensional strain determinations, only an incompressible distortional characterization can be conducted and in doing so the user should confine the characterization to strain levels below those where significant dilatation is expected. These strain levels can be determined with fair accuracy from the shape of the stress-strain curve (8,9).

F. SOME COMMENTS ON EFFICIENT CODE USAGE

The comments given below describe the best methods found to date to decrease the run times and efficiently eliminate bad data sets from characterizations.

1. Initial Characterization

Prior to running a full scale characterization on large masses of data where the cost per iteration is high, strictly from the volume of calculations, it makes good economic sense to make an initial characterization run on a few select experiments to obtain a good set of initial parameter estimates for the full scale characterizations. The experiments used in the initial characterization, roughly 10, should bracket the range of temperatures and pressures and will provide an excellent first approximation to the coefficients in the constitutive equation for large scale runs. This technique will greatly reduce the cost of characterization since it will provide good

initial estimates and hence rapid conversion on large runs. Whenever the initial values must be crudely estimated, this technique of a small scale initial characterization is recommended.

2. Removal of Bad Data

It appears that no matter how carefully the experimental data are screened, some bad data that are erroneously reduced will get into the data files. Generally these poor data stem from load, dilatational crosshead or chart scale notation errors, or data reduction errors, and will cause the resulting stresses, strains, dilatations, or times to be in error by factors of 2, 5, or 10. Some errors can also get into the system when transcribing the data to key punch sheets or in actual key punching, especially if a card verifier is not used. No matter what the cause, these types of errors can dominate the analysis because the error measure being minimized is a squared quantity. In this sense one datum point in error by 100%, or a factor of two, has the same effect on the error measure as 100 data points with an error or variability of 10%. A few very bad points in a large characterization will in general not negate the characterization, however one or two badly coded experiments will make a characterization run meaningless. The time to eliminate erroneous data is prior to key punching or, at least, before it gets into the data files. After the data are filed it is recommended that a library of the files be made using the Post Processor Code. It then takes only a few hours time to carefully examine this computer output to identify any poorly coded data.

Another way of eliminating poor data from the files is to limit the number of iterations on the first large scale characterization to one or two, or to fix all the parameters in the constitutive equation

and make only one iteration. If the initial estimates of the parameters were obtained from a representative small scale characterization the poorly coded experiments will stand out when comparing predicted versus observed states. The purpose of this screening operation is not to eliminate real material variability, but to eliminate from the files erroneous information. Once a good file has been built all of these precautions can be ignored since the only way bad data could be entered in the computer is through a reading error which is highly unlikely. Also once a test has been labeled as containing erroneous information it can be eliminated from the file, salvaged if possible, and put back in the files in corrected form. Even after careful examination of the raw data obtained from the three propellants tested on this program only one file was built wherein no data coding errors were found.

3. Separate Characterizations

Until one is familiar with the codes, it is recommended that the distortional, dilatational and failure characterizations be performed separately. The user can then become familiar with each portion of the code and its usage in a separate manner and become accustomed with the time required per iteration, initial parameter magnitudes, and other features. On runs of fair size this type of procedure will only add slightly to the total computer time and could provide great savings initially when a user is getting accustomed to the code.

4. Fixing Parameters

The characterization codes were developed in such a manner so that any of the constitutive parameters could be held constant thereby reducing the degrees of freedom in a characterization run. In general, this feature has been found very useful and in a few instances it appears

necessary, particularly in the dilatational characterization. Because the dilatation remains practically zero for a considerable range of strain it is impossible to get an accurate relative measure of the dilatation until some low level of dilatation is exceeded. This threshold level depends upon the measurement technique being employed, chart calibrations, and other experimental conditions. Thus a limiting parameter, VMIN, can be read in and values of dilatation less than this lower limit are not used in the characterization process. Because the very low strain-dilatation data is not used, the equations will not necessarily provide the near incompressible volumetric response observed at small strains. It has, therefore, been found necessary to hold the parameter C_1, which is essentially the reciprocal of the compressibility, constant. This parameter can be determined from bulk compressibility experiments and for most propellants C_1 ranges from 10^{-6} to 10^{-5} in magnitude.

G. LINEAR VISCOELASTICITY

The linear viscoelastic characterization code, SA034, has been used many times at Aerojet. Generally speaking, it is considerably slower in running than the nonlinear counterparts simply because it contains more unknowns and a great many hereditary integrals which are difficult to evaluate numerically. Like the nonlinear code it has the option to hold any of the unknown parameters fixed. The results of a demonstration run using Solithane 113 mechanical properties obtained at Aerojet are given in Table 1 and Figures 2 through 6. In this run a good approximation to the time-temperature shift function from a previous run was used so the run was limited to four iterations since it effectively is a linear problem. The run used 324 data points from 12 experiments which covered the range of temperature from -65°F to +150°F. The coefficient of variation between predicted and observed data was excellent being only 8.1%. Total run time

TABLE 1

COMPARISON OF CONSTITUTIVE PARAMETERS, B_i, FOR THE VISCOELASTIC CHARACTERIZATION OF SOLITHANE 113

i	B_i (Input)	B_i (After 4 Iterations)	Pivot Temperatures Input, °F	Reciprocal Relaxation Times, Input, B_i
1	-.072702	-.088769	-40	
2	-.099896	-.10368	-20	
3	-.30382	-.30333	0	
4	-.27654	-.27618	20	
5	-.074064	-.074813	77	
6	-.038682	-.038181	151	
7	0	352.7		0
8	0	45.5		$1. \times 10^{-1}$
9	0	-44.4		$1. \times 10^{0}$
10	0	107.5		$1. \times 10^{1}$
11	0	-998.8		$1. \times 10^{2}$
12	0	5448.6		$1. \times 10^{3}$
13	0	16227		$1. \times 10^{4}$
14	0	31695		$1. \times 10^{5}$
15	0	73105		$1. \times 10^{6}$
16	0	23856		$1. \times 10^{7}$
17	0	23327		$1. \times 10^{8}$
18	0	5773.1		$1. \times 10^{9}$
19	0	32206		$1. \times 10^{10}$
20	0	41328		$1. \times 10^{11}$
21	0	65353		$1. \times 10^{12}$

Initial Error Measure	324
Final Error Measure	2.27
Standard Deviation, %	8.125
Average Error, %	-0.736
Number of Experiments	12
Number of Data Points	324

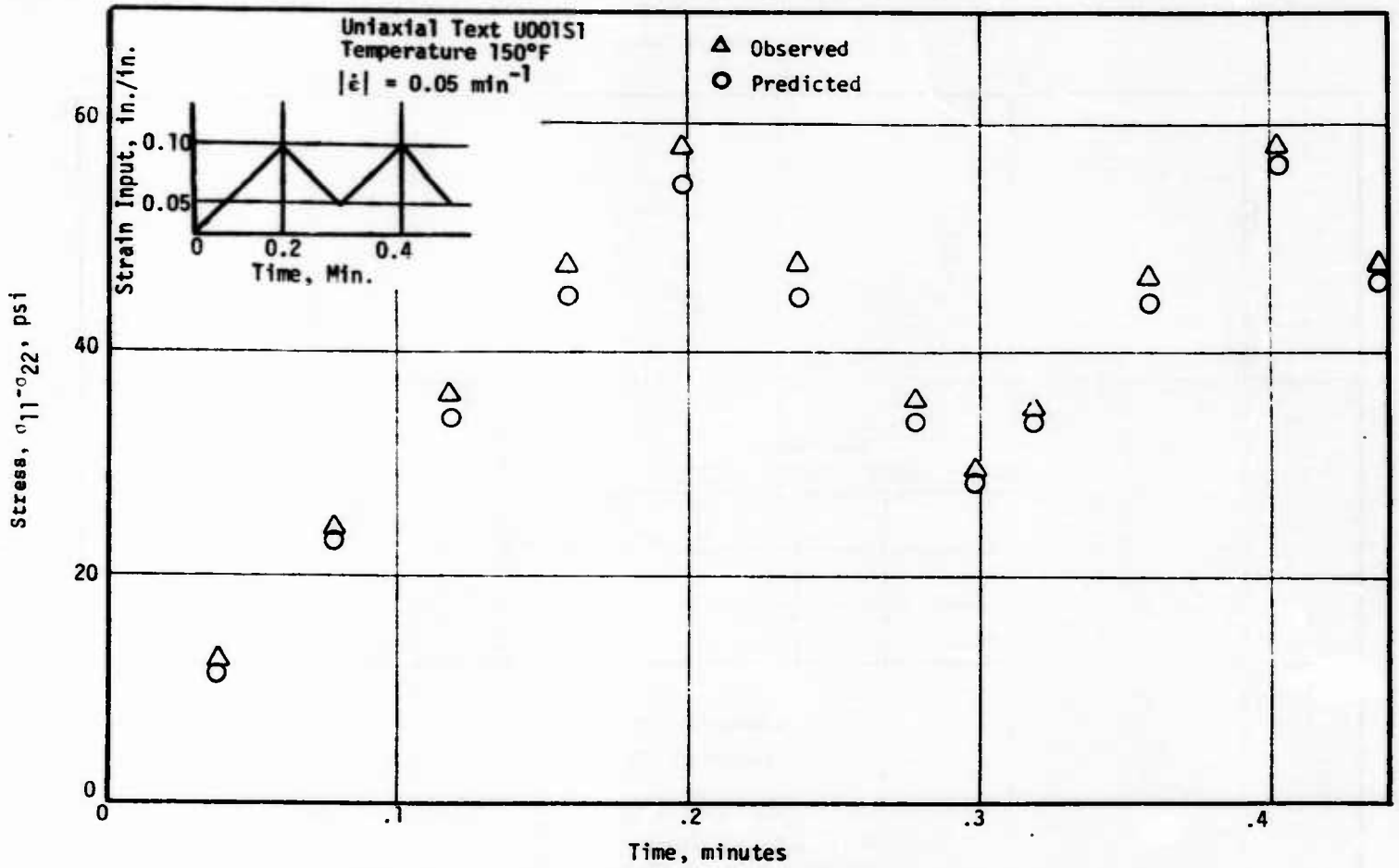

FIGURE 2. COMPARISON OF LINEAR VISCOELASTIC PREDICTIONS AND EXPERIMENTAL DATA FOR SOLITHANE 113

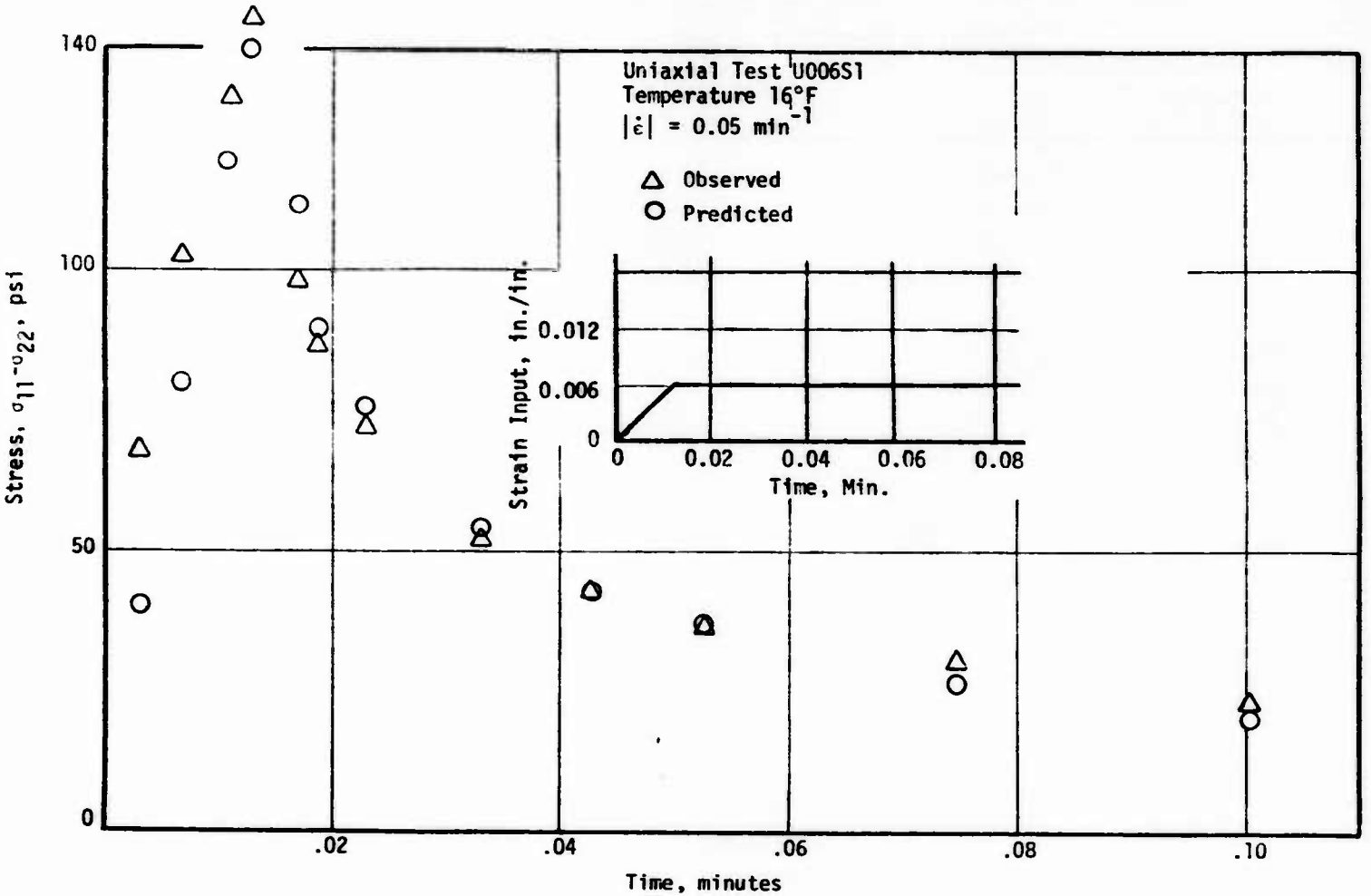

FIGURE 3. COMPARISON OF LINEAR VISCOLEASTIC PREDICTIONS AND EXPERIMENTAL DATA FOR SOLITHANE 113

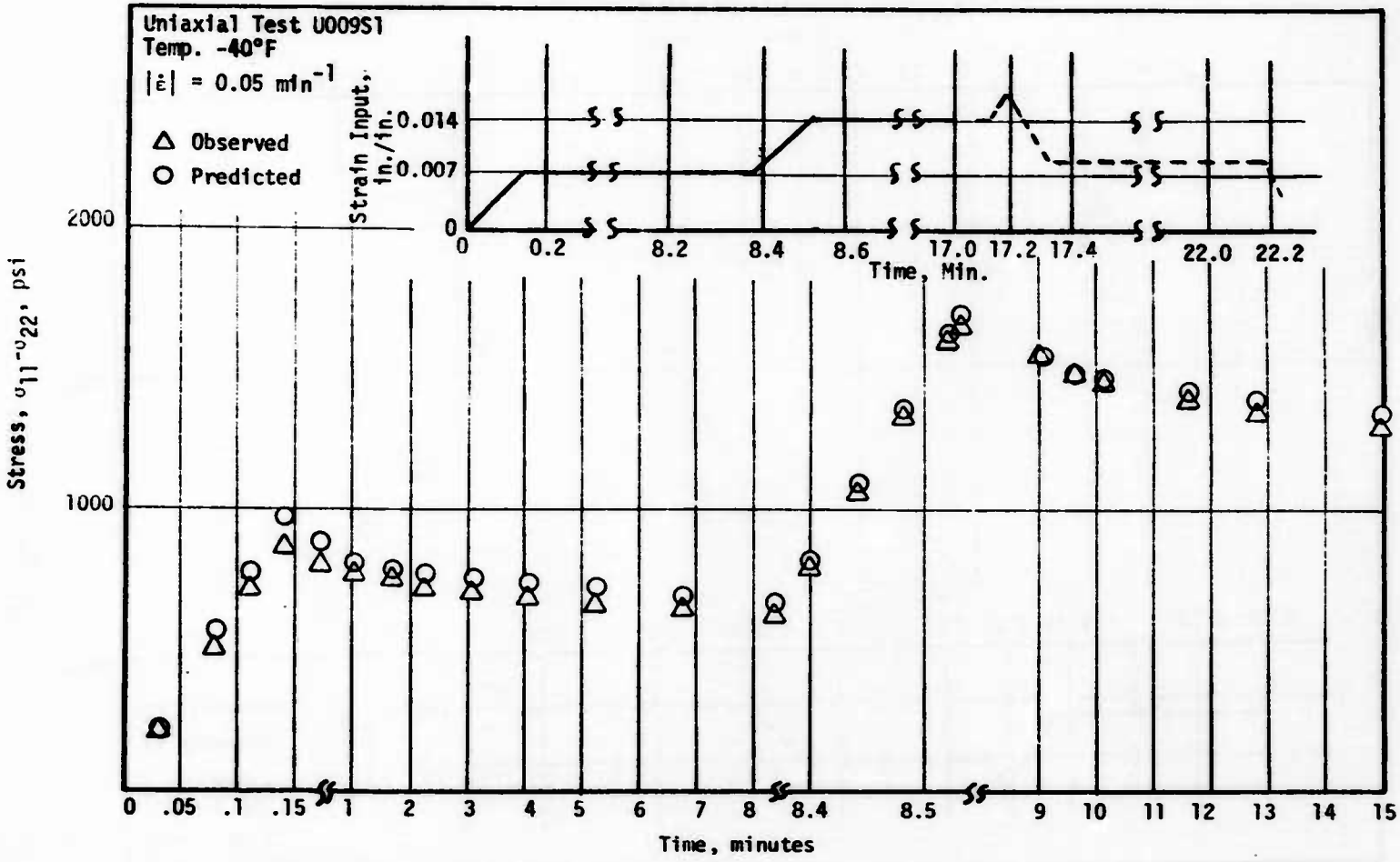

FIGURE 4a. COMPARISON OF LINEAR VISCOELASTIC PREDICTIONS AND EXPERIMENTAL DATA FOR SOLITHANE 113 (FIRST HALF OF TEST)

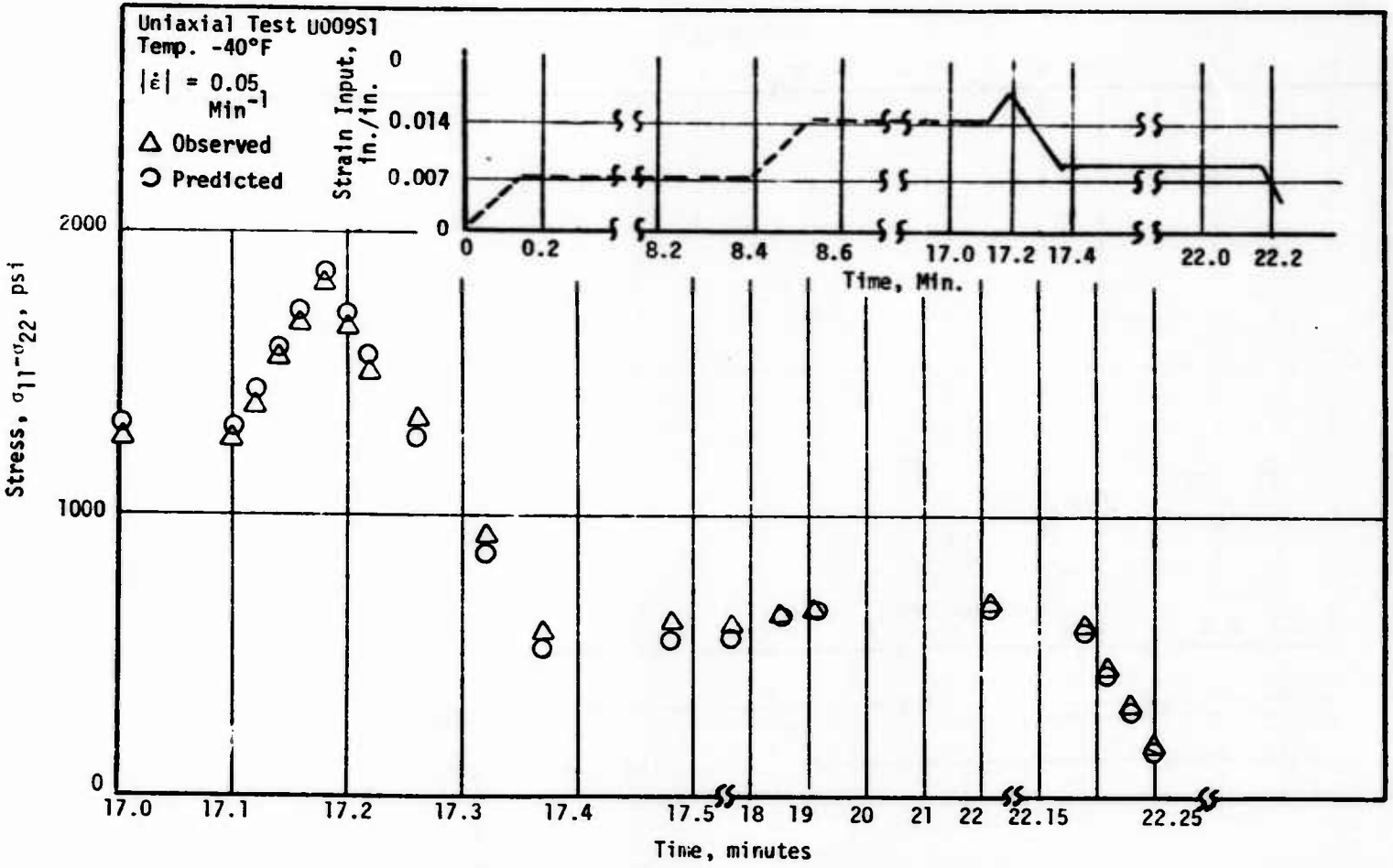

FIGURE 4b. COMPARISON OF LINEAR VISCOELASTIC PREDICTIONS AND EXPERIMENTAL DATA FOR SOLITHANE 113 (LAST HALF OF TEST)

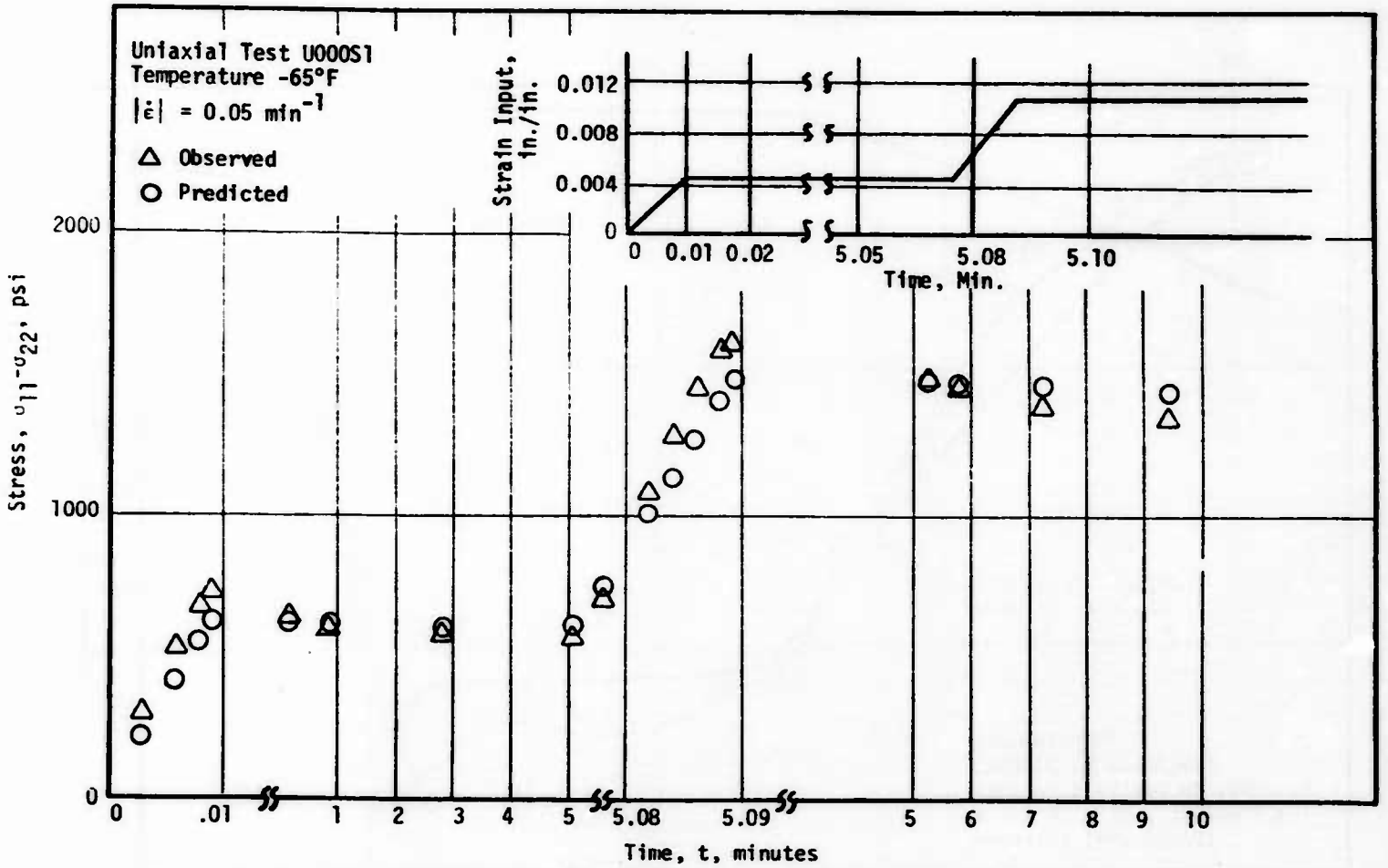

FIGURE 5. COMPARISON OF LINEAR VISCOELASTIC PREDICTIONS AND EXPERIMENTAL DATA FOR SOLITHANE 113

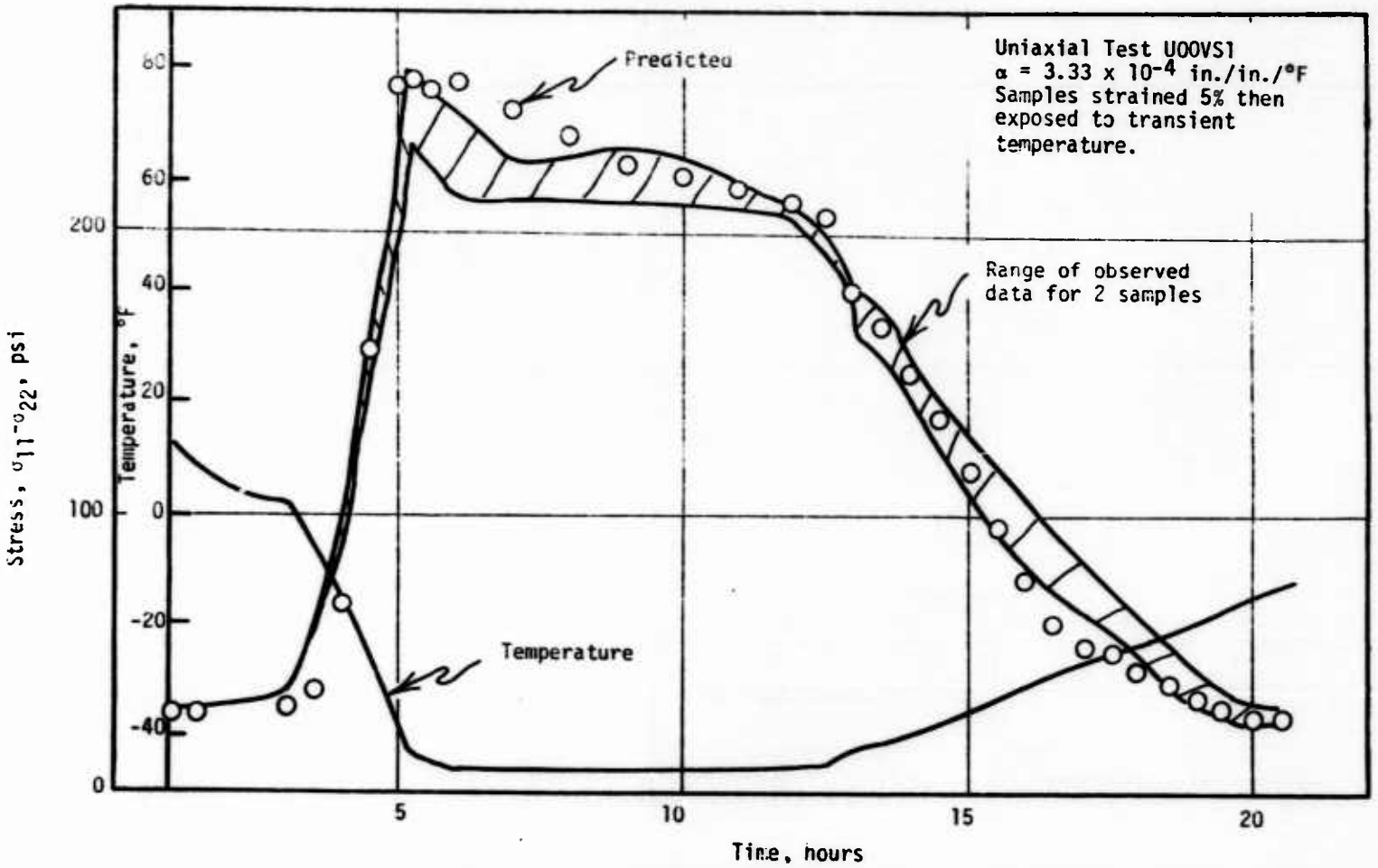

FIGURE 6. COMPARISON OF LINEAR VISCOELASTIC PREDICTIONS AND EXPERIMENTAL DATA FOR THERMOVISCOELASTIC EXPERIMENT ON SOLITHANE 113

was 3.3 minutes. Table 1 gives the initial and final values of parameters in the linear viscoelastic constitutive equation. Runs on propellant mechanical behavior generally give poor agreement since propellants are not linear viscoelastic materials.

H. NONLINEAR VISCOELASTIC CODE DEMONSTRATION

The discussion below demonstrates the capabilities of the nonlinear viscoelastic characterization codes for the three propellants tested during the course of this program. Since the results of the characterizations speak for themselves the discussion can be limited to highlighting deficiencies in the code or the constitutive representations. All of the characterizations discussed below include the complete stress-strain dilatational histories up to and including failure for a series of complex loading histories and different degrees of multiaxiality. These characterizations could no doubt be greatly improved upon by restricting the range of experimental conditions or by limiting the characterization to small strain levels. The data presented below represents, then, the severest of demonstration tests, something heretofore never undertaken for materials of this type. These characterizations test essentially three variables: The quality of experimental measurements including material variability; the capability of the constitutive equation to handle real propellant behavior, and the ability of nonlinear characterization codes to fit the constitutive theory to the experimental data. Overall the performance appears very good, however there are deficiencies, and these are discussed separately after the data are presented.

1. Aerojet Propellant (ANB-3124)

The Aerojet fast burning propellant was tested in uniaxial and biaxial strip tensile fields over the following range of conditions, temperature, -30°F to 125°F, superimposed pressures from 0 psig to 500

psig, and strain levels to 30%. Approximately 52 experiments were performed. This propellant contains large amounts of ultra fine (UFAP) oxidizers and exhibited little or no dilatation, even at large strains. For practically all test conditions the volumetric dilatation was only a small fraction of one percent volume increase with the maximum value being just over 1% dilatation at -30°F. This small amount of volume change, in comparison to 10 to 15% observable for many propellants at failure, does not have a strong influence on the mechanical response, and furthermore is difficult to measure with any precision. For this reason only distortional and failure characterizations were performed and an elastic volumetric compliance was assumed. The dilatation behavior is of little consequence for this propellant since it practically does not dilate, however the mechanical response is still highly nonlinear as clearly seen in the discussion below.

a. Distortional Characterization

Like all the characterizations carried out on this program, an initial characterization on a small sample of representative tests was performed to obtain a good set of estimated constitutive parameters. These estimated parameters were then used as starting values in the iterative large scale characterizations.

The large scale characterization consisted of 46 experiments which are identified in Table 2. In addition, the initial and final constitutive parameters and other detailed information regarding the distortional characterization are given in Table 3. Overall the quality of the distortional characterization is excellent. It gave a standard deviation of only $\pm$ 11.6 % and required 86 seconds of computer time. That means 68% of the stress values are predicted within $\pm$ 11.6% of the

TABLE 2

IDENTIFICATION OF CHARACTERIZATION EXPERIMENTS

FOR ANB-3124 PROPELLANT

Test No.	Test ID	Initial Temp.	Pressure
1	U00240	110	0
2	U11243	110	50
3	U11244	110	200
4	B00224	125	0
5	B00225	125	0
6	B00226	125	0
7	B11227	126	200
8	U00301	78	0
9	U00302	78	0
10	U00308	78	0
11	U00309	78	0
12	U00310	78	0
13	U00312	78	0
14	U00313	77	0
15	U00314	78	0
16	U00315	78	0
17	U11316	78	50
18	U11318	78	50
19	U11319	78	300
20	U11321	78	485
21	B00302	78	0
22	B00301	78	0
23	B00314	78	0
24	B00315	78	0
25	B00317	78	0
26	B11318	78	200
27	U00423	38	0
28	U00424	38	0
29	U00431	38	0
30	U11427	38	50
31	U11428	38	50
32	U11429	38	150
33	U11430	38	450
34	B00408	38	0
35	U00632	-1	0
36	U00633	-1	0
37	U11637	-1	50
38	U11638	-1	150
39	U11639	-1	450
40	B00621	0	0
41	B00622	0	0
42	B00623	0	0
43	B11619	0	200
44	U00958	-31	0
45	U00959	-31	0
46	U11961	-32	200

TABLE 3

DISTORTIONAL CHARACTERIZATION PARAMETERS

FOR ANB-3124 PROPELLANT

No. of Tests - 46
No. of Data Points = 598
Max. No. of Iterations = 0
Max. No. of Interval Halvings = 10
Numerical Derivative Increment = .1000-01
Print Parameter(s) = 0
Strains Greater Than .1000 + 01 were ignored.
No. of Shift Function Coefficients = 4
Total Number of Shear Coefficients = 13

The Initial Coefficients		Regression Coefficients After Convergence
K	B(K)	B(K)
1	-.804170-01	-.80551-01
2	-.775270-01	-.73185-01
3	-.534570-01	-.50543-01
4	-.894980-01	-.80392-01
5	.400000+02	.40000+02
6	-.100000+00	-.10000+00
7	-.182850+01	-.16218+01
8	-.924950+00	-.10823+01
9	.719380+01	.76860+01
10	.200000+01	.20000+01
11	.198490+03	.20908+03
12	.113040+03	.98814+02
13	.000000	.00000

There were 552 Experimental Test Points

The Average Deviation = -1.114 percent, and The Standard Deviation 10.901 percent.
The following 4 coefficients were held constant: 5 - 6 - 10 - 13

Calculated Shift Function, A_T	Temperature °F
.7624+05	-80.
.1522+05	-60.
.3040+04	-40.
.6070+03	-20.
.1212+03	0.
.2804+02	20.
.6489+01	40.
.2361+01	60.
.7857+00	80.
.1574+00	100.
.3153-01	120.
.6316-02	140.
.1265-02	160.
.2534-03	180.
.5077-04	200.

Pivot Points for Shift Function: 0., 40., 77., 130.

observed values, assuming normal statistical variability, and 95% of the predictions from the constitutive equation are within $\pm$ 23.2% of the experimental values. Considering the range of test conditions, the types of deformation histories, and the fact that the entire stress-strain curve to failure is being represented clearly demonstrates the applicability of the methods proposed in this report. Researchers unfamiliar with the mechanical properties of propellant materials should be made aware that these materials are not noted for their reproducibility, even for a constant test condition within the same small sample of bulk material. It is common for the standard deviation of properties such as modulus or strength to exceed 10% of the mean value at a single test condition. Considering these experiments were performed over a broad range of conditions and over a long period of time the results of the characterization are remarkably good. Indeed, much of the 11.6% standard deviation of predicted states must be attributed to material variability rather than errors in the representation. Figures 7 through 15 illustrate "Typical" fits of theory to measured stress response for this propellant. In addition, the cumulative damage index measure discussed in the next section is also illustrated on these curves. Failure, according to this type of theory, should occur when the damage index is unity.

b. Failure Characterizations

The failure characterization is different than the distortional characterization in that there is only one failure point per experiment whereas there were from 10 to 100 stress points selected per experiment for the distortional characterization. The cumulative damage theory uses the predicted stress history rather than the observed history in the damage equation. For the Aerojet propellant, only 44 of the 52 experiments were used in the failure characterization since 8 experiments were labeled as end-bond failures by the experimentalist. Because the

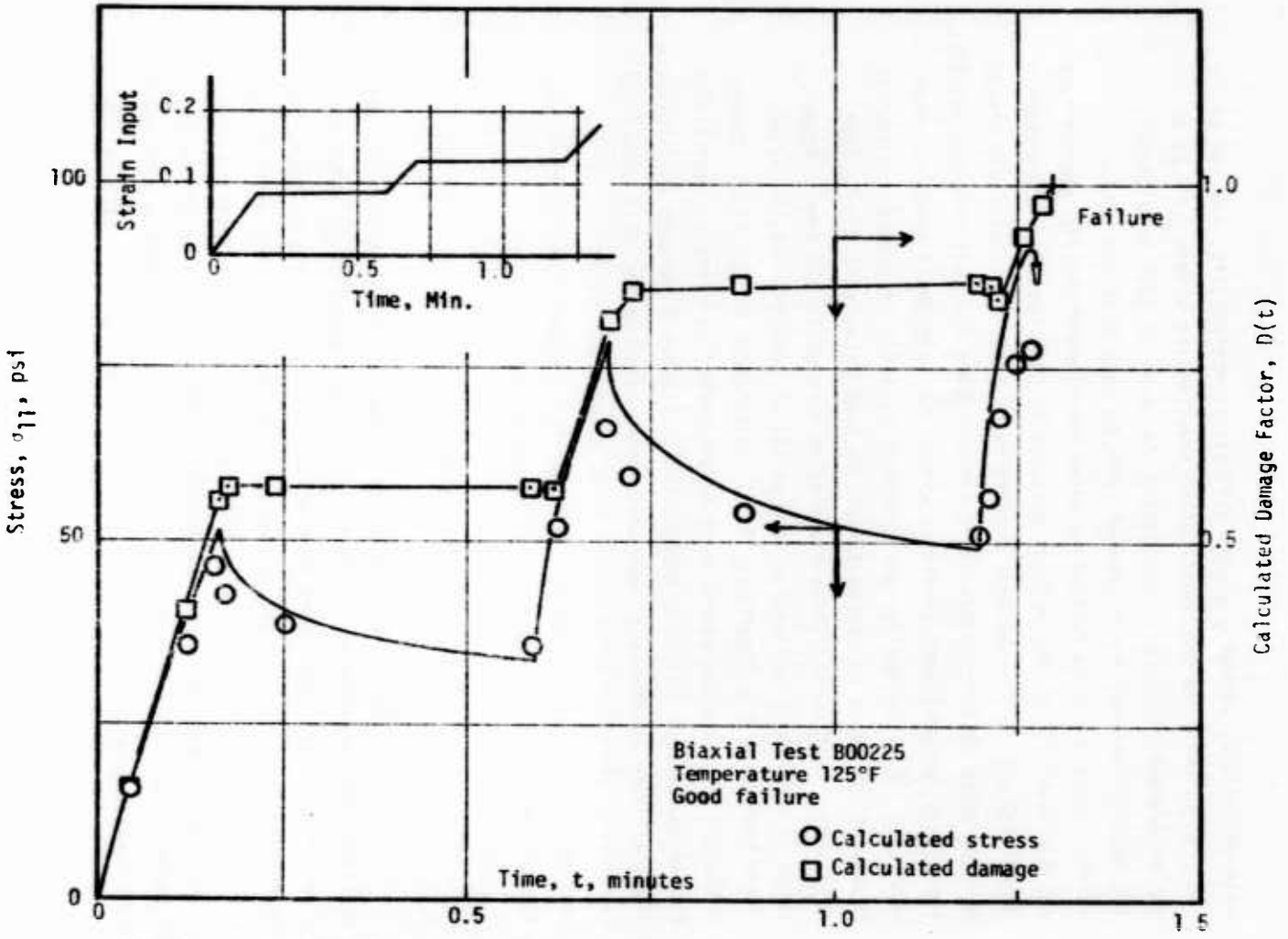

FIGURE 7. COMPARISON OF CALCULATED AND MEASURED RESPONSE OF THE ANB-3124 PROPELLANT

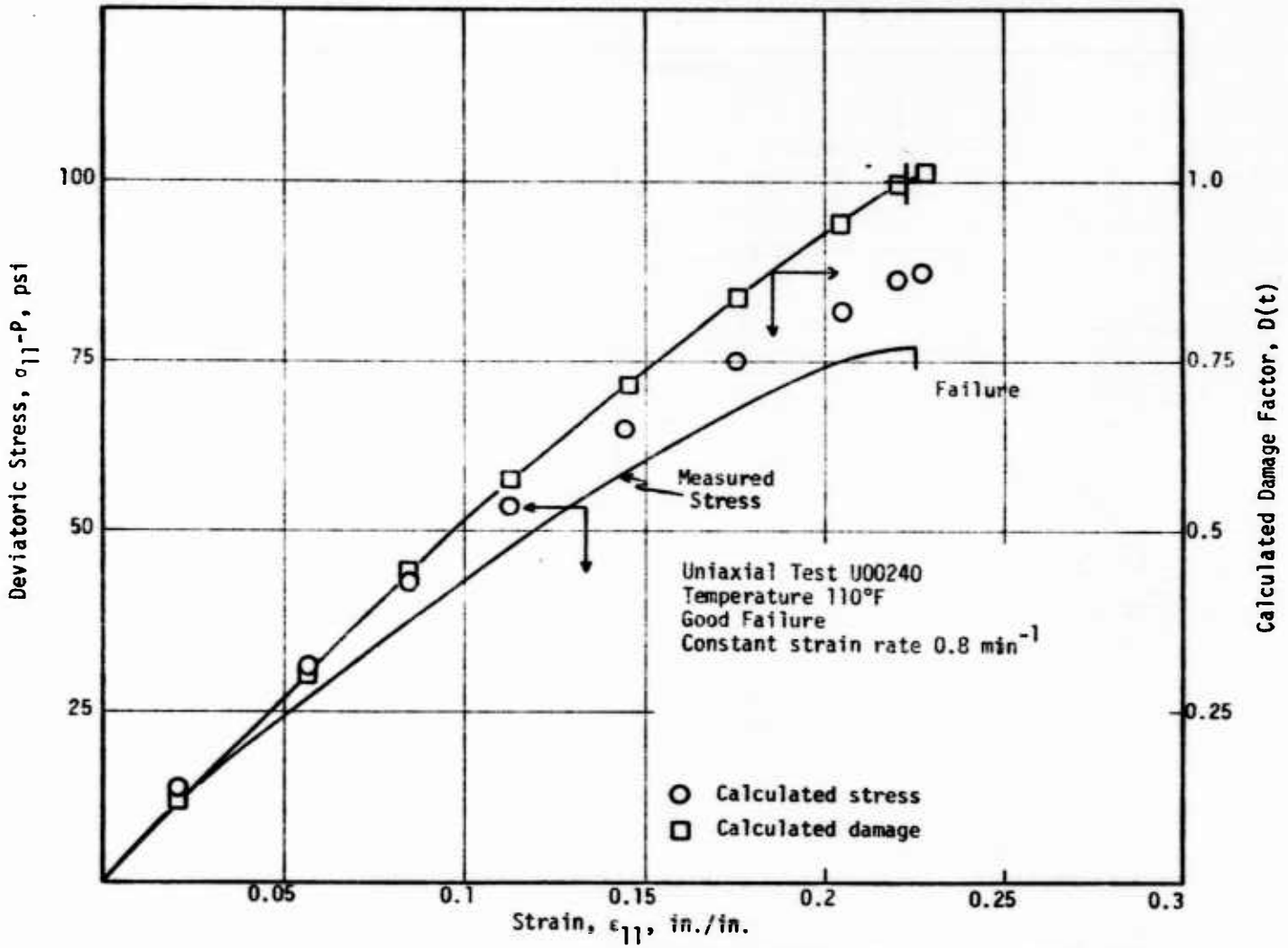

FIGURE 8. COMPARISON OF CALCULATED AND MEASURED RESPONSE OF THE ANB-3124 PROPELLANT

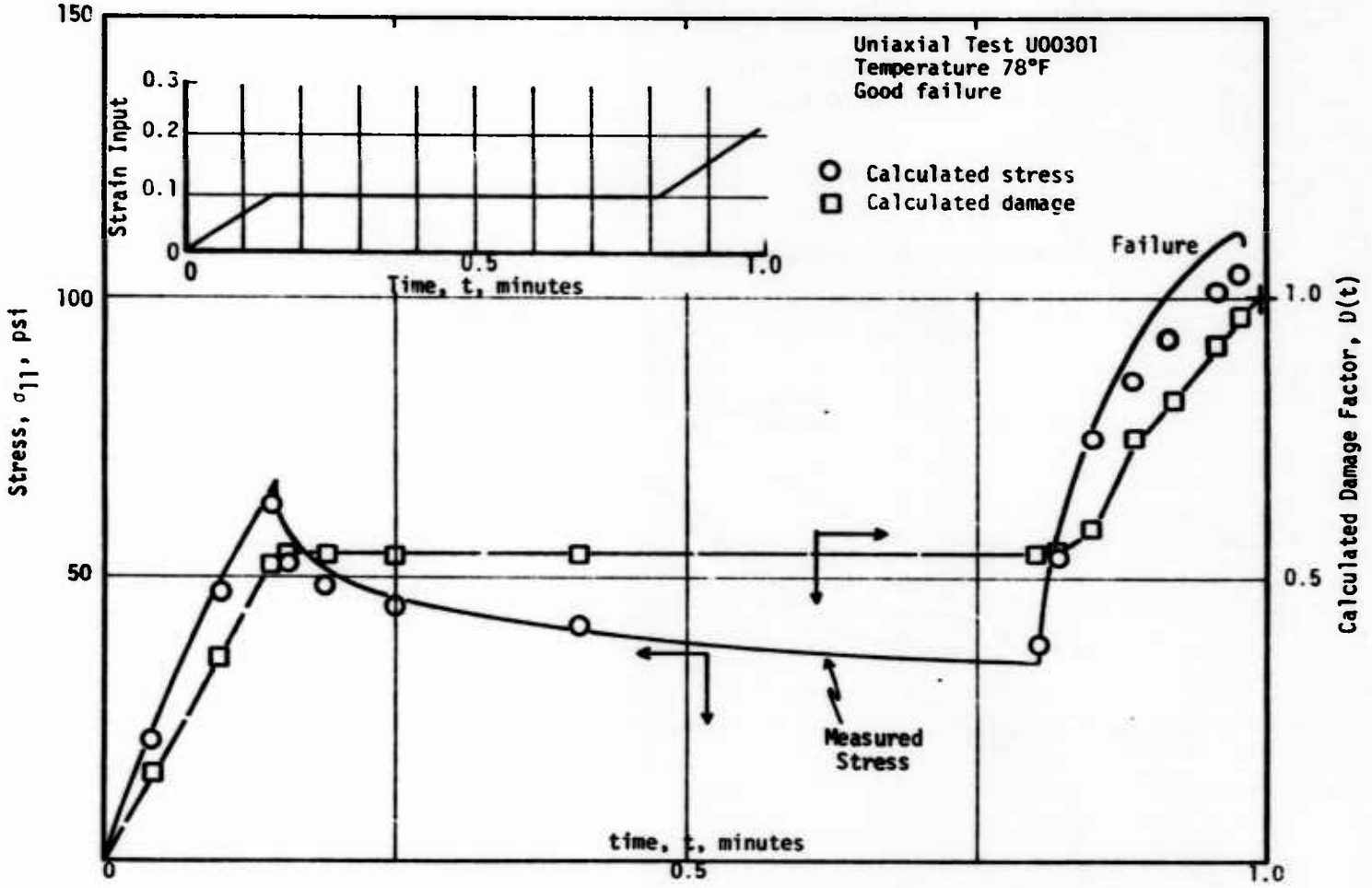

FIGURE 9. COMPARISON OF CALCULATED AND MEASURED RESPONSE OF THE ANB-3124 PROPELLANT

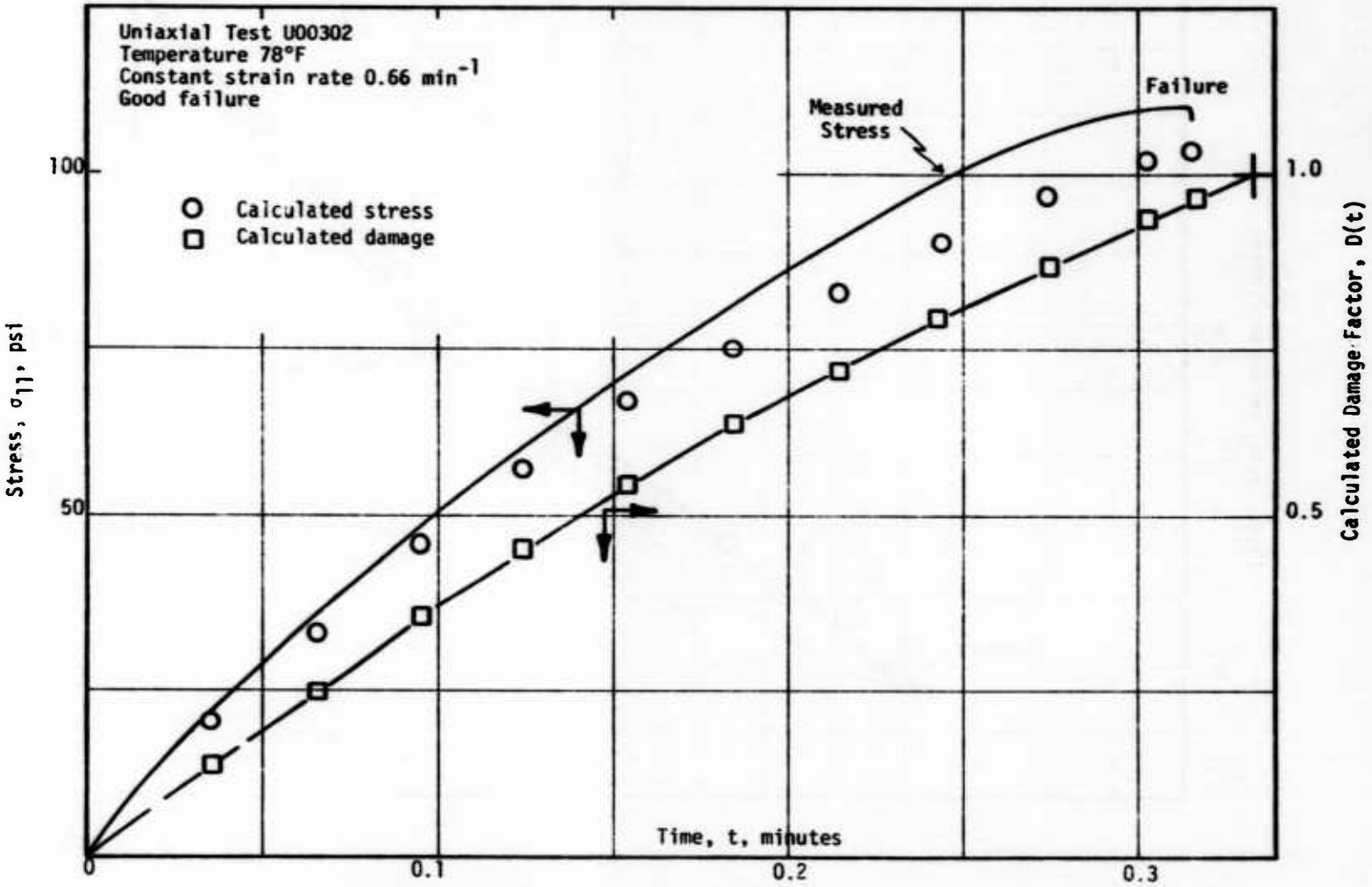

FIGURE 10. COMPARISON OF CALCULATED AND MEASURED RESPONSE OF THE ANB-3124 PROPELLANT

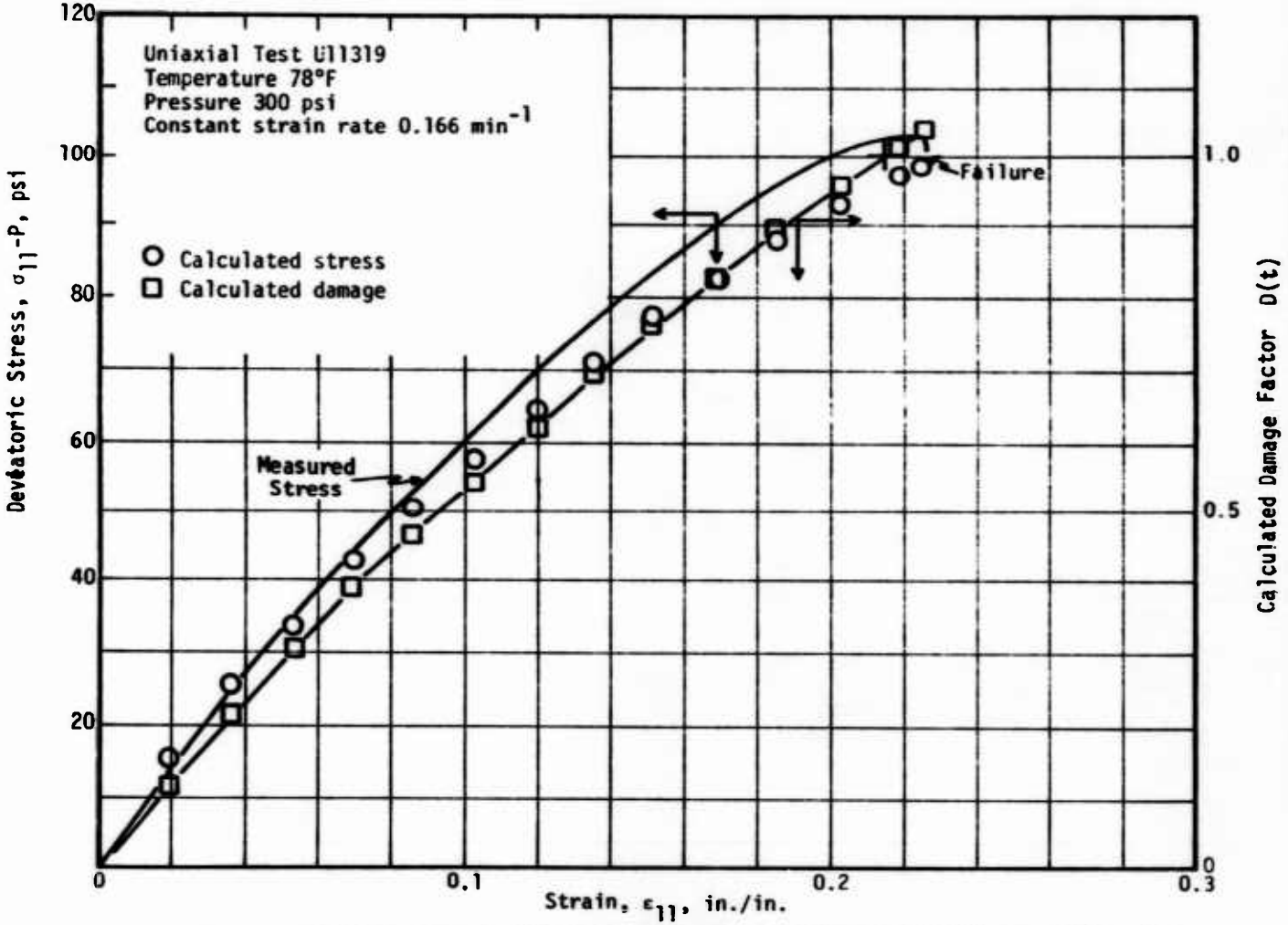

FIGURE 11. COMPARISON OF CALCULATED AND MEASURED RESPONSE OF THE ANB-3124 PROPELLANT

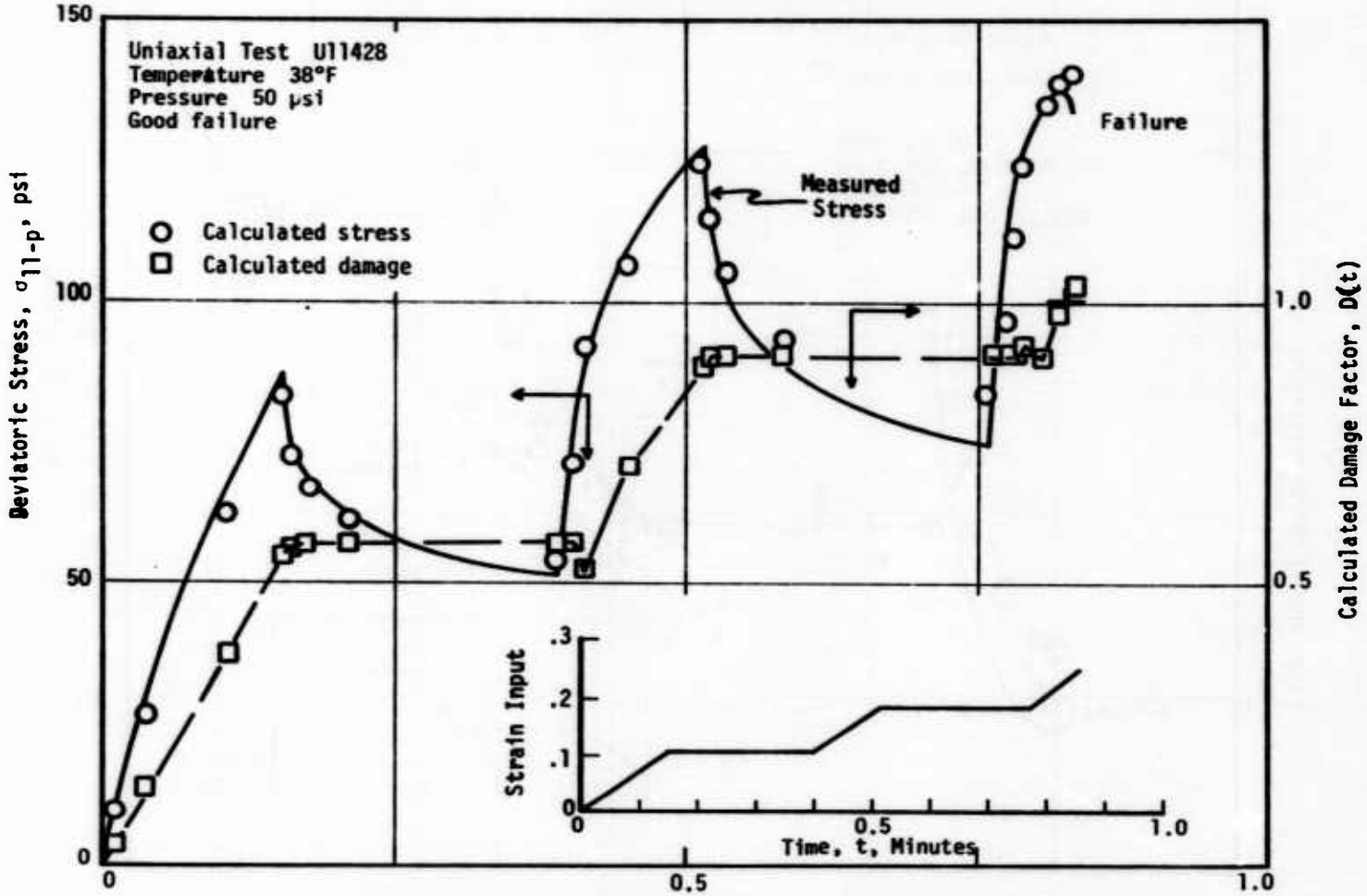

FIGURE 12. COMPARISON OF CALCULATED AND MEASURED RESPONSE OF THE ANB-3124 PROPELLANT

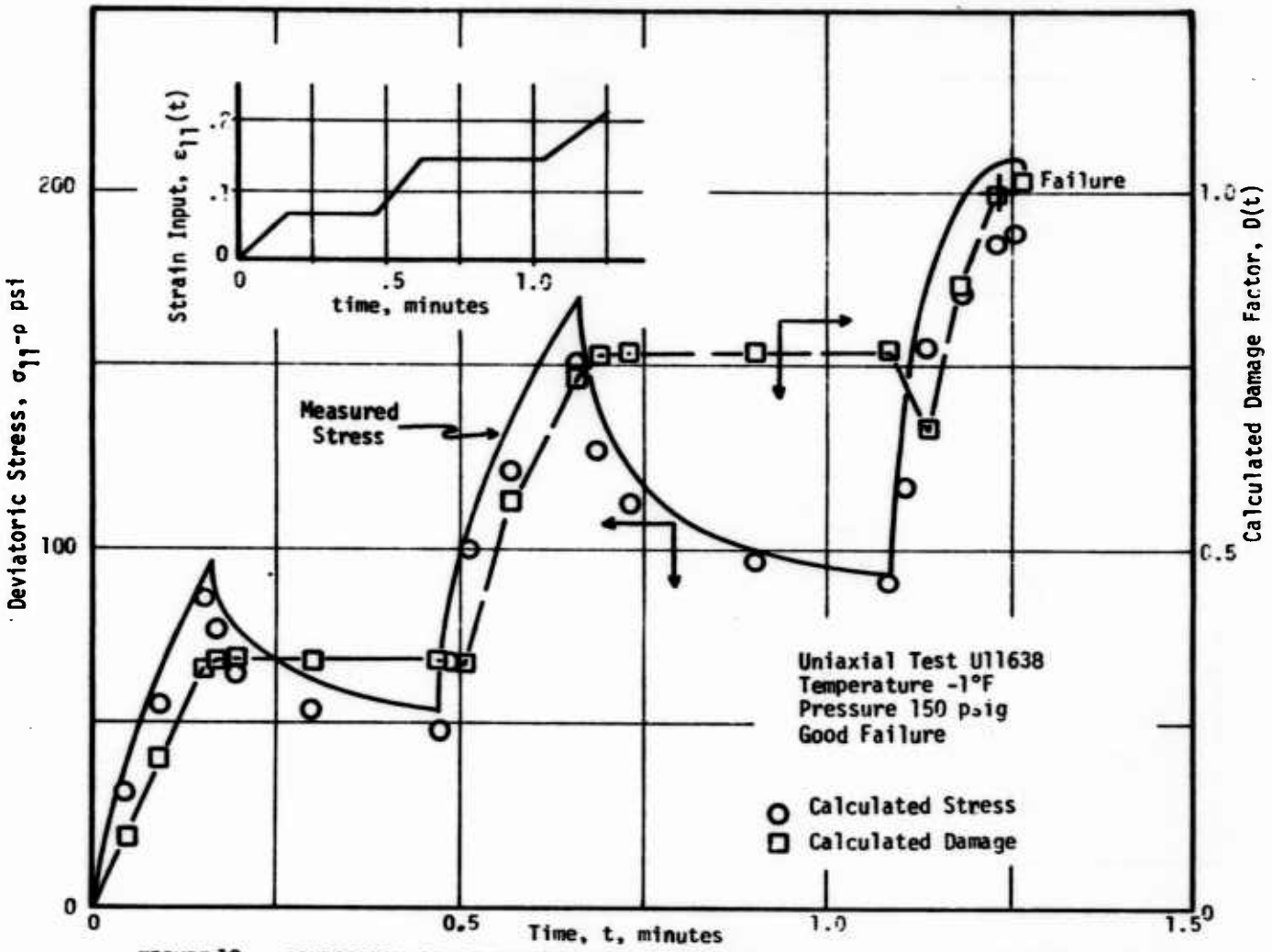

FIGURE 13. COMPARISON OF CALCULATED AND MEASURED RESPONSE OF THE ANB-3124 PROPELLANT

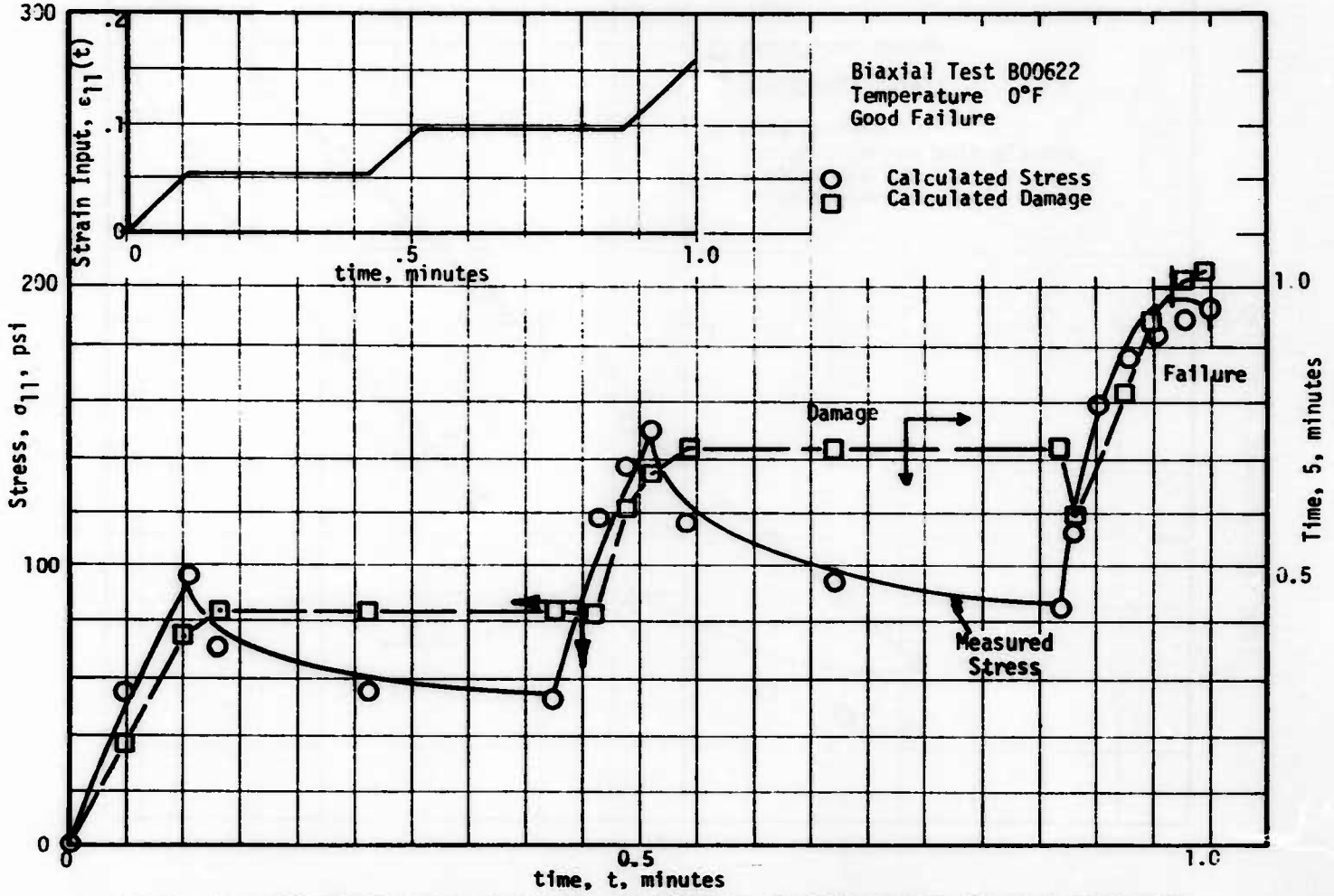

FIGURE 14. COMPARISON OF THE CALCULATED AND MEASURED RESPONSE OF THE ANB-3124 PROPELLANT

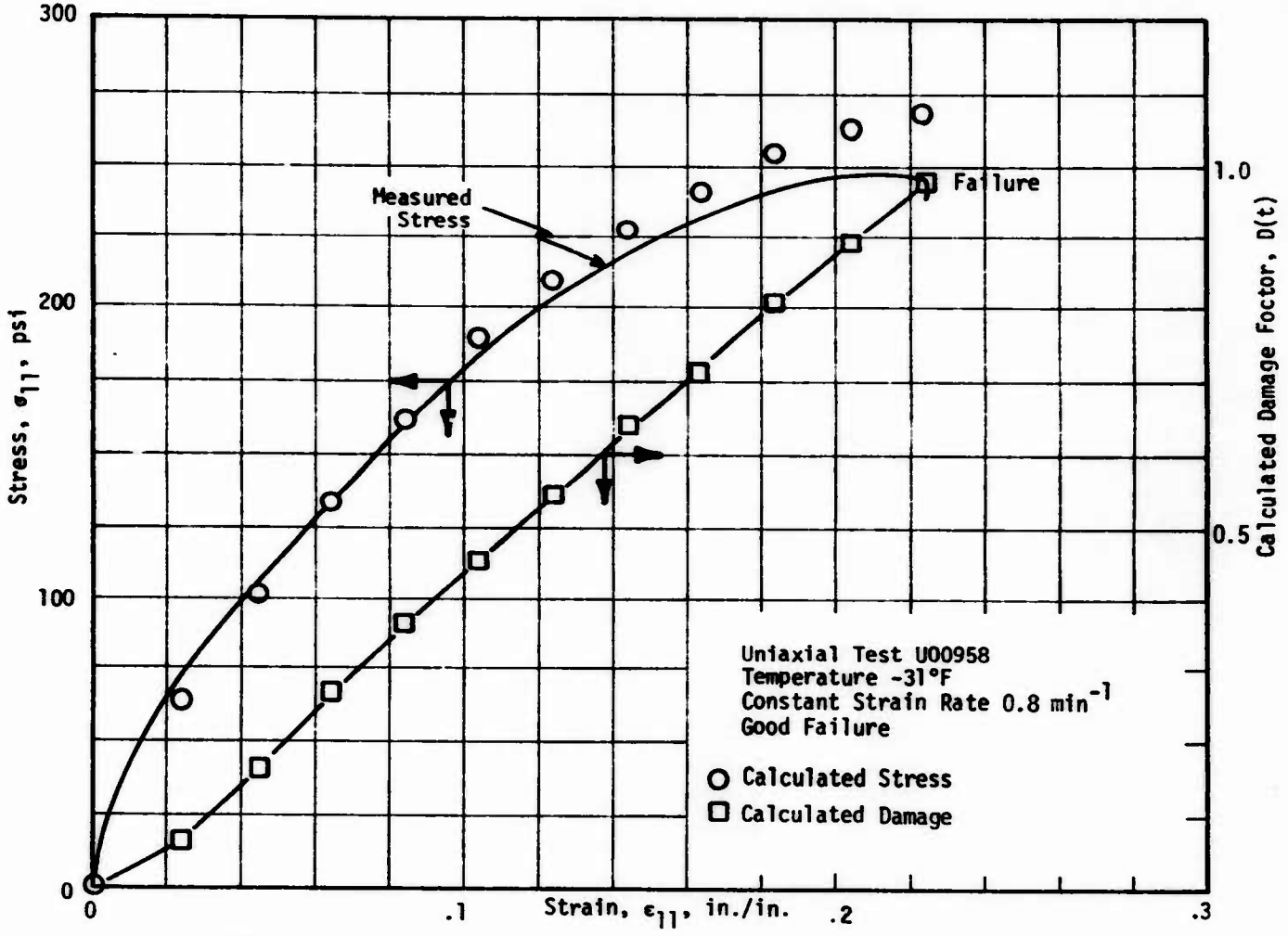

FIGURE 15. COMPARISON OF THE CALCULATED AND MEASURED RESPONSE OF THE ANB-3124 PROPELLANT

initial characterization suggested little dependency on six of the parameters in the failure equation these parameters were held constant, demonstrating the flexibility of the code. Actually the two exponents B_6 and B_7 were added at an early stage to include nonlinear damage measures and have never been found to be of any real value. They can be permitted to vary, but generally remain close to unity, hence in most failure characterizations they are simply fixed at unity. The parameters B_1 through B_4 were fixed at zero in this failure run. These parameters were designed to accommodate the dependency of the stress strain behavior on dilatation and since these propellants did not dilate to any appreciable extent and influence the stress-strain behavior it likewise should not influence the failure behavior. The failure characterization was therefore determined by four parameters which include two linear coefficients and two L_p norms, one which is fixed as L_∞. The failure characterization required 126 seconds of computer time. It started with an initial error measure of 44.0 and in 8 iterations had the error measure reduced to 0.794. The standard deviation of the damage measured at failure was 7.2%, which means that 68% of the failures could be expected to occur when the damage measure ranges from 0.928 to 1.072. The plots of damage versus history are included in Figures 7 through 15 for the experiments illustrated. In addition the initial and final values of the parameters in the failure equation and other information regarding this characterization are given in Table 4.

c. Discussion of Results

The results of the distortional and failure characterizations on the Aerojet propellant demonstrate that the techniques proposed in this report can actually work. The quality of the distortional characterization speaks for itself in that a standard deviation of only 11.6% of the predicted values not only demonstrates the computer routines but also must

TABLE 4

FAILURE ANALYSIS CONSTITUTIVE PARAMETERS FOR THE ANB-3124 PROPELLANT

K	The Initial Coefficients B(K)	Final Failure Coefficients B(K)
1	.000000	.000000
2	.000000	.000000
3	.000000	.000000
4	.000000	.000000
5	.100000 + 02	.424297 + 02
6	.100000 + 01	.100000 + 01
7	.100000 + 01	.100000 + 01
8	.000000	-.604433 - 01
9	.000000	.883460 - 01

The following 6 coefficients were held constant: 1, 2, 3, 4, 6 & 7

The following 38 tests were used in the Failure Characterization:

1	2	3	4	5	0	7	8	9	0	11	12	0	0	15	16	17	18	19	20
0	0	23	24	25	26	27	28	29	30	31	32	33	0	35	36	37	0	39	40
41	42	43	44	45	46														

There were 38 failure data points.

The Average Deviation = -.549 percent and

The Standard Deviation = 7.226 percent.

give credibility to the actual constitutive equations. Since the error is generally rather uniform over the entire stress-strain curve, much of the error or standard deviation stems from sample-to-sample variability and not from the constitutive equations.

The failure characterization is not as impressive as the distortional characterization and it can be improved upon considerably. One way of improving upon the failure characterization is to use more uniform method of defining failure on the stress strain curve. Many samples start to tear during the final portions of the tensile curve and failure should be defined when the tear first initiates rather than when it is completed, since the tear relieves surrounding stresses and nullifies the experimental conditions. Careful analysis of the damage index reveals that when the materials do not dilate significantly, the damage measure at failure for biaxial samples averages out to be less than unity, approximately 0.85, whereas for uniaxial samples it averages out somewhere near 1.10. The above values are for failure characterizations which include both uniaxial and biaxial experiments. When uniaxial or biaxial experiments are characterized for failure separately the damage relations do an excellent job and give very low standard deviations. Thus, part of the problem is in handling mixed stress states. The first conclusion one might draw from this argument is that the damage equations do not contain the proper relationships or dependency of failure on stress history. This argument can have merit, and if so, the codes can be easily changed to accommodate a new failure relationship. A simpler explanation of the discrepancies in uniaxial and biaxial failure predictions lies in using the wrong stress information. The biaxial samples tested have geometries roughly 1/4" x 1" x 7", and are commonly called strip biaxial, since effectively the normal strain in the 7" direction is held to zero in the central portion of the sample. An elastic analysis reveals that the axial stress is not uniform in this type of sample and has a peak value approximately 1.15 times the average stress measured for near

incompressible materials. If the stresses used in the damage criterion were amplified by this factor the agreement between uniaxial and biaxial would be excellent. Why not include such a fudge factor? Well it might be justified in a case like this, since the material does not dilate significantly, however for most propellants, which dilate greatly, there is little difference between uniaxial, biaxial, and triaxial constraints at failure. Hence the factor should float somewhere between 1.0 and 1.15. The problem is really not with the damage analysis but with the test specimen which does not produce a uniform biaxial stress field.

In summary, the distortional characterization of the ANB-3124 (HTPB-UFAP) propellant is excellent and the failure characterization is fair to good. The discrepancies in the failure characterization are mostly attributed to the poor definition of failure experimentally, especially in biaxial samples tested in a dilatometer where they cannot be viewed, and due to the nonuniform spatial stress distributions in the biaxial samples.

2. Thiokol Propellant (TPH-1135)

The high solids Thiokol propellant, TPH-1135, was the first propellant received. Because of the long delays in obtaining the other propellant candidates considerable experimental investigation was done on TPH-1135 to attempt to determine optimum testing conditions for characterization. Like the other two candidates the experimental work was confined to uniaxial and biaxial stress-strain-dilatation work over the following range of conditions: temperature -75°F to 150°F, superimposed pressures from 0 to 1000 psig, and strain levels to 40%. Approximately 100 experiments were included in the total characterization. Unlike the Aerojet propellant which contains large amounts of fine oxidizers, and consequently exhibits little or no dilatation, this propellant dilates considerably and therefore exhibits a strong dependency upon superimposed

pressure. The maximum dilatation levels experienced were roughly 10% volume increase. This propellant therefore is considerably different in its response characteristics than the Aerojet propellant, and certainly would have to be classified as being more complex. The discussion below describes the results of the distortional, dilatational and failure characterizations o· the TPH-1135 propellant using the computerized characterization codes. As summarized in Table 5, this large scale run used 54 experiments from -40°F to +150°F.

a. Distortional Characterization

The initial parameter estimates for the Thiokol characterization were based on a small sample characterization which used 10 experiments as input. The results of this small scale characterization, which provided an excellent fit of the data were than used as the starting parameters for the full scale characterization. In the small scale characterization the error measure for the distortional analyses was reduced from 178 to 26.7 to 10.9, to 5.6 to 2.20 to 1.846 and finally to 1.842 in six iterations. The final standard deviation on the predicted stresses was only 9.8% which is excellent by any standards. When the full scale characterization was performed 54 experiments were used with 951 data points. The coefficients in the full scale characterization were changed little from those of the small scale characterization and the final error measure resulted in a standard deviation of 12.9% of the predicted stress values. This value of the standard deviation is quite small since it is estimated that the reproducibility of the data is roughly $\pm$ 10% when experimental and material variability are considered. Comparisons of predicted and measured stress-strain response are shown in Figures 16 through 30 for typical experiments. Pertinent information from the characterization is provided in Table 5.

TABLE 5

CHARACTERIZATION PARAMETERS FOR TPH-1135 PROPELLANT

A. DISTORTIONAL CHARACTERIZATION

No. of Tests = 54

No. of Data Points = 951

Max. No. of Iterations = 3

Max. No. of Interval Halvings = 10

Numerical Derivative Increment = .1000-01

Print Parameter(s) = 0

Strains Greater Than .1000+01 were ignored

No. of Shift Function Coefficients = 5

Total Number of Shear Coefficients = 14

The Initial Coefficients		Final Regression Coefficients	
K	B(K)	I	B(I)
1	-.397070+00	1	-.41751+00
2	-.166950+00	2	-.16952+00
3	-.646620-01	3	-.72860-01
4	-.792770-01	4	-.80748-01
5	-.530700-01	5	-.53950-01
6	.600000+02	6	.60000+02
7	-.150000+00	7	-.15000+00
8	-.175090+01	8	-.16888+01
9	-.118320+01	9	-.12300+01
10	.107910+02	10	.10494+02
11	.200000+01	11	.20000+01
12	.102320+03	12	.10191+03
13	.235290+03	13	.23876+03
14	.529650+02	14	.56485+02

The following 3 coefficients were held constant: 6, 7 and 11

The Average Deviation = -1.740 percent, and the Standard Deviation = 12.896 percent.

Shift Function, A_T	Temperature °F
.8064+14	-80
.1906+11	-60
.4504+07	-40
.1271+05	-20
.4283+03	0
.9975+02	20
.1984+02	40
.3946+01	60
.8506+00	80
.2891+00	100
.9829-01	120
.3341-01	140
.1136-01	160
.3861-02	180
.1312-02	200

Pivot points for shift function: -30, 0, 20, 77 and 155.

TABLE 5 (Cont.)

CHARACTERIZATION PARAMETERS FOR THE TPH-1135 PROPELLANT

B. DILATATIONAL CHARACTERIZATION

No. of Tests = 54
No. of Data Points = 951
Max. No. of Iterations = 10
Max. No. of Interval Halvings = 10
Numerical Derivative Increment = .1000-01
Print Parameter(s) = 0
Dilatations Less Than .5000-02 Were Ignored
Total Number of Bulk Coefficients = 7

The Initial Coefficients K	B(K)	Final Regression Coefficients I	B(I)
1	-.100000-06	1	-.70722-02
2	-.100000-06	2	-.31083-03
3	.300000+01	3	.30000+01
4	-.100000-06	4	.92738-02
5	-.100000-06	5	-.48150-04
6	.133000-05	6	.13300-05
7	.000000	7	.56505+01

The following 2 coefficients were held constant: 3 6

The Average Deviation = .185 Percent, and
The Standard Deviation = 36.981 Percent.

TABLE 5 (Cont.)

CHARACTERIZATION PARAMETERS FOR THE TPH-1135 PROPELLANT

C. FAILURE ANALYSIS

The Initial Coefficients K	B(K)	Final Failure Coefficients I	B(I)
1	-.100000-06	1	.276944-03
2	-.100000-06	2	-.996347-07
3	-.100000-06	3	.973351-03
4	-.100000-06	4	-.100658-06
5	.100000+02	5	.711298+01
6	.100000+01	6	.100000+01
7	.100000+01	7	.100000+01
8	.000000	8	.169195-02
9	.000000	9	.153631-01

The following 2 coefficients were held constant: 6 and 7

The following 49 tests were used in the failure characterization:

1	2	0	4	5	6	0	8	9	10	11	12	13	14	15
16	17	0	19	20	21	22	23	24	25	26	27	28	29	30
31	32	33	34	35	36	37	38	39	40	41	42	43	44	45
0	47	48	49	50	0	52	53	54						

There were 49 failure data points.

The Average Deviation = -2.777 Percent, and

The Standard Deviation = 12.084 Percent.

TABLE 5 (Cont.)

CHARACTERIZATION PARAMETERS FOR THE TPH-1135 PROPELLANT

D. EXPERIMENTS USED IN THE CHARACTERIZATION

Test No.	Test ID	No. Pts.	Initial Temp.	Pressure
1	B00152	11	110.	0.
2	B11251	9	150.	100.
3	U00991	10	-40.	0.
4	U00994	12	-40.	0.
5	U00997	10	-40.	0.
6	U11998	10	-40.	50.
7	U11999	9	-40.	100.
8	U00996	17	-40.	0.
9	U00142	22	150.	0.
10	U00233	23	110.	0.
11	U00565	30	20.	0.
12	B11153	24	150.	100.
13	B11154	10	150.	200.
14	B00250	24	110.	0.
15	B11321	65	77.	100.
16	B11317	22	77.	50.
17	B11779	26	-19.	100.
18	B11778	9	-19.	50.
19	U11232	12	110.	100.
20	U00141	9	150.	0.
21	U11146	11	150.	50.
22	U00427	8	40	0.
23	U00140	27	150.	0.
24	B00631	34	0.	0.
25	U00780	11	-20.	0.
26	U11240	13	110.	50.
27	U00550	27	20.	0.
28	U11675	11	0.	100.
29	U11567	28	20.	100.
30	U11569	15	20.	300.
31	U11566	14	20.	50.
32	U00564	16	20.	0.
33	U11147	10	150.	100.
34	B00641	9	0.	0.
35	B00633	9	0.	0.
36	U00231	11	110.	0.
37	U00428	28	38.	0.
38	B00627	8	0.	0.
39	B11630	11	0.	100.
40	B00628	6	0.	0.
41	B11323	44	77.	200.
42	B00434	10	40.	0.
43	B00426	7	40.	0.
44	B00435	7	40.	0.
45	B11320	10	77.	550.
46	U00319	29	77.	0.
47	U11324	24	77.	400.
48	U11325	24	77.	500.
49	U11326	23	77.	0.
50	U11321	22	77.	0.
51	B00318	10	77.	0.
52	U00314	22	77.	200.
53	U00313	24	77.	100.
54	U00312	24	77.	0.

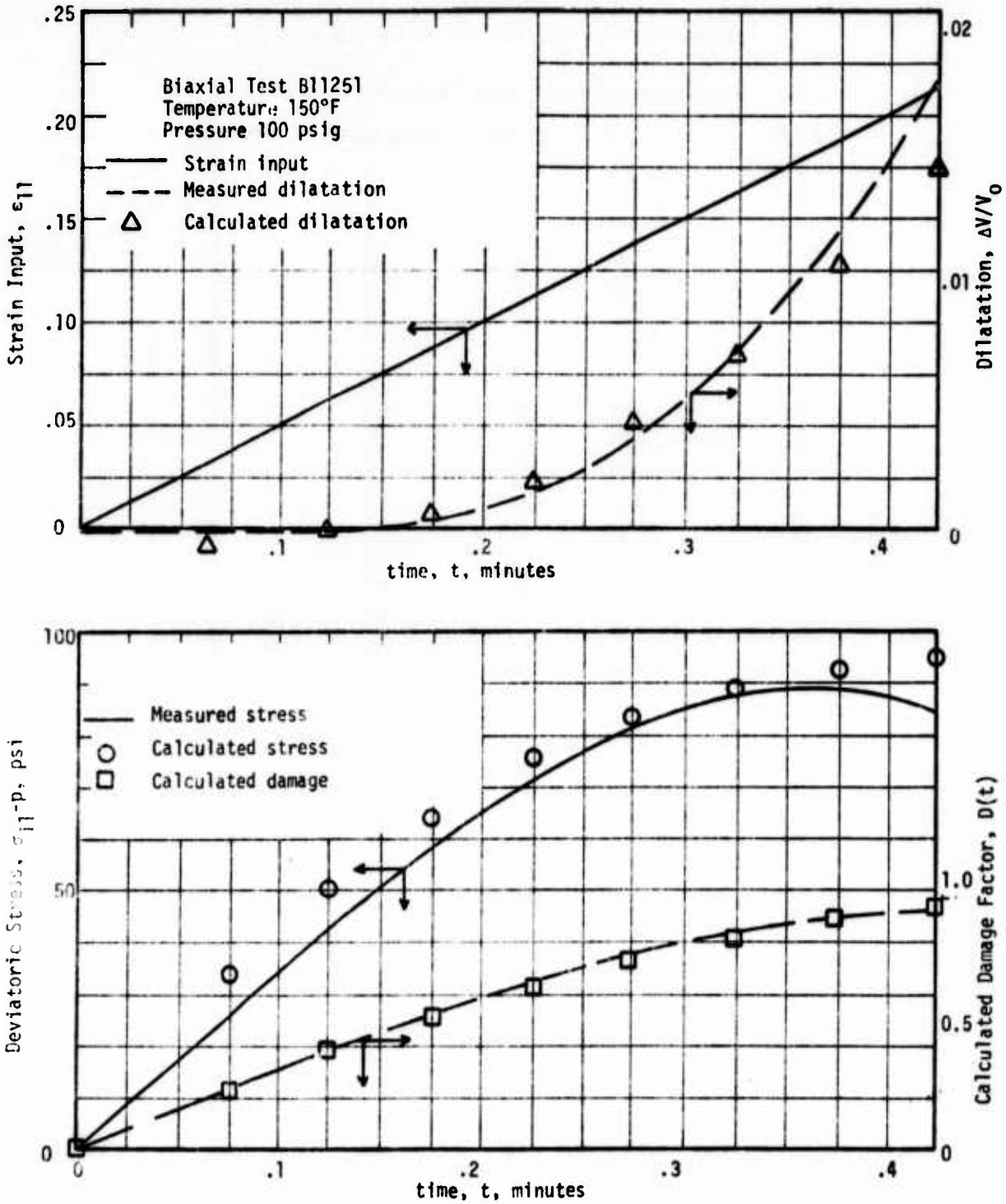

FIGURE 16. COMPARISON OF CALCULATED AND MEASURED RESPONSE OF THE TPH-1135 PROPELLANT

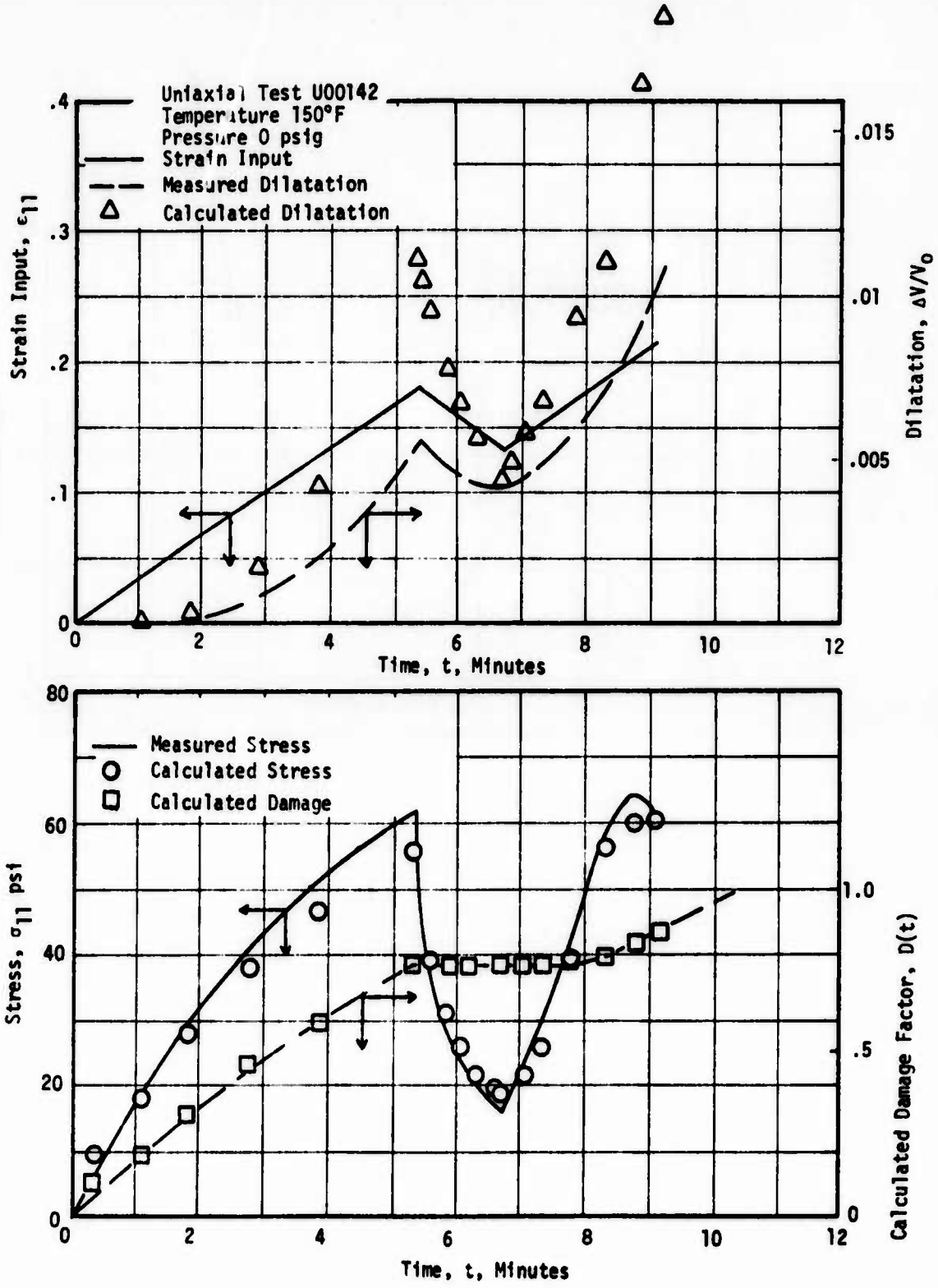

FIGURE 17. COMPARISON OF CALCULATED AND MEASURED RESPONSE OF THE TPH-1135 PROPELLANT

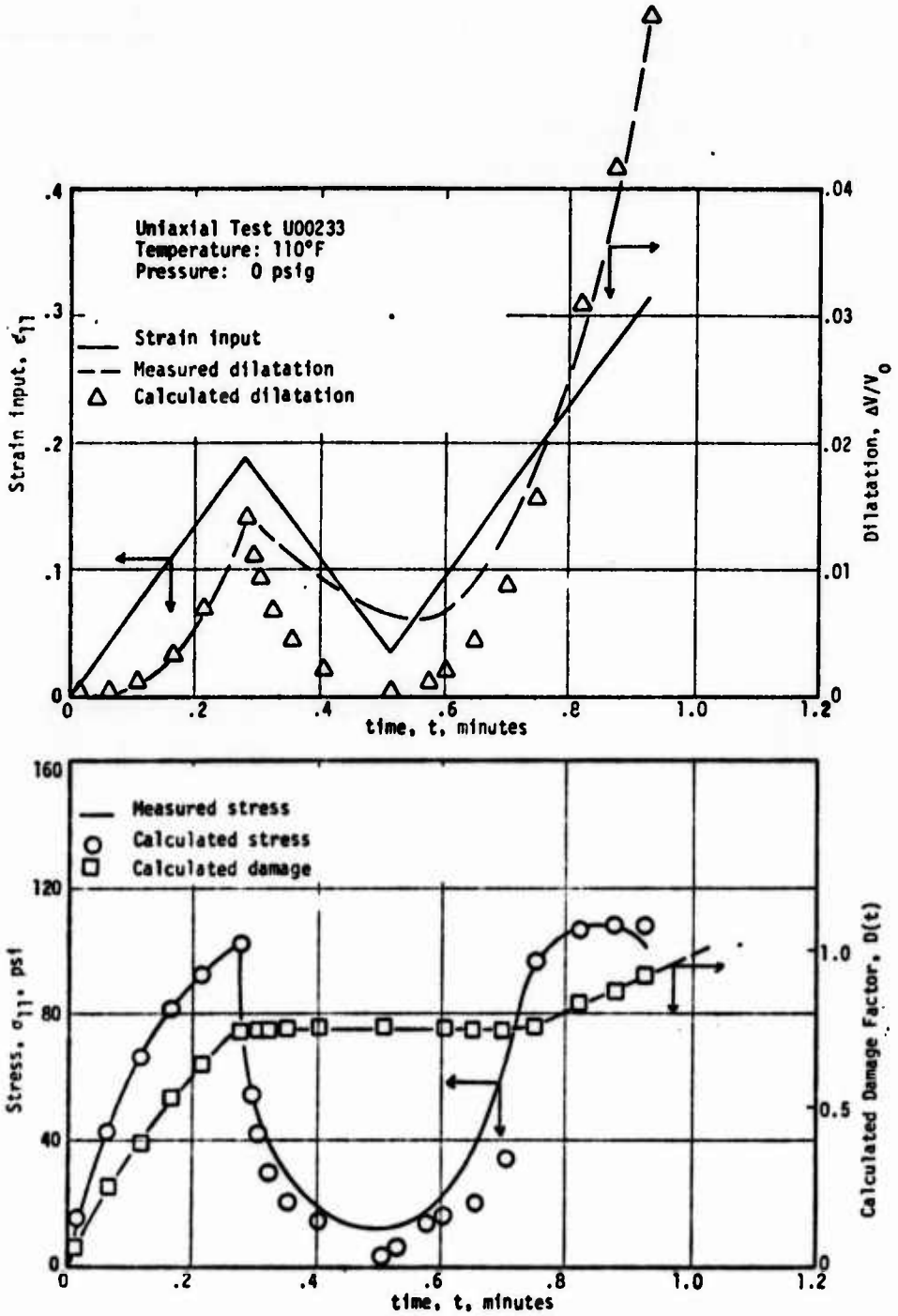

FIGURE 18. COMPARISON OF CALCULATED AND MEASURED RESPONSE OF THE TPH-1135 PROPELLANT

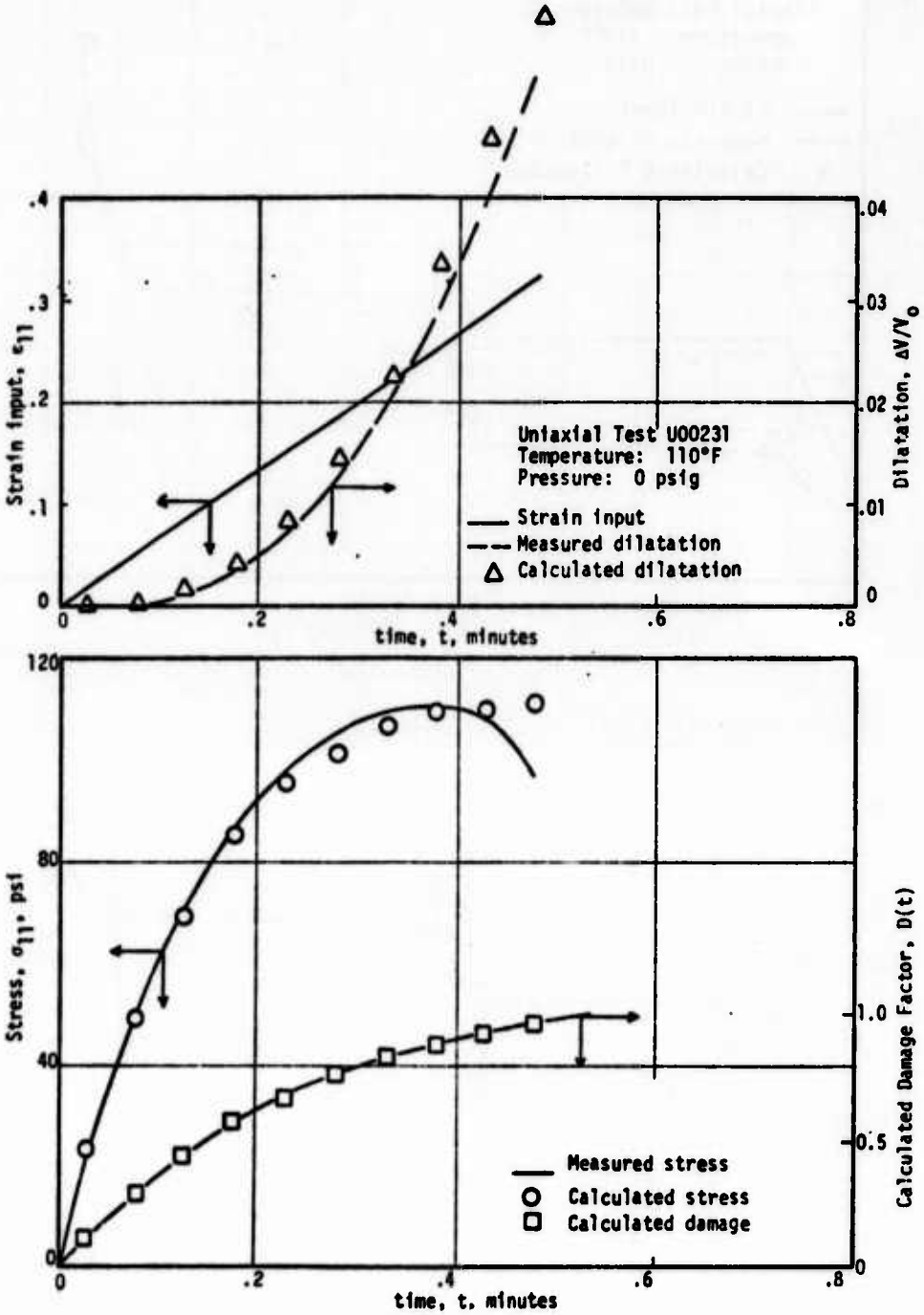

FIGURE 19. COMPARISON OF THE CALCULATED AND MEASURED RESPONSE OF THE TPH-1135 PROPELLANT

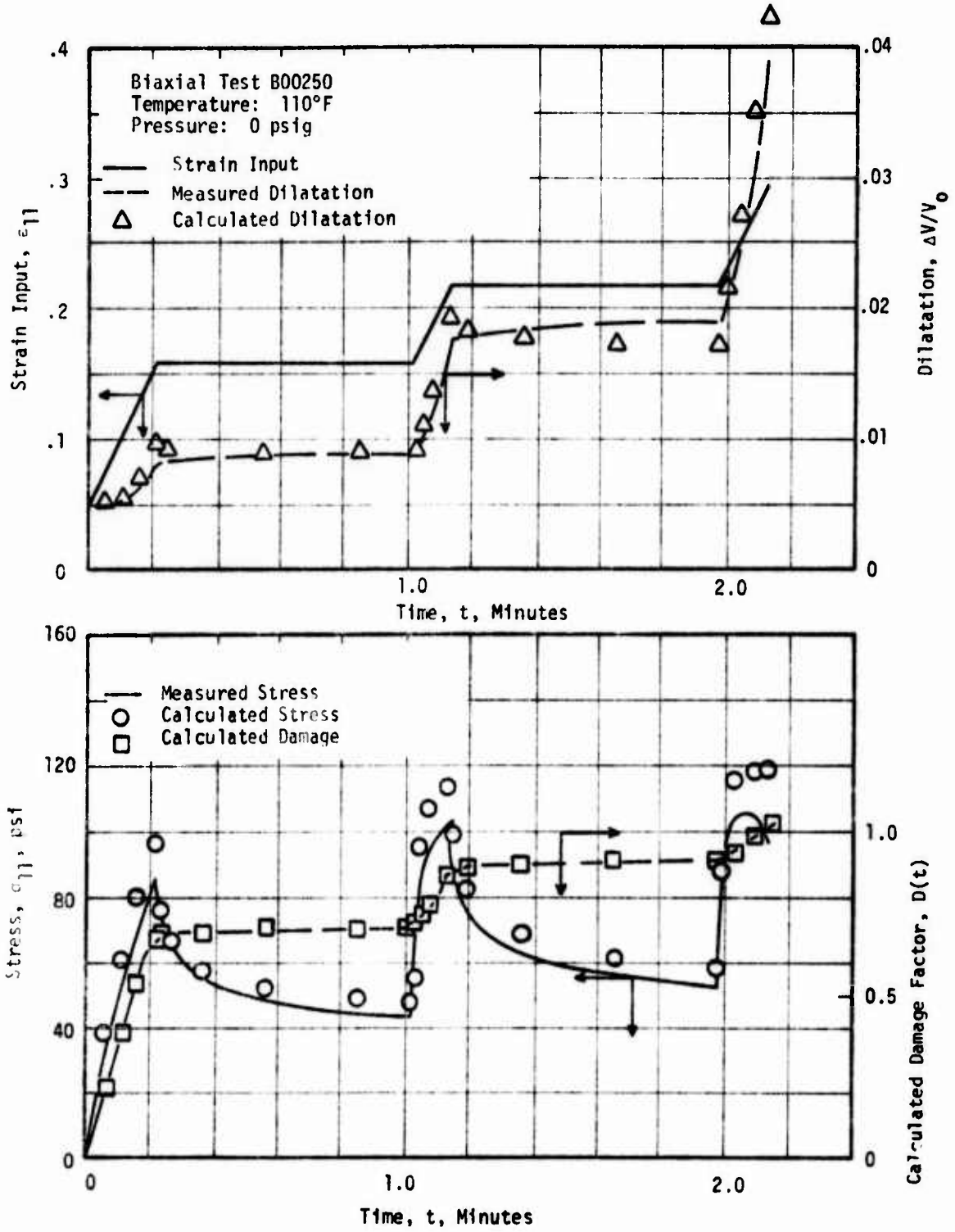

FIGURE 20. COMPARISON OF THE CALCULATED AND MEASURED RESPONSE OF THE TPH-1135 PROPELLANT

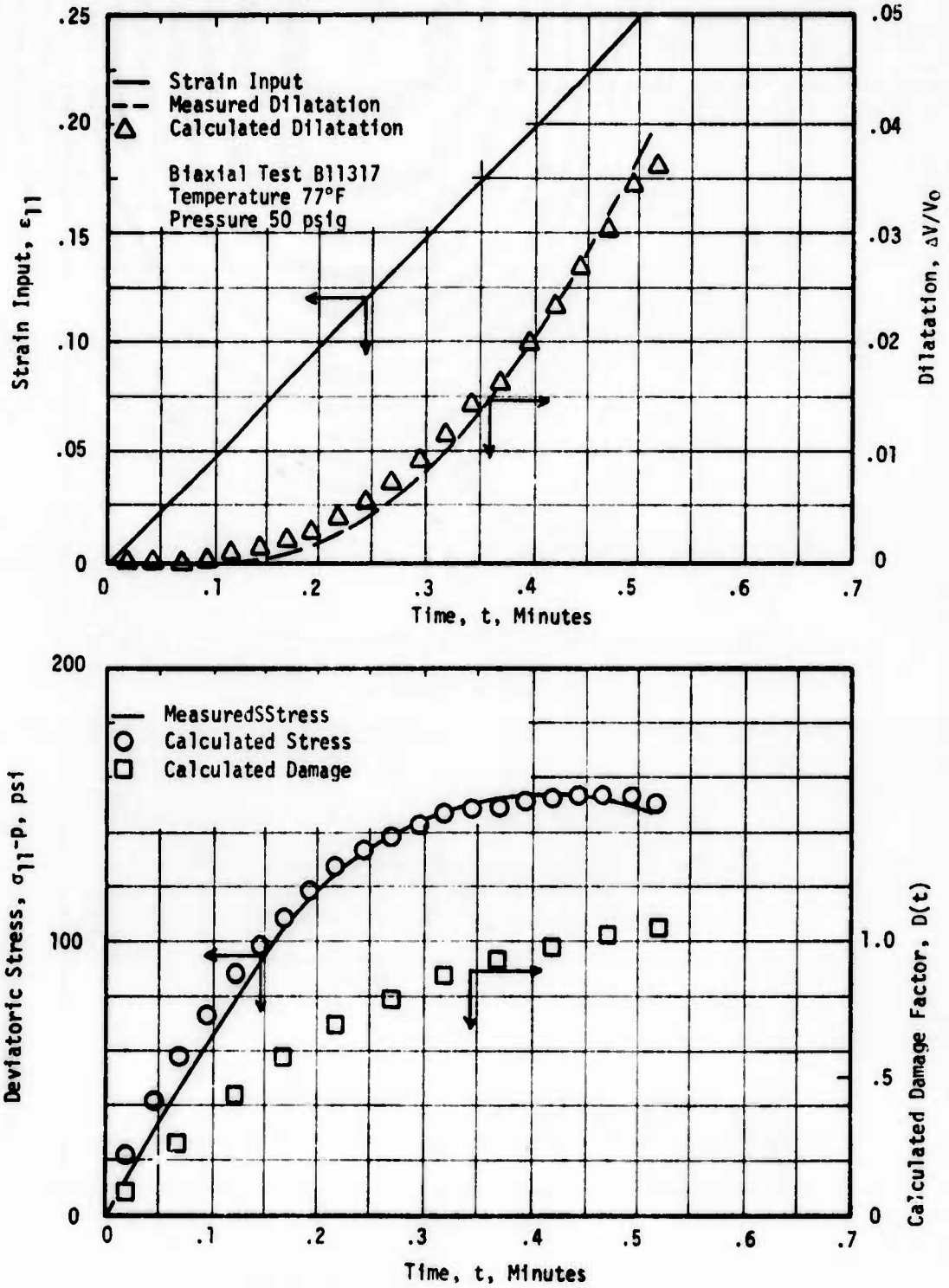

FIGURE 21. COMPARISON OF CALCULATED AND MEASURED RESPONSE OF THE TPH-1135 PROPELLANT

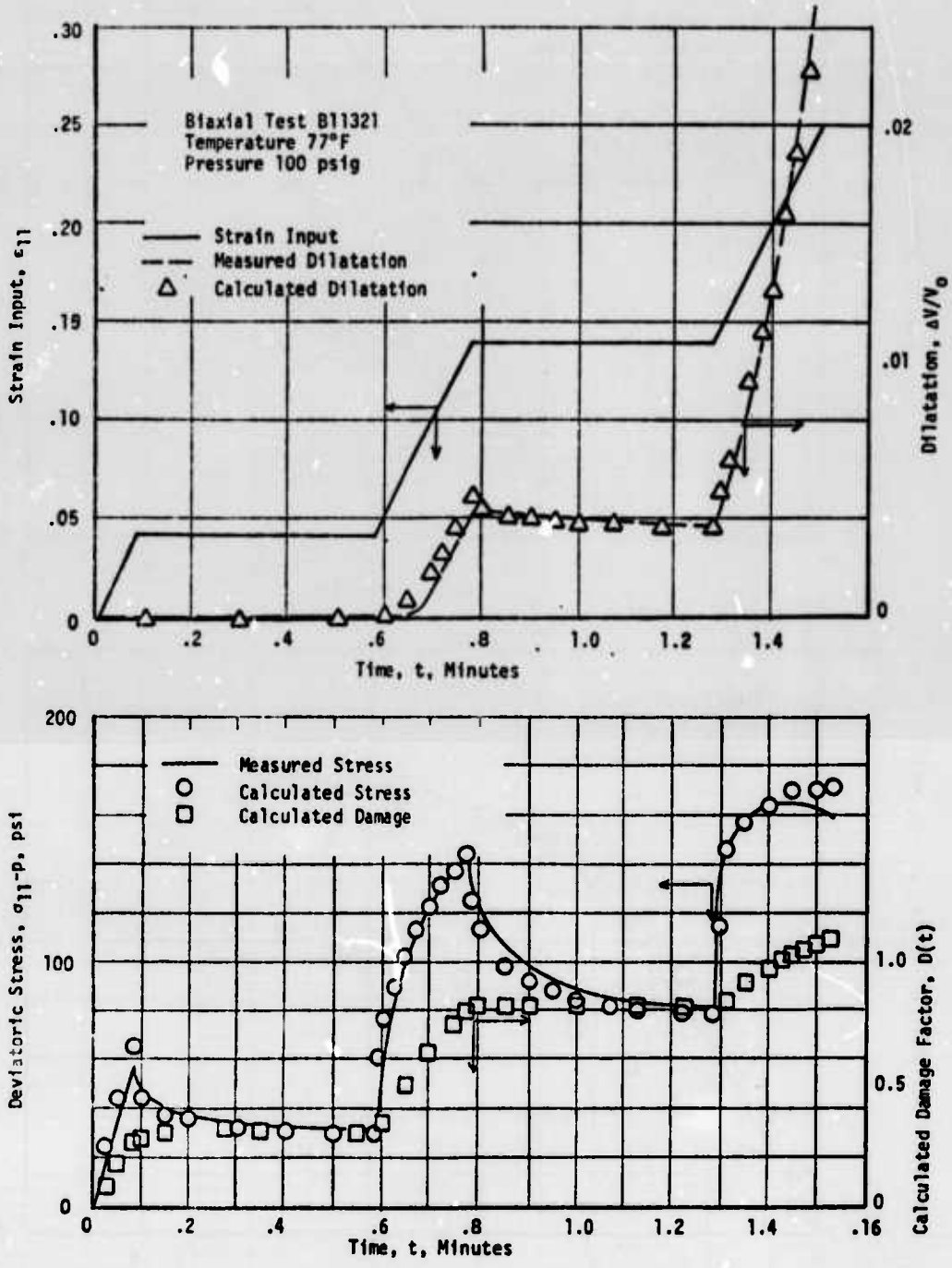

FIGURE 22. COMPARISON OF CALCULATED AND MEASURED RESPONSE OF THE TPH-1135 PROPELLANT

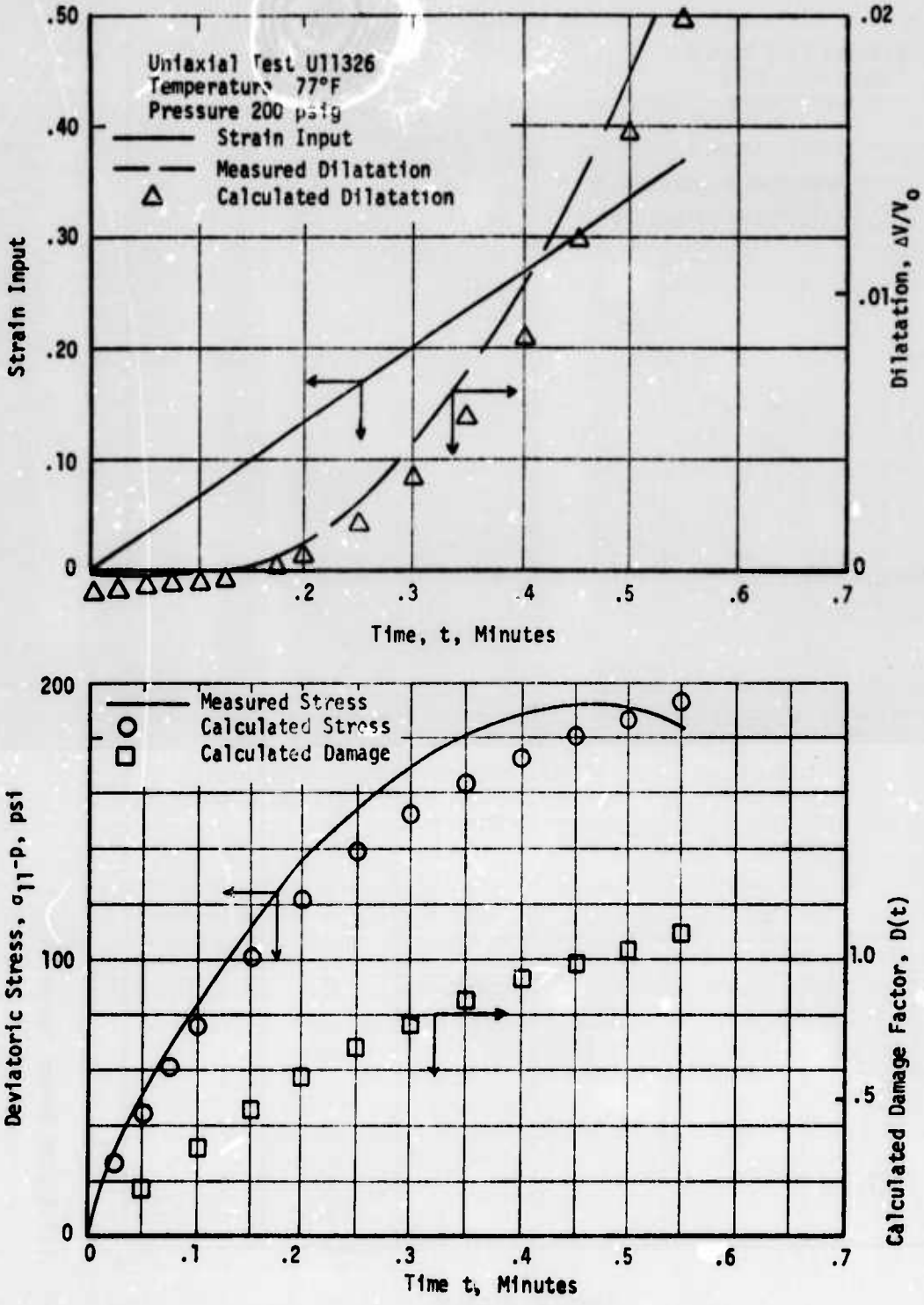

FIGURE 23. COMPARISON OF CALCULATED AND MEASURED RESPONSE OF THE TPH-1135 PROPELLANT

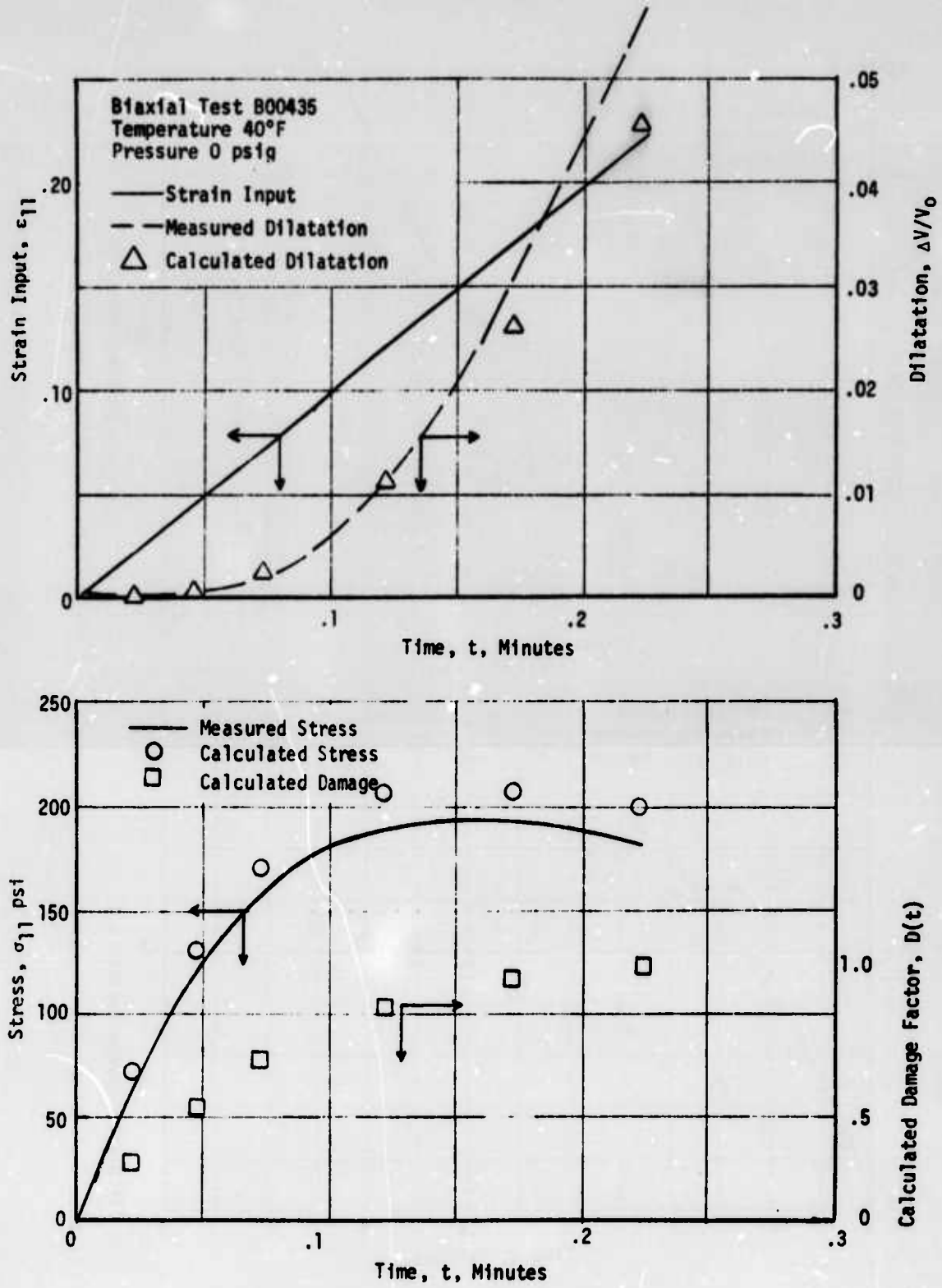

FIGURE 24. COMPARISON OF CALCULATED AND MEASURED RESPONSE OF THE TPH-1135 PROPELLANT

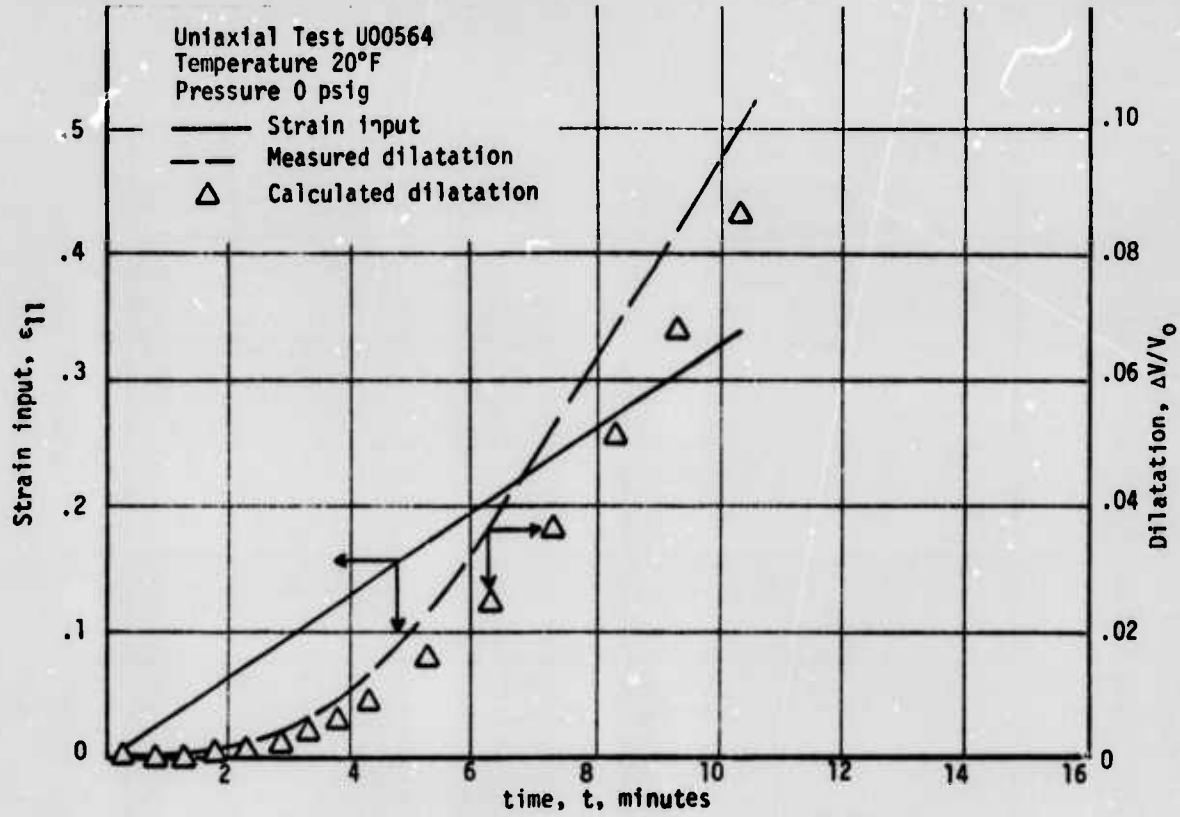

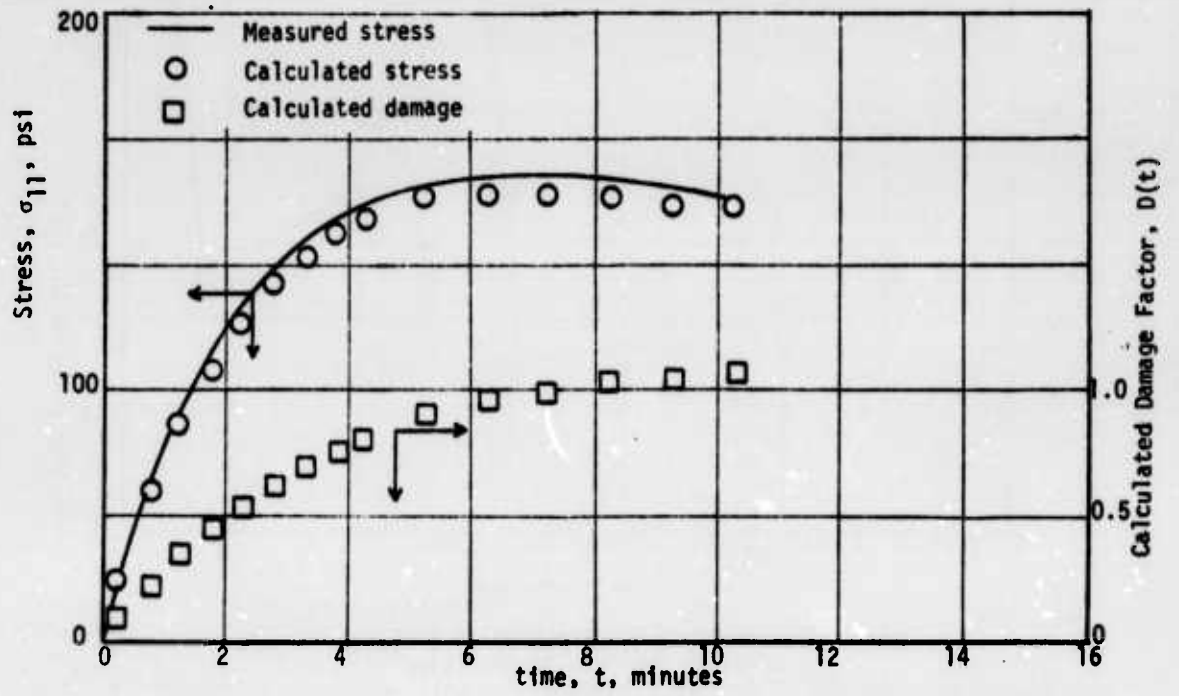

FIGURE 25. COMPARISON OF CALCULATED AND MEASURED RESPONSE OF THE TPH-1135 PROPELLANT

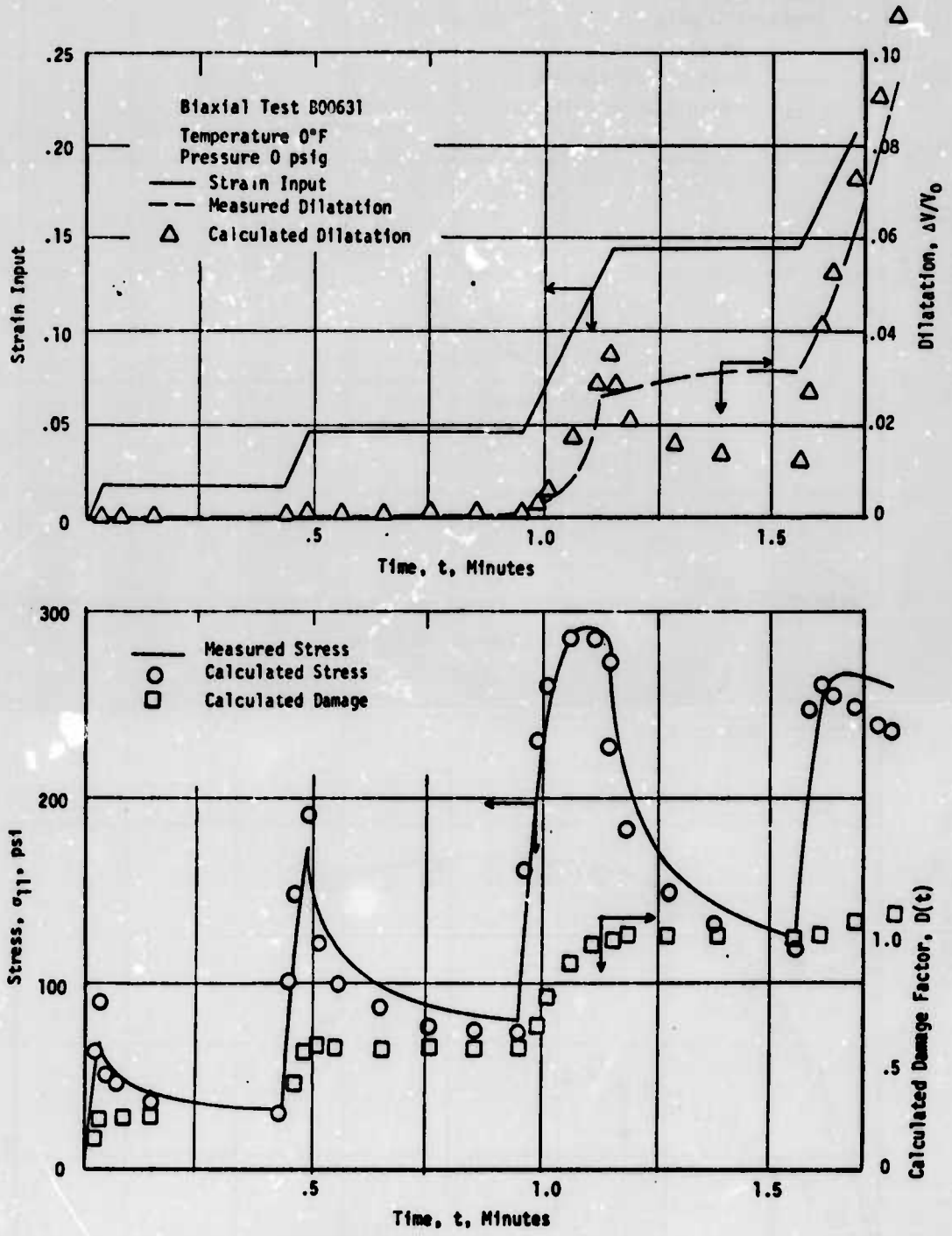

FIGURE 26. COMPARISON OF CALCULATED AND MEASURED RESPONSE FOR THE TPH-1135 PROPELLANT

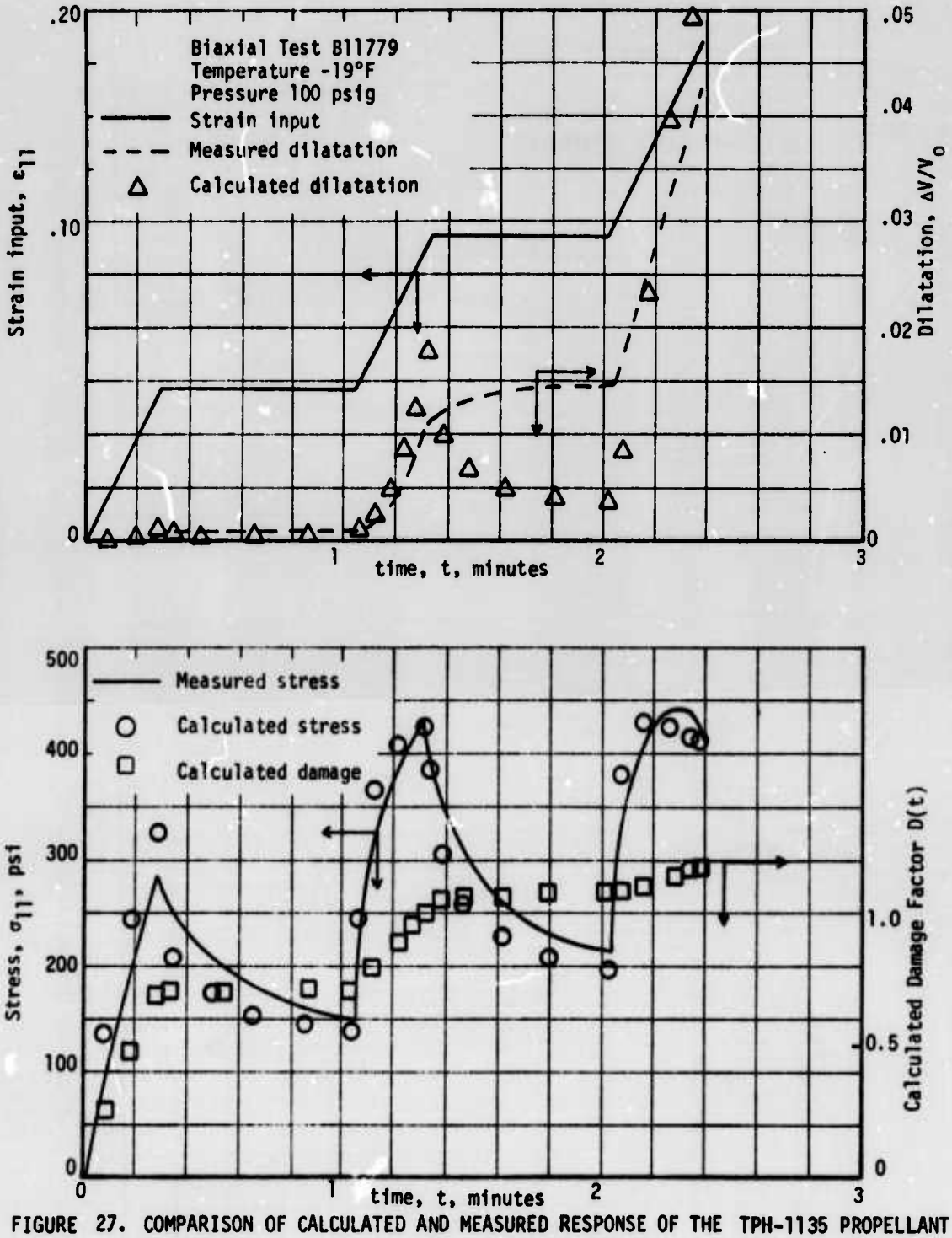

FIGURE 27. COMPARISON OF CALCULATED AND MEASURED RESPONSE OF THE TPH-1135 PROPELLANT

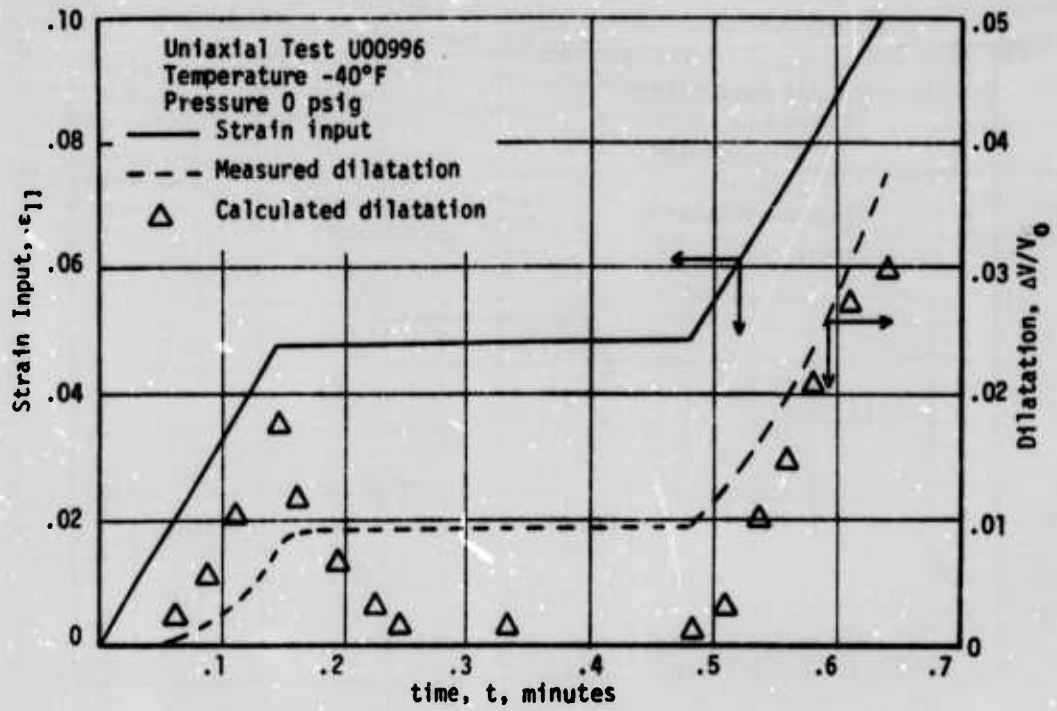

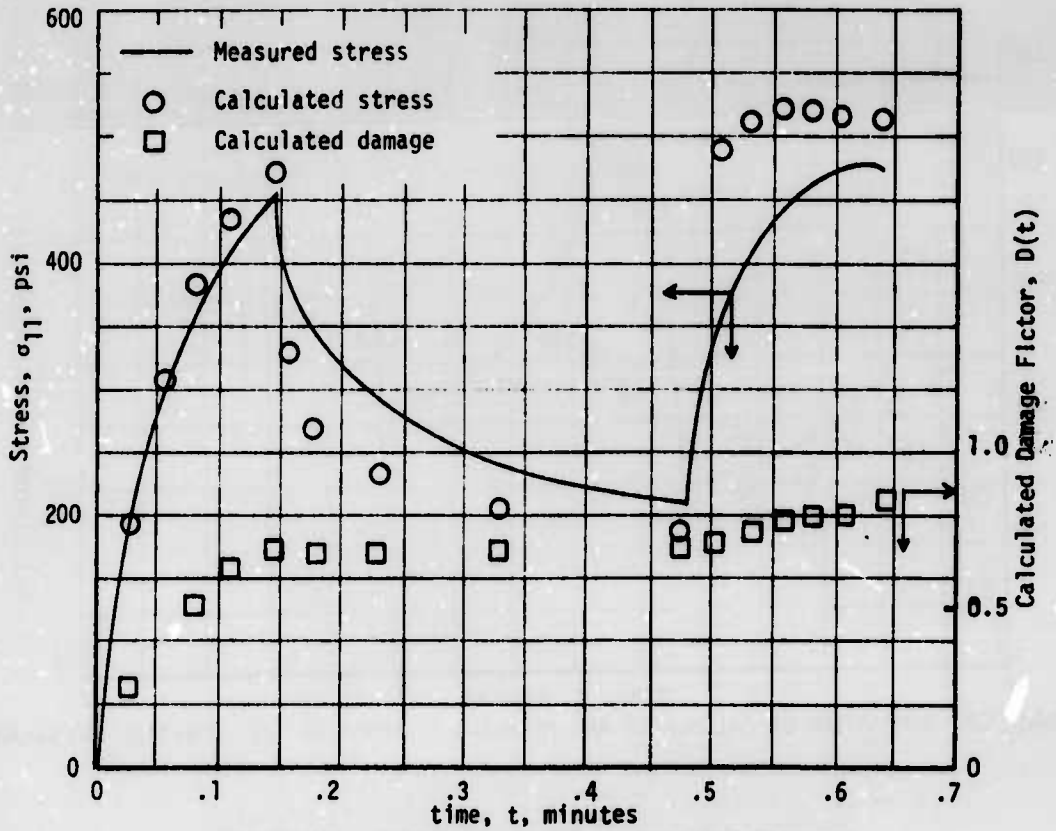

FIGURE 28. COMPARISON OF CALCULATED AND MEASURED RESPONSE FOR THE TPH-1135 PROPELLANT

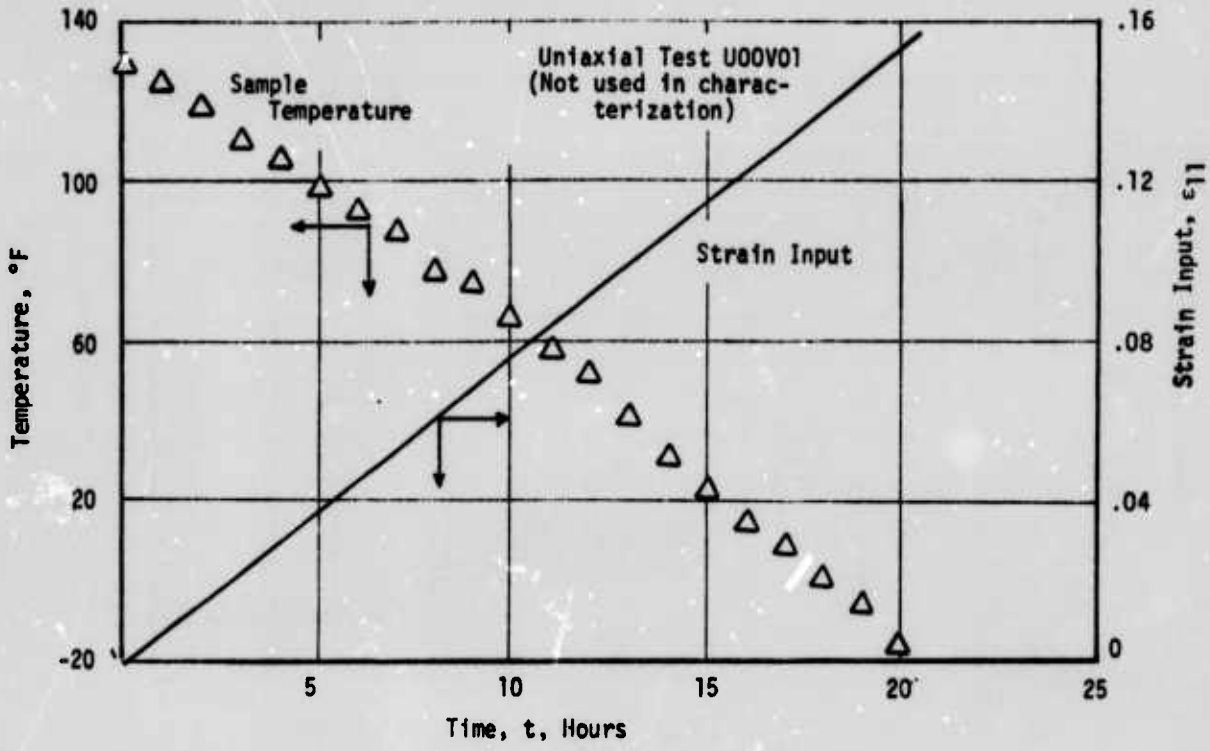

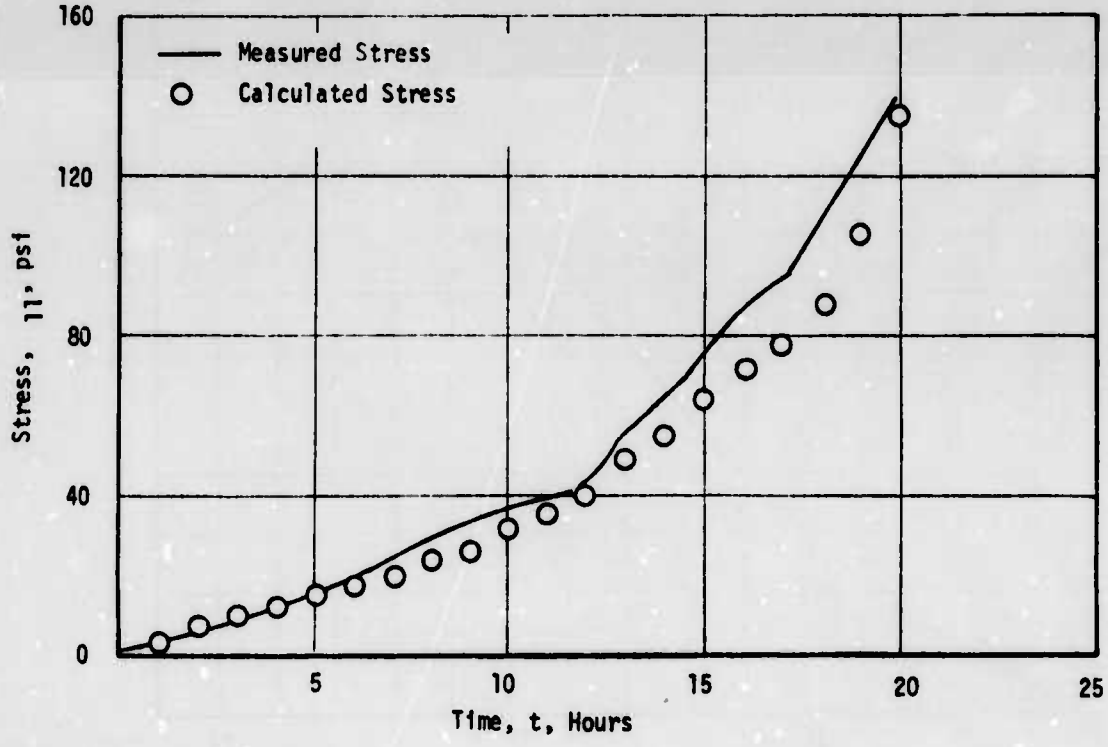

FIGURE 29. COMPARISON OF CALCULATED AND MEASURED RESPONSE FOR THE TPH-1135 PROPELLANT

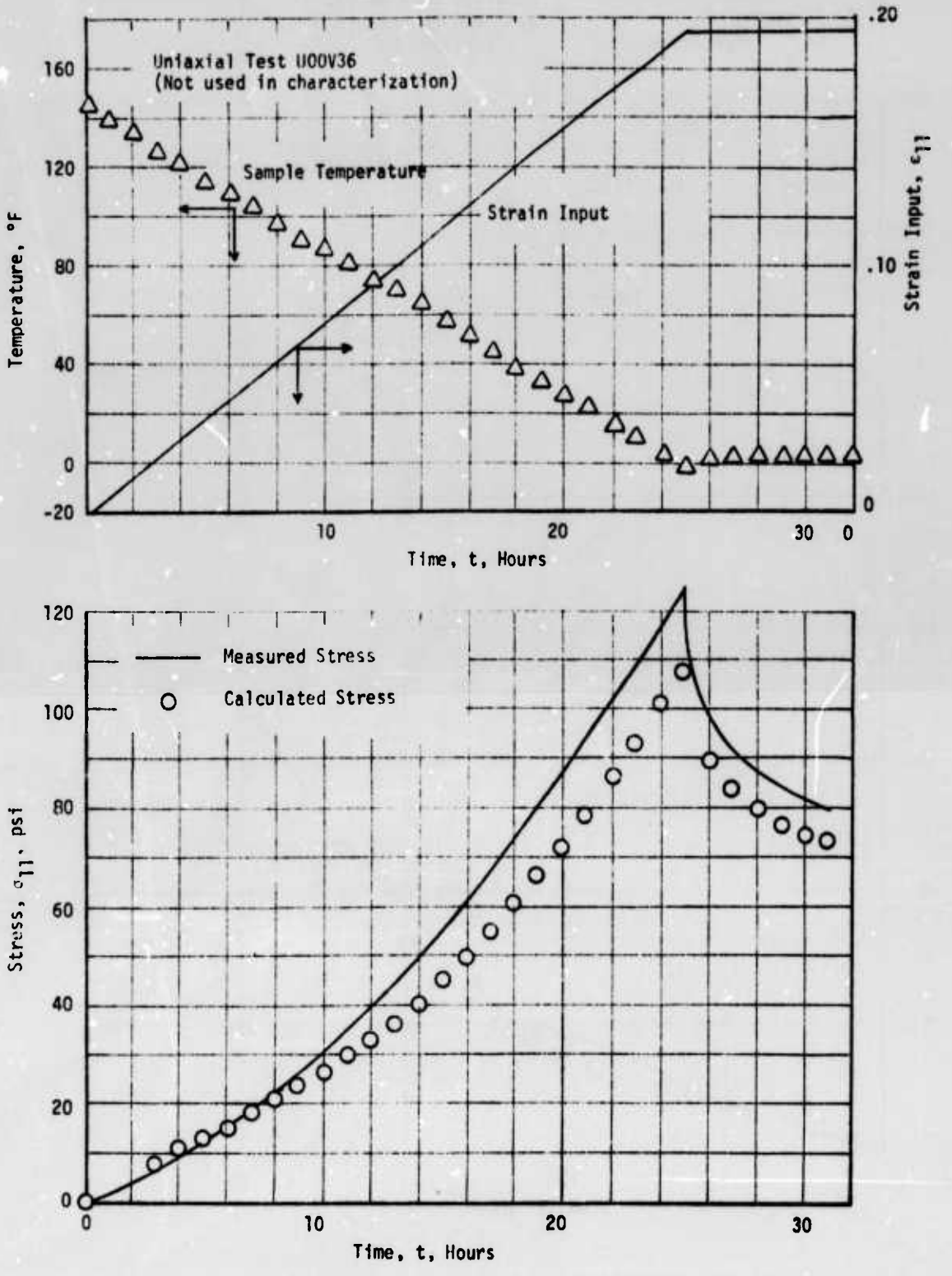

FIGURE 30. COMPARISON OF CALCULATED AND MEASURED RESPONSE OF THE TPH-1135 PROPELLANT

b. Dilatational Characterization

The dilatational characterization of TPH-1135 was performed at the same time as the distortional characterization. As mentioned earlier the dilatation measurements have considerable experimental variability when they are compared on a percentage error basis because volume change is an increasing function which changes from near zero values to very large values. In order to retain realistic compressibility predictions it was found necessary to fix the coefficient B_6 at 0.133×10^{-5} which represents a bulk modulus of 600,000 psi for pure hydrostatic compression. In addition the coefficient B_3 has never changed significantly from 3.0 in dilatational characterization and so was fixed at 3.0. This feature of being able to hold one or more parameters constant in the characterization demonstrates the flexibility of the codes. In addition, dilatation values less than 0.005 were ignored in the characterization process since for values less than this the errors of experimentation can be quite large. Another feature which can be used to advantage on dilatational characterizations is the ability to change the error measure from a relative to an absolute measure, giving more weight to the large values. This feature was also used on this run to demonstrate the method.

In the actual run, the initial value of the absolute error was 0.32095 and was reduced on following iterations to 0.2838, 0.12214, 0.07278, 0.04942, 0.04817, 0.04766. The actual fit of the dilatational constitutive equation to the laboratory data is shown in Figures 16 through 30 along with the stress-strain data. The quality of these response predictions must be considered poor in comparison to the distortional predictions since they yield a standard deviation of 36.9%. This standard deviation could have been further reduced by using a relative error measure, however, that would have given more weight to the smaller values of dilatation which are measured with a much poorer precision than the larger values. Ignoring dilatational values less than 0.005 essentially removes half of the data from the dilatational analysis.

c. Failure Characterization

The failure characterization of TPH-1135 used the same experiments for input as the distortional and dilatational characterizations. Of the 54 experiments, five were labeled as poor failures in the laboratory effort, hence the 54 experiments provided 49 data points for a failure analysis. Coefficients B_6 and B_7 in the failure run were held at unity as discussed in Section 4.H.2.a. The error measure associated with the damage calculations went from 49 to 1.60, 1.085, 0.8196, and 0.8155 in subsequent iterations. The standard deviation on predicted damage at failure was 12.08%. This value compares well with other data on cumulative damage calculations. Comparisons of damage level vs deformation are provided in Figures 16 through 30. In addition, pertinent information on the characterizations are provided in Table 5.

d. Discussion of Results

There is little to be said about the quality of the distortional characterization. The predictions of distortional stresses are considered excellent since the standard deviation of only 12.9% approaches the estimated total precision of the experimentation and material variability.

The dilatational characterization is considered to be of poor quality, and although much can be said about the difficulty in obtaining good measurements, it would appear that much of the problem lies in deficiencies in the mathematical representations. It appears that the mathematical constitutive descriptions cannot properly describe all of the data in a single representation. This problem was discussed in detail in a previous final report (1) and the problem was greatly reduced

by going to an inverse representation wherein the dilatation is computed as the variable rather than the mean pressure. Although the consequences of errors are less now it would appear that the basic problem remains. Briefly stated, propellants dilate positively under net hydrostatic pressures due to distortion. This type of nonlinear coupling appears to be very complex and more work must be done to improve upon the representations used in this phase of the characterization. Once new representations are developed they can be included in the characterization code by simply changing two subroutines. The current characterizations appear to have all the proper trends and order of magnitude of the dilatation effect, but they do need some fine tuning beyond the current mathematics. To date however, it still is probably the best that can be offered and can do a quite adequate job over a narrower range of conditions.

The failure characterization is again quite good and examination of the data indicates that the damage computed for the -40°F tests is only 0.71 at failure. It appears that the mathematical methods used to describe the damage for this propellant cannot cover the entire temperature range, although it works well to -20°F. Eliminating the -40°F data would reduce the standard deviation for the remaining data by more than 50%, since roughly 80% of the total error measure results from the -40°F tests.

3. Hercules Propellant (VMO)

The characterization of the Hercules VMO, an XLDB propellant, was limited in temperature from -10°F to +110°F on the recommendation of the Hercules Company. Like the other propellants it was tested using uniaxial and biaxial strip specimens at pressures to 1000 psi. Unlike the other two propellants, the uniaxial specimens were truncated JANNAF samples which appear to have caused some additional difficulties as discussed later in this section. The overall response of this propellant appears to fall between that of the Aerojet propellant and the Thiokol propellant. It

dilates more than the Aerojet material but considerably less than the Thiokol propellant. Mathematically it appears to obey the same constitutive equation as the rubber base propellants and the quality of the characterization is essentially the same. The biggest difference appears to be the materials modulus sensitivity to temperature. As expected the modulus increases more rapidly at lower temperatures than does that of the conventional rubber base propellant, which would have a much lower glass transition temperature. This however is not a fair comparison since this propellant was never intended for use at extremely low temperatures and in the higher temperature regions its behavior is undestinguishable from rubber base propellants. Other small differences in the response can probably be attributed to a lower volumetric filler content, since a propellant of this type does not require the high solids loadings to get a high specific impulse because it derives much of its energy from the liquid plasticizers. The discussion below presents a brief synopsis of the characterization of the Hercules propellant and a discussion of the results.

a. Distortional Characterization

The distortional characterization of the Hercules propellant was carried out using 933 data points from 46 experiments covering the full range of experimental conditions. This characterization had a standard deviation of 16.9% which is about 25% higher than those of the other characterizations made to date. Careful analysis of the data indicates statistical discrepancies between the uniaxial and biaxial predictions. When only uniaxial or only biaxial data were characterized the standard deviation was about 6% lower indicating difficulties in predicting the change in strain state.

It is interesting to note that this was the only propellant tested wherein a truncated JANNAF specimen was used for the uniaxial specimen. An average gage length was used in the measurements however; it is known to vary strongly during the course of a test (10). A small change or error in the gage length of this sample during an experiment would cause an error in the input deformation history and could easily cause the increase in the standard deviation between the predicted and observed responses. The truncated JANNAF samples also make it difficult to accurately measure the relative dilatation since the samples total volume change is measured and there surely must be a gradient of the dilatation within such a sample.

In an attempt to demonstrate an improved characterization for a specific analysis, such as thermal cycling, the Hercules propellant was also characterized using just the atmospheric pressure data. In this run the standard deviation was reduced to 11.2% with only a minor change in the parameters in the constitutive equation. This specialized characterization was conducted using 30 experiments with 610 data points from the same set of 54 experiments. The data from this improved and specialized characterization are presented in Figures 31 through 42 for typical tests. Table 6 gives detailed information regarding the characterization of the Hercules propellant.

b. Dilatational Characterization

The dilatational characterization of the Hercules propellant was performed using the relative error measure. As discussed in Section 4.H.2.b the constant B_6 was held fixed to insure proper volumetric compliance at small strains. The standard deviation for this characterization was 25.4%, about double that for the distortional characterization. When all the pressure data was included the standard deviation was again up to 36% indicating the pressure dependence of dilatation is probably not being handled correctly by the mathematics in the dilatational constitutive equation. These data are presented in Figures 31 through 42.

TABLE 6

NONLINEAR THERMOVISCOELASTIC CHARACTERIZATION OF THE VMO PROPELLANT

A. DISTORTIONAL CHARACTERIZATION

Input Parameters

No. of Tests = 30
No. of Data Points - 610
Max. No. of Iterations = 8
Max. No. of Interval Halvings = 10
Numerical Derivative Increment = .1000-01
Print Parameter(s) = 0
Strains Greater than .1000 + 01 were ignored.
No. of Shift Function Coefficients = 3
Total Number of Shear Coefficients = 12

The Initial Coefficients		Regression Coefficients	
K	B(K)	I	B(I)
1	-.131480 + 00	1	-.13182 + 00
2	-.736000 - 01	2	-.73511 - 01
3	-.668100 - 01	3	-.67013 - 01
4	.400000 + 02	4	.40000 + 02
5	-.323270 - 01	5	-.32327 - 01
6	-.442120 + 01	6	-.44161 + 01
7	0.727330 - 00	7	.73331 + 00
8	.554460 + 01	8	.56227 + 01
9	.547600 + 01	9	.54723 + 01
10	.000000	10	.10051 + 03
11	.000000	11	.14547 + 03
12	.000000	12	-.23308 + 01

The following coefficients were held constant:

There were 580 experimental test points.

The average deviation = -1.065 percent, and
the standard deviation = 11.258 percent.

Calculated Shift Function, A_T	Temperature - °F
.1125 + 09	-80
.8055 + 07	-60
.5769 + 06	-40
.4132 + 05	-20
.2959 + 04	0
.2119 + 03	20
.1518 + 02	40
.3489 + 01	60
.8179 + 00	80
.2141 + 00	100
.5605 - 01	120
.1467 - 01	140
.3841 - 02	160
.1005 - 02	180
.2632 - 03	200

Pivot Temperatures Used: 40, 77, and 120.

TABLE 6 (CONTINUED)

B. DILATATIONAL CHARACTERIZATION

No. of Tests = 30

No. of Data Points = 610

Maximum number of Iterations = 10

Maximum number of Interval Halvings = 10

Numerical Derivative Increment = .1000-01

Print Parameter(s) = 0

Dilatations less than .5000-02 were ignored.

The Initial Coefficients		Final Regression Coefficients	
K	B(K)	I	B(I)
1	-.989350 - 01	1	.92033 - 02
2	.947250 - 02	2	.49184 - 02
3	.155560 + 01	3	.16977 + 01
4	-.199880 - 01	4	-.53702 - 02
5	-.611000 - 03	5	-.51252 - 03
6	.125000 - 05	6	.12500 - 05
7	.243190 + 00	7	.15658 + 00

The following 1 Coefficients were Held Constant: B(6)

The Average Deviation = -7.026 percent, and

The Standard Deviation = 25.435 percent

TABLE 6 (CONTINUED)

C. FAILURE ANALYSIS

The Initial Coefficients		Final Failure Coefficients	
K	B(K)	I	B(I)
1	.764300 - 04	1	.334482 - 03
2	.000000	2	.000000
3	.799500 - 04	3	.339822 - 03
4	.000000	4	.000000
5	.200847 + 02	5	.206912 + 02
6	.100000 + 01	6	.814669 + 00
7	.100000 + 01	7	.739861 + 00
8	-.162847 - 01	8	-.282510 - 01
9	.554122 - 01	9	.123466 + 00

The following 28 tests were used in the failure characterization:

1	2	3	4	5	6	0	8	9	10	11	12	13
14	15	0	17	18	19	20	21	22	23	24	25	26
27	28	29	30									

There were 28 failure data points

The Average Deviation = -4.086 Percent and

The Standard Deviation = 5.212 Percent

TABLE 6 (CONTINUED)

D. LIST OF EXPERIMENTS USED IN THE HERCULES CHARACTERIZATION

Test No.	Test ID	No. Pts.	KODE*	Initial Temp.
1	U00217	19	1	111
2	U00218	22	1	112
3	U00220	28	1	110
4	B00222	23	1	110
5	B00223	24	2	112
6	B00223	9	2	110
7	B00236	11	2	113
8	B00241	24	2	113
9	U00301	20	1	77
10	U00302	19	1	77
11	U00304	37	1	77
12	U00315	22	1	78
13	U00316	20	1	77
14	B00301	12	2	78
15	B00302	13	2	78
16	B00303	16	2	78
17	B00304	25	2	78
18	U00433	20	1	39
19	U00434	13	1	39
20	U00435	29	1	39
21	U00437	23	1	40
22	U00438	22	1	40
23	B00413	11	2	42
24	U00649	15	1	7
25	U00650	11	1	-6
26	U00651	30	1	-8
27	U00652	25	1	-2
28	U00653	22	1	-2
29	U00654	21	1	-2
30	B00628	24	2	2

* 1 = Uniaxial 2 = Biaxial

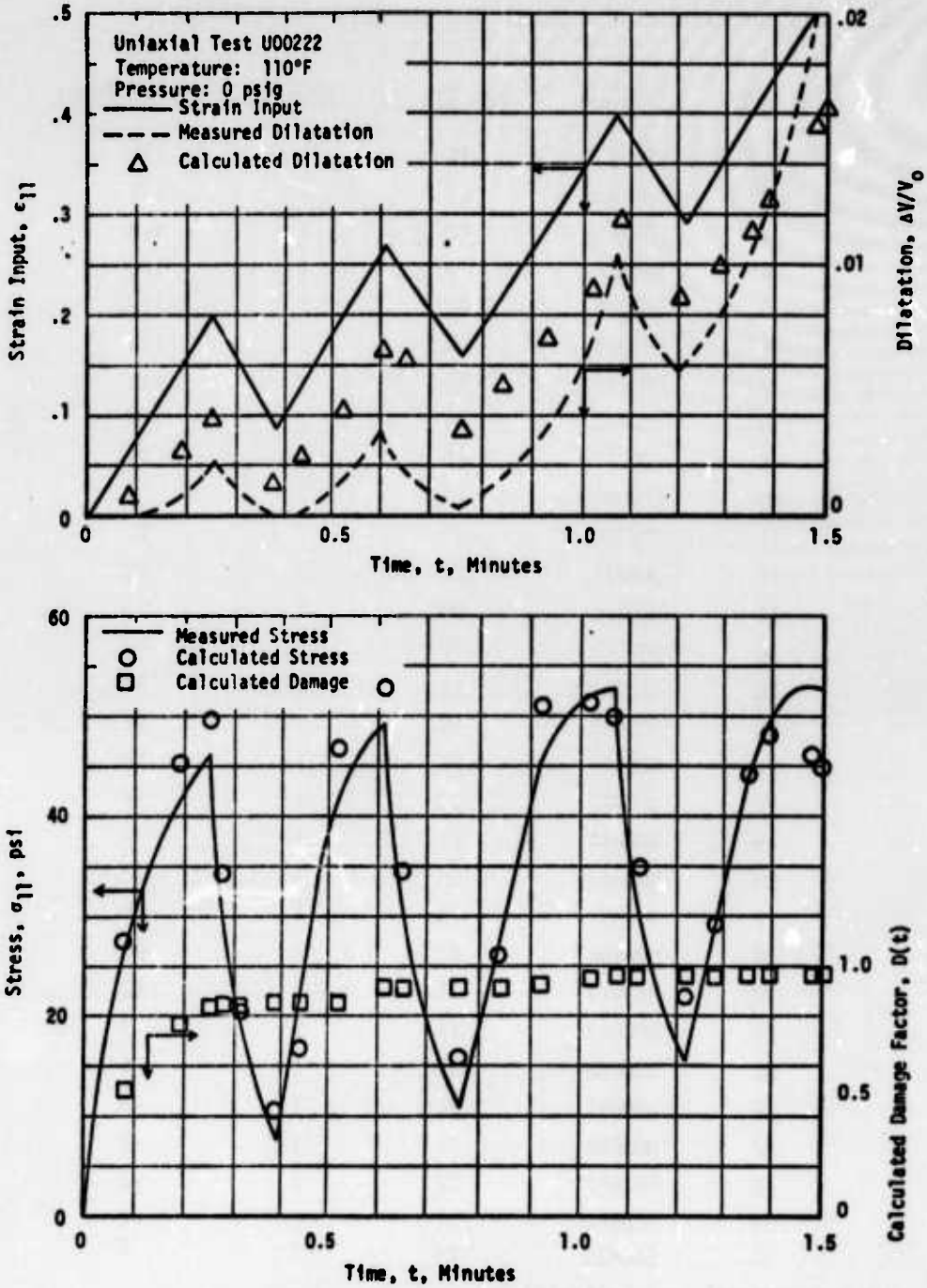

FIGURE 31. COMPARISON OF CALCULATED AND MEASURED RESPONSE OF THE VMO PROPELLANT

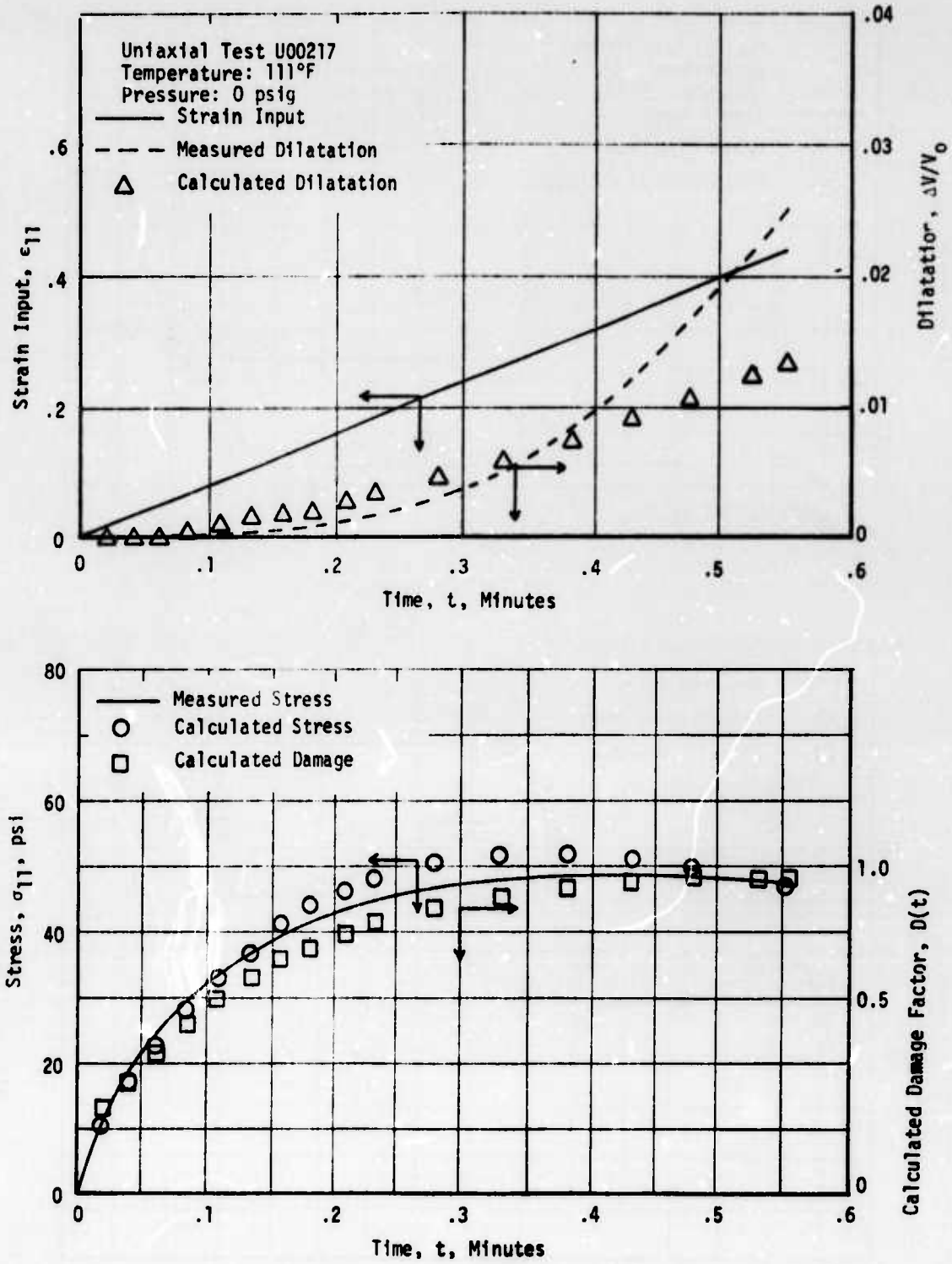

FIGURE 32. COMPARISON OF MEASURED AND CALCULATED RESPONSE OF THE VMO PROPELLANT

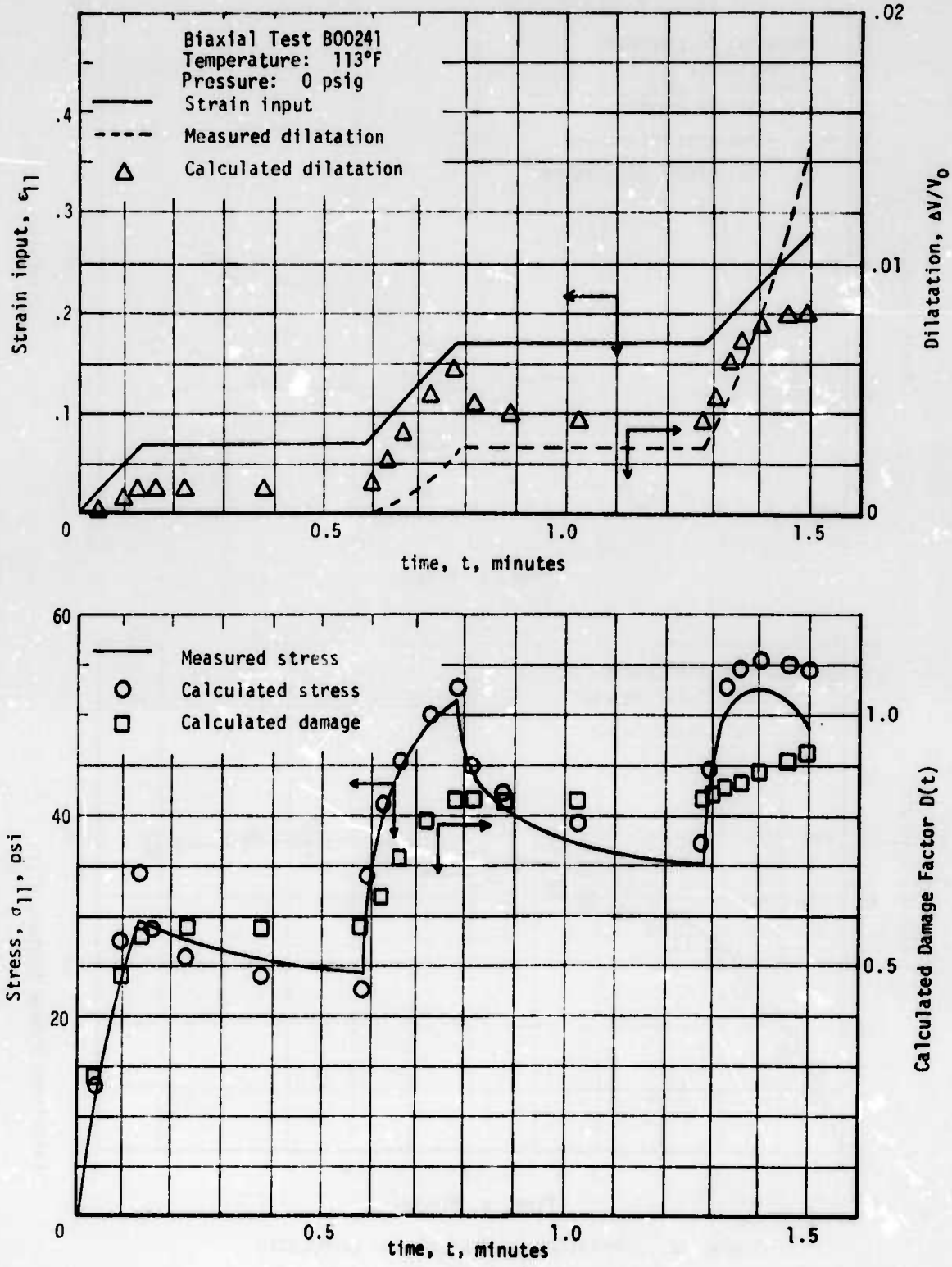

FIGURE 33. COMPARISON OF CALCULATED AND MEASURED RESPONSE OF THE VMO PROPELLANT

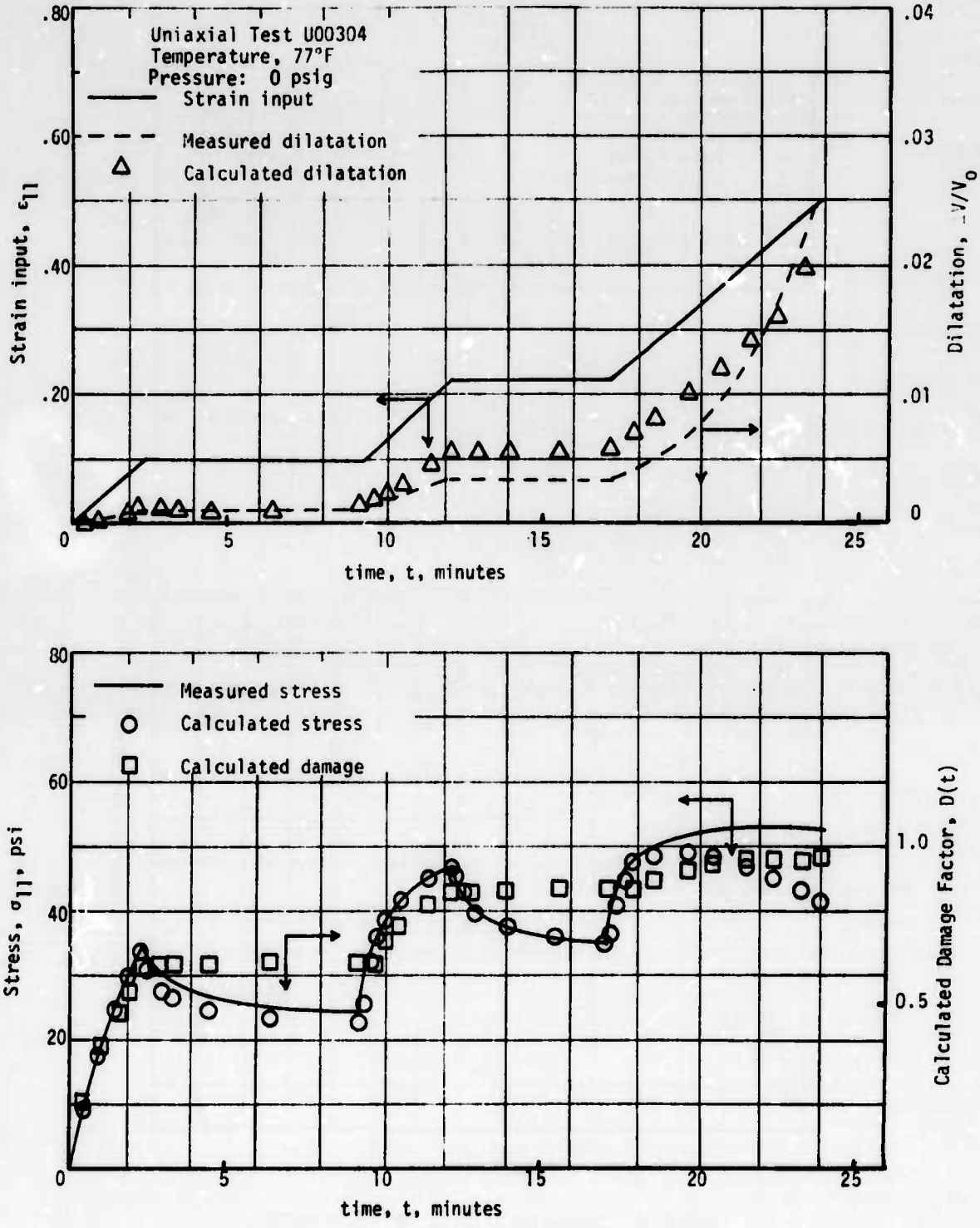

FIGURE 34. COMPARISON OF CALCULATED AND MEASURED RESPONSE OF THE VMO PROPELLANT

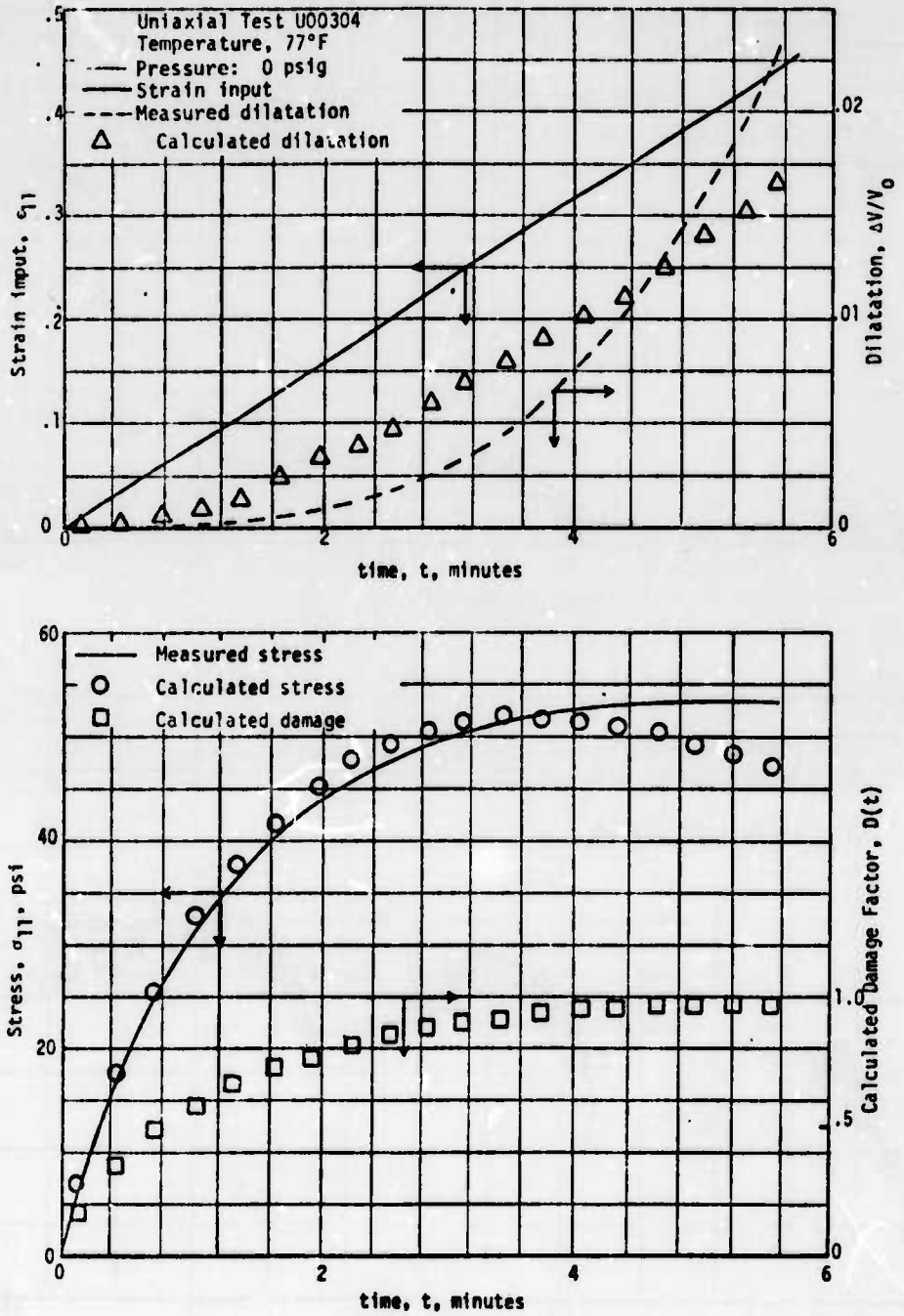

FIGURE 35. COMPARISON OF CALCULATED AND MEASURED RESPONSE OF THE VMO PROPELLANT

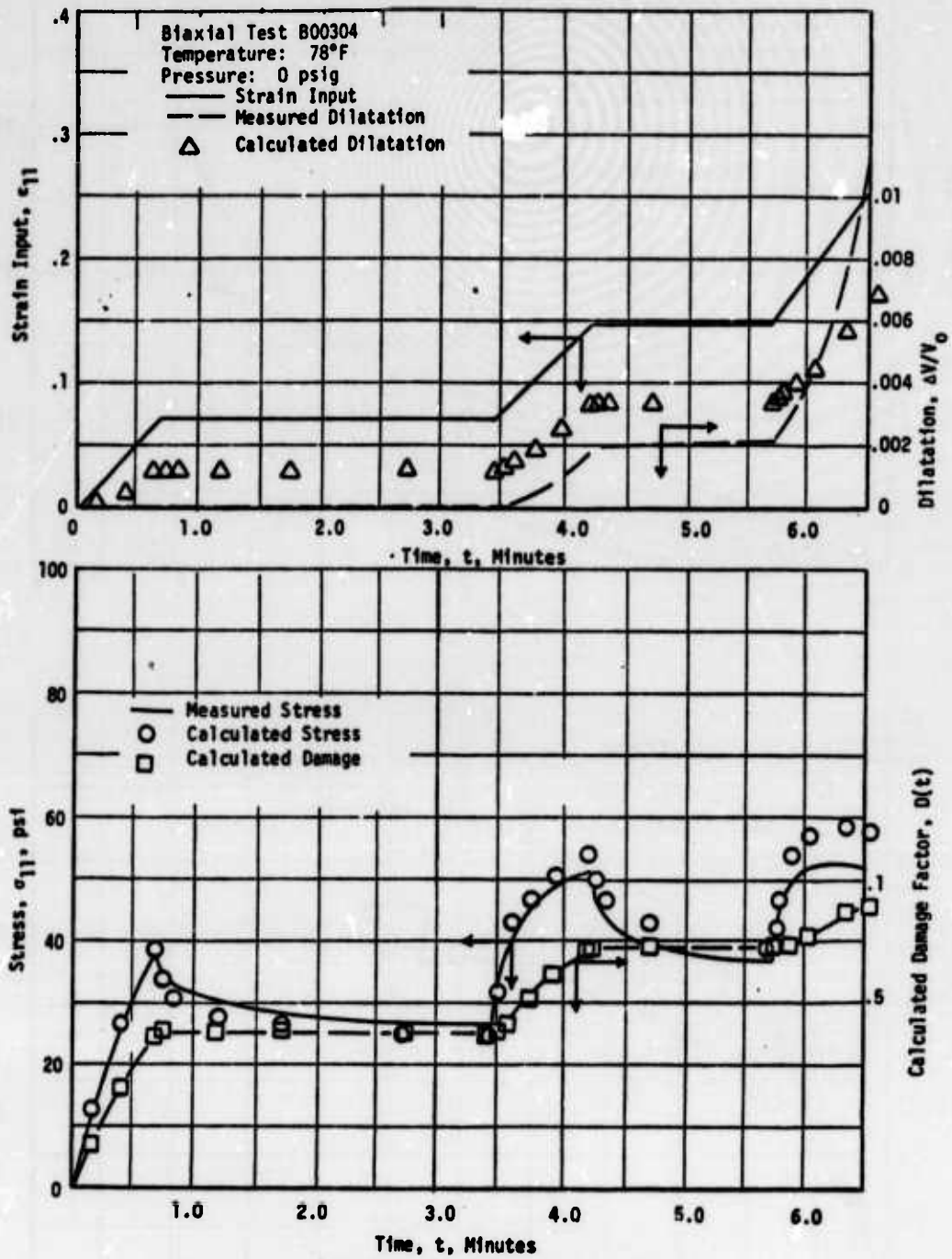

FIGURE 36. COMPARISON OF THE CALCULATED AND MEASURED RESPONSE OF THE VMO PROPELLANT

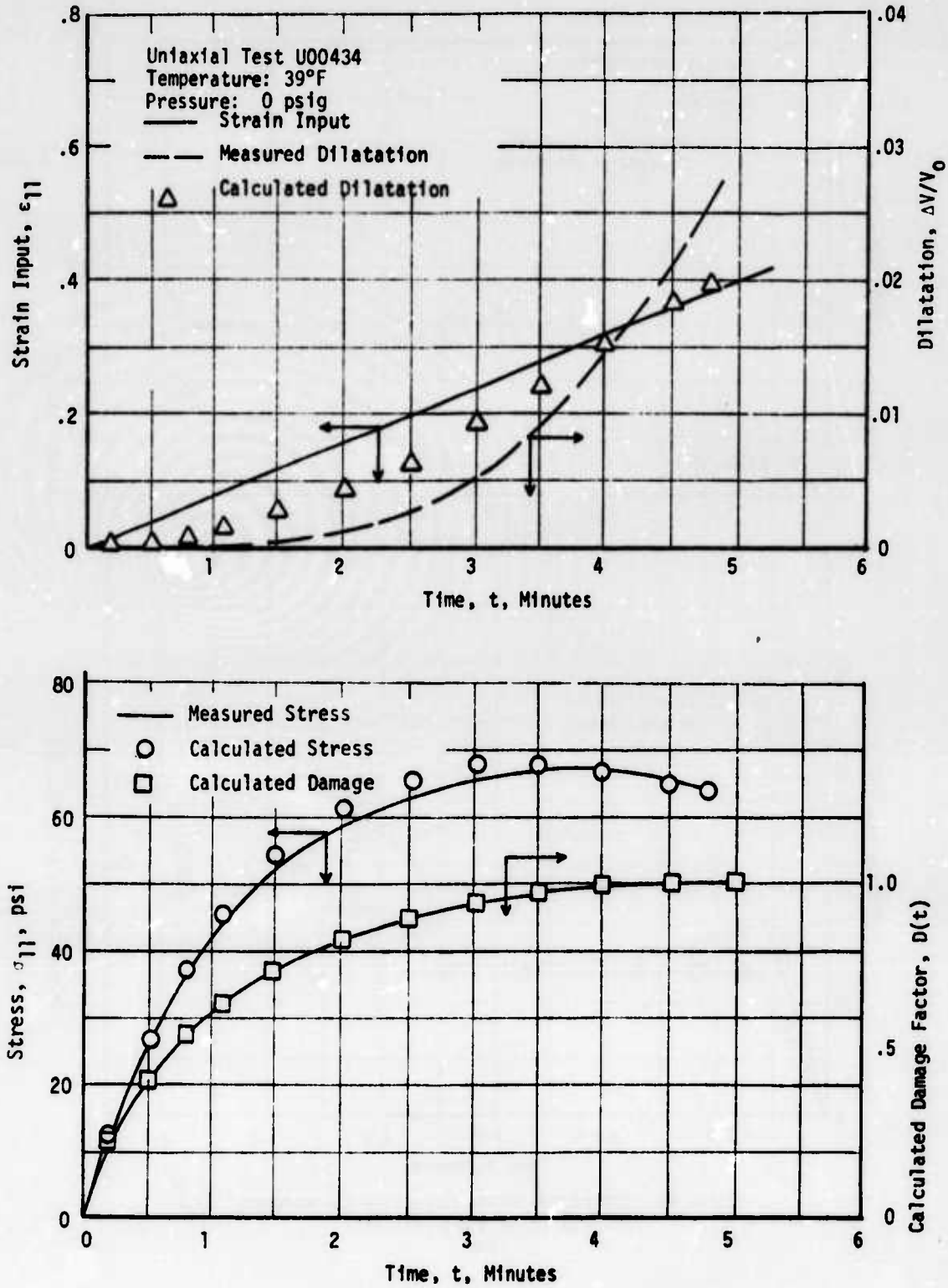

FIGURE 37. COMPARISON OF CALCULATED AND MEASURED RESPONSE OF THE VMO PROPELLANT

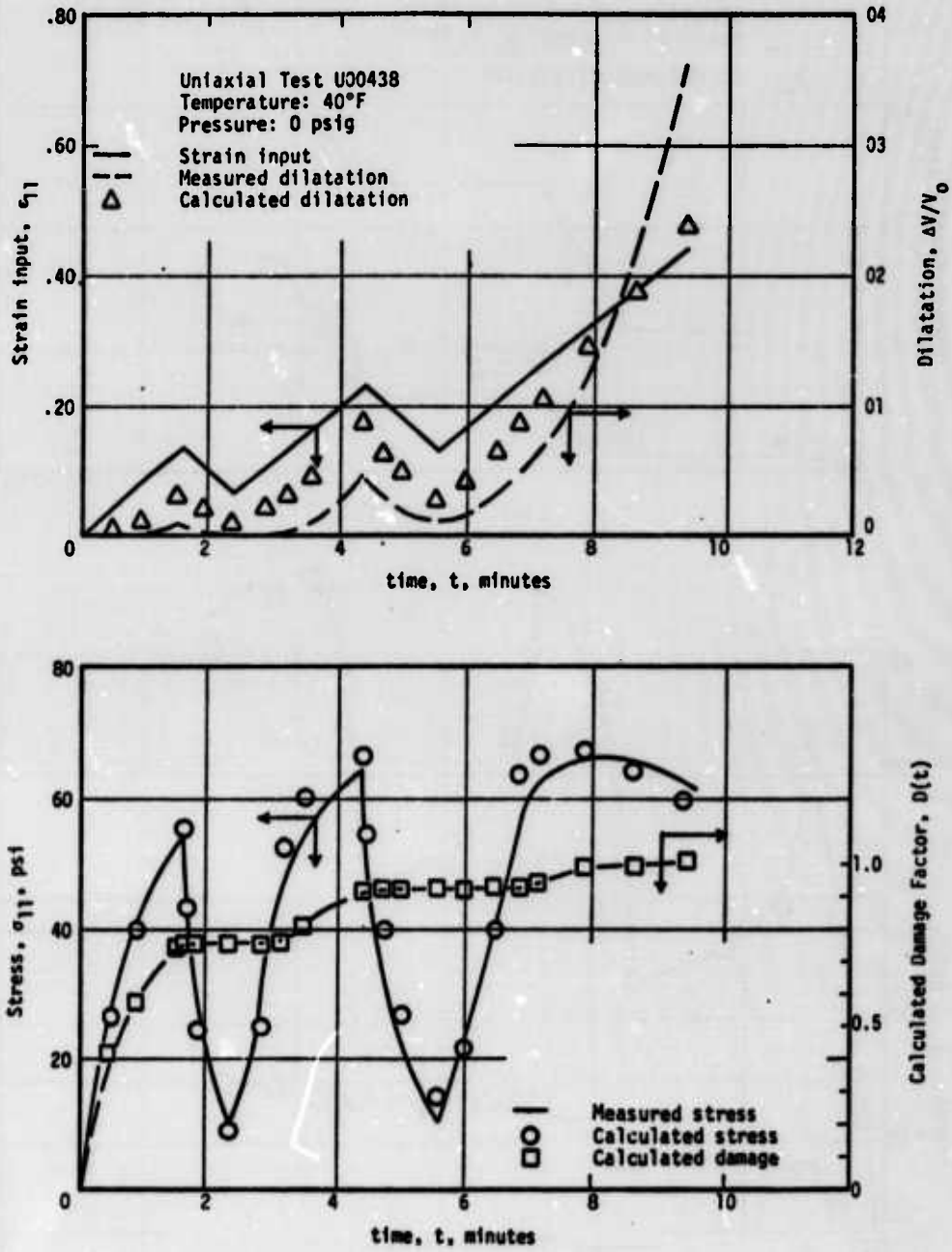

FIGURE 38. COMPARISON OF CALCULATED AND MEASURED RESPONSE OF THE VMO PROPELLANT

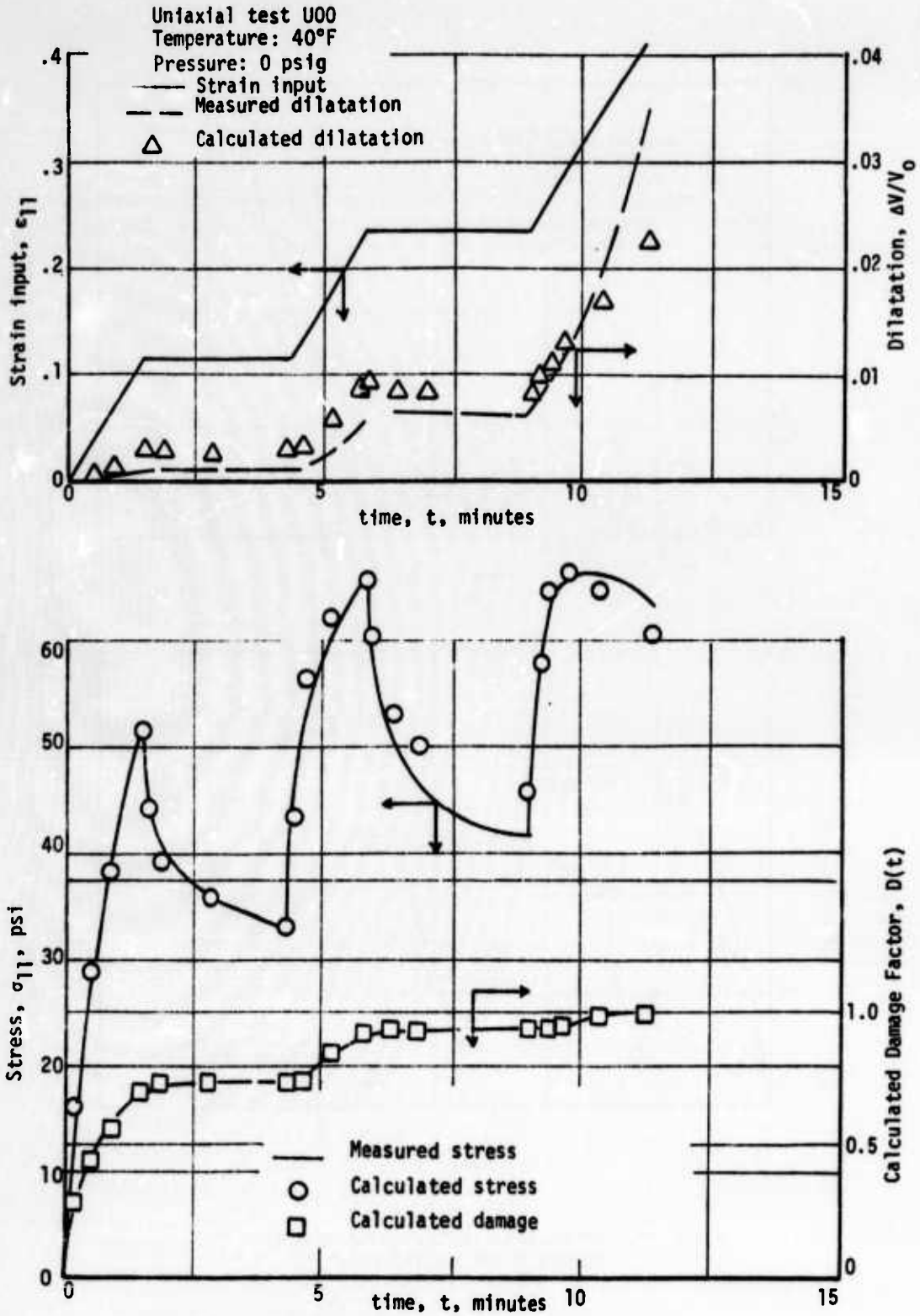

FIGURE 39. COMPARISON OF CALCULATED AND MEASURED RESPONSE OF THE VMO PROPELLANT

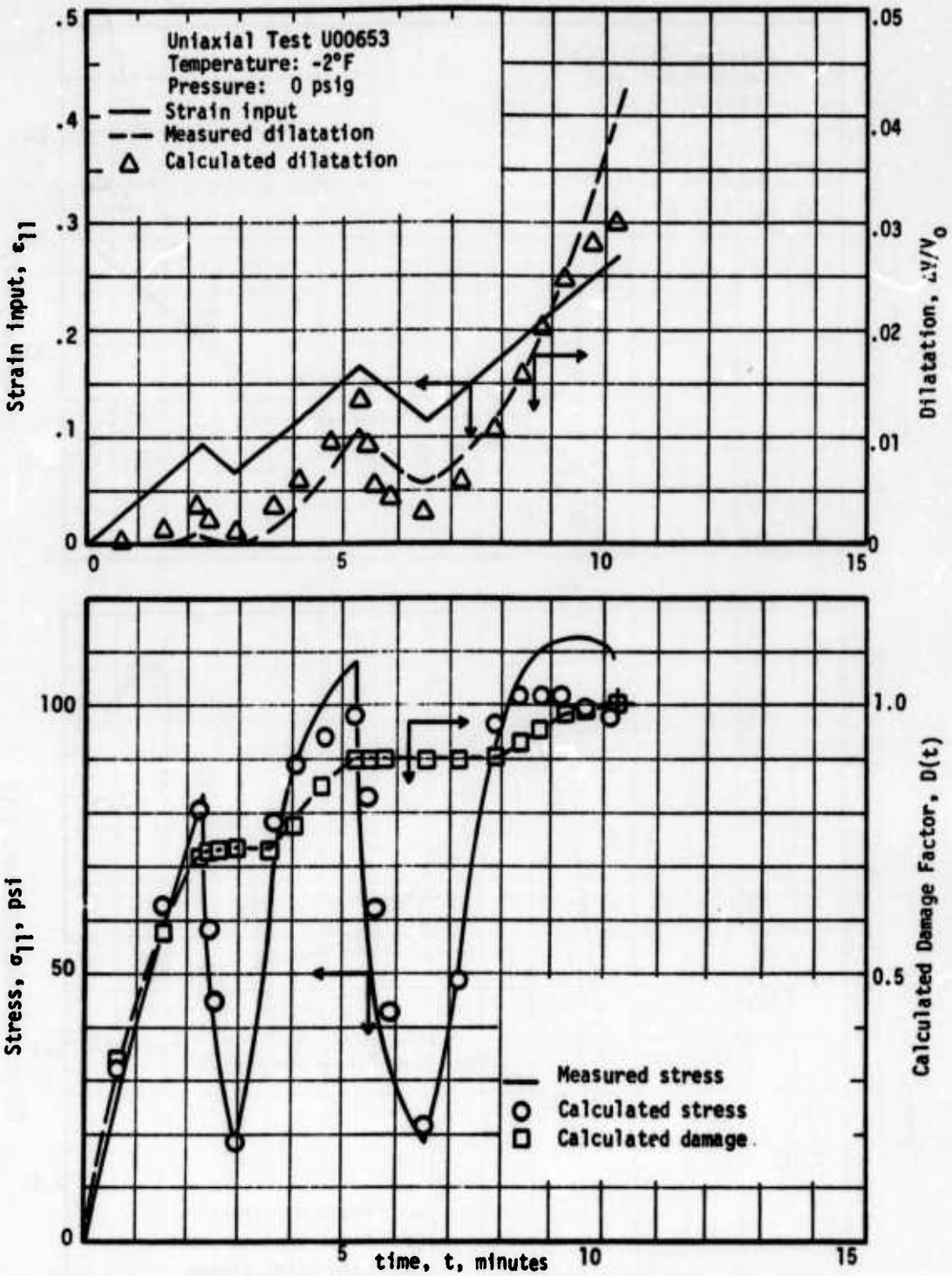

FIGURE 40. COMPARISON OF MEASURED AND CALCULATED RESPONSE OF THE VMO PROPELLANT

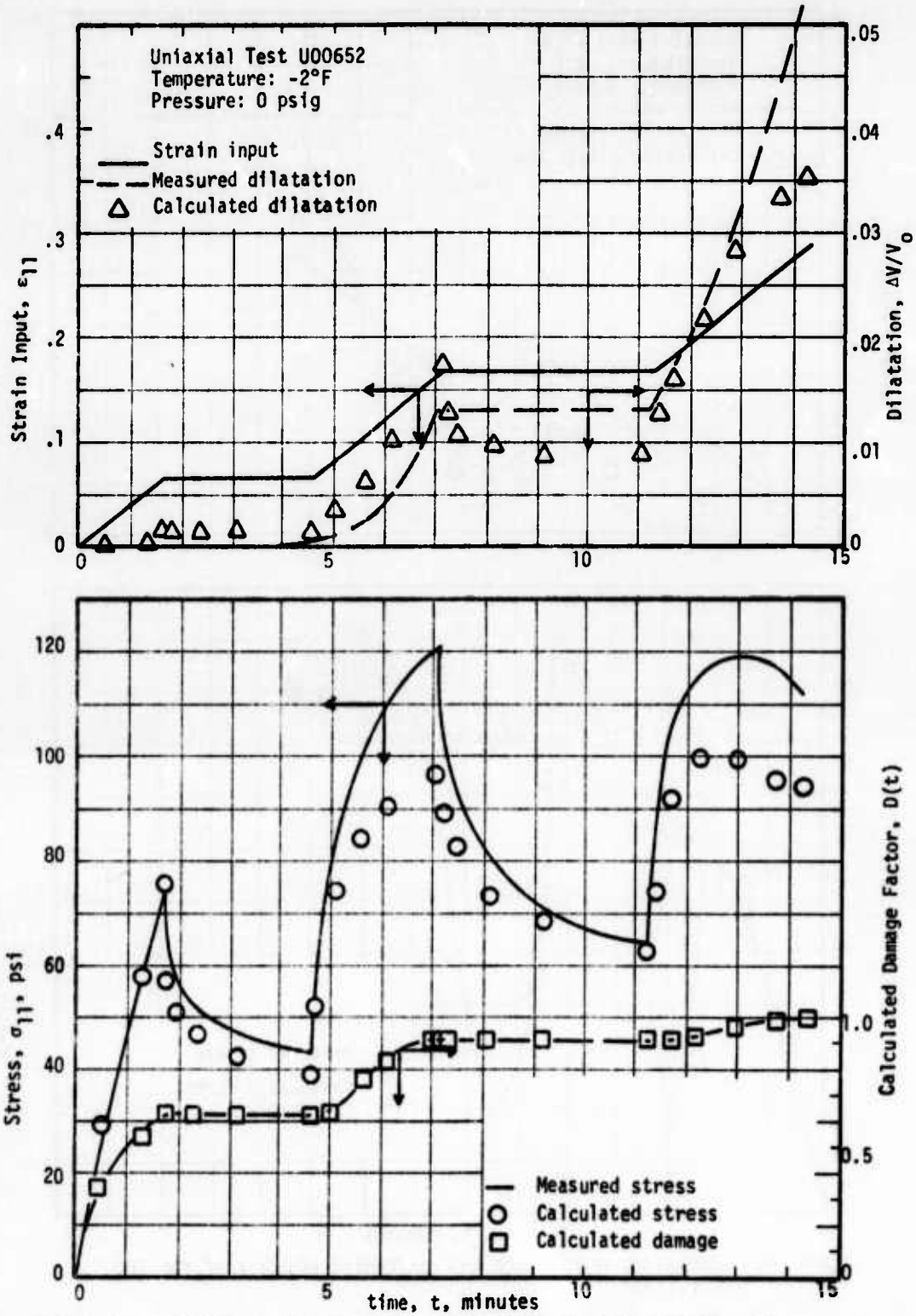

FIGURE 41. COMPARISON OF CALCULATED AND MEASURED RESPONSE OF THE VMO PROPELLANT

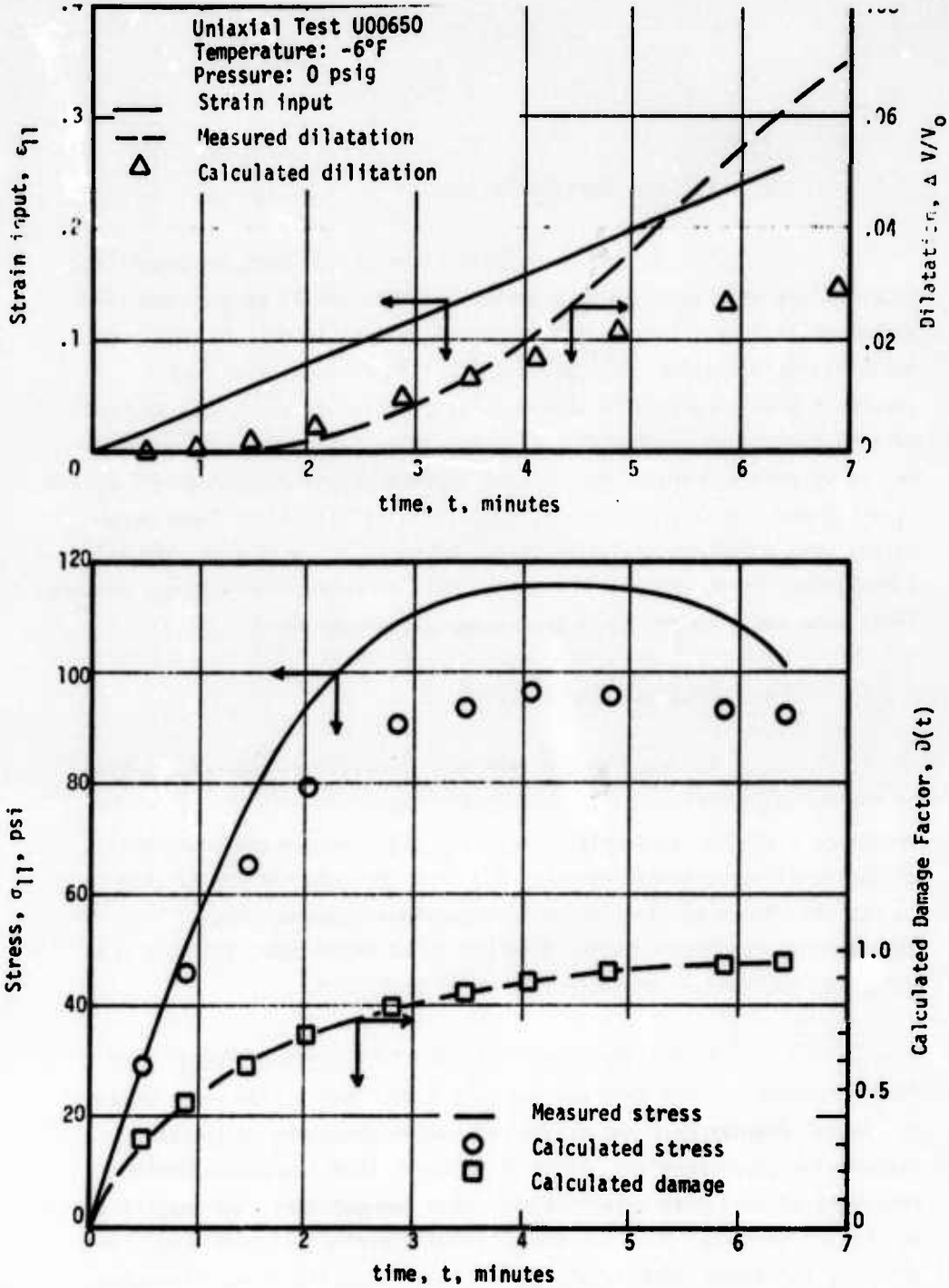

FIGURE 42. COMPARISON OF CALCULATED AND MEASURED RESPONSE OF THE VMO PROPELLANT

c. Failure Characterization

The failure characterization of the Hercules propellant is excellent and has a standard deviation of only 5.2% on the predicted damage at failure. This is the lowest value seen to date on any large scale characterization, indicating the nonlinear cumulative damage equations work very well on the Hercules propellant, as is seen by the data in Figures 31 through 42. This characterization was one of the few in which the computer was allowed to vary the damage parameters B_6 and B_7 which are normally held at unity as discussed earlier. These parameters were optimized out at roughly 2.0 and 0.8 respectively indicating a nonlinear damage measure is probably more in order than a linear measure. These data are also presented in Figures 31 through 42.

d. Discussion of Results

It would appear that the distortional characterization of the Hercules VMO propellant, like the other two propellants can be described with good to excellent accuracy with the proposed nonlinear distortional constitutive equation and that the computer can be used to fit the theory to experimentally determined response data. The dilatational characterization, although by no means poor, still is not good, and the failure characterization is excellent.

It was fortunate that Hercules supplied Aerojet with JANNAF specimens since this was the only propellant tested whose uniaxial or biaxial samples were not simple end bonded specimens of constant rectangular cross-section. Since it is known that truncated JANNAF specimens of nonlinear materials will have non-constant gage lengths the quality of the input data for the uniaxial experimental data reduction probably introduces considerable error into the distortional characterization. This poor specimen definition is further illustrated by

significant statistical discrepancies between the uniaxial and biaxial distortional and dilatational characterizations.

Obviously a characterization can be no more accurate than the experimentation and it would appear that even though our experimental methods are far more sophisticated than normal, large improvements can still probably be made. Ideally, an ordinary JANNAF specimen has a gage length of 2.7 inches, however, at small strains it has an actual measured gage length closer to 3.6 inches, an error of 33%. For propellant materials at larger strains it does approach the 2.7 inch value. The gage length and the change in gage length have also been shown to be strongly dependent on stress-strain curve shape (10). This type of data would argue strongly for avoiding samples of the JANNAF type and continuing with simple specimens, even though they present bonding problems.

The same arguments can be made about dilatation measurements using the JANNAF or strip biaxial specimens. The strip biaxial sample is known to have peak normal stresses about 15% higher than the average normal stresses if the material making up the sample is linear elastic and has a Poisson's ratio of near 1/2. Strain gradients of the same order of magnitude can, therefore, be expected. If the dilatation were linearly related to the stress state, as it is in linear elastic materials, then the average sample dilatation would be a good measure. In the case of propellants the dilatation is an extremely nonlinear function of the stress or strain, indicating that an average measure would introduce errors. Much of the possible error in dilatation predictions stems from the differences between uniaxial and biaxial data, and the uniaxial data are surely the higher quality data when simple samples are being used because the stress field is simple and near constant. A highly probable cause of the large errors

in the dilatation predictions could be due to the poor dilatation measure of the biaxial strip sample. This type of problem is the same problem facing those working with embedded stress transducers wherein the data cannot be properly interpreted without an accurate analysis, which, if possible, would make the transducer measurements unnecessary. Added support for this argument stems from the fact that when all uniaxial or all biaxial data are used the characterizations, both dilatational and distortional, are improved.

The failure characterization of the Hercules propellant is excellent. Unlike the distortional and dilatational characterizations which require a point by point description of a response function versus history of input, a failure characterization only has one point per experiment. In this sense an average measure of stress and other parameters is probably more than adequate since the failure condition is represented by an L_p norm which is nothing but a sophisticated means of averaging a history. It would appear that cumulative damage relations can do a very good job in predicting failure for the Hercules VMO propellant.

4. Other Propellants

In addition to the three propellants discussed above, three other propellants have been characterized using the codes and constitutive representations described in this report. The Aerojet space satellite propellant, ANB 3335, an unplasticized propellant; AAP 3124, an Aerojet high energy propellant; and ANB 3066, the Minuteman propellant. Overall, the characterization of these materials is essentially equivalent to the three discussed above. The distortional characterizations are always

excellent, the failure characterizations good to excellent, and the dilatation characterization is generally poor. Data for five of the six propellants tested have been included in the magnetic tape library of experimental data and can be used as input to these codes. The only propellant not included is ANB 3066.

I. SUMMARY OF THE TASK II EFFORT

The data presented in this section clearly demonstrates that iterative computerized characterization of linear and nonlinear viscoelastic constitutive equations using measured material response is not only practical but can be a powerful tool. This technique not only eliminates the requirements for specialized tests but also eliminates the requirement that those utilizing this type of characterization be highly skilled in mathematics. It enables the user to select tests that simulate real motor conditions and to use this information in characterizing the material.

The one real problem in utilizing this or any other characterization technique is obtaining quality laboratory data, since the characterization is limited in its precision by the validity of the experimental input. The discussion at the end of the Hercules characterization points out probable weakness in the truncated JANNAF sample and the strip biaxial sample because of the difficulties in obtaining reliable stress and dilatation measures. Just how such problems can be eliminated or minimized is difficult to envision. However, they must be solved if good experimental input into characterization processes is to be a reality.

It should be mentioned that the characterizations presented for the propellant materials covers their entire range of capability to failure for a wide range of conditions. Further improvements in the

characterizations can be obtained by limiting the range of strain to the maximum value expected in real motor conditions and the stress states and deformation histories to realistic simulations of the analyses under consideration. Overall the quality of the distortional and failure characterizations is from good to excellent in all cases tried to date with the dilatation characterization being generally poor in comparison. The codes have been designed so that they can be easily modified,if it is demonstrated that superior constitutive equations exist for any of the representations. In conclusion,one point should be made with regard to the dilatation representation. It is felt that it contains all of the necessary features but still requires some fine tuning. Researchers who feel it can be simply improved are encouraged to develop better relations. The real test, however, is in comparing predictions with real experimental data, something rarely done, and that is a problem of considerable difficulty.

There currently exists five magnetic tape libraries of propellant data covering a broad range of experimental conditions complete with dilatation data. Those interested in trying their hand at nonlinear constitutive theory and relating it to the behavior of real materials have at least half of their problems solved, since a volume of data exists. Hopefully, this code and possible modifications of it will ease, improve, and possibly standardize the material characterization procedures of the industry.

SECTION 5

TASK III - FINITE ELEMENT COMPUTER CODE DEVELOPMENT

A. WORK TO BE ACCOMPLISHED

The contractor shall incorporate the constitutive theory (developed under previous Air Force contract) into a finite element computer code. This finite element code will be able to handle quasi-static problems in addition to varying material properties and elastic motor case capabilities. The code shall allow for time varying pressure (within the quasi-static restrictions) and transient thermal loads. This code will be completely compatible with the constitutive equation characterization code. All information generated by the characterization code will be directly applicable to the finite element code input format. In addition, the finite element code shall be capable of utilizing the cumulative damage information generated by the characterization program. The finite element code will be completely documented. User's information and data on code construction shall be included in the documentation.

B. GENERAL OVERVIEW OF THE FINITE ELEMENT CODE DEVELOPMENT

The work described in this section was performed by Professors Leonard Herrmann and James Hutchinson of the University of California, Davis. They were contracted as consultants to perform the Task III effort. To accomplish the goals described above they developed a new finite element code based on previous viscoelastic computer codes developed by Professor Herrmann on past Aerojet contracts. The code they developed has considerably more features than requested in the work statement, all designed to increase its capability as regards propellant grain stress analyses. These additional capabilities and features include automatic grid generation and the ability to handle linear elastic and linear viscoelastic propellant properties as well

as orthotropic case properties. This code is an excellent tool which the industry can build and improve upon to make nonlinear viscoelastic analysis of propellant grains a reality in future years. Described below are details of the code construction while the user's manual is given in Appendix F. Both the code and the user's manual were provided by the consultants.

C. COMPATIBILITY WITH CHARACTERIZATION CODE

Since the characterization codes and the finite element codes were being developed during the same time period it was difficult to make them fully compatible during their development phases. This compatibility problem was resolved when the input to the finite element code was finalized. Since the input to the finite element code is much more complex than the output of the characterization code, the characterization code was modified by simply renaming the coefficients at the end of each phase of the nonlinear characterization. At the end of each type of characterization, distortional, dilatational, and failure, a set of coefficients is output that are identical to the input requirements of the finite element code. In addition, they are preceded by a statement indicating that they are the specific values to be used for the stress analyses input. These coefficients are different from the ones used in the characterization calculations.

D. FINITE ELEMENT CODE CAPABILITIES

The finite element program may be used for quasi-static plane strain, plane stress or axisymmetric analyses of elastic or viscoelastic structures. The structure may consist of elastic, linear viscoelastic and nonlinear viscoelastic continuum components; and isotropic and/or orthotropic shell components. In addition, the viscoelastic materials may have thermo-rheologically simple temperature dependent properties. The structure may be subjected to a combination of time-dependent externally-applied loads (or displacements), body forces and thermal effects. The program includes a finite element, transient heat conduction

analysis which may be used to calculate the time-dependent temperature distribution within the structure. Automatic grid generation has also been included as have damage measure calculations for key element locations.

The description of the types of elements, the numerical procedures, employed in the program, and a User's Manual are provided in the following sections.

E. KEY FEATURES OF THE FINITE ELEMENT CODE

1. Introduction

A brief description is given of the more important features of the numerical methods used in the development of a nonlinear thermo-viscoelastic finite element analysis for solid propellant rocket motors. A description of the computer code is given in the accompanying User's Manual (Appendix F). The analysis and the computer code are a continuation and augmentation of work carried out and reported during previous projects. Only those features unique to this analysis will be reported herein; the remaining items will be referred to by reference to previous reports.

2. Theory and Analysis

a. Type of Elements

(1) Continuum Element: The element used in the stress analysis is developed from the variational theorem for incompressible and nearly incompressible solids reported in Reference (11) (for plane stress, a modified form of the special formulation given in Reference (12) is used). The approximations for the displacements are expressed in terms of the 4-node isoparametric quadrilateral element (13); the hydrostatic stress variable (H) is approximated as a constant within each element. The integration of the element stiffness and load matrices is performed using a Gaussian quadrature numerical integration rule; the User may elect to use a 9 or 25 point formula.

(2) Thermal Element: In the thermal analysis, a quadrilateral element constructed of 4 constant heat flux triangles is employed, see Reference (14).

(3) Case Element: The case element (for axisymmetry) is a conventional cone element; a cubic approximation is used for the transverse displacement and a linear approximation for the in-plane displacement, see Reference 13.

b. Nonlinear Analysis

(1) Incremental-Iterative Analysis: Because of the time dependence of viscoelasticity problems, in general, an incremental analysis procedure is required. The nonlinearities introduced by the nonlinear volume change measure and the nonlinear viscoelastic material properties require that iteration be introduced within each time increment. In addition, because of the way that the system stiffness matrix is handled in this analysis (see following section), even linear viscoelasticity problems may require iteration. Hence, in general, the analysis is performed by taking small steps in time (adding appropriate increments of load to the structure, etc.) and iterating within each time step to obtain the correct response. The one exception, when the incremental-iterative procedure is not required, is when the analysis is used for linear elasticity problems with a linear measure of volume change. Incremental-iterative procedures naturally require a large computational effort; an attempt to substantially reduce this effort is described below.

(2) Modified Newton Type of Analysis: One of the two (the second will be discussed in a later section) main contributing factors to the computation effort is solving, for each iteration of each increment, the set of simultaneous equations which arise from the finite element analysis (a linear viscoelasticity problem with a linear

measure of volume change would not require iteration). The fact that, in general, the coefficients of the simultaneous equations differ for each time step and hence the equations must be completely solved anew is due to the fact that the incremental properties of a viscoelastic material change each increment (the exception is when constant length time steps are used for linear viscoelasticity without temperature effects). In the solution of the set of simultaneous equations, by far the most expensive operation is the reduction of the system stiffness matrix; thus, if means could be found for avoiding this operation, considerable computational effort could be avoided.

Consider first the case of linear viscoelasticity with a linear measure of volume change (i.e., a linear problem that does not inherently require iteration). For increment N, the set of simultaneous equations that is given by the finite element method may be written in the form:

$$[S]_N[\Delta U]_N = [L]_N \tag{19}$$

$[S]_N$ = matrix of coefficients of the simultaneous equations

$[\Delta U]_N$ = vector of global unknowns

$[L]_N$ = vector of non-homogeneous terms

Let M denote the number of some previous increment. Write Equation (19) in the form:

$$[S]_M[\Delta U]_N = [L]_N - \left\{[S]_N - [S]_M\right\}[\Delta U]_N \tag{20}$$

Equation (20) will be solved by iteration; denote the "i^{th}" approximation to $[\Delta U]_N$ as $[\Delta U]_{N_i}$. In the "i^{th}" iteration, the term $\left\{[S]_N - [S]_M\right\}[\Delta U]_{N_i}$

will be approximated by $\left\{[S]_N - [S]_M\right\}[\Delta U]_{N_{i-1}}$ (assuming that $[S]_N - [S]_M$ is small, this will be a convergent procedure, in fact for temperature independent problems with constant length time steps, $[S]_N = [S]_M$), i.e.

$$[S]_M[\Delta U]_{N_i} = [L]^*_{N_i} \tag{21}$$

where

$$[L]^*_{N_i} = [L]_N - \left\{[S]_N - [S]_M\right\}[\Delta U]_{N_{i-1}} \tag{22}$$

In order to start the iteration procedure ($i = 1$), the following definition is used:

$$[\Delta U]_{N_0} \equiv [\Delta U]_{N-1} \tag{23}$$

Thus, for each iteration in each increment, beyond increment M, the left-hand side of Equation (21) remains the same and thus the reduction of the left-hand side need not be repeated; instead only the reduction and back-substitution of the right-hand side is performed.

It is to be noted that, for linear viscoelasticity problems with a linear measure of volume changed, and with temperature effects and/or non-constant time steps, the above procedure introduces iteration where it was previously not needed (for nonlinear problems, it is of course in general always a requirement). Thus, for a given increment a savings is only achieved if the increased computational effort introduced by the iteration is less than the savings effected by not having to reduce the $[S]_N$ matrix.

To this point, the only statement made concerning the value of M (Equation (21)) is that $M \leq N$. The decision concerning the value of M is handled as follows: To begin the solution procedure, of course $M = 1$ (thus for linear problems no iteration is required in the first increment). The value of $M = 1$ is used until it

is judged that there is no longer any savings of computation effort by using this scheme; denote the number of this increment as I. In the next increment $[S]_{M=I+1}$ is used and for a linear problem, no iteration is required. The value of M = I + 1 is used until it is judged that another update is justified. The criteria that is used to judge when the $[S]_M$ matrix should be updated is when:

$$\text{No. of iterations} \geq \text{Bandwidth}/4 \tag{24}$$

This criterion is an out-growth of a previous study of the efficiency of the Gaussian elimination equation solving procedure. This criterion could be improved by placing timing statements in the program and accurately measuring the computational time involved in the competing operations of iteration and reduction of the system stiffness matrix; time was not available for such a study.

Nonlinearities introduced by the nonlinear measure of volume char., and/or nonlinear material properties are handled by introducing iteration into each increment; the nonlinear effects are successively approximated by using the strain values calculated in the previous iteration. The procedure outlined in the previous paragraph for linear viscoelasticity may be easily modified to account for the nonlinearities. Equation (22) is written in the form:

$$[L]^{*}_{N_i} = [L]_{N_i} - \left\{ [S]_{N_i} - [S]_{M_1} \right\} [\Delta U]_{N_{i-1}} \tag{25}$$

where the N_i subscript of $[L]_{N_i}$ and $[S]_{N_i}$ denote that these matrices change in value each iteration due to the successive approximation of the nonlinearities. The criterion for updating M is written in the form:

$$\text{No. of iterations} \geq \text{No. of iteration in increment M} + \text{Bandwidth}/4 \tag{26}$$

The additional term in this expression (compared to expression (24)) is introduced to account for the fact that even if $[S]_{N_i}$ were used in

Equation (21), iteration would still be required to account for the non-linearities; thus it is the cost of the additional iterations introduced by the fact that M≠N that must be weighed against the cost of reducing $[S]_N$.

In order to effectively implement the above scheme, means had to be found for avoiding the direct evaluation of the term $\left\{ [S]_{N_i} - [S]_{M_1} \right\} [\Delta U]_{N_{i-1}}$. The direct evaluation would require that storage be provided for both $[S]_{N_i}$ and $[S]_{M_1}$ in addition to the storage required for the reduced form of $[S]_{M_1}$; the providing for storage (and manipulation) of these very large matrices would be prohibitively expensive. In place of the indicated operations, what was actually done was to write the incremental stress-strain relationship for increment N ($[C]_{N_i}$ is the matrix of incremental properties for iteration "i" of increment N, for a given point in the system).

$$[\Delta\sigma]_{N_i} = [C]_{N_i} [\Delta\varepsilon]_{N_i} + [T]_{N_i} . \tag{27}$$

in the iterative form:

$$[\Delta\sigma]_{N_i} = [C]_{M_1} [\Delta\varepsilon]_{N_i} + [T]^*_{N_i} \tag{28}$$

where

$$[T]^*_{N_i} = [T]_{N_i} + \left\{ [C]_{N_i} - [C]_{M_1} \right\} [\Delta\varepsilon]_{N_{i-1}} \tag{29}$$

The fact that $[C]_{M_1}$ does not change from one increment to the next means that the left hand side of the simultaneous equation does not change and thus only a new right hand side need be calculated. Therfore, all that needs to be stored is the information needed to reconstruct the incremental material properties $[C]_{M_1}$ and the previous estimate of the displacements $[\Delta U]_{N_{i-1}}$ ($[\Delta\varepsilon]_{N_{i-1}}$ is calculated from $[\Delta U]_{N_i}$). Thus, the term $\left\{ [S]_{N_i} - [S]_{M_1} \right\} [\Delta U]_{N_{i-1}}$ is effectively calculated by forming $[T]^*_{N_i}$ for each of the elements and directly combining them to form $[L]^*_{N_i}$. Now if in forming the element load matrix, $[L]^*_{N_1}$, a partial reduction is effected, due to the "static consideration" of element unknowns and/or

the specification of non-homogeneous displacement boundary conditions, the element stiffness matrix (for M_1) would need to be available. In order to avoid the necessity of storing the element stiffness matrices, an element without a center point (the 4-node isoparametric element) was used (to avoid the "static condensation" of center point displacements) and a scheme for specifying non-homogeneous displacement boundary conditions which does not partially reduce the element load matrix was employed. The scheme that was used to account for non-homogeneous displacement boundary conditions is the one suggested by Irons (13) wherein the appropriate diagonal term is set equal to X and the corresponding right-hand side term to $X \cdot U_o$; where X is a very large number (10^{20} for this program) and U_o is the specified displacement.

(3) Iteration Factor: To improve the rate of convergence of the iteration procedure an "iteration factor" is introduced. Thus an improved estimate $[\Delta U]^*_{N_i}$ of the solution for iteration "i" of increment N is expressed in the form (note $[\Delta U]_{N_0}$ is defined by Equation (23)).

$$[\Delta U]^*_{N_i} = R \cdot [\Delta U]_{N_i} + (1-R) \cdot [\Delta U]_{N_{i-1}} \tag{30}$$

A discussion of a practical procedure that may be used to make an effective choice for the value of R is given in Reference 2. It is to be noted, due to a change in definition, that in terms of the iteration factor R' used in Reference 2:

$$R = R' + 1 \tag{31}$$

(4) Convergence Criteria: The criteria for convergence of the iteration procedure that are used are based upon a comparison of the sucessive predictions for the system unknowns, i.e., $[\Delta U]_{N_{i-1}}$ and $[\Delta U]_{N_i}$; two comparisons are made. (They both must be satisfied for convergence, however, either may be avoided by setting the acceptable limit excessively large.) The first criterion limits the maximum relative difference between individual components of $[\Delta U]_{N_{i-1}}$ and $[\Delta U]_{N_i}$, i.e., the difference between the individual components are divided by the average magnitude of the components of $[\Delta U]_{N_i}$

and compared to a prescribed acceptable value. For the second criterion the absolute values of the differences between the components of $[\Delta U]_{N_{i-1}}$ and $[\Delta U]_{N_i}$ are summed and divided by the sum of the absolute values of $[\Delta U]_{N_i}$, the result is then compared to an acceptable value prescribed by the User.

Because of the possibility that a circumstance might arise when convergence would not occur, the iteration procedure is arbitrarily aborted if the number of iterations should exceed 10 + Bandwidth; it may prove to be desirable to modify the program so that the User may easily modify this limit.

(5) Incremental Material Properties: The relationship at a given point in the structure between the incremental stresses and strains is written in the form:

$$[\Delta\sigma]_{N_i} = [C]_{N_i}\,[\Delta\varepsilon]_{N_i} + [T]_{N_i} \tag{32}$$

This equation is developed by writing the exact nonlinear expressions relating stress and strain at t_N and t_{N-1} (note in general $f([\varepsilon]_N)$ involves values of $[\varepsilon]$ for $t = o \longrightarrow t_N$, etc.), i.e.

$$[\sigma]_{N-1} = f([\varepsilon]_{N-1}) \tag{33}$$

$$[\sigma]_N = f([\varepsilon]_N) \tag{34}$$

and subtracting the results to yield:

$$[\Delta\sigma]_N = [\sigma]_N - [\sigma]_{N-1} = f([\varepsilon]_N) - f([\varepsilon]_{N-1}) \tag{35}$$

The expression of $f([\varepsilon]_N) - f([\varepsilon]_{N-1})$ in the form $[C]_N[\Delta\varepsilon]_N + [T]_N$ uses numerical procedures similar to those employed in Reference 2. For the nonlinear viscoelastic material (characterized by the equation given in the Users' Manual) after considerable manipulation the following equations are obtained:

$$\Delta\sigma_{ij} = \Delta S_{ij} + \delta_{ij}\Delta\bar{\sigma} \tag{36}$$

$$\Delta\varepsilon_{ij} = \Delta e_{ij} + \frac{1}{3}\delta_{ij}\Delta\theta \tag{37}$$

where

$$\Delta S_{ij_N} = 2\mu_N \Delta e_{ij_N} + L_{ij_N} \tag{38}$$

$$\Delta\bar{\sigma}_N = K_N(\Delta\theta_N - 3\alpha\Delta T_N) + \chi_N \tag{39}$$

$\Delta T_N \equiv$ Temperature change in increment N

$$\mu_N = G_N\left\{A_3 + A_4 g_{1N} + A_6\, g_{2N} + (1-g_{3N}) \sum_{m=1}^{M} a_m J_{Nm}\right\} \tag{40}$$

$$G = e^{(A_1 I_\gamma + A_2 I_d/I_\gamma)} \tag{41}$$

$$I_d = \theta + \theta_c \tag{42}$$

$$\theta = \varepsilon_{11} + \varepsilon_{22} + \varepsilon_{33} \tag{43}$$

$$\theta_c = \varepsilon_{11}\varepsilon_{22} + \varepsilon_{11}\varepsilon_{33} + \varepsilon_{22}\varepsilon_{33} - \varepsilon_{12}^2 + \varepsilon_{11}\varepsilon_{22}\varepsilon_{33} - \varepsilon_{33}\varepsilon_{12}^2 \tag{44}$$

$$I_\gamma = \frac{1}{3}\sqrt{(\varepsilon_{11} - \varepsilon_{22})^2 + (\varepsilon_{22} - \varepsilon_{33})^2 + (\varepsilon_{33} - \varepsilon_{11})^2 + 6\varepsilon_{12}^2} \tag{45}$$

$$g_i = \left(\frac{||f||_{p_i}}{||f||_{q_i}}\right)^{\eta_i} \quad \text{where} \quad ||f||_\eta = \begin{cases} |f| & \eta < 0 \\ ||f||_\infty & \eta > 100 \\ (\phi_\eta)^{1/\eta} & 0 < \eta \leq 100 \end{cases} \tag{46}$$

$$\phi_n = \int_0^{\xi} |f(\xi')|^n d\xi = \int_0^{t} e^{-\beta(\tau)} |f(t')|^n dt', \tag{47}$$

and

$$\phi_{n_N} = \phi_{n_{N-1}} + \int_{\xi_{N-1}}^{\xi_N} ||f(\xi')|^n \, d\xi = \phi_{n_{N-1}} + \int_{t_{N-1}}^{t_N} e^{-\beta(\tau)} |f(t')|^n dt' \tag{48}$$

$$J_{Nm} = \frac{1 - e^{-\beta_m \Delta\xi_N}}{\beta_m \Delta\xi_N} + J^*_{Nm} = (1/2) \int_{-1}^{1} e^{-\beta_m(\xi_N - \xi)} d\tau \quad \text{if } \beta_m = 0;\ J_{Nm} = 1 \tag{49}$$

$$J^*_{Nm} = \frac{1}{2} \int_{-1}^{1} \left[e^{-\beta_m(\xi_N - \xi)} - e^{-\beta_m \frac{\Delta\xi_N}{2}(1-\tau)}\right] d\tau \tag{50}$$

$$L_{ij_N} = 2.0 \Big\{ A_3(G_N - G_{N-1}) + A_4 \left(G_N g_{1_N} - G_{N-1}\, g_{1_{N-1}}\right) +$$

$$A_6\left(G_N\, g_{2_N} - G_{N-1}\, g_{2_{N-1}}\right)\Big\} e_{ij_{N-1}} + \tag{51}$$

$$2.0 \left\{ G_N\left(1 - g_{3_N}\right) \sum_{m=1}^{M} \alpha_m e^{-\beta_m \Delta\xi} \psi_{ij_{Nm}} - G_{N-1}\left(1 - g_{3_{N-1}}\right) \sum_{m=1}^{M} \alpha_m \psi_{ij_{Nm}} \right\}$$

$$\psi_{ij_{Nm}} = \int_0^{t_{N-1}} e^{-\beta_m (\xi_{N-1} - \xi')} \frac{\partial e_{ij}}{\partial t'} dt' \tag{52}$$

$$K_N = 1/C_1 h_{1_N} \tag{53}$$

$$h_1 = e^{[C_{4_1} + C_{5_1}(T-77°F)]\bar{\sigma}} \tag{54}$$

NOTE: $\bar{\sigma}_N = (\sigma_{11_{N-1}} + \sigma_{22_{N-1}} + \sigma_{33_{N-1}})/3 + \Delta\bar{\sigma}_N$

$$\Delta\bar{\sigma}_N = \mu_N \Delta H_N$$

$$x_N = K_N[(\theta_{C_N} - \theta_{C_{N-1}}) - C_1 (h_{1_N} - h_{1_{N-1}})\bar{\sigma}_{N-1} \tag{55}$$

$$-C_2(h_{2_N} I_{\gamma_N}^{C_3} - h_{2_{N-1}} I_{\gamma_{N-1}}^{C_3})]$$

In the above equations the subscript "i" is used to indicate a particular component of a matrix or a vector not the iteration number.

Equation (27) is obtained by combining and expressing Equations (36) and (17) in matrix form. For iteration "i" the nonlinear terms involving $[\varepsilon]_N$ are estimated in terms of $[\varepsilon]_{N_i} = [\varepsilon]_{N-1} + [\Delta\varepsilon]_{N_{i-1}}$; i.e., Equations (41), (44) to (48) and (55).

The need for an estimate for the strains results in a unique difficulty for plane stress problems. This stems from the fact, that the thickness strain cannot be expressed directly in terms of displacement gradients but instead must be solved for, such, that the thickness stress has the prescribed value; such a calculation requires a knowledge of the incremental stress-strain relationship. For linear materials, this offers no difficulty because the incremental stress-strain relationship is, of course, directly known. However, for nonlinear materials it is not. For nonlinear materials this relationship is a function of the strain state which is in turn, of course, a function of the thickness strain; i.e., the quantity we are attempting to solve for. Thus, for plain stress problems a new dimension is added to the iterative analysis that is not present in plain strain or axisymmetric analyses. This additional difficulty may, if the nonlinearities are strong, greatly slow down convergence or prevent it all together.

(6) Measure of Volume Change - I_d: The linear measure of volume change is the first strain invariant; in the above equations set $\theta_c = 0$. The nonlinear measure includes the second and third strain invariants, which is an exact measure.

c. Evaluation of Viscoelastic History Effects

(1) Hereditary Integrals: The procedure used to evaluate the hereditary integrals is similar to what was used in Reference 2; the resulting equations are summarized above (Section 5.E.2.b(5)). The major drawback offered by the use of these equations is the large amount of storage required for the $\psi_{ij_{Nm}}$ array. In Reference 2 these equations were calculated by means of the following recursive relationship:

$$\psi_{ij_{Nm}} = [e^{-\beta_m \Delta \xi_{N-1}} \psi_{ij_{N-1,m}} + \Delta e_{ij_{N-1}} J_{N-1,m}] \qquad (56)$$

If the $\psi_{ij_{Nm}}$ array is stored directly there is a need for $n = j \cdot k \cdot \ell \cdot m$ storage locations where

j = number of strain components (for axisymmetry $j = 4$)
k = number of elements
ℓ = number of terms in exponential series
m = number of integration points in element for which the history effects are evaluated

Very often (e.g. see Reference (2)) for the purposes of evaluating the history effects the strains are approximated as constant within each element, i.e., all integration points are assumed to have the same history effects, ($m = 1$); the significance of this approximation has not been determined. By proceeding in a slightly different way this storage requirement can be nearly cut in half and the noted approximation avoided. Expressing e_{ij} in terms of a numerical operator on the node point displacement components (u_k) (the form of D_{ij} is obtained by operating on the element shape functions, Reference (13) with the differential operator which relates strains to displacements);

$$e_{ij} = D_{ij}\,(u_k) \qquad (57)$$

Thus, Equation (52) may be written in the form:

$$\psi_{ij_{Nm}} = \int_0^{t_{N-1}} e^{-\beta_m(\xi_{N-1} - \xi')} \frac{\partial\, D_{ij}\,(u_k)}{\partial t'}\, dt' \qquad (58)$$

or

$$\psi_{ij_{Nm}} = D_{ij}\left\{\int_0^{t_{N-1}} e^{-\beta_m(\xi_{N-1}-\xi')}\,\frac{\partial u_k}{\partial t'}\,dt'\right\} . \tag{59}$$

Let

$$\psi^*_{k_{Nm}} = \int_0^{t_{N-1}} e^{-\beta_m(\xi_{N-1}-\xi')}\,\frac{\partial u_k}{\partial t'}\,dt' . \tag{60}$$

Thus,

$$\psi_{ij_{Nm}} = D_{ij}\left\{\psi^*_{K_{Nm}}\right\} . \tag{61}$$

The $\psi^*_{K_{Nm}}$ array can be calculated with an equation similar to Equation (56). Thus, the storage requirement is now $n = j^* \cdot K^* \cdot \ell$ where

j^* = number of displacement components (2 for 2-dimensions)
k^* = number of nodes (only slightly larger than k)

Thus, the storage requirement for evaluation of the hereditary integral has been effectively cut in half and, in addition, the approximation that the hereditary effects are constant within each element has been avoided.

In using this procedure reduced time is calculated at the nodes instead of at the element centers as was done in Reference (2). This method is complicated for non-homogeneous bodies, i.e., where all the elements framing into a given nodes do not consist of the same material. For such situations a separate $\psi^*_{K_{Nm}}$ is calculated and stored for each of the several materials framing into a given node.

The method is further complicated for plane stress problems because Equation (57) may not be used to express the thickness strain in terms of the displacements and thus this strain component must be treated in a special way.

(2) Norm Terms: The nonlinear effects introduced by the norm terms are treated in a fashion similar to that used in Reference (2) (also,see Reference (2) for a definition of the "Scale Factor").

d. Computer Code

The computer code developed in Reference (2) for nonlinear viscoelastic problems has been extensively modified. The modifications include (1) incorporation of a more general nonlinear viscoelastic material characterization, (2) usage of the modified Newton iteration scheme, (3) usage of the modified method of accounting for the hereditary history terms, and (4) the incorporation of extensive input data generation schemes. The use of the computer code is described in the accompanying "Users Manual" (Appendix F).

SECTION 6

TASK IV - FINITE ELEMENT CODE DEMONSTRATION

A. WORK TO BE ACCOMPLISHED

The contractor shall conduct an experimental effort to verify the validity of the finite element computer code developed in Task III. Samples of all propellants characterized in Task II having very high stress/strain gradients will be tested for total volumetric and force response on appropriate test equipment and compared with the finite element predictions.

B. ORIGINAL TASK IV EFFORT

The original Task IV effort required subjecting small instrumented propellant grains to pressure and thermal loads and to compare the experimentally determined stress and deformation histories with those obtained by finite element analyses. The stress transducers for these motors were to be provided by AFRPL and because of problems the Air Force had in obtaining these devices the transducers arrived several months late. The transducers in question were 150 lb normal stress transducers which were to be used to measure bondline radial stresses at the propellant-case interface. To eliminate adhesion and void problems the transducers were pre-potted with a small hemisphere of inert propellant by the manufacturers. The quality of the potting appeared poor in that it looked porous as shown in Figure 43. Since this portion of the program was already several months behind at that time there was nothing to do but try them. The transducers were bonded to the inside diameter of 5" I.D. steel tubes, which were to be used for the bases, and calibrated at several temperatures from 135°F to -65°F. During the calibration the behavior appeared quite linear and could be represented by a linear algebraic equation which included a temperature dependent zero shift and slope of the form:

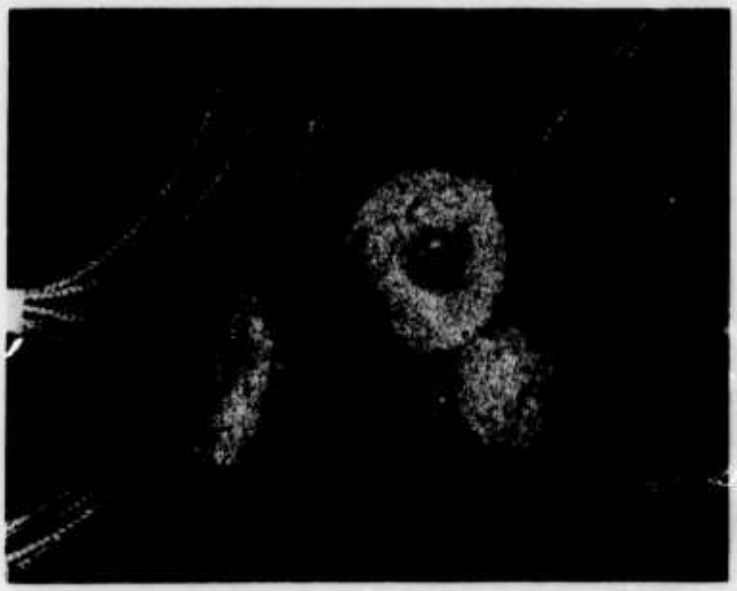

FIGURE 43. PHOTOGRAPH OF 150 PSI NORMAL STRESS TRANSDUCERS AS DELIVERED FROM THE MANUFACTURER WITH PROPELLANT POTTING

$$\text{Pressure} = A(T) + B(T) \cdot Mv \qquad (62)$$

In the above equation A(T) is the zero shift and B(T) is the sensitivity factor which changes little. The actual calibration process consisted of letting the whole system come to equilibrium at a temperature and obtaining a pressure versus millivolt curve from 0 to 100 psia. Under these conditions the transducers performed normally.

In order to further test the validity of the linear algebraic interpretation of transducer output another experiment was performed wherein the cylinders were first pressurized to 50 psia and than cooled to -65°F, holding the 50 psia constant, and then recalibrated. Hence the state of 50 psia and -65°F was arrived at via two different paths, first in the normal calibration by cooling at zero pressure and then pressurizing and then in the special calibration by pressurizing to 50 psia and then cooling. In a rocket motor subjected to a transient thermal field the gages would be exposed to a path somewhere between these two extremes. The results of these two different calibrations are shown in Table 7 for the six double bridge transducers. In the table each transducer bridge is shown separately and also included are the results of a repeat experiment. All readings were taken using a digital voltmeter and the readings were quite stable. These data indicate that the bore transducers themselves, with only a small amount of potting, are path sensitive and that the algebraic equation used to interpret the gage output is not valid for transient thermal conditions since the same pressure and temperature yield two different voltage outputs. The data in Table 7 evince output changes of as much as 15 millivolts, with many transducers showing 6 to 10 millivolts change. Since 10 millivolts is roughly equivalent to a 14 psi change in pressure this represents a very large error. The peculiar part of the experiment is that each half of the bridge seems to behave differently, yet the results were reproducible.

TABLE 7

TRANSDUCER READINGS IN MILLIVOLTS AT -65°F FOR TWO

PRESSURE-TEMPERATURE CALIBRATION HISTORIES

Transducer Ident.	Path I*		Path II**		Path II	
	0 psi	50 psi	0 psi	50 psi	0 psi	50 psi
122-1	6.5	32.1	8.7	40.2	5.88	38.4
122-2	8.1	35.4	11.5	44.5	8.88	42.5
123-1	-10.3	15.8	-13.8	17.7	-12.2	22.1
123-2	- 1.6	25.5	- 0.4	31.1	- 1.7	31.0
124-1	0	28.0	4.8	34.9	2.5	35.5
124-2	10.2	39.3	18.8	50.3	11.8	44.9
125-1	4.4	32.9	14.2	43.6	5.8	37.8
125-2	- 0.3	28.0	7.5	37.7	1.1	33.7
126-1	9.3	38.1	17.3	46.0	11.1	42.6
126-2	18.5	48.5	28.5	58.7	21.3	54.4
127-1	14.5	40.4	28.6	57.2	20.4	50.6
127-2	3.8	30.7	9.4	39.6	3.8	36.5

* Path I -- Cool to -65 with 0 psig and pressurize.

** Path II - Pressurize to 50 psig at ambient and cool to -65°F.

Because of this contradicting data indicating path sensitivity the transducers were rejected and this portion of the program was revised. Whether the fault was with the particular transducers or if the observed data was characteristic of all transducers of this type is unknown, however the effects were reproducible for similar thermal histories. The transducers were even calibrated down to a vacuum to demonstrate that for isothermal conditions they were linear and voids, if they existed in the potting, were of no consequence. There was also some criticism with the manner in which the transducers were connected to the instrumentation, by crimping, rather than soldering. The experiments however were repeated by H. Leeming and Associates for the Air Force and they obtained similar results. If these results are to be accepted they would suggest that for very wide temperature excursions the gage output depends upon its thermal and pressure histories as well as the current state of pressure and temperature. Such effects can be expected with a viscoelastic potting that had a high modulus. It would appear that for the extreme temperatures considered a linear hereditary interpretation of gage output is required.

Because the gages were not performing according to manufacturers specifications and were displaying path dependent hereditary response, this portion of the Task IV program was dropped with the Air Force's approval and the Task IV effort was rewritten as illustrated in the description of the work to be accomplished at the beginning of this section.

C. TASK IV - DEMONSTRATION

1. Description of Experiments

The experimental program described in the Task IV work statement above was carried out on all three propellants. The sample dimensions selected were roughly 1" x 2" x 1/4". The one inch faces were end-bonded to metal tabs and the specimens were elongated in the two inch direction using the uniaxial dilatometer for isothermal test conditions and a special Aerojet slow rate tester for transient thermal experiments. The isothermal measurements consisted of measuring the total pulling force and the total volumetric change as a function of deformation. In the transient thermal experiments only the total force was measured. The isothermal experiments used several deformation histories and superimposed pressure levels. To introduce large strain and stress gradients, holes or fillets were cut into the samples. The reason for this selection of sample geometry was that the maximum sample width that can fit into the dilatometer is just over one inch and to introduce large strain gradients the sample length was fixed at two inches. The one quarter inch dimension was as thin as possible to approximate plane stress conditions and yet retain a quality sample. Actually, the one quarter inch thickness is a little on the large size for a good plane stress approximation, however it was impractical to make good test specimens much thinner than this considering the particulate nature of propellant.

2. Finite Element Code Problems

The intent of this experimental effort was to model the sample geometries and boundary conditions using the finite element code and predict for the same deformation histories the total force

and volumetric response of the samples versus time. The quality of the constitutive equations, the characterization codes, and the finite element codes could then be judged on the basis of this comparison of experiment to predictions using samples that had deformation and stress gradients. Unfortunately such comparisons proved impossible.

During the final check out phases of the finite element code development in Task III problems started emerging regarding convergence for plane stress boundary conditions using the nonlinear constitutive equations. Numerically or analytically plane stress solutions are always more difficult to develop than plane strain solutions because the thickness strain is unknown and an iterative solution technique must be developed that finds the strain that makes the thickness stress zero. In plane strain calculations the thickness strain is known and the thickness stress can be determined by the constitutive equation. The plane stress portion of the code was then modified in an attempt to correct this situation of poor convergence for plane stress problems and the problem was thought to have been solved. The program was then checked using actual characterizations on simple trial problems. During this check out phase the codes appeared to work well and the Task III effort was completed.

When the time came to actually perform the comparisons between experiment and theory using the finite element analyses on specimens using a large number of elements the convergence to plane stress conditions was poor and often times the code would not converge. This section of the code was then again studied, some changes made, but no further improvements were obtained. Since the program was in its final stages the problem still remains largely unsolved.

To determine if it was actually the finite element codes plane stress section or the constitutive characterizations that was causing the difficulties some of the same problems that failed to converge for plane stress conditions were modeled as axisymmetric problems and performed perfectly. Hence the problem appears to be numerical and not associated with the constitutive equations. In a final attempt to get some comparative data from the computer codes the convergence criterion for the plane stress condition was greatly relaxed, which means a sacrifice in accuracy, and some problems ran, although slowly, but for others even the relaxed criterion would not suffice. The few simple cases that did run are shown in Figures 44 and 45 for the Aerojet propellant. Figure 46 illustrates the finite element grid used which has 65 elements. This grid was generated using the automatic grid generation features of the code. The comparisons of the analyses and experiment are not really worth discussing since the convergence criteria were greatly relaxed and failure to converge prior to completion of the run was the reason for termination in two cases. Generally speaking the comparisons look good. However, considering the test conditions it would be difficult to be greatly in error. After spending considerable money on the computer attempting to get quality runs in a short period of time this task was abandoned for future work.

As it currently stands the finite element code functions well for plane strain or axisymmetric problems but will not always converge for plane stress boundary conditions when the nonlinear constitutive equations are used for material response description. These problems do not influence the linear elastic or linear viscoelastic portions of the finite element code (this fact was substantiated by the solution of a number of sample problems).

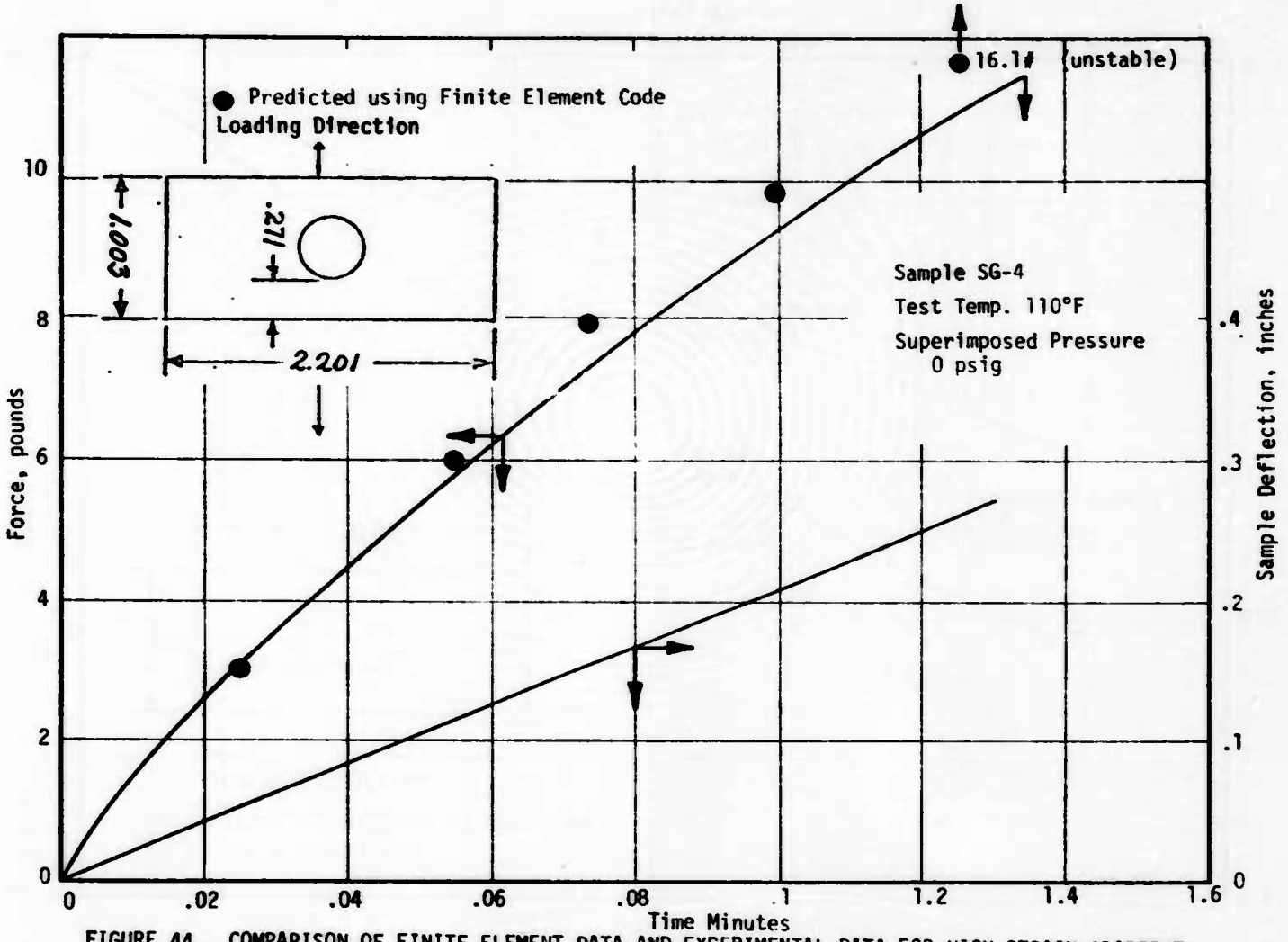

FIGURE 44. COMPARISON OF FINITE ELEMENT DATA AND EXPERIMENTAL DATA FOR HIGH STRAIN GRADIENT SAMPLES USING THE ANB-3124 PROPELLANT

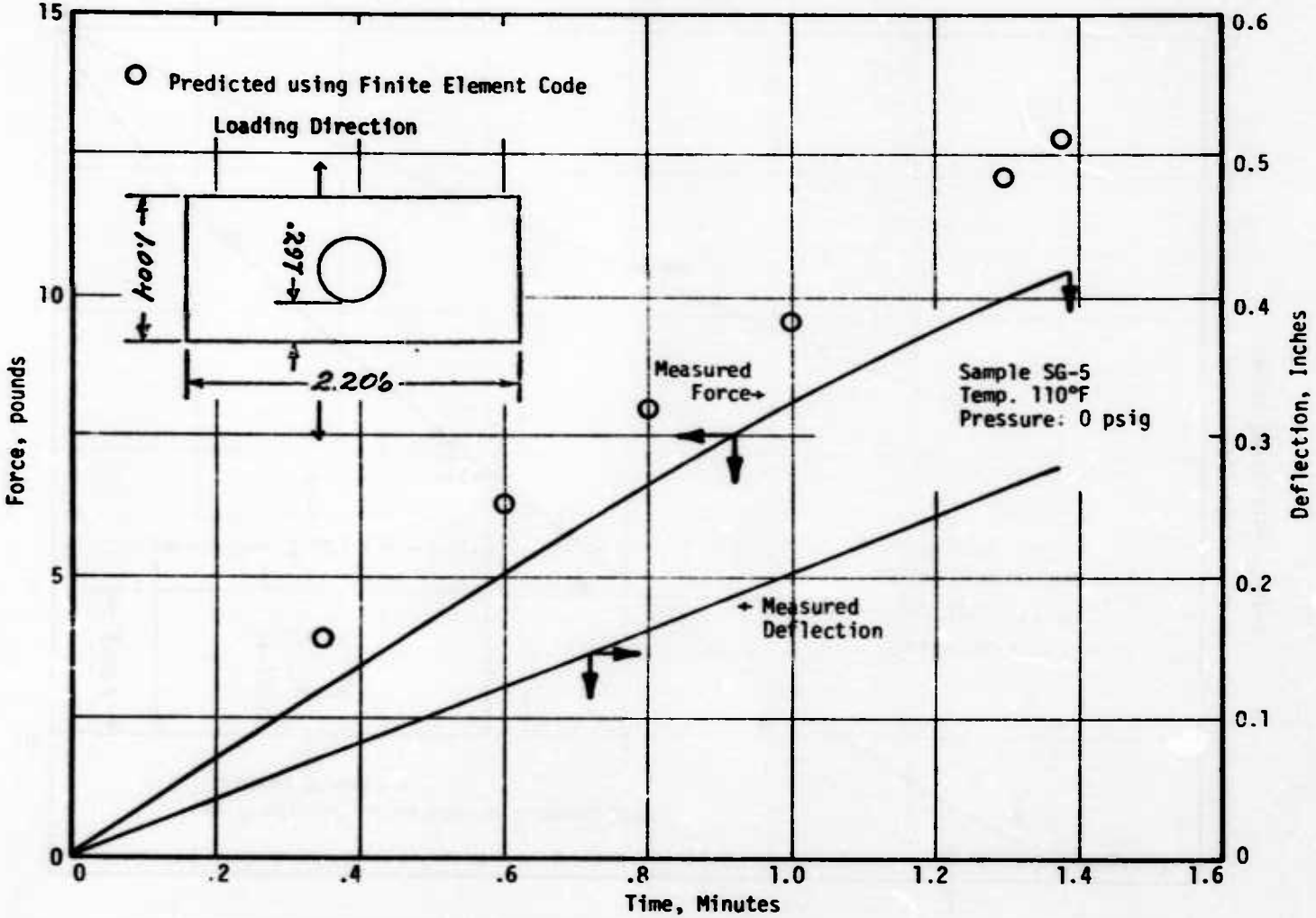

FIGURE 45. COMPARISON OF FINITE ELEMENT DATA AND EXPERIMENTAL DATA FOR HIGH STRAIN GRADIENT SAMPLES USING THE ANB-3124 PROPELLANT

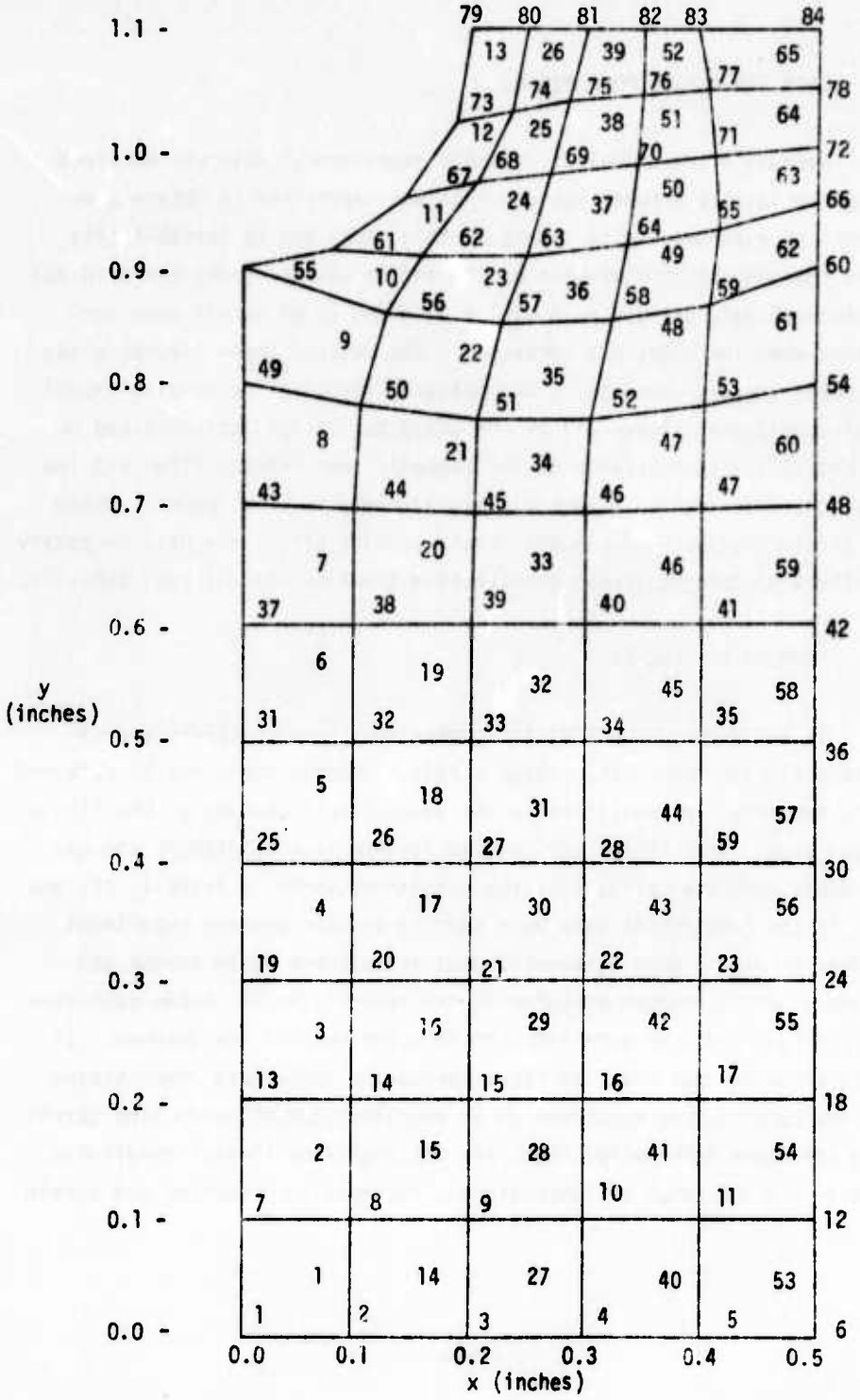

FIGURE 46. FINITE ELEMENT GRID MADE BY AUTOMATED GRID GENERATION PORTION OF CODE FOR SPECIMEN ANALYSES

D. DATA FOR FUTURE COMPARISONS

Because a great deal of valuable experimental data was obtained during the Task IV effort, for which it was impossible to obtain comparisons of experiment with theory at this time, due to instabilities within the plane stress protion of the finite element code, the original experimental data are given in Tables 8, 9 and 10 to permit such comparisons when the codes are corrected. The data in these figures gives the sample shapes, dimensions, and measured response for varying experimental conditions. Since all of the characterization data obtained on each propellant is available on the magnetic tape library files and the actual characterization parameters are included in this report. These high strain gradient experiments should provide all of the data necessary for others to test nonlinear constitutive theories against real behavior.

E. SUMMARY OF TASK IV

It was unfortunate that the comparisons between theory and experiment for specimens having high strain gradients could not be obtained due to numerical instabilities in the plane stress section of the finite element code. This leaves the program lacking in completeness and may cast doubt upon the validity of the results obtained in Tasks I, II, and III. If the comparisons were made and the results between experiment and theory were in good agreement, most researchers would accept the equations and techniques proposed in the report. As it stands such comparisons have not been made and, therefore, the results are unknown. It should be emphasized that the characterization codes have demonstrated that the constitutive equations do an excellent job of predicting stress state for known deformation histories for highly multiaxial conditions and over a great range of temperatures, deformation histories and strain

magnitudes to failure. The test conditions for these characterization experiments are actually idealized as having no spatial gradients of strain or stress since that, by definition, is an ideal characterization experiment. In reality, as has been discussed earlier, the biaxial strip sample does have strain gradients that can influence and introduce errors into the characterization when it is idealized as having no gradients.

No constitutive equation to date used in mechanics of materials considers the state of stress to be functionally related to the spatial gradients of strain. The stress state in continuum mechanics theory is developed through a series of axioms and postulates for the class of materials termined "Simple Materials" wherein, by definition, the stress state is at most dependent upon the history of the deformation gradients (strains) and independent of the strain gradients. The implications and consequences of stress being constitutively related to strain gradients would make characterization virtually impossible especially in materials that are not microscopically homogeneous such as propellants. Dealing then with the difficult but practical side and considering propellants to be within the domain of "Simple Materials", it has already been demonstrated that the proposed equations work well for specimens having no spatial gradients. Now in a finite element analysis using constant strain elements, such as the code described in Task III, the stress state in each element is determined solely by the history of the strains within that element and in no case is the constitutive equation in one element dependent upon the state of neighboring elements. That is not to say that the state of stress and strain in each element is not influenced by its neighbors through the equations of stress equilibrium and geometric strain compatibility, but rather that the constitutive equation does not depend upon

strain gradients. The finite element code is simply a sophisticated tool that determines the distribution of strain such that the compatibility, equilibrium and boundary conditions are satisfied.

Thus if the constitutive equation worked well for a great variety of characterization experiments and failed to compare with samples having strain gradients the fault must be in either of three areas: (1) the finite element codes are in error, (2) the experiments are in error, or (3) the constitutive equations are in error. In the first two situations comparisons cannot be made because of faulty technique.

TABLE 8

FORCE-VOLUME-DEFLECTION DATA FOR HIGH STRAIN GRADIENT EXPERIMENTS USING THE HERCULES PROPELLANT

Data Pt.	Temp. °F	Def. in.	Time	Force lb	ΔV_1 in^3
1	78	.014	.014	1.0	0.0
2	78	.034	.034	2.3	0.0
3	78	.054	.054	3.5	0.0
4	78	.074	.074	4.7	0.0
5	78	.094	.094	5.6	0.0
6	78	.114	.114	6.5	0.00015
7	78	.134	.134	7.2	0.00020
8	78	.154	.154	7.9	0.00025
9	78	.174	.174	8.3	0.00030
10	78	.194	.194	8.9	0.00040
11	78	.214	.214	9.2	0.00050
12	78	.234	.234	9.5	0.00070
13	78	.254	.254	9.8	0.00080
14	78	.274	.274	10.0	0.00100
15	78	.294	.294	10.0	0.00120
16	78	.314	.314	8.5	0.00135
17	78	.009	0.09	0.40	0.0
18	78	.019	0.19	0.90	0.0
19	78	.039	0.39	1.94	0.0
20	78	.059	0.59	2.90	0.0
21	78	.079	0.79	3.80	0.00004
22	78	.099	0.99	4.60	0.00006
23	78	.119	1.19	5.23	0.00010
24	78	.139	1.39	5.80	0.00015
25	78	.159	1.59	6.30	0.00019
26	78	.179	1.79	6.70	0.00020
27	78	.199	1.99	7.01	0.00024
28	78	.219	2.19	7.30	0.00035
29	78	.239	2.39	7.56	0.00040
30	78	.259	2.59	7.70	0.00050
31	78	.279	2.79	7.82	0.00060
32	78	.289	2.89	7.78	0.00065

(Pressure = 0 psig)

No. 1

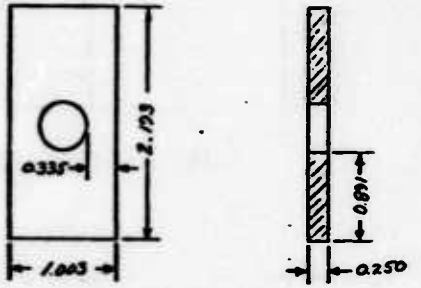

(Pressure = 0 psig)

No. 2

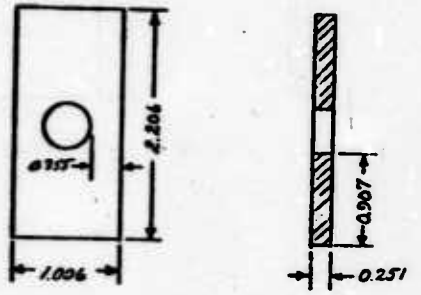

TABLE 8

FORCE-VOLUME-DEFLECTION DATA FOR HIGH STRAIN GRADIENT EXPERIMENTS USING THE HERCULES PROPELLANT (CONT.)

Data Pt.	Temp. °F	Def. in.	Time	Force lb	ΔV_1 in^3
1	79	.016	.016	1.03	0.0
2	79	.036	.036	2.25	0.0
3	79	.056	.056	3.48	0.0
4	79	.076	.076	4.50	0.0
5	79	.096	.096	5.40	0.00005
6	79	.116	.116	6.20	0.00010
7	79	.136	.136	6.90	0.00010
8	79	.156	.156	7.40	0.00015
9	79	.176	.176	7.90	0.00019
10	79	.196	.196	8.30	0.00022
11	79	.216	.216	8.61	0.00034
12	79	.236	.236	9.00	0.00043
13	79	.256	.256	8.22	0.00055
14	79	.276	.276	9.40	0.00070
15	79	.296	.296	9.50	0.00085
16	77	.01	.01	0.67	0.0
17	77	.03	.03	1.80	0.0
18	77	.05	.05	2.80	0.0
19	77	.07	.07	3.74	0.0
20	77	.09	.09	4.60	0.0
21	77	.11	.11	5.27	0.0
22	77	.13	.13	5.90	0.00010
23	77	.15	.15	6.30	0.00010
24	77	.17	.17	6.70	0.00015
25	77	.19	.19	7.02	0.00020
26	77	.21	.21	7.26	0.00029
27	77	.23	.23	7.42	0.00040
28	77	.25	.25	7.59	0.00060
29	77	.27	.27	7.62	0.00082
30	77	.29	.29	7.60	0.00122
31	77	.31	.31	7.20	0.00152

(Pressure = 0 psia)

No. 3

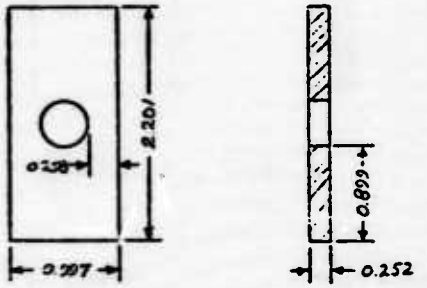

(Pressure = 0 psia)

No. 4

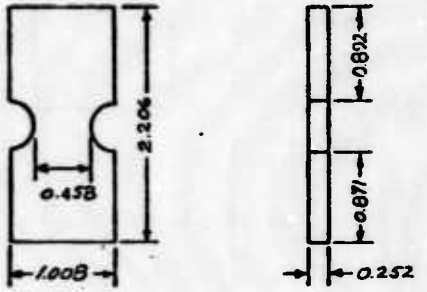

TABLE 8

FORCE-VOLUME-DEFLECTION DATA FOR HIGH STRAIN GRADIENT EXPERIMENTS USING THE HERCULES PROPELLANT (CONT.)

Data Pt.	Temp. °F	Def. in.	Time	Force lb	ΔV_1 in^3
1	77	.009	0.09	0.40	0.0
2	77	.029	0.29	1.40	0.0
3	77	.049	0.49	2.40	0.0
4	77	.069	0.69	3.20	0.0
5	77	.089	0.89	3.90	0.00006
6	77	.109	1.09	4.47	0.00010
7	77	.129	1.29	4.97	0.00012
8	77	.149	1.49	5.40	0.00015
9	77	.169	1.69	5.75	0.00018
10	77	.189	1.89	6.05	0.00021
11	77	.209	2.09	6.30	0.00027
12	77	.229	2.29	6.49	0.00036
13	77	.249	2.49	6.62	0.00041
14	77	.269	2.69	6.77	0.00060
15	77	.289	2.89	6.81	0.00078
16	77	.309	3.09	6.81	0.00100
17	77	.319	3.19	6.75	0.00120

(Pressure = 0 psig)

No. 5

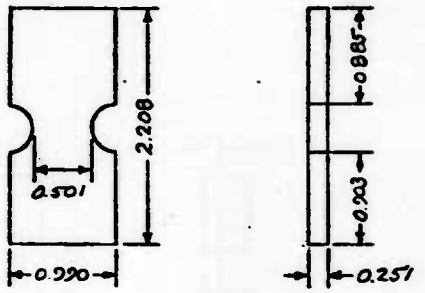

TABLE 8

FORCE-VOLUME-DEFLECTION DATA FOR HIGH STRAIN GRADIENT EXPERIMENTS USING THE HERCULES PROPELLANT (CONT.)

Data Pt.	Temp. °F	Def. in.	Time	Force lb	ΔV_1 in^3
1	77	0.012	0.12	0.74	0.0
2	77	0.022	0.22	1.10	0.0
3	77	0.042	0.42	1.74	0.0
4	77	0.052	0.52	2.13	0.0
5	77	0.062	0.62	2.50	0.0
6	77	0.072	0.72	2.85	0.0
7	77	0.077	0.77	3.00	0.0
8	77	0.077	0.82	2.83	0.0
9	77	0.077	0.92	2.70	0.0
10	77	0.077	1.12	2.55	0.0
11	77	0.077	1.62	2.40	0.0
12	77	0.077	2.12	2.32	0.0
13	77	0.077	3.12	2.20	0.0
14	77	0.077	3.39	2.20	0.0
15	77	0.080	3.42	2.55	0.0
16	77	0.090	3.52	3.16	0.0
17	77	0.100	3.62	3.54	0.00004
18	77	0.110	3.72	3.85	0.00010
19	77	0.120	3.82	4.10	0.00014
20	77	0.130	3.92	4.33	0.00018
21	77	0.140	4.02	4.50	0.00018
22	77	0.140	4.12	4.10	0.00018
23	77	0.140	4.32	3.85	0.00010
24	77	0.140	4.62	3.65	0.00010
25	77	0.140	5.12	3.51	0.00010
26	77	0.140	6.12	3.36	0.00017
27	77	0.140	6.56	3.32	0.00017
28	77	0.146	6.62	3.92	0.00019
29	77	0.156	6.72	4.44	0.00021
30	77	0.166	6.82	4.80	0.00024
31	77	0.176	6.92	5.00	0.00027
32	77	0.186	7.02	5.16	0.00030
33	77	0.196	7.12	5.35	0.00033
34	77	0.216	7.32	5.60	0.00043
35	77	0.241	7.57	5.87	0.00050
36	77	0.241	7.62	5.50	0.00050
37	77	0.241	7.82	5.04	0.00055
38	77	0.241	8.32	4.71	0.00059
39	77	0.241	9.12	4.44	0.00060
40	77	0.241	10.02	4.30	0.00061
41	77	0.251	10.12	5.10	0.00065
42	77	0.271	10.32	5.85	0.00074
43	77	0.301	10.62	6.24	0.00090
44	77	0.351	11.12	6.50	0.00130
45	77	0.381	11.42	6.35	0.00160

(Pressure = 0 psig)

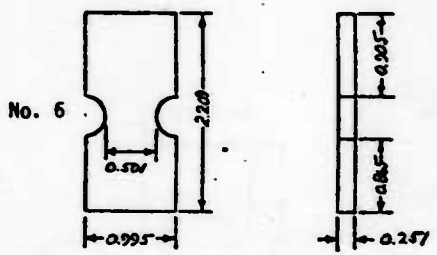

TABLE 8

FORCE-VOLUME-DEFLECTION DATA FOR HIGH STRAIN GRADIENT EXPERIMENTS USING THE HERCULES PROPELLANT (CONT.)

Data Pt.	Temp. °F	Def. in.	Time	Force lb	ΔV_1 in^3
1	77	.004	.004	0.40	0.0
2	77	.014	.014	1.27	0.0
3	77	.024	.024	2.04	0.0
4	77	.034	.034	2.80	0.0
5	77	.044	.044	3.50	0.0
6	77	.054	.054	4.12	0.0
7	77	.064	.064	4.65	0.0
8	77	.084	.084	5.55	0.0
9	77	.104	.104	6.40	0.0
10	77	.124	.124	7.10	0.00006
11	77	.144	.144	7.67	0.00014
12	77	.164	.164	8.26	0.00017
13	77	.184	.184	8.67	0.00020
14	77	.204	.204	9.05	0.00027
15	77	.224	.224	9.40	0.00035
16	77	.244	.244	9.75	0.00045
17	77	.264	.264	9.90	0.00060
18	77	.284	.284	10.00	0.00070
19	77	.304	.304	10.10	0.00085
20	77	.324	.324	9.88	0.00100
21	77	.029	0.29	1.70	0.0
22	77	.049	0.49	2.65	0.0
23	77	.069	0.69	3.55	0.0
24	77	.089	0.89	4.25	0.0
25	77	.109	1.09	4.85	0.0
26	77	.129	1.29	5.40	0.0
27	77	.149	1.49	5.90	0.0
28	77	.169	1.69	6.24	0.0
29	77	.189	1.89	6.60	0.0
30	77	.209	2.09	6.90	0.00005
31	77	.229	2.29	7.20	0.00010
32	77	.249	2.49	7.40	0.00010
33	77	.269	2.69	7.63	0.00012
34	77	.289	2.89	7.80	0.00012
35	77	.309	3.09	8.00	0.00018
36	77	.329	3.29	8.10	0.00020
37	77	.349	3.49	8.25	0.00022
38	77	.369	3.69	8.39	0.00035
39	77	.389	3.89	8.45	0.00039
40	77	.409	4.09	8.47	0.00041

No. 7 (Pressure = 0 psig)

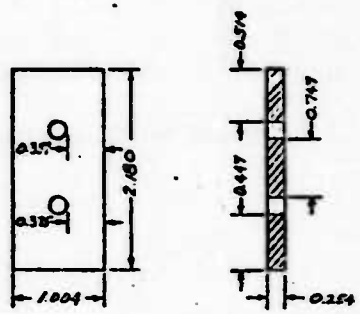

No. 8 (Pressure = 0 psig)

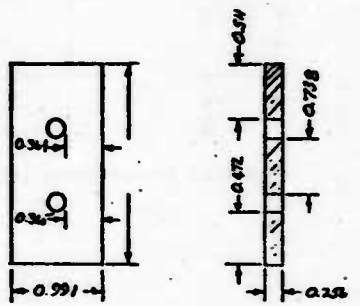

TABLE 8

FORCE-VOLUME-DEFLECTION DATA FOR HIGH STRAIN GRADIENT EXPERIMENTS USING THE HERCULES PROPELLANT (CONT.)

Data Pt.	Temp. °F	Def. in.	Time	Force lb	ΔV_1 in^3
1	77	.020	0.20	1.52	0.0
2	77	.040	0.40	2.63	0.0
3	77	.060	0.60	3.60	0.0
4	77	.080	0.80	4.40	0.0
5	77	.102	1.02	5.10	0.0
6	77	.132	1.32	6.00	0.0
7	77	.162	1.62	6.66	0.0
8	77	.192	1.92	7.23	0.0
9	77	.222	2.22	7.70	0.0
10	77	.252	2.52	8.10	0.0
11	77	.282	2.82	8.47	0.0
12	77	.312	3.12	8.76	0.0
13	77	.342	3.42	9.00	0.00004
14	77	.372	3.72	9.22	0.00006
15	77	.402	4.02	9.50	0.00007
16	77	.432	4.32	9.75	0.00008
17	77	.462	4.62	9.93	0.00009
18	77	.492	4.92	10.10	0.00011
19	77	.522	5.22	10.35	0.00014
20	77	.552	5.52	10.40	0.00017
21	77	.582	5.82	10.40	0.00017
22	77	.612	6.12	9.69	0.00018
23	77	.018	.018	1.00	0.0
24	77	.048	.048	2.73	0.0
25	77	.078	.078	4.22	0.0
26	77	.108	.108	5.60	0.0
27	77	.138	.138	6.75	0.0
28	77	.168	.168	7.65	0.0
29	77	.198	.198	8.40	0.0
30	77	.228	.228	9.02	0.0
31	77	.258	.258	9.50	0.0
32	77	.288	.288	9.92	0.0
33	77	.318	.318	10.33	0.0
34	77	.348	.348	10.70	0.0
35	77	.378	.378	11.10	0.0
36	77	.408	.408	11.30	0.0
37	77	.438	.438	11.56	0.0
38	77	.478	.478	11.80	0.0
39	77	.508	.508	11.65	0.0

(100 psi Superimposed Pressure)

No. 9

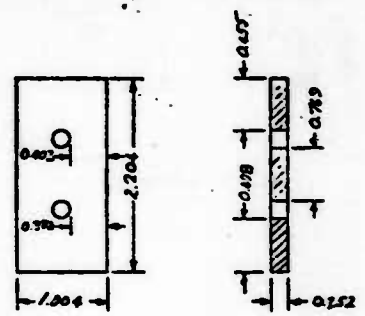

(100 psi Superimposed Pressure)

No. 11

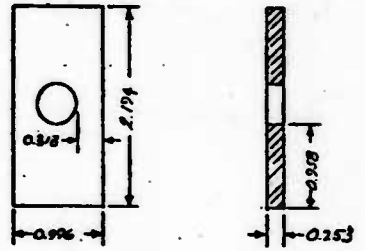

TABLE 8

FORCE-VOLUME-DEFLECTION DATA FOR HIGH STRAIN GRADIENT EXPERIMENTS USING THE HERCULES PROPELLANT (CONT.)

Data Pt.	Temp. °F	Def. in.	Time	Force lb	ΔV_1 in^3
1	77	0.014	0.14	1.30	0.0
2	77	0.044	0.44	2.91	0.0
3	77	0.074	0.74	4.15	0.0
4	77	0.104	1.04	5.17	0.0
5	77	0.134	1.34	5.99	0.0
6	77	0.164	1.64	6.65	0.0
7	77	0.194	1.94	7.10	0.0
8	77	0.224	2.24	7.67	0.0
9	77	0.254	2.54	8.09	0.0
10	77	0.284	2.84	8.43	0.0
11	77	0.314	3.14	8.74	0.0
12	77	0.344	3.44	9.00	0.0
13	77	0.374	3.74	9.30	0.0
14	77	0.404	4.04	9.50	0.0
15	77	0.434	4.34	9.70	0.0
16	77	0.474	4.74	9.80	0.0
17	77	0.494	4.94	9.20	0.0
18	77	.027	0.27	1.64	0.0
19	77	.057	0.57	3.03	0.0
20	77	.087	0.87	4.06	0.0
21	77	.117	1.17	4.99	0.0
22	77	.147	1.47	5.64	0.0
23	77	.177	1.77	6.19	0.0
24	77	.207	2.07	6.60	0.0
25	77	.237	2.37	7.00	0.0
26	77	.267	2.67	7.34	0.0
27	77	.297	2.97	7.60	0.0
28	77	.327	3.27	7.85	0.00006
29	77	.357	3.57	8.06	0.00009
30	77	.387	3.87	8.21	0.00013
31	77	.417	4.17	8.20	0.00015

(100 psi Superimposed Pressure)

No. 12

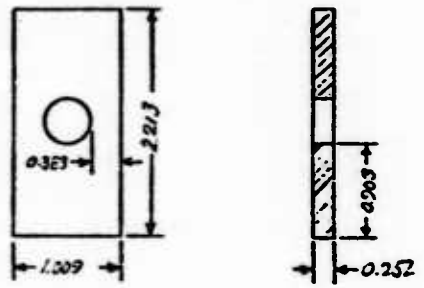

(100 psi Superimposed Pressure)

No. 13

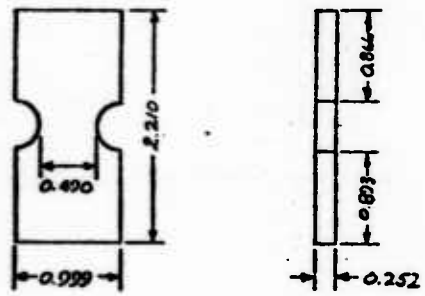

TABLE 8

FORCE-VOLUME-DEFLECTION DATA FOR HIGH STRAIN GRADIENT EXPERIMENTS USING THE HERCULES PROPELLANT (CONT.)

Data Pt.	Temp. °F	Def. in.	Time	Force lb	ΔV_1 in^3
1	78	.02	.02	1.25	0.0
2	78	.04	.04	2.30	0.0
3	78	.06	.06	3.20	0.0
4	78	.09	.09	4.30	0.0
5	78	.12	.12	5.15	0.0
6	78	.15	.15	5.90	0.0
7	78	.18	.18	6.50	0.0
8	78	.21	.21	6.90	0.0
9	78	.24	.24	7.40	0.0
10	78	.27	.27	7.67	0.0
11	78	.30	.30	8.00	0.00006
12	78	.33	.33	8.30	0.00008
13	78	.36	.36	8.56	0.00010
14	78	.39	.39	8.80	0.00015
15	78	.42	.42	9.04	0.00018
16	78	.45	.45	9.20	0.00022
17	78	.48	.48	9.20	0.00027
18	112	.02	.02	1.30	0.0
19	112	.07	.07	3.94	0.0
20	112	.12	.12	5.56	0.00008
21	112	.17	.17	6.59	0.00015
22	112	.22	.22	7.20	0.00030
23	112	.27	.27	7.50	0.00060
24	112				

(100 psi Superimposed Pressure)

No. 14

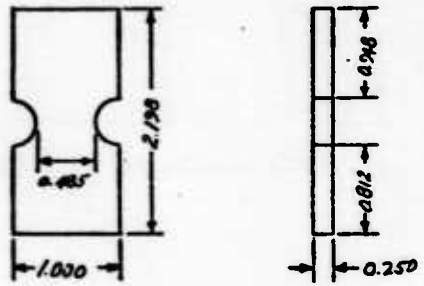

(Pressure = 0 psi)

No. 15

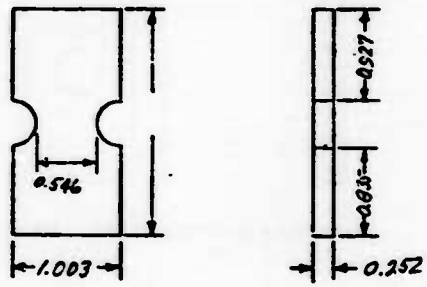

TABLE 8

FORCE-VOLUME-DEFLECTION DATA FOR HIGH STRAIN GRADIENT EXPERIMENTS USING THE HERCULES PROPELLANT (CONT.)

Data Pt.	Temp. °F	Def. in.	Time	Force lb	ΔV_1 in^3
1	77	.012	.012	1.04	0.0
2	77	.032	.032	2.80	0.0
3	77	.052	.052	4.20	0.0
4	77	.072	.072	5.49	0.0
5	77	.092	.092	6.45	0.0
6	77	.112	.112	7.40	0.0
7	77	.132	.132	8.13	0.00004
8	77	.152	.152	8.80	0.00005
9	77	.172	.172	9.39	0.00005
10	77	.192	.192	9.90	0.00005
11	77	.222	.222	10.50	0.00006
12	77	.252	.252	11.14	0.00006
13	77	.282	.282	11.64	0.00010
14	77	.312	.312	12.06	0.00010
15	77	.342	.342	12.40	0.00015
16	77	.372	.372	12.70	0.00019
17	77	.402	.402	13.05	0.00020
18	77	.432	.432	13.30	0.00021
19	77	.462	.462	13.50	0.00025
20	77	.492	.492	13.46	0.00030
21	112	.014	.014	0.80	0.0
22	112	.064	.064	3.30	0.00006
23	112	.114	.114	5.04	0.00010
24	112	.164	.164	6.18	0.00014
25	112	.214	.214	6.90	0.00026
26	112	.241	.241	7.16	0.00032
27	112	.254	.254	6.50	0.00040
28	112	.254	.254	6.04	0.00040
29	112	.254	.254	5.40	0.00038
30	112	.254	.729	4.90	0.00033
31	112	.259	.734	5.60	0.00034
32	112	.269	.744	6.20	0.00040
33	112	.289	.764	7.00	0.00044
34	112	.309	.784	7.40	0.00050
35	112	.339	.814	7.60	0.00070
36	112	.369	.844	7.70	0.00100
37	112	.379	.854	7.60	0.00112

(100 psi Superimposed Pressure)

No. 16

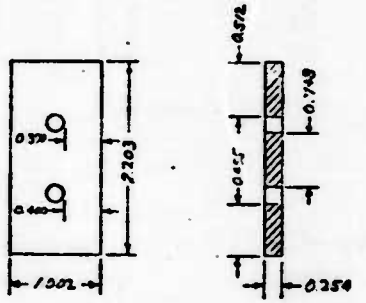

(Pressure = 0 psig)

No. 20

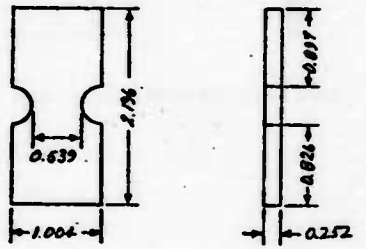

TABLE 8

FORCE-VOLUME-DEFLECTION DATA FOR HIGH STRAIN GRADIENT EXPERIMENTS USING THE HERCULES PROPELLANT (CONT.)

Data Pt.	Temp. °F	Def. in.	Time	Force lb	ΔV_1 in^3
1	78	.009	.009	0.63	0.0
2	78	.029	.029	1.80	0.0
3	78	.049	.049	2.97	0.0
4	78	.069	.069	4.00	0.0
5	78	.089	.089	4.90	0.0
6	78	.109	.109	5.78	0.0
7	78	.129	.129	6.63	0.0
8	78	.149	.149	7.40	0.0
9	78	.169	.169	7.98	0.0
10	78	.189	.189	8.50	0.0
11	78	.209	.209	9.00	0.0
12	78	.229	.229	9.46	0.0
13	78	.249	.249	9.90	0.0
14	78	.269	.269	10.17	0.0
15	78	.289	.289	10.55	0.0
16	78	.309	.309	10.79	0.0
17	78	.329	.329	11.05	0.0
18	78	.349	.349	11.30	0.0
19	78	.369	.369	11.50	0.0
20	78	.389	.389	11.60	0.0
21	78	.409	.409	11.24	0.0
22	112	.026	0.26	1.26	0.00002
23	112	.076	0.76	3.40	0.00014
24	112	.126	1.26	4.90	0.00020
25	112	.176	1.76	5.85	0.00034
26	112	.226	2.26	6.50	0.00040
27	112	.276	2.76	6.99	0.00059

(100 psi Superimposed Pressure)

No. 22

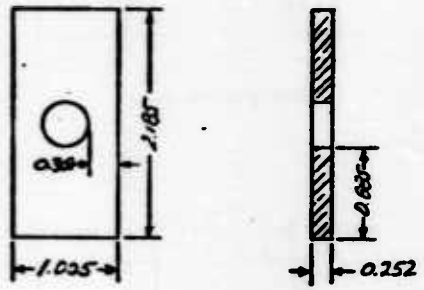

(Pressure = 0 psig)

No. 23

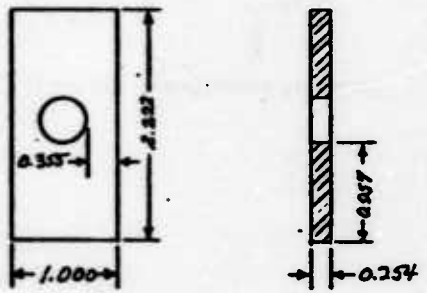

TABLE 8

FORCE-VOLUME-DEFLECTION DATA FOR HIGH STRAIN GRADIENT EXPERIMENTS USING THE HERCULES PROPELLANT (CONT.)

Data Pt.	Temp. °F	Def. in.	Time	Force lb	ΔV_1 in^3
1	110	.02	.02	1.10	0.0
2	110	.05	.05	2.45	0.0
3	110	.10	.10	4.55	0.00008
4	110	.15	.15	6.00	0.00018
5	110	.20	.20	7.00	0.00020
6	110	.25	.25	7.70	0.00040
7	110	.30	.30	8.19	0.00060
8	110	.33	.33	8.20	0.00078
9	107.0	0.0	0.0	0.0	
10	89.5	0.030	300.0	0.0	
11	65.0	0.066	660.0	1.1	
12	47.0	0.090	900.0	2.0	
13	43.0	0.096	960.0	2.9	
14	34.5	0.108	1080.0	3.4	
15	-2.5	0.150	1500.0	15.5	
16	-24.0	0.186	1860.0	10.0	
17	-42.0	0.216	2160.0	21.3	
18	-44.5	0.228	2280.0	26.5	
19	-45.0	0.234	2340.0	27.6	
20	107.0	0.0	0.0	0.0	
21	89.5	0.030	300.0	0.5	
22	65.0	0.066	660.0	2.0	
23	47.0	0.090	900.0	3.0	
24	43.0	0.096	960.0	4.0	
25	34.5	0.108	1080.0	4.5	
26	-2.5	0.150	1500.0	7.4	
27	-24.0	0.186	1860.0	13.3	
28	-42.0	0.216	2160.0	26.5	
29	-43.5	0.222	2220.0	28.0	

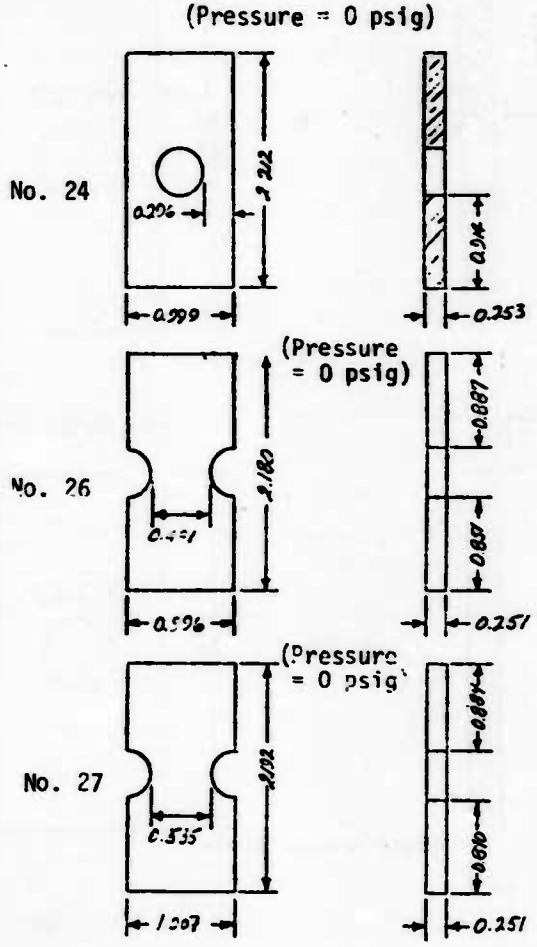

TABLE 9

FORCE-VOLUME-DEFLECTION DATA FOR HIGH STRAIN GRADIENT EXPERIMENTS USING THE AEROJET PROPELLANT

Data Pt.	Temp. °F	Def. in.	Time	Force lb	ΔV_1 in^3
1	110	.05	.025	3.00	0.0
2	110	.10	.055	5.75	0.0
3	110	.15	.075	7.30	0.0
4	110	.20	.100	9.20	0.0
5	110	.25	.125	10.90	0.0015
6	110	.27	.135	11.30	0.00020
7	110	.07	.35	3.0	0.0
8	110	.12	.60	5.0	0.0
9	110	.12	.30	6.5	0.0
10	110	.20	1.00	8.0	0.0
11	110	.26	1.30	10.0	0.0
12	110	.270	1.38	10.4	0.0

(Pressure = 0 psig)

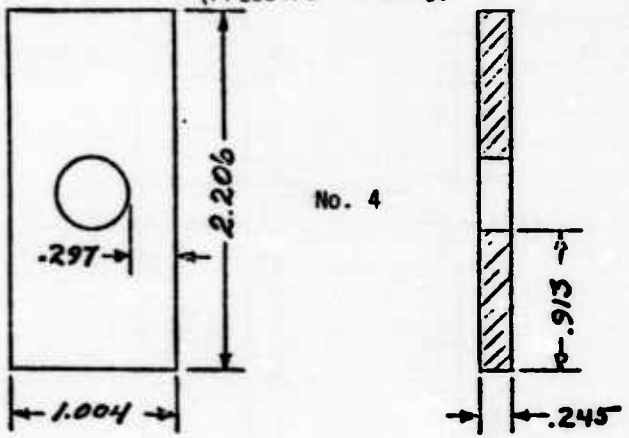

(Pressure = 0 psig)

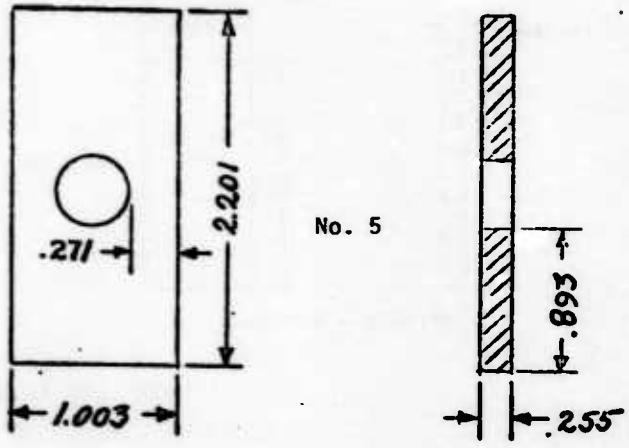

TABLE 9

FORCE-VOLUME-DEFLECTION DATA FOR HIGH STRAIN GRADIENT EXPERIMENTS USING THE AEROJET PROPELLANT (CONT.)

Data Pt.	Temp. °F	Def. in.	Time	Force lb	ΔV_1 in^3
1	110	.033	.066	1.90	0.0
2	110	.103	.206	5.00	0.0
3	110	.147	.294	6.80	0.0
4	110	.147	.326	6.00	0.0
5	110	.147	.526	5.00	0.0
6	110	.147	.700	4.75	0.0
7	110	.1775	.761	7.10	0.0
8	110	.2275	.861	9.50	0.0
9	110	.2675	.941	10.90	0.0

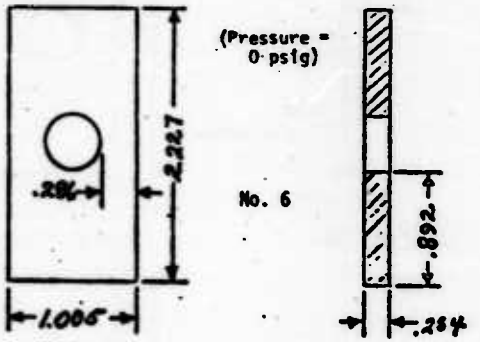

10	37	.040	.040	4.0	0.0
11	37	.070	.070	6.0	0.0
12	37	.120	.120	10.0	0.0
13	37	.160	.160	12.0	0.0
14	37	.210	.210	15.0	0.0002
15	37	.260	.260	17.0	0.0005
16	37	.280	.280	17.5	0.0007

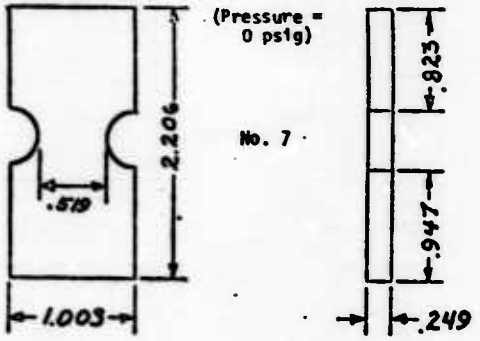

17	-1	.040	.040	6.7	0.0
18	-1	.080	.080	12.2	0.0
19	-1	.120	.120	16.7	0.00008
20	-1	.160	.160	20.5	0.00022
21	-1	.200	.200	23.5	0.00048
22	-1	.240	.240	25.4	0.00110
23	-1	.250	.250	25.7	0.00120

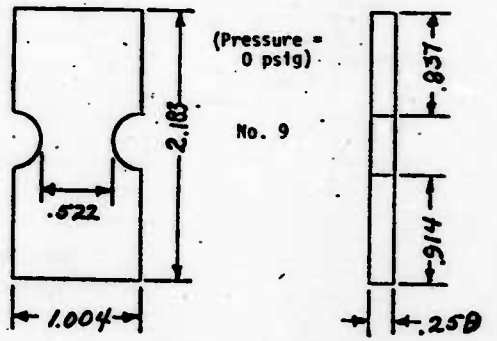

TABLE 9

FORCE-VOLUME-DEFLECTION DATA FOR HIGH STRAIN GRADIENT EXPERIMENTS USING THE AEROJET PROPELLANT (CONT.)

Data Pt.	Temp. °F	Def. in.	Time	Force lb	ΔV_1 in^3
1	110	.02	.019	1.5	0.0
2	110	.06	.030	4.0	0.0
3	110	.13	.065	8.0	0.00010
4	110	.19	.095	10.9	0.00016
5	110	.24	.120	12.9	0.00025
6	110	.26	.130	13.6	0.00035
7	110	.064	.32	3.2	0.0
8	110	.114	.57	5.5	0.0
9	110	.164	.82	7.7	0.0
10	110	.214	1.07	9.9	0.0
11	110	.264	1.32	11.8	0.0
12	110	.284	1.42	12.3	0.0
13	-1	.019	.019	4.0	0.0
14	-1	.039	.039	7.0	0.0
15	-1	.064	.064	9.8	0.0
16	-1	.104	.104	14.0	0.00008
17	-1	.139	.139	17.3	0.00016
18	-1	.174	.174	20.0	0.00032
19	-1	.204	.204	22.0	0.00055
20	-1	.239	.239	23.75	0.00088

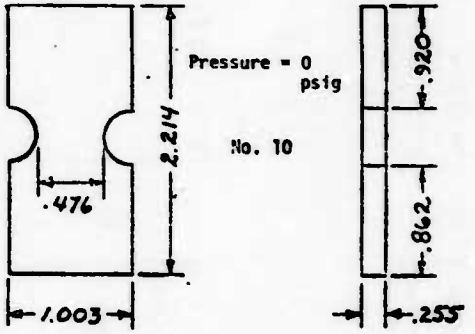

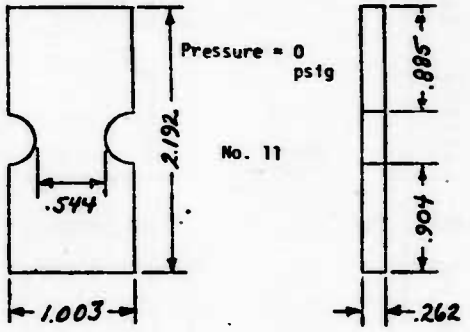

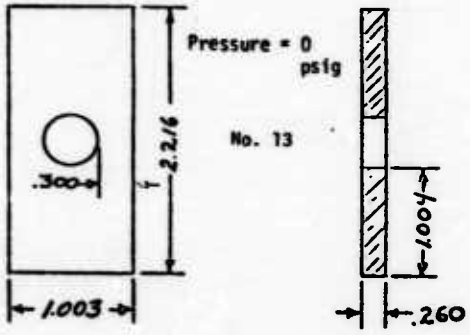

TABLE 9

FORCE-VOLUME-DEFLECTION DATA FOR HIGH STRAIN GRADIENT EXPERIMENTS USING THE AEROJET PROPELLANT (CONT.)

Data Pt.	Temp. °F	Def. in.	Time	Force lb	ΔV_1 in^3
1	-3	.026	.013	6.4	0.0
2	-3	.066	.033	13.3	0.0
3	-3	.096	.048	17.0	0.0
4	-3	.136	.068	21.5	0.00007
5	-3	.176	.088	25.1	0.00020
6	-3	.206	.103	27.0	0.00041
7	-3	.216	.108	27.3	0.00054
8	78	.026	.026	2.0	0.0
9	78	.066	.066	4.0	0.0
10	78	.116	.116	6.5	0.0
11	78	.166	.166	8.7	0.0
12	78	.216	.216	10.5	0.0
13	78	.236	.236	11.1	0.0
14	78	.246	.246	11.1	0.0
15	78	.04	.400	1.80	0.0
16	78	.09	.900	3.80	0.0
17	78	.14	1.400	5.60	0.0
18	78	.19	1.900	7.40	0.0
19	78	.24	2.400	9.05	0.0
20	78	.28	2.800	10.25	0.0
21	78	.29	2.900	10.30	0.0

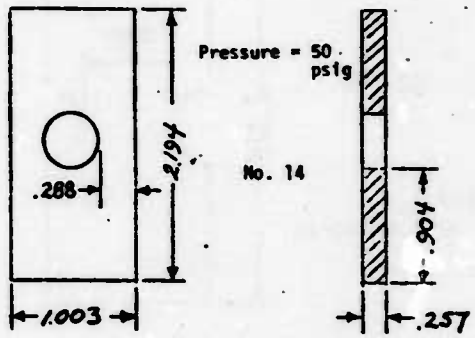

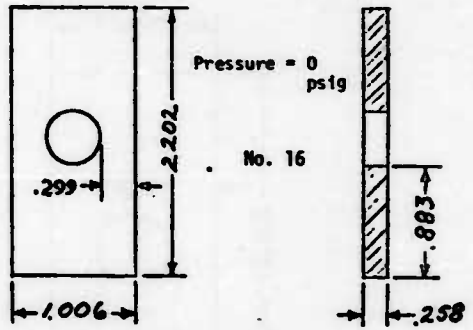

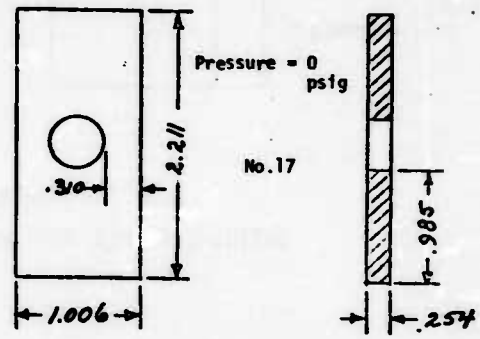

TABLE 9

FORCE-VOLUME-DEFLECTION DATA FOR HIGH STRAIN GRADIENT EXPERIMENTS USING THE AEROJET PROPELLANT (CONT.)

Data Pt.	Temp. °F	Def. in.	Time	Force lb	ΔV_1 in^3
1	78	.0205	.041	1.40	0.0
2	78	.0555	.111	3.40	0.0
3	78	.0875	.175	5.04	0.0
4	78	.0875	.221	4.30	0.0
5	78	.0875	.351	3.80	0.0
6	78	.0875	.504	3.55	0.0
7	78	.1060	.541	5.30	0.0
8	78	.1310	.591	6.80	0.0
9	78	.1610	.651	8.25	0.0
10	78	.1610	.691	7.20	0.0
11	78	.1610	.811	6.40	0.0
12	78	.1610	1.001	5.90	0.0
13	78	.1760	1.031	7.90	0.0
14	78	.1960	1.071	9.40	0.0
15	78	.2360	1.151	11.40	0.0
16	78	.2560	1.191	11.90	0.0
17	78	.2610	1.201	11.90	0.0
18	-3	.03	.06	5.5	0.0
19	-3	.06	.12	9.0	0.0
20	-3	.11	.22	14.0	0.0
21	-3	.11	.26	11.2	0.0
22	-3	.11	.44	9.0	0.0
23	-3	.11	.66	8.0	0.0
24	-3	.13	.70	14.0	0.00005
25	-3	.17	.78	18.9	0.00014
26	-3	.215	.87	22.4	0.00045
27	-3	.215	.90	18.7	0.00043
28	-3	.215	1.02	15.0	0.00040
29	-3	.215	1.46	12.3	0.00039
30	-3	.235	1.50	20.2	0.00050
31	-3	.255	1.90	23.3	0.00069
32	-3	.265	2.10	23.4	0.00074

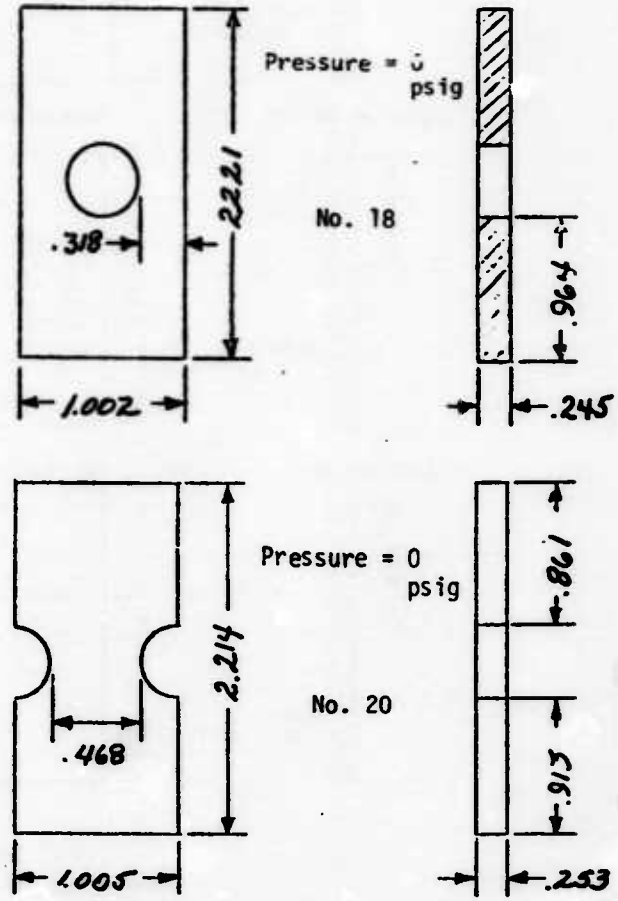

TABLE 9

FORCE-VOLUME-DEFLECTION DATA FOR HIGH STRAIN GRADIENT EXPERIMENTS USING THE AEROJET PROPELLANT (CONT.)

Data Pt.	Temp. °F	Def. in.	Time	Force lb	ΔV_1 in^3
1	-3	.036	.018	5.5	0.0
2	-3	.076	.038	10.5	0.0
3	-3	.146	.073	18.2	0.0
4	-3	.206	.103	23.6	0.00007
5	-3	.266	.133	25.5	0.00038
6	-3	.296	.148	29.2	0.00073
7	78	.03	.03	2.3	0.0
8	78	.08	.08	5.3	0.0
9	78	.12	.12	7.2	0.0
10	78	.15	.15	8.6	0.00006
11	78	.20	.20	10.7	0.00011
12	78	.24	.24	12.2	0.00020
13	78	.27	.27	13.2	0.00030
14	78	.03	.30	1.50	0.0
15	78	.08	.80	3.45	0.0
16	78	.13	1.30	5.25	0.0
17	78	.18	1.80	7.00	0.0
18	78	.23	2.30	8.60	0.0
19	78	.28	2.80	9.90	0.0
20	78	.29	2.90	9.96	0.0

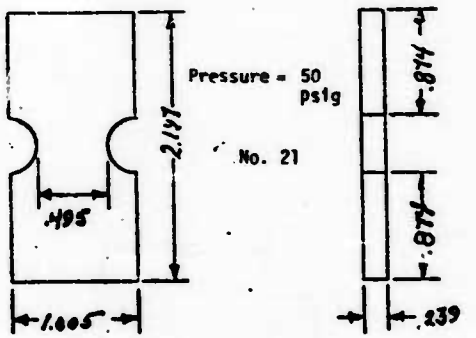

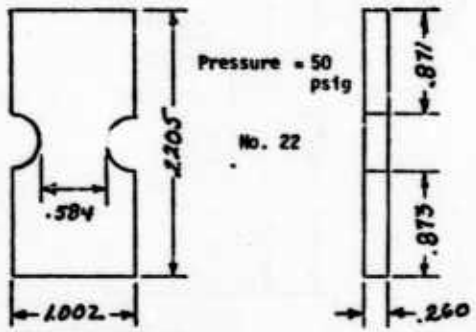

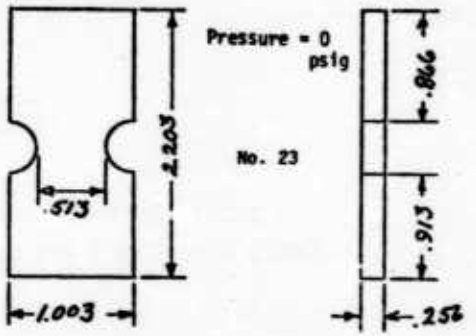

TABLE 9

FORCE-VOLUME-DEFLECTION DATA FOR HIGH STRAIN GRADIENT EXPERIMENTS USING THE AEROJET PROPELLANT (CONT.)

Data Pt.	Temp. °F	Def. in.	Time	Force lb	ΔV_1 in^3
1	78	.0500	.100	2.60	0.0
2	78	.0400	.180	4.80	0.0
3	78	.0500	.280	7.00	0.0
4	78	.0500	.310	6.20	0.0
5	78	.0500	.550	5.00	0.0
6	78	.0500	.788	4.70	0.0
7	78	.0710	.830	7.00	0.0
8	78	.1060	.900	9.00	0.0
9	78	.1285	.945	10.00	0.0
10	78	.1285	.970	8.85	0.0
11	78	.1285	1.160	7.40	0.0
12	78	.1285	1.474	6.70	0.0
13	78	.1415	1.500	8.80	0.0
14	78	.1765	1.570	11.40	0.0
15	78	.2115	1.640	12.80	0.0
16	78	.2215	1.660	12.95	0.0

(Pressure = 0 psig)

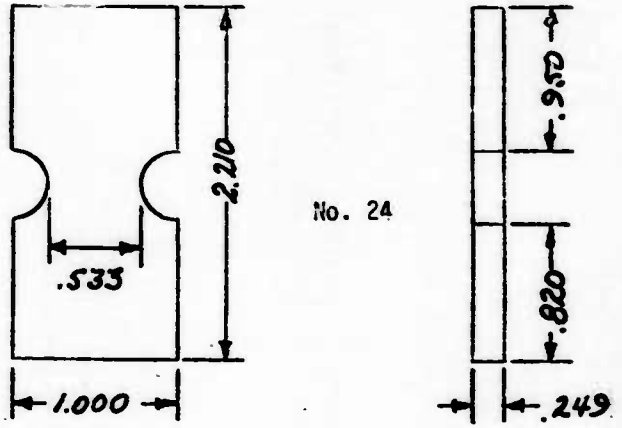

TABLE 10

FORCE-VOLUME-DEFLECTION DATA FOR HIGH STRAIN GRADIENT EXPERIMENTS USING THE THIOKOL PROPELLANT

Data Pt.	Temp. °F	Def. in.	Time	Force lb	ΔV_1 in^3
1	76	.025	.025	5.3	0.0
2	76	.050	.050	10.5	0.0
3	76	.075	.075	14.5	0.0
4	76	.100	.100	18.2	0.0002
5	76	.125	.125	21.4	0.0004
6	76	.150	.150	24.2	0.0007
7	76	.175	.175	26.5	0.0012
8	76	.225	.225	30.0	0.0027
9	76	.275	.275	32.1	0.0050
10	76	.325	.325	33.4	0.0082
11	76	.375	.375	34.0	0.0121
12	76	.425	.425	34.2	0.0166
13	76	.475	.475	34.1	0.0216
14	76	.525	.525	33.8	0.0268
15	76	.575	.575	32.8	0.0320
16	76	.625	.625	30.5	0.0371
17	76	.010	.010	3.50	0.0
18	76	.020	.020	5.50	0.0
19	76	.045	.045	10.50	0.0
20	76	.095	.095	18.50	0.0001
21	76	.145	.145	25.00	0.0005
22	76	.170	.170	27.70	0.0012
23	76	.220	.220	31.20	0.0027
24	76	.270	.270	33.50	0.0051
25	76	.320	.320	35.00	0.0086
26	76	.370	.370	35.50	0.0126
27	76	.420	.420	35.50	0.0174
28	76	.470	.470	35.00	0.0227
29	76	.520	.520	34.20	0.0280
30	76	.545	.545	33.50	0.0306

(Pressure = 0 psig)

No. 1

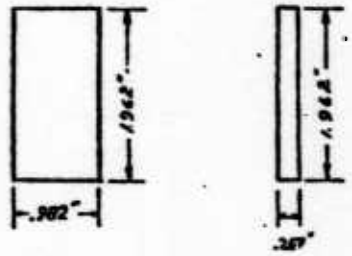

(Pressure = 0 psig

No. 2

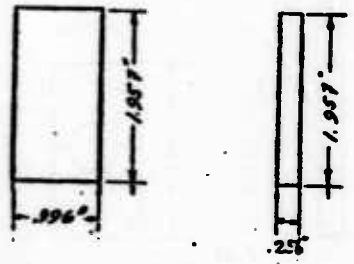

TABLE 10

FORCE-VOLUME-DEFLECTION DATA FOR HIGH STRAIN GRADIENT EXPERIMENTS USING THE THIOKOL PROPELLANT (CONT.)

Data Pt.	Temp. °F	Def. in.	Time	Force lb	ΔV_1 in^3	
1	71	.005	.005	1.25	0.0	(Pressure = 0 psig)
2	71	.015	.015	3.00	0.0	
3	71	.030	.030	4.80	0.0	
4	71	.055	.055	7.50	0.0	
5	71	.080	.080	10.20	0.0	No. 3
6	71	.105	.105	12.60	0.0	
7	71	.130	.130	14.90	0.0003	
8	71	.155	.155	16.85	0.0004	
9	71	.180	.180	18.55	0.0007	
10	71	.205	.205	19.60	0.0013	
11	71	.230	.230	19.70	0.0019	
12	71	.255	.255	15.25	0.0024	
13	71	.008	.008	1.60	0.0	(Pressure = 0 psig)
14	71	.023	.023	4.00	0.0	
15	71	.033	.033	5.50	0.0	
16	71	.058	.058	8.75	0.0	
17	71	.083	.083	11.50	0.0	
18	71	.108	.108	14.20	0.0002	No. 4
19	71	.133	.133	16.50	0.0004	
20	71	.158	.158	18.50	0.0006	
21	71	.183	.183	20.25	0.0009	
22	71	.208	.208	21.40	0.0015	
23	71	.233	.233	22.20	0.0023	
24	71	.258	.258	22.10	0.0030	
25	71	.283	.283	18.80	0.0040	
26	78	.010	.010	1.60	0.0	(Pressure = 0 psig)
27	78	.020	.020	2.90	0.0	
28	78	.070	.070	7.80	0.0	
29	78	.120	.120	12.60	0.0	
30	78	.170	.170	16.90	0.0004	
31	78	.195	.195	18.60	0.0008	No. 5
32	78	.220	.220	20.00	0.0012	
33	78	.245	.245	21.00	0.0018	
34	78	.270	.270	21.60	0.0025	
35	78	.295	.295	21.90	0.0034	
36	78	.320	.320	20.90	0.0043	
37	78	.345	.345	18.50	0.0049	

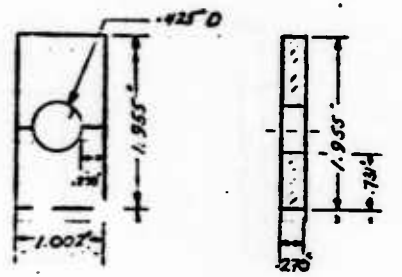

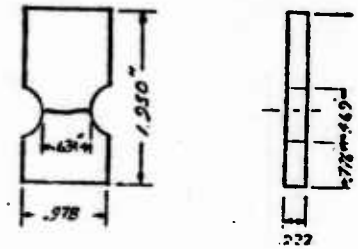

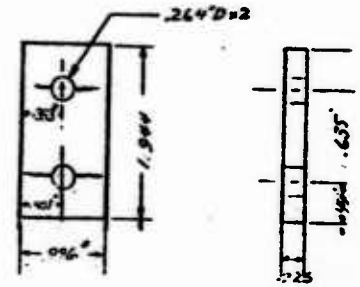

TABLE 10

FORCE-VOLUME-DEFLECTION DATA FOR HIGH STRAIN GRADIENT EXPERIMENTS USING THE THIOKOL PROPELLANT (CONT.)

Data Pt.	Temp. °F	Def. in.	Time	Force lb	ΔV_1 in^3	
1	78	.012	.012	1.90	0.0	
2	78	.027	.027	3.80	0.0	
3	78	.077	.077	9.30	0.0	
4	78	.127	.127	13.70	0.0	No. 6
5	78	.177	.177	17.20	0.0004	
6	78	.227	.227	19.50	0.0013	
7	78	.277	.277	20.50	0.0027	
8	78	.307	.307	19.50	0.0038	
9	77	.025	.025	2.70	0.0	
10	77	.075	.075	6.50	0.0	
11	77	.125	.125	9.60	0.0002	No. 7
12	77	.175	.175	12.00	0.0005	
13	77	.225	.225	13.20	0.0013	
14	77	.245	.245	12.30	0.0015	
15	77	.010	.010	3.00	0.0	
16	77	.060	.060	10.25	0.0	
17	77	.110	.110	16.25	0.0003	
18	77	.160	.160	20.90	0.0008	
19	77	.185	.185	24.20	0.0013	No. 8
20	77	.205	.205	20.00	0.0018	

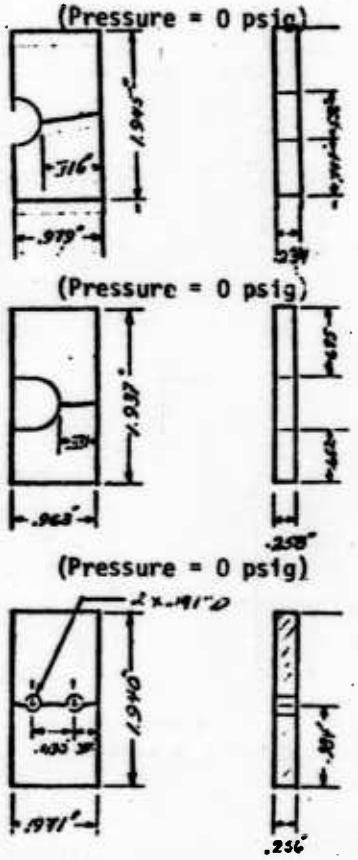

TABLE 10

FORCE-VOLUME-DEFLECTION DATA FOR HIGH STRAIN GRADIENT EXPERIMENTS USING THE THIOKOL PROPELLANT (CONT.)

Data Pt.	Temp. °F	Def. in.	Time	Force lb	ΔV_1 in^3
1	76	.010	.010	2.00	0.0
2	76	.060	.060	8.30	0.0
3	76	.110	.110	13.50	0.0
4	76	.160	.160	18.00	0.0004
5	76	.210	.210	21.00	0.0012
6	76	.235	.235	21.25	0.0018
7	76	.250	.250	19.00	0.0022
8	77	.018	.018	3.00	0.0
9	77	.038	.038	5.75	0.0
10	77	.063	.063	8.75	0.0
11	77	.088	.088	11.30	0.0
12	77	.113	.113	13.70	0.0
13	77	.138	.138	15.85	0.0003
14	77	.163	.163	17.60	0.0007
15	77	.188	.188	19.00	0.0012
16	77	.213	.213	19.50	0.0018
17	77	.238	.238	17.90	0.0024
18	77	.013	.026	1.85	0.0
19	77	.033	.066	3.85	0.0
20	77	.058	.116	6.40	0.0
21	77	.083	.166	8.75	0.0
22	77	.108	.216	10.85	0.00008
23	77	.133	.266	12.90	0.00019
24	77	.158	.316	14.80	0.00040
25	77	.183	.366	16.30	0.00078
26	77	.208	.416	17.50	0.00110
27	77	.233	.466	18.50	0.00176
28	77	.258	.516	18.90	0.00254
29	77	.283	.566	18.75	0.00340

No. 9

(Pressure = 0 psig)

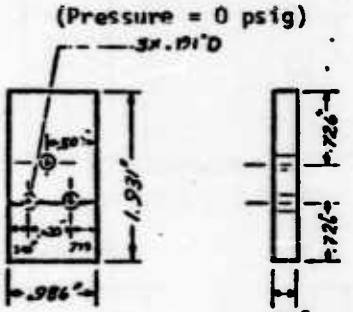

No. 10

(Pressure = 0 psig)

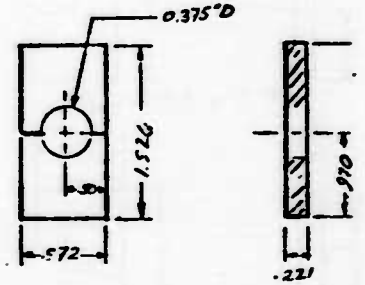

No. 11

(Pressure = 0 psig)

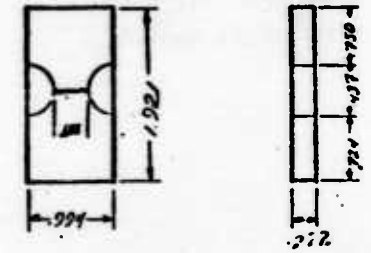

TABLE 10

FORCE-VOLUME-DEFLECTION DATA FOR HIGH STRAIN GRADIENT EXPERIMENTS USING THE THIOKOL PROPELLANT (CONT.)

Data Pt.	Temp. °F	Def. in.	Time	Force lb	ΔV_1 in^3
					(Pressure = 0 psig)
1	81	.01	.05	1.25	0.0
2	81	.04	.20	3.60	0.0
3	81	.07	.35	6.30	0.0
4	81	.10	.50	8.80	0.0
5	81	.13	.65	11.00	0.0
6	81	.16	.80	13.00	0.0003
7	81	.19	.95	14.75	0.0006
8	81	.22	1.10	16.25	0.0010
9	81	.25	1.25	17.25	0.0015
10	81	.28	1.40	18.00	0.0025
11	81	.31	1.55	18.05	0.0034
12	81	.34	1.70	16.80	0.0043
					(Pressure = 0 psig)
13	78	.011	.011	2.10	0.0
14	78	.026	.026	4.50	0.0
15	78	.041	.041	6.50	0.0
16	78	.056	.056	8.50	0.0
17	78	.071	.071	10.40	0.0
18	78	.086	.086	12.00	0.00005
19	78	.101	.101	13.60	0.0001
20	78	.116	.116	15.10	0.00024
21	78	.131	.131	16.40	0.00040
22	78	.146	.146	17.70	0.00046
23	78	.161	.161	18.75	0.00065
24	78	.176	.176	19.65	0.00090
25	78	.191	.191	20.40	0.00125
26	78	.206	.206	20.75	0.00175
27	78	.221	.221	20.60	0.00202
28	78	.236	.236	18.60	0.00240

No. 12

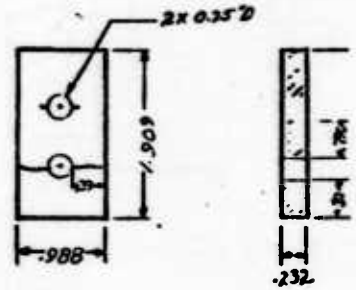

No. 13

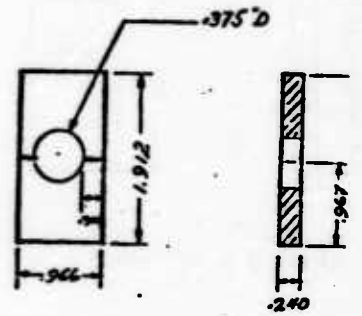

TABLE 10

FORCE-VOLUME-DEFLECTION DATA FOR HIGH STRAIN GRADIENT EXPERIMENTS USING THE THIOKOL PROPELLANT (CONT.)

Data Pt.	Temp. °F	Def. in.	Time	Force lb	ΔV_1 in^3
					(Pressure = 0 psig)
1	78	.015	.03	2.40	0.0
2	78	.030	.06	4.10	0.0
3	78	.045	.09	5.70	0.0
4	78	.060	.12	7.15	0.0
5	78	.075	.15	8.65	0.0
6	78	.090	.18	10.00	0.0
7	78	.105	.21	11.40	0.00007
8	78	.120	.24	12.70	0.00012
9	78	.135	.27	13.80	0.00020
10	78	.150	.30	14.80	0.00032
11	78	.165	.33	15.80	0.00050
12	78	.180	.36	16.55	0.00072
13	78	.195	.39	17.40	0.00098
14	78	.210	.42	17.90	0.00130
15	78	.225	.45	18.20	0.00170
16	78	.240	.48	18.20	0.00218
17	78	.255	.51	16.70	0.00260
					(Pressure = 0 psig)
18	78	.02	.10	2.50	0.0
19	78	.05	.25	5.75	0.0
20	78	.08	.40	8.90	0.0
21	78	.11	.55	11.60	0.0
22	78	.14	.70	14.00	0.00014
23	78	.17	.85	16.00	0.00024
24	78	.20	1.00	17.55	0.00045
25	78	.23	1.15	18.80	0.00070
26	78	.26	1.30	19.30	0.00107
27	78	.29	1.45	17.50	0.00136

No. 14

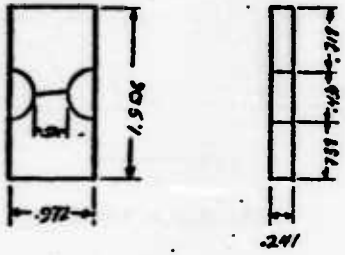

No. 15

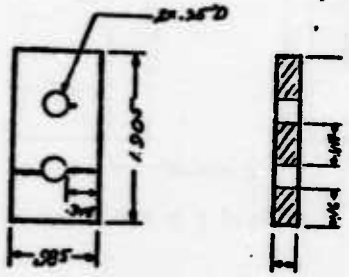

TABLE 10

FORCE-VOLUME-DEFLECTION DATA FOR HIGH STRAIN GRADIENT EXPERIMENTS USING THE THIOKOL PROPELLANT (CONT.)

Data Pt.	Temp. °F	Def. in.	Time	Force lb	ΔV_1 in^3
1	77	.011	.011	1.80	0.0
2	77	.026	.026	3.80	0.0
3	77	.041	.041	5.80	0.0
4	77	.056	.056	7.65	0.0
5	77	.071	.071	9.50	0.0
6	77	.086	.086	11.00	0.0
7	77	.101	.101	12.60	0.00004
8	77	.116	.116	14.10	0.00008
9	77	.131	.131	15.55	0.00014
10	77	.146	.146	16.85	0.00020
11	77	.161	.161	18.10	0.00030
12	77	.176	.176	19.25	0.00040
13	77	.191	.191	20.40	0.00055
14	77	.206	.206	21.25	0.00070
15	77	.221	.221	22.00	0.00090
16	77	.236	.236	22.70	0.00110
17	77	.251	.251	23.10	0.00135
18	77	.266	.266	22.70	0.00155
19	78	.010	.010	2.20	0.0
20	78	.020	.020	3.90	0.0
21	78	.030	.030	5.25	0.0
22	78	.045	.045	7.10	0.0
23	78	.065	.065	9.50	0.0
24	78	.090	.090	12.40	0.00005
25	78	.115	.115	15.20	0.00010
26	78	.140	.140	17.90	0.00020
27	78	.165	.165	20.30	0.00035
28	78	.190	.190	22.30	0.00055
29	78	.215	.215	24.20	0.00085
30	78	.240	.240	25.49	0.00124
31	78	.265	.265	26.40	0.00173
32	78	.290	.290	25.60	0.00233

(Pressure = 0 psig)

No. 16

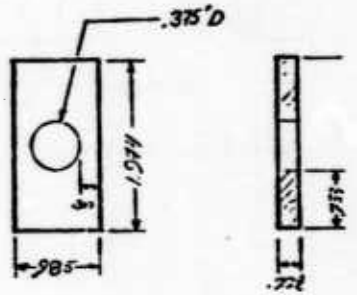

(Pressure = 0 psig)

No. 18

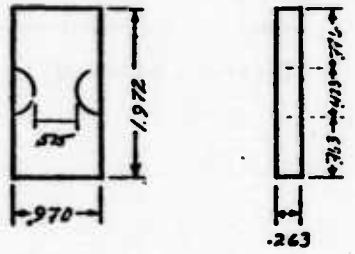

TABLE 10

FORCE-VOLUME-DEFLECTION DATA FOR HIGH STRAIN GRADIENT EXPERIMENTS USING THE THIOKOL PROPELLANT (CONT.)

Data Pt.	Temp. °F	Def. in.	Time	Force lb	ΔV_1 in^3
1	77	.0125	.125	1.25	0.0
2	77	.0275	.275	2.60	0.0
3	77	.0425	.425	3.80	0.0
4	77	.0575	.575	5.05	0.0
5	77	.0725	.725	6.25	0.0
6	77	.0875	.875	7.50	0.0
7	77	.1025	1.025	8.60	0.0
8	77	.1175	1.175	9.80	0.0
9	77	.1325	1.325	11.00	0.00004
10	77	.1475	1.475	12.25	0.00008
11	77	.1625	1.625	13.35	0.00010
12	77	.1775	1.775	14.30	0.00015
13	77	.1925	1.925	15.15	0.00020
14	77	.2075	2.075	16.10	0.00030
15	77	.2225	2.225	17.00	0.00040
16	77	.2375	2.375	17.80	0.00050
17	77	.2525	2.525	18.50	0.00061
18	77	.2675	2.675	19.00	0.00079
19	77	.2825	2.825	19.55	0.00095
20	77	.2975	2.975	19.90	0.00115
21	77	.3125	3.125	19.25	0.00130
22	78	.009	.009	1.50	0.0
23	78	.019	.019	3.20	0.0
24	78	.034	.034	5.15	0.0
25	78	.059	.059	8.30	0.0
26	78	.084	.084	11.00	0.0
27	78	.109	.109	13.55	0.0
28	78	.134	.134	16.10	0.0001
29	78	.159	.159	18.40	0.0002
30	78	.184	.184	20.50	0.0004
31	78	.209	.209	22.40	0.0006
32	78	.234	.234	24.00	0.0008
33	78	.259	.259	25.30	0.0012
34	78	.284	.284	26.25	0.0016
35	78	.309	.309	26.50	0.0020

(Pressure = 0 psig)

No. 19

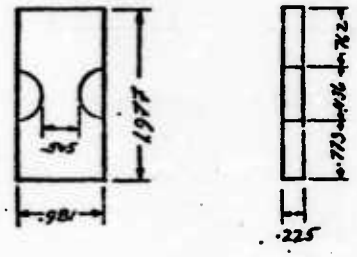

(Pressure = 0 psig)

No. 20

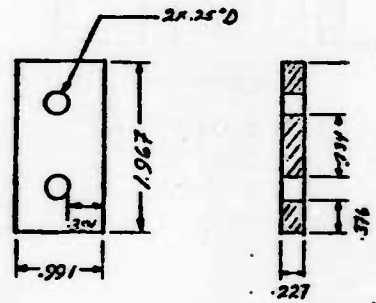

TABLE 10

FORCE-VOLUME-DEFLECTION DATA FOR HIGH STRAIN GRADIENT EXPERIMENTS USING THE THIOKOL PROPELLANT (CONT.)

(Pressure = 0 psig)

No. 21

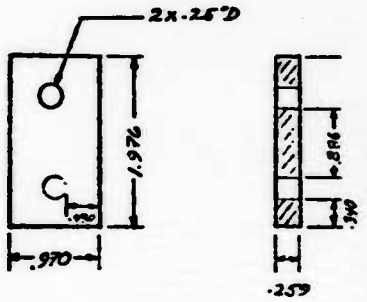

Data Pt.	Temp. °F	Def. in.	Time	Force lb	ΔV_1 in^3
1	77	.010	.10	1.10	0.0
2	77	.035	.35	3.25	0.0
3	77	.060	.60	5.50	0.0
4	77	.085	.85	7.75	0.0
5	77	.110	1.10	10.00	0.0
6	77	.135	1.35	12.45	0.00005
7	77	.160	1.60	14.55	0.00011
8	77	.185	1.85	16.60	0.00019
9	77	.210	2.10	18.60	0.00030
10	77	.235	2.35	20.40	0.00044
11	77	.260	2.60	22.00	0.00061
12	77	.285	2.85	23.40	0.00090
13	77	.310	3.10	24.45	0.00118
14	77	.335	3.35	24.50	0.00150

TABLE 10

FORCE-VOLUME-DEFLECTION DATA FOR HIGH STRAIN GRADIENT EXPERIMENTS USING THE THIOKOL PROPELLANT (CONT.)

(Pressure = 0 psig)

No. 22

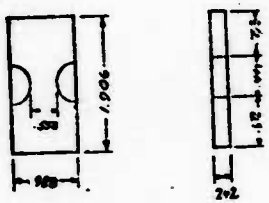

Data Pt.	Temp. °F	Def. in.	Time	Force lb	ΔV_1 in^3
1	77	.02	.10	2.50	0.0
2	77	.04	.20	4.60	0.0
3	77	.06	.30	6.50	0.0
4	77	.08	.40	8.40	0.0
5	77	.098	.49	10.00	0.0
6	77	.098	.50	8.80	0.0
7	77	.098	.55	7.65	0.0
8	77	.098	.65	6.80	0.0
9	77	.098	.80	6.20	0.0
10	77	.098	1.05	5.65	0.0
11	77	.098	1.55	5.14	0.0
12	77	.098	1.78	5.00	0.0
13	77	.102	1.80	7.60	0.0
14	77	.112	1.85	10.00	0.0
15	77	.122	1.90	11.50	0.0
16	77	.132	1.95	12.55	0.0001
17	77	.142	2.00	13.50	0.0002
18	77	.148	2.03	14.00	0.0003
19	77	.148	2.05	12.20	0.0003
20	77	.148	2.10	10.70	0.0003
21	77	.148	2.15	10.05	0.0003
22	77	.148	2.25	9.25	0.0003
23	77	.148	2.40	8.63	0.0003
24	77	.148	2.55	8.22	0.00025
25	77	.148	2.80	7.80	0.00020
26	77	.148	3.30	7.25	0.00020
27	77	.148	3.44	7.20	0.00015
28	77	.150	3.45	9.70	0.00015
29	77	.160	3.50	13.60	0.00030
30	77	.170	3.55	15.10	0.00040
31	77	.180	3.60	16.00	0.00050
32	77	.190	3.65	16.70	0.00060
33	77	.200	3.70	17.30	0.00075
34	77	.210	3.75	17.80	0.00100
35	77	.216	3.78	17.92	0.00120
36	77	.216	3.80	15.60	0.00120
37	77	.216	3.85	13.66	0.00120
38	77	.216	3.90	12.75	0.00120
39	77	.216	4.00	11.70	0.00130
40	77	.216	4.30	10.40	0.00130
41	77	.216	4.92	9.30	0.00130
42	77	.222	4.95	13.40	0.00140
43	77	.232	5.00	16.80	0.00150
44	77	.242	5.05	17.80	0.00190
45	77	.252	5.10	18.15	0.00220
46	77	.262	5.15	17.60	0.00250

TABLE 10

FORCE-VOLUME-DEFLECTION DATA FOR HIGH STRAIN GRADIENT EXPERIMENTS USING THE THIOKOL PROPELLANT (CONT.)

Data Pt.	Temp. °F	Def. in.	Time	Force lb	ΔV_1 in^3
1	-1.0	.015	.015	13.0	0.0
2	-1.0	.030	.030	25.0	0.0
3	-1.0	.045	.045	33.6	0.0
4	-1.0	.060	.060	39.9	0.0
5	-1.0	.075	.075	44.0	0.0001
6	-1.0	.090	.090	48.0	0.0004
7	-1.0	.105	.105	51.0	0.00075
8	-1.0	.120	.120	52.7	0.00135
9	-1.0	.135	.135	54.0	0.00180
10	-1.0	.150	.150	54.1	0.00250
11	-1.0	.165	.165	54.1	0.00335
12	-1.0	.180	.180	53.9	0.00425
13	-1.0	.195	.195	49.0	0.00500
14	-1.0	.0075	.075	3.0	0.0
15	-1.0	.0175	.175	6.9	0.0
16	-1.0	.0325	.325	12.4	0.0
17	-1.0	.0475	.475	16.6	0.0
18	-1.0	.0625	.625	20.7	0.0
19	-1.0	.0775	.775	24.6	0.0
20	-1.0	.0925	.925	27.9	0.0
21	-1.0	.1075	1.075	30.1	0.00025
22	-1.0	.1225	1.225	32.2	0.00050
23	-1.0	.1375	1.375	33.5	0.00090
24	-1.0	.1525	1.525	34.9	0.00120
25	-1.0	.1675	1.675	35.4	0.00190
26	-1.0	.1825	1.825	36.0	0.00250
27	-1.0	.1975	1.975	36.0	0.00320
28	-1.0	.2125	2.125	35.4	0.00400
29	-1.0	.2275	2.275	33.6	0.00480

(Pressure = 0 psig)

No. 27

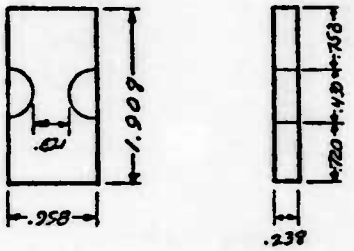

(Pressure = 0 psig)

No. 28

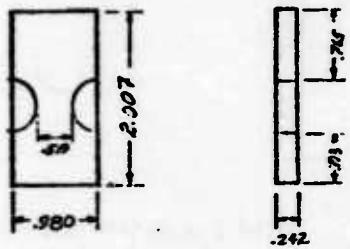

TABLE 10

FORCE-VOLUME-DEFLECTION DATA FOR HIGH STRAIN GRADIENT EXPERIMENTS USING THE THIOKOL PROPELLANT (CONT.)

Data Pt.	Temp. °F	Def. in.	Time	Force lb	ΔV_1 in^3
					(Pressure = 0 psig)
1	-1.0	.006	.006	7.4	0.0
2	-1.0	.016	.016	16.5	0.0
3	-1.0	.026	.026	23.0	0.0
4	-1.0	.036	.036	28.5	0.0
5	-1.0	.046	.046	32.2	0.0001
6	-1.0	.056	.056	37.8	0.0001
7	-1.0	.071	.071	43.4	0.0003
8	-1.0	.086	.086	47.3	0.0005
9	-1.0	.101	.101	50.5	0.0008
10	-1.0	.116	.116	53.0	0.0012
11	-1.0	.131	.131	54.8	0.0018
12	-1.0	.146	.146	55.0	0.0026
13	-1.0	.161	.161	55.0	0.0035
14	-1.0	.176	.176	51.0	0.0043
					(Pressure = 0 psig)
15	0.0	.008	.08	4.6	0.0
16	0.0	.013	.13	4.8	0.0
17	0.0	.018	.18	8.8	0.0
18	0.0	.028	.28	11.9	0.0
19	0.0	.038	.38	15.4	0.0
20	0.0	.053	.53	21.3	0.0
21	0.0	.068	.68	25.8	0.0
22	0.0	.083	.83	29.6	0.0001
23	0.0	.098	.98	32.3	0.0004
24	0.0	.113	1.13	35.0	0.0007
25	0.0	.128	1.28	37.0	0.0010
26	0.0	.143	1.43	38.8	0.0014
27	0.0	.158	1.58	40.0	0.0018
28	0.0	.173	1.73	40.9	0.0025
29	0.0	.188	1.88	41.2	0.0037
30	0.0	.203	2.03	41.0	0.0040
31	0.0	.218	2.18	39.5	0.0048
32	0.0	.233	2.33	35.0	0.0055

No. 29

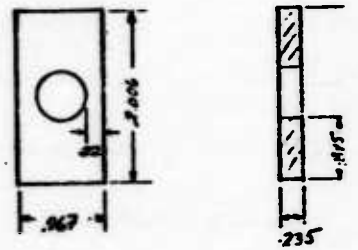

No. 30

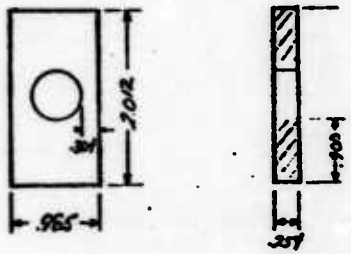

TABLE 10

FORCE-VOLUME-DEFLECTION DATA FOR HIGH STRAIN GRADIENT EXPERIMENTS USING THE THIOKOL PROPELLANT (CONT.)

Data Pt.	Temp. °F	Def. in.	Time	Force lb	ΔV_1 in^3
1	0.0	.0175	.175	5.70	0.0
2	0.0	.0375	.375	12.00	0.0
3	0.0	.0575	.575	18.70	0.0
4	0.0	.0735	.735	22.80	0.0
5	0.0	.0735	.739	19.50	0.0
6	0.0	.0735	.839	16.00	0.0
7	0.0	.0735	.989	13.80	0.0
8	0.0	.0735	1.489	11.10	0.0
9	0.0	.0735	2.489	9.06	0.0
10	0.0	.0735	3.989	7.80	0.0
11	0.0	.0735	5.489	7.00	0.0
12	0.0	.0785	5.539	14.00	0.0
13	0.0	.0885	5.639	21.25	0.0001
14	0.0	.1035	5.789	26.60	0.0003
15	0.0	.1235	5.989	31.10	0.0006
16	0.0	.1485	6.239	34.75	0.0011
17	0.0	.1535	6.289	35.10	0.0013
18	0.0	.1535	6.339	30.00	0.0014
19	0.0	.1535	6.489	23.75	0.0015
20	0.0	.1535	6.739	20.15	0.0015
21	0.0	.1535	6.989	18.48	0.0015
22	0.0	.1535	7.989	15.15	0.0015
23	0.0	.1535	8.989	13.55	0.0015
24	0.0	.1535	9.939	12.65	0.0018
25	0.0	.1585	9.989	20.00	0.0020
26	0.0	.1635	10.039	25.00	0.0020
27	0.0	.1735	10.139	31.50	0.0024
28	0.0	.1835	10.239	34.55	0.0026
29	0.0	.1985	10.389	37.00	0.0032
30	0.0	.2135	10.539	37.75	0.0039
31	0.0	.2285	10.689	37.50	0.0050
32	0.0	.2435	10.839	36.50	0.0061
33	0.0	.2585	10.989	34.00	0.0069
34	151	.048	.048	3.20	0.0
35	151	.073	.073	4.75	0.0
36	151	.098	.098	6.25	0.0
37	151	.123	.123	7.60	0.0
38	151	.148	.148	9.00	0.0
39	151	.173	.173	10.25	0.00008
40	151	.198	.198	11.50	0.00015
41	151	.223	.223	12.60	0.00020
42	151	.248	.248	13.60	0.00030
43	151	.273	.273	14.40	0.00044
44	151	.298	.298	14.95	0.00061

(Pressure = 0 psig)

No. 31

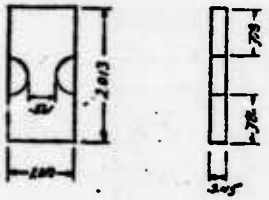

(Pressure = 0 psig)

No. 32

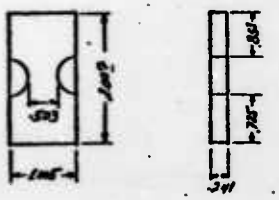

TABLE 10

FORCE-VOLUME-DEFLECTION DATA FOR HIGH STRAIN GRADIENT EXPERIMENTS USING THE THIOKOL PROPELLANT (CONT.)

Data Pt.	Temp. °F	Def. in.	Time	Force lb	ΔV_1 in^3
1	150	.060	.060	3.75	0.0
2	150	.085	.085	5.30	0.0
3	150	.110	.110	6.90	0.0
4	150	.135	.135	8.50	0.0
5	150	.160	.160	10.00	0.0
6	150	.185	.185	11.50	0.00009
7	150	.210	.210	12.90	0.00017
8	150	.235	.235	14.20	0.00022
9	150	.260	.260	15.50	0.00038
10	150	.285	.285	16.50	0.00051
11	150	.310	.310	17.25	0.00070
12	150	.320	.320	17.40	0.00075
13	77	.020	.20	1.80	0.0
14	77	.045	.45	4.00	0.0
15	77	.070	.70	6.05	0.0
16	77	.095	.95	8.30	0.0
17	77	.120	1.20	10.25	0.00008
18	77	.145	1.45	12.25	0.00014
19	77	.170	1.70	14.25	0.00020
20	77	.195	1.95	15.90	0.00030
21	77	.220	2.20	17.50	0.00042
22	77	.245	2.45	18.80	0.00070
23	77	.270	2.70	19.00	0.00092

(Pressure = 0 psig)

No. 35

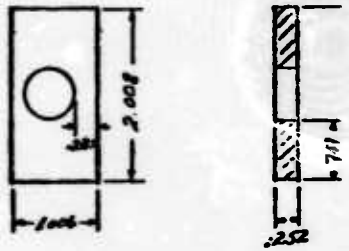

(Pressure = 0 psig)

No. 38

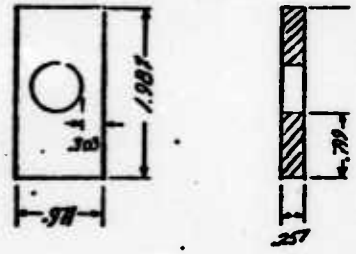

TABLE 10

FORCE-VOLUME-DEFLECTION DATA FOR HIGH STRAIN GRADIENT EXPERIMENTS USING THE THIOKOL PROPELLANT (CONT.)

Data Pt.	Temp. °F	Def. in.	Time	Force lb	ΔV_1 in^3
1	121.0	.006	60	0.0	
2	116.0	.012	120	0.0	
3	116.0	.018	180	0.0	
4	112.0	.024	240	0.5	
5	111.5	.030	300	0.8	
6	108.0	.042	420	0.8	
7	104.0	.054	540	0.9	
8	99.5	.060	660	1.0	
9	96.0	.078	780	2.0	
10	86.0	.102	1020	3.6	
11	76.0	.126	1260	5.0	
12	68.0	.150	1500	6.3	
13	52.0	.174	1740	8.1	
14	30.0	.198	1980	10.0	
15	9.5	.222	2220	13.8	
16	-5.0	.234	2340	16.5	
17	-12.0	.240	2400	17.2	
18	-14.5	.246	2460	14.8	
19	-19.0	.251	2508	12.0	
20	-22.0	.252	2520	6.0	
21	-25.0	.258	2580	8.2	
22	-35.0	.270	2700	12.0	
23	-36.0	.294	2940	12.8	
24	121.0	.006	60	0.0	
25	116.0	.012	120	0.0	
26	116.0	.018	180	0.0	
27	112.0	.024	240	0.5	
28	111.5	.030	300	0.8	
29	108.0	.042	420	0.8	
30	104.0	.054	540	0.9	
31	99.5	.066	660	1.0	
32	96.0	.078	780	2.0	
33	86.0	.102	1020	3.2	
34	76.0	.126	1260	4.5	
35	68.0	.150	1500	5.4	
36	52.0	.174	1740	7.1	
37	30.0	.198	1980	9.0	
38	9.5	.222	2220	12.0	
39	-14.5	.246	2460	17.0	
40	-25.0	.258	2580	19.0	
41	-30.0	.264	2640	17.4	
42	-35.0	.270	2700	10.3	
43	-34.0	.276	2760	1.2	

(Pressure = 0 psig)

No. 39

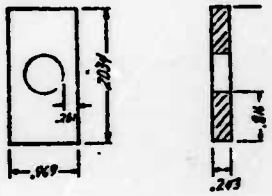

(Pressure = 0 psig)

No. 40

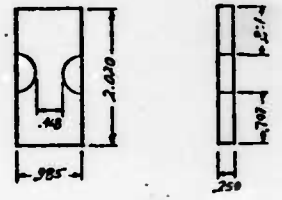

SECTION 7

RECOMMENDATIONS FOR FUTURE WORK

All of the problems associated with obtaining an accurate structural analysis of a solid propellant motor were not addressed during this program. Although this contract was successful in meeting the objective defined in Tasks I, II, and III, analytical computer difficulties prevented completion of the analyses section of Task IV. However, even if this program had been one hundred percent successful and the methods proposed were put into immediate use, many problems significant to practical propellant grain stress analyses would remain unresolved. The discussion below defines problems that must be studied sometime in the future if accurate analytical techniques are to be employed in obtaining accurate grain stress analyses.

A. FINITE ELEMENT CODE DEVELOPMENT

The computer code developed in Task III of this contract is the first 2-dimensional finite element code capable of linear elastic, linear viscoelastic, and nonlinear viscoelastic stress analyses. Features included in the code are the capability of using orthotropic shell elements, a finite measure of dilatation and hence conservation of mass, and the capability to handle transient thermal and pressure loads. Overall this is an excellent code and has features designed specifically for handling real propellant behavior. Since this represents the first attempt at such a code, some deficiencies such as the poor convergence experienced during nonlinear plane stress solutions are to be expected. It is therefore recommended that an effort be funded to improve and refine this nonlinear finite element code so that it can be of better use to the industry.

B. DILATATIONAL CONSTITUTIVE EQUATION

The nonlinear viscoelastic constitutive equations developed to date on this and previous contracts appear to do an excellent job handling the distortional stress-strain behavior of propellants, but appear to be lacking in precision for the dilatational relationships. There are several possible reasons for such behavior: namely dilatation is difficult to measure, the bulk stress must be calculated in many experiments, and the dilatation changes by several orders of magnitude during an experiment. Nevertheless there appears to be a deficiency in describing dilatational behavior that when found will greatly improve the precision of the dilatational constitutive equation. To date there has been little actual work in this area and much could be accomplished. If such relationships could be developed they would be excellent equations to use in preliminary design and failure analyses since dilatation caused by vacuoles is the first sign of failure in propellant.

C. AGING EFFECTS

Even after the problems of improved analysis methods and failure criteria are successfully handled for unaged propellants, the accuracy of grain structural integrity evaluations will still be subjected to the limitations imposed by inadequate knowledge of propellant aging behavior. If the propellant were aged while in the unstressed state, or if the propellant were truly elastic, the problem would be quite simple, since only a re-characterization of the properties would be required. However, when aging occurs under conditions of stress and strain, the problem is more complex, even if the aging process is not coupled by stress. The differences between aging then deforming, deforming then aging, or deforming and aging simultaneously can result in large stress differences similar to those observed when specimens are cooled then stretched, stretched then

cooled, or cooled and stretched simultaneously. Obviously, the aging stress-strain functional should be very path sensitive. Experimental observations indicate that during aging under deformed conditions such things as postcure, oxidative crosslinking, or any mechanism leading to chain scission and reformation can cause large changes in the grain stress-free temperature, or the grain stress-free configuration.

Today aged propellant structures are generally treated as though they were purely elastic, that is, their reference stress-free configurations never changes, and the aging process is not stress or strain-coupled. This is an oversimplification. It is interesting to note from the work of Tobolsky (15) that many crosslinked amorphous polymeric materials, which are normally thought of as elastic, can undergo large amounts of permanent set or changes in reference configuration during aging while exhibiting little or no change in response properties. Similar behavior has been observed with propellants but it usually receives little attention in aging evaluations, even though the shifting in the stress-free configuration for many systems is probably more important to consider in an analysis than changes in response properties.

The need for aging type constitutive equations will be very difficult to satisfy for many reasons. First, aging is a chemical phenomenon which in itself is not clearly understood. Secondly, aging-type constitutive equations are in principle easy to construct, but in practice, interpreting the chemical or physical phenomenon in an abstract mathematical functional relationship will require a significant effort. Further, to make the mathematical development possible the proper types of experimental data must be obtained. Currently, all that is done is to age and then test. What is really required is to test and age simultaneously, something that is relatively difficult and rarely done except in real motors. Again, to make this information useful stress analysis programs would have to be rewritten to account for the aging phenonomenon.

Conventionally, aging studies are conducted by chemists or statisticians with little training or experience in the area of applied mechanics. Aging tests historically have not been designed to characterize the material response, but as quality control tests which hopefully will show trends and give some estimate of useful life. Factors important to a stress analysis, such as changes in reference configuration, are rarely, if ever, considered. Any insight gained into the chemical-mechanical response of aged grains is valuable and can be used qualitatively, if not quantitatively.

In summary, good constitutive theory and good analysis methods are needed for unaged propellant grains to initially design a good system. Aging constitutive equations are needed to predict what will happen to that system with time, and thereby allow determination of environmental restrictions and margins of safety required in the initial design to assure a successful storage and service life.

SECTION 8

REFERENCES

1. Farris, R. J., and Schapery, R. A., "Development of a Solid Rocket Propellant Nonlinear Constitutive Theory", Report No. AFRPL-TR-73-50 (June 1973).

2. "Applications of Non-Linear Viscoelasticity and Cumulative Damage (A Realistic Evaluation of Real Propellant Behavior)" NOSC Contract No. N00017-70-C-4441, Aerojet Solid Propulsion Company, Final Report 1565-26F (May 1971).

3. AFOSR, Themis Contract F-44620-68-C-0022, University of Utah Report, UTEC TH 70-083 (June 1970).

4. Farris, R. J., "Homogeneous Constitutive Equations for Materials with Permanent Memory", Ph.D. Dissertation, College of Engineering, University of Utah (June 1970).

5. Farris, R.J., "Applications of Viscoelasticity of Filled Materials", Master's Thesis, University of Utah, Department of Civil Engineering (June 1969).

6. Leeming, H. et. al., "Final Report, Solid propellant Structural Test Vehicle and Systems Analysis", Final Report No. AFRPL-TR-70-10, Lockheed Propulsion Company (March 1970).

7. Williams, M. L., Landel, R. R., and Ferry, J. D., J Am. Chem. Soc. 77, 3701 (1955).

8. Farris, R. J., "Dilatation of Granular Filled Elastomers Under High Rates of Strain", J. Appl. Polymer Sci., 8, page 25 (1964).

9. Farris, R. J., "The Influence of Vacuole Formation on the Response and Failure of Highly Filled Polymers", Trans. Soc. Rheol., 12, 315-334 (1968).

10. Farris, R. J., and Steele, R. D., "Strain Measuring Extensometer", Bulletin of the 5th Meeting of the ICRPG Mechanical Behavior Working Group, CPIA Publication No. 119, Vol. I, p. 1 (October 1966).

11. Herrmann, L. R., "Elasticity Equations for Incompressible and Nearly Incompressible Materials by a Variational Theorem", AIAA J., 3, No. 10, pp. 1896-1901 (October 1965).

12. Herrmann, L. R., "Developments Relating to the Linear and Nonlinear Thermo-Viscoelastic Analysis of Solid propellant Grains", Consulting Report to the Aerojet-General Corporation (December 1969).

13. Zienkiewicz, O. C., "The Finite Element Method in Engineering Science", McGraw-Hill, London (1971).

14. Bills, K. W., Jr., et. al., "Solid Propellant Cumulative Damage Program", Final Report No. AFRPL-TR-68-131, Contract No. F04611-67-C-0102 (October 1968).

15. Tobolsky, A. v., Properties and Structure of Polymers, 160, John Wiley and Sons, Inc., New York (1960).

APPENDIX A

APPLICATION OF VISCOELASTIC FRACTURE MECHANICS TO NONLINEAR BEHAVIOR AND FRACTURE OF SOLID PROPELLANT

APPLICATION OF VISCOELASTIC FRACTURE MECHANICS TO NONLINEAR BEHAVIOR AND FRACTURE OF SOLID PROPELLANT

R. A. Schapery

July 1974

I. INTRODUCTION AND SUMMARY

Farris and Fitzgerald (A-1) first proposed the use of Lebesgue norms of strain in a constitutive theory for solid propellant in order to account for the effect of microstructural damage. Farris then successfully characterized nonlinear viscoelastic behavior of solid propellant under constant and transient temperatures, first in the range of negligible vacuole dilatation (A-2, A-3) and then with vacuole dilatation (A-4); the effect of superposed hydrostatic pressure is included in the study in (A-4). A physical basis for the Lebesgue norm of strain was provided by Farris (A-5) using a one-dimensional model; this norm was shown to be a natural measure for representing the global effect of microstructural damage in particle-reinforced (elastic) rubber when local failure of polymer strands obeys a linear cumulative damage rule in strain.

An alternative approach to characterizing the effect of microstructural damage on overall mechanical response was recently proposed by Schapery (A-4). Specifically, a constitutive equation was derived by bringing together a recently developed viscoelastic theory of crack growth (A-6), statistical properties of the microstructure, and an idealized model that accounts for the influence of microcracking on softening of the bulk composite material. This fracture mechanics approach enabled Schapery to relate global mechanical response to basic fracture and viscoelastic properties and to variations in these quantities (such as produced by environmental changes and chemical aging).

In this Appendix, the same basic theory of crack growth is used to predict the effect of stress and temperature histories and aging on the statistical distribution of failure times of specimens. Such predictions form an important part of structural reliability analysis. Also included in this report are further considerations in the area of nonlinear constitutive equations which deal with the effects of superposed pressure and healing of microcracks.

A brief review of the equations governing viscoelastic crack growth is given in Section II. Determination of the frequency distribution of failure times and prediction of the probability of failure under time-varying loads, pressure, and temperature are covered in Section III. In Section IV some experimental results are given which appear to bring out the effect of microcrack healing on overall stress-strain behavior. Also examined briefly is the effect of pressure and the question of whether or not Lebesgue norms of stress or strain (or both) should be used in a basic constitutive theory for solid propellant.

II. VISCOELASTIC CRACK GROWTH THEORY

In this section we model the small initial (natural) flaws as cracks and use the viscoelastic fracture mechanics theory in (A-6) to predict the effect of applied loading history on the extent of microcrack and macrocrack growth. (A "microcrack" is defined as a crack whose length and/or width is on the order of or less than the mean particle diameter; a "macrocrack" is a crack whose length and width are much larger than the mean particle diameter and spacing.) It will be seen how the analysis of microcrack growth and arrest can be used to develop a nonlinear constitutive equation for solid propellant, and how macrocrack growth considerations yield a stochastic model for gross specimen failure. Although the former analysis was detailed previously (A-4), we shall cover the essential points here in order to help bring out the similarities and differences in the use of fracture mechanics for constitutive equations and failure theory.

A. Microcrack Model

We assume, for simplicity, that a propellant specimen is subjected to an external uniaxial tensile stress, $\sigma = \sigma(t)$, and that all cracks propagate in only the so-called opening mode. Generalization to account for other crack propagation modes and more general states of stress are discussed later. It is supposed that there exists an initial distribution of microcracks within the binder and possibly between binder and particles; the size of each crack is assumed to be defined by a single parameter, $2a_o$, representing the initial length or diameter of the crack. As the loading on the body is increased from zero, a given crack will start to grow when the stress intensity factor* at the tip, N_o, exceeds a certain critical value, N_{or}. This value is identical to that for an elastic continuum whose Young's modulus, E, and Poisson's ratio, ν, are equal to the long-time (rubbery) values E_r and ν_r, respectively, for the actual viscoelastic material; thus

$$N_{or} = \sqrt{\frac{\Gamma E_r}{\pi(1 - \nu_r^2)}} \tag{A-1}$$

where Γ is the fracture energy appropriate to cohesive or adhesive failure (depending on the location of the crack tip). If the stress intensity factor equals or exceeds the value based on initial (glassy) modulus E_g and Poisson's ratio ν_g (which value is given by Eq. (A-1) except the subscript "r" is replaced by "g") then the crack velocity is

---

*The stress intensity factor is defined in the singular stress distribution near the crack tip,

$$\sigma_y = N_o/\sqrt{x} \tag{A-2}$$

where σ_y is the stress normal to the crack plane and x is the distance ahead of the tip.

predicted to be very high, and is limited only by wave action. We shall say that the binder material in the neighborhood of a microcrack of interest is "failed" if $N_o \geq N_{og}$; the time at which N_{og} is first reached will be called the failure time.

The crack growth theory in (A-6) can be used to predict time-dependent crack size (when $N_{or} < N_o < N_{og}$) and failure time for each microcrack in a specimen under the following assumptions: (i) the rubber binder is linearly viscoelastic; (ii) the Poisson's ratio of the binder is constant (we shall assume $\nu = 1/2$); (iii) all filler particles are rigid relative to the binder; and (iv) the composite specimen is linearly viscoelastic with crack sizes fixed, and is under a spacewise uniform temperature.

Now the crack velocity, $\dot{a}$, when $N_{or} < N_o < N_{og}$, is governed by the equation

$$D_m(t_\alpha) = \frac{4\Gamma}{3\pi N_o^2} \tag{A-3}$$

with

$$t_\alpha = \alpha/3\dot{a} \tag{A-4}$$

and

$$\alpha = \pi^2 N_o^2/\sigma_m^2 I_1^2 \tag{A-5}$$

where existing information on rubber suggests that the fracture energy, Γ, and the stress distribution in the failure zone next to the tip (as defined by $\sigma_m I_1$ in (A-6)*) are constant. The quantity $D_m(t_\alpha)$ is the in situ creep compliance of the binder in uniaxial tension expressed in terms of the "effective time," t_α; also, α is the length of the failure zone next to the crack tip over which the material disintegrates.

It is next assumed that during most or all of the time required for local failure, the binder creep compliance is given by the power law,†

$$D_m(t) = (t/a_T)^n D_1 \tag{A-6}$$

---

*σ_m is the maximum stress in the failure zone and $0 < I_1 \leq 2$; for a uniformly distributed stress in this zone, $I_1 = 2$.

†However, at very short and long times, $D_m(t) \to E_g^{-1}$ and $D_m(t) \to E_r^{-1}$, respectively.

where n is a constant; D_1 is assumed constant except for effects of aging. Also, from the time the body is first loaded, t = 0, to the failure time for a given crack, we assume the crack is isolated. That is, the crack is assumed to be so small that the only geometric parameter affecting crack growth is its own instantaneous length or diameter, 2a. In support of this point for cracks which are initially isolated, it is shown in (A-6) that the crack size at 90 percent of the failure time is only 10^n x $(2a_o)$; e.g., if n = 0.3, most of the time required for failure is consumed while the crack doubles in size.

The stress intensity factor for the i^{th} isolated crack satisfying the assumptions (i) - (iv) listed just above Eq.(A-3) can be written in the form (A-6):

$$N_{oi} = \sqrt{a_i}\, f_i\, \sigma \qquad \text{(A-7)}$$

where $2a_i$ is the size of the i^{th} crack, and the coefficient f_i is a measure of the state of stress existing in the binder in the neighborhood of the i^{th} crack relative to the applied stress σ; the coefficient f_i, which will be called a stress concentration factor, is independent of material properties and stress, and depends only on the local particle geometry and spacing; dimensional analysis can be used to easily prove this statement. According to the theory in (A-6), Eq. (A-7) is identical to the stress intensity factor in an elastic binder; thus, in principle, elastic analysis can be used to derive f_i. f_i is assumed to be unaffected by other cracks.

We combine Eqs. (A-3 - A-7) and find the instantaneous size of the i^{th} crack at time t:

$$\frac{1}{a_{oi}^{1/n}} - \frac{1}{a_i^{1/n}} = f_i^{\,q} \int_o^t \left\{ \frac{3^{(1-n)}\, D_1\, \pi^{(2n+1)}}{4n^n \Gamma\, \sigma_m^{\,2n} I_1^{\,2n}} \right\}^{1/n} \left(\frac{\sigma}{a_T}\right)^q dt \qquad \text{(A-8)}$$

where the curly bracket in the integrand will be a function of time if chemical aging occurs and/or there is healing following unloading (which effects are accounted for through time-dependent properties). Also q is a constant:

$$q \equiv 2\left(1 + \frac{1}{n}\right) \qquad \text{(A-9)}$$

The failure time of this crack is denoted by t_i, and is obtained by setting $a_i = a_{gi}$, where $2a_{gi}$ is the crack length for which $N_o = N_{og}$; viz, from Eq. (A-7) and the glassy counterpart of Eq. (A-1) with

$\nu_g = 1/2$:

$$a_{gi} = \frac{4\Gamma E_g}{3\pi f_i^2 \sigma^2} \qquad \text{(A-10)}$$

If power law Eq.(A-6) is assumed to apply for all $t > 0$, then $E_g = \infty$ and consequently $a_{gi} = \infty$. For simplicity, in this section we shall use this infinite value for a_i in Eq.(A-8) at the time of failure, which is, of course, essentially the same as assuming $(a_{gi} / a_{oi})^{1/n} >> 1$. This latter inequality is not valid for small values of failure time and/or low temperatures; the effect of a finite value of a_{gi} will be analyzed in Section III-B of this appendix. Thus, letting $a_{gi} \to \infty$ in Eq. (A-8) and rewriting it yields,

$$1 = \int_0^{t_i} \frac{dt}{t_{ci}} \qquad \text{(A-11)}$$

where t_{ci} would be the failure time for the $i^{\underline{th}}$ crack if the specimen had been subjected to a timewise constant stress, σ, equal to the actual stress at the time t, and if it had constant material and fracture properties equal to those <u>actually</u> existing at the time t:

$$t_{ci} = (A^{-\frac{1}{n}}) (f_i^{-q}) (a_{oi}^{-\frac{1}{n}}) (\sigma^{-q}) a_T (M^{-\frac{1}{n}}) \qquad \text{(A-12)}$$

where A is a constant and is the group of terms in curly brackets in Eq.(A-8) at a preselected <u>reference state</u>, and M is the ratio of this group at current time t to the reference value; thus

$$M = \frac{D_1}{D_{1r}} \frac{\Gamma_r}{\Gamma} \frac{\sigma_{mr}^{2n} I_{1r}^{2n}}{\sigma_m^{2n} I_1^{2n}} \qquad \text{(A-13)}$$

where the subscript "r" denotes constant quantities corresponding to the reference state. <u>Without</u> aging and healing M is unity; otherwise $M = M(t)$, and, although not essential, we assume M is the same function for all cracks. It is interesting to observe that Eq. (A-11) is one form of a <u>linear cumulative damage relation</u>.

Next, substitute Eq. (A-12) onto Eq. (A-11) and solve for the stress concentration factor required to produce failure at time t_i:

$$f_i = \frac{B a_{oi}^{-\frac{1}{nq}}}{||\sigma||_{Mq}} \qquad \text{(A-14)}$$

where

$$B \equiv A^{-\frac{1}{nq}} \tag{A-15}$$

and $||\sigma||_{Mq}$ is a "weighted" Lebesgue norm,

$$||\sigma||_{Mq} \equiv \left\{ \int_0^{t_i} M^{\frac{1}{n}} \sigma^q \frac{dt}{a_T} \right\}^{\frac{1}{q}} = \left\{ \int_0^{\xi_i} M^{\frac{1}{n}} \sigma^q \, d\xi \right\}^{\frac{1}{q}} \tag{A-16}$$

in which ξ is reduced time,

$$\xi \equiv \int_0^t \frac{dt}{a_T} \tag{A-17}$$

Of course, without aging and healing we set M = 1 and obtain the Lebesgue norm itself in terms of reduced time. Note also that, from Eq. (A-9),

$$\frac{1}{nq} = \frac{1}{2(n+1)} = \frac{1}{2} - \frac{1}{q} \tag{A-18}$$

Thus, for all cracks in which $f \geq f_i$ failure of the surrounding material has occurred. Cracks with smaller concentration factors have not yet failed. When the time t_i is exceeded for a given crack, the growth will be very rapid until the tips are arrested at filler particles and/or the tips move into a region of low stress concentration. In the analysis in (A-4) we assumed the applied stress is low enough that most cracks are eventually arrested and that the increase in the $i^{\underline{th}}$ crack size from the time t_i to the time the crack is arrested, t_{ai}, say (or, at least, until its velocity reduces to a relatively small value) is much larger than $2a_{oi}$; the time difference $t_{ai} - t_i$ was assumed to be negligible compared to t_i.

Let us denote the crack size at time t_{ai} as $2a_{ai}$; since $a_{ai} >> a_{oi}$ and in view of the comments immediately following Eq. (A-6) we concluded that the influence of the $i^{\underline{th}}$ crack on overall mechanical response is felt approximately at the time t_i, and the magnitude of this influence is directly related to the total growth, $2a_{ai} - 2a_{oi} \simeq 2a_{ai}$. (Interaction between cracks when $t > t_i$ was allowed.)

The above considerations, together with stochastic representations of f_i, a_{oi}, and a coefficient S_i (defining the overall softening effect of the $i^{\underline{th}}$ crack) yield the following constitutive equation (which was derived in (A-4)) for strain due to stress:

$$\varepsilon = \int_0^{\xi} D(\xi - \xi') \frac{d}{d\xi'} \left\{ \sigma[1 + H'] \right\} d\xi' \qquad \text{(A-19)}$$

in which

$$H' \equiv \int_{g'}^{\infty} G(g)\, dg \qquad \text{(A-20)}$$

where $D(\xi)$ is the creep compliance for the propellant in its linear viscoelastic range and g' is the reciprocal of the weighted Lebesgue norm, Eq. (A-16), evaluated at reduced time ξ',

$$g' \equiv \left\{ \int_0^{\xi'} M^{\frac{1}{n}} \sigma^q \, d\xi \right\}^{-\frac{1}{q}} \qquad \text{(A-21)}$$

The function $G(g)$ is non-negative since it is a statistical distribution function; all three of the distribution functions associated with the random variables f_i, a_{oi}, and S_i collapse into the one function G as a consequence of using power law Eq. (A-6) for creep compliance. In view of Eq.(A-21) and because $G \geq 0$, we find H' is a non-decreasing function of time if healing does not occur (i.e. if M is independent of ξ).

B. Macrocrack Model

The theory of crack growth developed in (A-6) and reviewed in the above subsection provides the basis for predicting failure times of composite materials and structures under time varying loads and environments. Rather than adding the effects of all microcracks, as we did in developing a constitutive theory, one follows only the growth of the one or more cracks which are directly involved in producing structural failure; as a conservative simplification, we will assume that these cracks are not arrested through interaction with particles and/or other flaws. By including paramecers that define the randomness of the various factors which influence failure time, it is possible to predict the probability of failure within the desired service life.

As a simple illustration, consider a bar subjected to a constant or transient uniaxial tensile stress; we allow for aging and a transient temperature, but assume that on a macro-scale any changes are essentially independent of spacial location. For simplicity, only small-scale geometric randomness will be taken into account; however,

the example could be extended to account for randomly varying temperatures, loading and properties.

Let us focus our attention on the growth of a single crack that is assumed to propagate in the opening mode during the entire lifetime of the specimen. This crack is further assumed to be the one that ultimately causes specimen failure when its growth becomes unstable. It is supposed that during most or all of the specimen's lifetime the instantaneous stress intensity factor depends on a single crack dimension. These assumptions may be at least approximately satisfied with solid propellant specimens. For example, they are met for an internal, penny-shaped crack whose plane is perpendicular to the applied stress and whose initial diameter ($2a_o$) is large compared to filler particles in its immediate neighborhood; for creep exponents, n, typical of solid propellant, crack velocity increases very rapidly with size, and therefore the crack would normally remain close to its initial size during most of the specimen's lifetime (A-6). As one final simplifying assumption, the composite material in the neighborhood of the crack of interest is assumed to be linearly viscoelastic, having Poisson's ratio $\nu=1/2$ and the power law creep compliance

$$D(\xi) = \xi^n D_1 \tag{A-22}$$

The failure time of this idealized fracture model is predicted from Eq. (A-14), where the subscript "1" now refers to the one crack which, by assumption, ultimately causes specimen failure. For later use, we write Eq. (A-14) in the form

$$g = g(\xi_f) = \frac{1}{||\sigma||_{Mq}} \equiv \left\{ \int_0^{\xi_f} \frac{1}{M^n} \sigma^q d\xi \right\}^{-\frac{1}{q}} \tag{A-23}$$

where, by definition,

$$g \equiv \frac{f a_o^{\frac{1}{nq}}}{B} \tag{A-24}$$

The reduced failure time is denoted here by ξ_f. Although for notational convenience we have dropped the subscript "1", it should be noted that f and a_o (and therefore g) are random variables; viz., the stress concentration factor and initial flaw size corresponding to the most critical crack in each specimen will vary from specimen-to-specimen. Observe from Eq. (A-17) and (A-23), in which $\xi_f \equiv \xi(t_f)$ and $a_T > 0$, that g is a single-valued, monotonically decreasing function of failure times ξ_f and t_f; this observation implies the most critical crack in a specimen is the one for which the g-value is the <u>largest</u>.

III. STOCHASTIC MODELS OF FAILURE

A. Power-Law Material

The idealized model described in Section II-B for failure of a material whose creep compliance is the power law Eq. (A-22) will be used here. We consider a universe of specimens which are identical except for the values of f and a_o (and therefore g). Denote the frequency distribution of the largest g in each specimen by $p_g(g)$. Thus, by definition the proportion of specimens having their largest g-values between g and g + dg is $p_g dg$. Since Eq.(A-23) is a monotonic deterministic relation, $p_g dg$ is also the relative number of times between ξ_f and $\xi_f + d\xi_f$; denoting the frequency distribution of ξ_f by $p = p(\xi_f)$, we write

$$-p d\xi_f = p_g dg \tag{A-25}$$

where the minus sign is introduced because $dg/d\xi_f < 0$. Evaluating $dg/d\xi_f$ from Eq. (A-23) there results

$$p(\xi_f) = p_g(||\sigma||_{Mq}^{-1}) \left. \frac{\frac{1}{M^n}\sigma^q}{q\,||\sigma||_{Mq}^{(1+q)}} \right|_{\xi = \xi_f} \tag{A-26}$$

Now, according to Eq. (A-24), the distribution p_g is determined entirely by the small-scale, geometric irregularities in the specimens through f and a_o; recall that B is a constant. Therefore, in principle, one can find p_g experimentally using one stress and temperature history (e.g. isothermal creep tests) and then substitute this function into Eq.(A-25) or (A-26) to predict the frequency distribution of failure times for other thermal and mechanical histories.

In order to illustrate the use of experimental data and to show how Eq. (A-26) can be by-passed when predicting failure probabilities, suppose isothermal creep tests are conducted on a set of specimens; without loss in generality, we can set M=1 for these tests if appreciable aging does not occur during the time these tests are conducted. It is desired to use non-aging creep-rupture data to obtain an equation for predicting failure probability under more general conditions. As the first step, it will be helpful to introduce two new variables:

$$L \equiv -q \log g, \qquad \ell \equiv \log t_f \tag{A-27}$$

where t_f is an experimental creep-rupture time and $\log \equiv \log_{10}$. The corresponding distribution functions are $p_L(L)$ and $p_1(\ell)$, where $p_L dL = -p_g dg$; also, $p_1 d\ell = p_L dL$. After specializing the Lebesgue norm

in Eq. (A-23) to isothermal creep we find

$$p_L(L) = p_1(\xi) \qquad \text{(A-28a)}$$

with

$$L = \xi + q\log\sigma - \log a_T \qquad \text{(A-28b)}$$

Observe that p_1 is the frequency distribution of log-failure times found from creep-rupture data (if the sample size is sufficiently large); for solid propellant, p_1 commonly can be represented by the normal distribution function (A-7, 8, 9). Now Eq. (A-28) shows that, if the present theory is valid, plots of distributions of log t_f obtained at different constant stresses and temperatures can be translated horizontally along the log t_f axis to form a <u>master distribution curve</u>; this latter point follows from the fact that p_g (and therefore p_L) is independent of stress, temperature, and age. $p_L(L)$ is, of course, equal to this master curve when the latter is the (measured or predicted) distribution of log t_f for which $a_T=\sigma=1$. Furthermore, under arbitrary aging and thermal and mechanical loading p_L continues to define the distribution of failure times.

The probability of failure, P_f, say, can now be predicted. For any one specimen in which $M=M(\xi)$, $\sigma=\sigma(\xi)$, and $T=T(\xi)$ are known over the time period $0 \leq t \leq t_T$, the probability of failure occuring at any time during this period is

$$P_f(0 \leq t \leq t_T) = \int_0^{L_T} p_L(L)\, dL \qquad \text{(A-29)}$$

where p_L is the <u>master distribution curve</u> obtained from creep-rupture tests, and L_T is the value of L at the end of the period, t_T. In order to evaluate P_f, calculate ξ from Eq. (A-17), g from Eq. (A-23), and L from Eq.(A-27); note that

$$L(\xi) = \log \left| \int_0^{\xi} M^{\frac{1}{n}} \sigma^q d\xi \right| \qquad \text{(A-30)}$$

and $L_T \equiv L(\xi_T)$ where $\xi_T \equiv \xi(t_T)$. According to Eq. (A-29), the final step consists of integrating the master distribution curve, p_L:

It should be emphasized that the above theory provides a means for predicting the <u>probability of failure</u> of an aging or nonaging material, under simple or complex temperature and loading histories, <u>in terms of the distribution of isothermal creep-rupture times</u>. This prediction method turns out to be identical to that

proposed by Bills (A-7, 8, 9) on the basis of empirical evidence. He obtained good agreement between theory and experiment in the reduced-time range for which the relation between the logarithm of applied stress and the mean of log-time (in creep tests) was linear. It is a simple matter to show that Eq. (A-28) predicts this linear relationship in creep. Specifically, starting with the definition of mean log-time, $\overline{\ell}$,

$$\overline{\ell} \equiv \int_{-\infty}^{\infty} \ell\, p_1(\ell)\, d\ell \tag{A-31}$$

change the variable of integration to L by using Eq. (A-28); there results

$$\overline{(\log t_f/a_T)} = \overline{L} - q \log \sigma \tag{A-32}$$

where $\overline{L}$ is the mean value of L,

$$\overline{L} \equiv \int_{-\infty}^{\infty} L\, p_L\, dL \tag{A-33}$$

which is independent of stress and temperature.

B. Generalization to Include Small Values of Reduced Time

In view of these encouraging results, we shall now extend the theory to account for behavior outside the range for which the power law form of creep compliance, Eq. (A-22), is applicable. In particular, the effect of a finite glassy modulus, E_g, will be considered in order to obtain an improved model for predicting failures at small values of reduced time. It should be added that this short-time range may be important even when the temperature is quite far above the glass transition value. This point is based on the fact that high strain rates can exist at crack tips although the overall specimen strain rate may be small; these high rates are reflectd in t_a, Eq. (A-4), which can be much less than the physical time. For the same reason, creep failure data at large values of reduced times usually are unaffected by Eq. (A-8) and therefore do not normally deviate from the predictions based on a power-law compliance.

Generalization of the underlying crack growth theory will be accomplished by simply using Eq. (A-8) with $a_1 = a_{gi}$ (instead of $a_1 = \infty$) at the time of failure, t_f; recall that a_{gi} is given by Eq. (A-10). The resulting equation can be written in the form

$$g = \left\{ B_1 \frac{\sigma_f^{\frac{2}{n}}}{f^2} + \int_0^{\xi_f} \frac{1}{M^n}\, \sigma^q\, d\xi \right\}^{-\frac{1}{q}} \tag{A-34}$$

where σ_f is the stress at $\xi = \xi_f$, B_1 is a constant,

$$B_1 \equiv \left(\frac{3\pi}{4\Gamma E_g A}\right)^{\frac{1}{n}} \tag{A-35}$$

and the relation between random variables g, f, and a_o, Eq. (A-24), is still valid. Thus, the net effect of using a finite value of glassy modulus is to replace Eq. (A-23) by Eq. (A-34).

It should be added that the same result, viz. Eq.(A-34), would have been obtained had we started with Eq. (A-3), instead of Eq. (A-8), and used the creep compliance (with D_m replaced by D)

$$D(\xi) = \begin{cases} 1/E_g \text{ for } o<\xi<\xi_o \\ \\ D_1\xi^n \text{ for } \quad \xi \geq \xi_o \end{cases} \tag{A-36}$$

where $\xi_o \equiv (E_g D_1)^{-\frac{1}{n}}$. Although this $D(\xi)$ is continuous for all $\xi>o$, its first derivative is discontinuous at $\xi = \xi_o$ and, therefore, one might expect Eq. (A-36) to produce a noticeable error in short-time failure predictions. However, the failure time calculation involves an integration process, which tends to smooth out the effect of this discontinuity. We have compared the prediction in (A-6) for creep-rupture times of Solithane (in which a very accurate representation of creep compliance was used) to those predicted from Eq. (A-34), and the results were found to be quite close for all $\xi>o$; it was interesting to find that the latter approximate predictions agreed with experiment better than the predictions given in (A-6). This closeness between the predictions existed in spite of the fact that Eq. (A-36) is a rather poor representation for Solithane at times in the neighborhood of ξ_o. Also, it should be added that when the more realistic creep compliance, $D(\xi) = E_g^{-1} + D_1 \xi^n$, is used to predict failure times, the result is for more involved than Eq. (A-34), which, in turn, produces considerable complexity in the stochastic analysis; even for constant stress and temperature, and without statistical effects, failure-time prediction requires evaluation of an incomplete Beta function (A-6).

Both g and f in Eq. (A-34) are random variables. However, for flaws which are initially large compared to the mean particle size and spacing it seems reasonable to assume that f is close or equal to that for a penny-shaped crack; i.e. $f = \sqrt{2}/\pi$ (A-6). For <u>now</u>, therefore, let us suppose that f has the same value for all specimens. Extension to random variations of f will be made later.

With this condition, Eq. (A-34), just as Eq. (A-23), is a deterministic relation in g and ξ_f. However, with sufficiently rapid oscillations of stress, $g(\xi_f)$ will not now be monotonic; this problem is easily removed

by recognizing that failure of any given specimen occurs the first time Eq.(A-34), in terms of the specimen's largest g-value, is satisfied. Thus, by defining g_{min} as the smallest value of $g(\xi_f)$ up to the current time, Eq. (A-34) should be replaced by the condition

$$g = g_{min} \tag{A-37}$$

whenever Eq.(A-34) predicts $g > g_{min}$. With this modification, Eq. (A-25) can be used to calculate $p(\xi_f)$. Note that when $g > g_{min}$, then in this interval of time $dg/d\xi_f = 0$; in turn, Eq.(A-25) yields the physically correct value of $p = 0$ (i.e. no failures) in this same interval.

Pursuing this model further, let us use the logarithmic variable L in Eq.(A-27) and calculate the frequency distribution $p(\xi_f)$ for isothermal nonaging, creep tests. Starting with $p d\xi_f = p_L dL$ and drawing upon Eq. (A-34) (after specializing it to isothermal creep) in order to calculate $dL/d\xi_f$, there results

$$p(\xi_f) = \left\{ \left[\frac{2}{n} \frac{B_1}{f^2} \delta(\xi_f) + \sigma^2 \right] \Big/ \left[\frac{B_1}{f^2} + \sigma^2 \xi_f \right] \right\} p_L \tag{A-38}$$

Note that $\delta(\xi_f)$ is the Dirac delta function, which appears because some specimens may fail when the stress σ is first applied. Also the argument of P_L is

$$L = L(\xi_f) = \log \left\{ \sigma^{\frac{2}{n}} \left[\frac{B_1}{f^2} + \sigma^2 \xi_f \right] \right\} \tag{A-39}$$

Now, p_L is independent of E_g. Consequently, if p_L has already been established from the intermediate and long-time tests (e.g., for propellant p_L is usually the normal distribution function, as mentioned earlier) then Eqs. (A-38) and (A-39) enable one to predict the statistical distribution of creep failure times at small values of reduced time; such a prediction, when compared with experimental data, should be useful in checking the theory and evaluating the constant B_1/f^2 appearing in this generalized theory.

The probability of failure for the general case of $M = M(\xi)$, $\sigma = \sigma(\xi)$, and $T = T(\xi)$ is still calculated from Eq. (A-29); L_T is now given by $L_T \equiv L(\xi_T)$ in which $\xi_T \equiv \xi(t_T)$ and where

$$L(\xi) = \log \left\{ B_1 \frac{\sigma_f^{\frac{2}{n}}}{f^2} + \int_0^{\xi} M^{\frac{1}{n}} \sigma^q \, d\xi \right\} \qquad \text{(A-40)}$$

In light of the earlier discussion for the situation in which $g > g_{min}$, we must set $L = L_{max}$ whenever Eq.(A-40) predicts $L < L_{max}$; by definition L_{max} is the largest value of $L(\xi)$, as predicted by Eq. (A-40), up to the current time.

We shall now extend the theory to allow for statistical variations of the stress concentration factor f as well as L (where L is defined in Eq. (A-27). First, considering all cracks in a single specimen, and for specified time variations of M, σ, and T, there will be one crack whose f and L values produce the smallest value of ξ_f, as predicted by Eq. (A-34); without loss of generality in the result, we can assume no two cracks in this specimen have the same f and L values. This crack will be termed the "critical" crack for the specimen. Now, consider the set of pairs of values (L,f) corresponding to each critical crack in all specimens; introduce the frequency distribution $p_s = p_s(L,f)$, where $p_s \, dL \, df$ is the proportion of specimens having L-values between L and L + dL and f -values between f and f + df. We are interested in calculating $p d\xi_f$, which is the proportion of specimens having failure times between ξ_f and $\xi_f + d\xi_f$. This latter proportion is equal to the integral of $p_s \, d\, L \, df$ over the area in the L - f plane bounded by the curves ξ_f = constant and $\xi_f + d\xi_f$ = constant. We obtain, finally, with L given by Eq. (A-40) evaluated at ξ_f,

$$p(\xi_f) = \sigma_f^q \int_0^{\infty} p_s(L,f) \; 10^{-L \left\{ \frac{2}{n} \frac{B_1 d\sigma_f/d\xi_f}{f^2 \sigma_f^3} + M^{\frac{1}{n}} \right\}} df \qquad \text{(A-41)}$$

In order to recover the distribution p for the previous case in which f is a specified constant(f_o, say), let $p_s = \delta(f-f_o) \, p_1(L)$. For example, for a nonaging, isothermal creep test, Eq.(41) reduces immediately to Eq. (A-38).

Let us now assume that the distribution of values (L,f), corresponding to the critical cracks in the universe of specimens of interest, does not change with stress history and age. With this condition, it appears to be possible to evaluate $p_s(L,f)$ from isothermal creep tests conducted at different stress levels. Specifically, determine the distribution $p(\xi_f)$ for each stress. Then approximate the infinite integral in Eq. (A-41) by a finite sum. With p specified at a finite set of values of ξ_f and σ, solve for p_s by matrix inversion. The size of the surface

$p_s = p_s(L,f)$ that is traced out by this process will obviously depend on the range of value of ξ_f and σ.

C. Effect of Superimposed Pressure

In a study of creep failure of tensile specimens under superimposed pressure, Bills et al. (A-10) observed a very simple dependence of creep failure times on the pressure. Specifically, they found that pressure, p, could be taken into account through replacing the temperature-dependent shift factor a_T by the product $a_T a_p$, where a_p is a function of only the pressure, and replacing tensile stress by $\sigma_1 + p$, where σ_1 is the axial stress; note that $\sigma_1 + p$ is twice the maximum shear stress, $\sigma_1 - \sigma_2$, where σ_2 ($= -p$) is the lateral stress. These observations were made in the power-law range of failure time; i.e. where the mean value of log t_f is related linearly to stress. In the context of Eq. (A-30), we may therefore account for pressure by letting M be a function of pressure (or possibly the mean stress $(\sigma_1 + 2\sigma_2)/3$) and letting $\sigma \to \sigma_1 + p$.

These experimental results seem to imply that cracks grow as readily in shear as in the opening mode, and that the fracture energy Γ and/or the crack tip strength σ_m vary with pressure. The effect of friction between crack faces is apparently small since the driving force for crack growth is the maximum shear stress $\sigma_1 - \sigma_2$, regardless of the magnitude of the pressure in the range studied ($p \leq 1000$ psi). It should be added that had we included shearing modes in the crack propagation theory, the results would have taken the same analytical form as these for the opening mode (e.g. Eqs. (A-23) and (A-34)), assuming the direction of propagation of the critical crack does not vary appreciably with time (A-6). Furthermore, with this broader interpretation of the theory, the value of the factor f for each crack can be thought of as representing the effect of both local stress concentration and crack direction.

IV. ON THE CONSTITUTIVE THEORY BASED ON FRACTURE MECHANICS

As a means of providing some experimental verification of the basic fracture model for nonlinearity described in Section II-A, electron microscopy and dual-rate mechanical property tests were used in a study of Aerojet's ANB 3066 propellant.

Representative results using TAMU's scanning electron microscope are shown in Figures 1a and 1b. Shown is a microtoned surface of a propellant specimen under various amounts of elongation. It is interesting to observe that until the propellant is close to gross failure, the flaws are crack-like rather than rounded or ellipsoidal cavities; of course, this observed flaw shape is probably somewhat

different from what exists in the interior of the specimen. Also, at least in the early stages, a significant proportion of the flaws have a random orientation because they tend to follow the boundaries of the larger adjacent particles; therefore, both shearing and opening modes of flaw initiation and growth are present. Incidentally, a greater magnification of the surface reveals that a thin skin of binder remains on the particles, even though the specimen in Figure 1 appears to exhibit the dewetting phenomenon.

Recall that the analysis in Section II-A of this appendix was based on the assumption that most of the growth of an individual flaw, and the consequent overall softening effect on the propellant, occur in a very short period of time following instability of the extremely small initial flaw; arrest was assumed to occur after this rapid growth, at least if the load was not too high. The microscopy investigation seemed to confirm this assumed behavior. Observable flaws in Figure 1 popped into view only during the time the elongation was being increased; the time at which a flaw suddenly appears is to be identified with the time of unstable growth in the theory. Subsequent growth and coalescence with nearby flaws was very gradual.

Results from a series of mechanical property tests on ANB 3066 at room temperature are shown in Figures 2-7. Each curve represents an average of the data obtained from two specimens; however, the specimen-to-specimen differences were found to be quite small. Standard JANNAF dogbone type specimens were employed. Two different crosshead rates were used: 0.1 and 5 inches per minute. Generally, each test consisted of loading a virgin specimen at the high (low) rate, allowing it to rest at zero load (after a relaxation and/or a ramp unloading period), and then reloading the same specimen at the low (high) rate. In most cases the specimen was then subjected to additional cycles of loading and unloading. The unloading ramp rate was always the same as that used to load the specimen.

Figures 2 and 3 give results for the tests in which a period of constant elongation followed a ramp loading. Curve 2 is for the second loading of a pair of specimens that had initially been strained at a low rate (curve 3 in Figure 3). Similarly, curve 4 in Figure 3 was obtained after the two specimens had been subjected to a high rate (curve 1 in Figure 2). A period of constant elongation was not employed in obtaining the data in Figures 4-7. Observe that the past history of the pair of specimens used to obtain each curve is shown in the table included with the figures.

Two points especially are worth noting in the behavior revealed by these tests: (i) The load-time trace for the second loading eventually climbs above the virgin curve if the rest period is sufficiently long; see Figures 2-4, and especially curve 6 in Figure 4. (ii) The peak load reached in the first loading has much less effect on the

subsequent reloading-time trace than the peak elongation if the rest time is long enough (>10 minutes); for example, curve 4 in Figure 3 intersects the virgin curve at approximately the peak elongation from the previous loading, even though the previous peak load was much greater; in contrast, this intersection does not occur with short rest periods, as may be seen in Figure 6.

On the basis of the behavior exhibited in Figures 1-7 and discussed above, it is believed a realistic physical model of propellant nonlinearity must include (at least) the following mechanisms: (i) stress-dependent microcrack growth and instability, such as described in Section II-A (appendix). (ii) healing of microcracks, with the amount of healing depending on the maximum strain imposed up to the current time and the time elapsed while the specimen is under zero load. (iii) increased resistance to crack growth due to crack-tip blunting. This latter mechanism would be capable of predicting the response in which a reloading-time trace climbs above the virgin curve; i.e., cracks due to the first loading would blunt during the early portion of the reloading, and therefore would not propagate as readily as cracks in the first loading.

It is expected that one effect of superimposed pressure on microcrack growth is the same as described in Section III-C of this appendix. Namely, the weighting function M in the Lebesgue norm, Eq. A-21), depends on this pressure or the mean stress. However, in addition, the pressure may accelerate the rate of healing and permit healing to occur even though applied deviatoric stresses are not zero. The fact shear-type cracks exist implies significant healing may occur under stress, even without superimposed pressure.

Whether or not a physical model which is both practical and realistic can be synthesized to describe these various phenomena is not clear at this time. However, it is very encouraging that the simple crack growth model in Section III of this appendix has proven to be quite accurate for predicting failure behavior.

REFERENCES FOR APPENDIX A

A-1. R. J. Farris and J. E. Fitzgerald, "Deficiences of Viscoelastic Theories as Applied to Solid Propellants," Bulletin JANNAF Mech. Beh. Wkg. Group, 8th Meeting, CPIA Pub. 193, March 1970.

A-2. R. J. Farris, "The Stress-Strain Behavior of Mechanically Degradable Polymers," Polymer Networks: Structural and Mechanical Properties, A. J. Chompff and S. Newman, Eds., Plenum, 1971.

A-3. R. J. Farris, "Applications of Nonlinear Viscoelasticity and Cumulative Damage (A Realistic Evaluation of Real Propellant Behavior)", Aerojet Solid Propulsion Co., NOSC Final Rpt. 1565-26F, May 1971.

A-4. R. J. Farris and R. A. Schapery, "Development of a Solid Rocket Propellant Nonlinear Viscoelastic Constitutive Theory," Final Rpt. AFRPL-TR-73-50, June 1973.

A-5. R. J. Farris, "Homogeneous Constitutive Equations for Materials with Permanent Memory," Ph.D. Thesis, Univ. of Utah, Dept. of Civil Eng'g, June 1970.

A-6. R. A. Schapery, "A Theory of Crack Growth in Viscoelastic Media," Texas A&M U. Rpt. No. MM 2764-73-1, March 1973.

A-7. K. W. Bills, Jr., D. M. Campbell, R. D. Steele, and J. D. McConnell, Applications of Cumulative Damage in the Preparation of Parametric Grain Design Curves and the Prediction of Grain Failures on Pressurization, Aerojet Solid Propulsion Co., Final Report 1341-26F, August 1970.

A-8. K. W. Bills, Jr., F. E. Peterson, and R. D. Steele, "Study of Cumulative Damage Techniques for the Prediction of Motor Failure", Aerojet-General Corporation Report No. 4158-81F (Contract No. NOw 66-0545-c) (July 1967).

A-9. K. W. Bills, Jr., F. E. Peterson, R. D. Steele, and R. C. Sampson, "Development of Criteria for Solid Propellant Screening and Preliminary Engineering Design", Aerojet Report 1159-81F (Contract No. N00017-67-C-2415) (December 1968).

A-10. K. W. Bills, Jr., et. al, "Solid Propellant Cumulative Damage Program", Final Report No. AFRPL-TR-68-131, Contract No. F04611-67-C-0102, (October 1968).

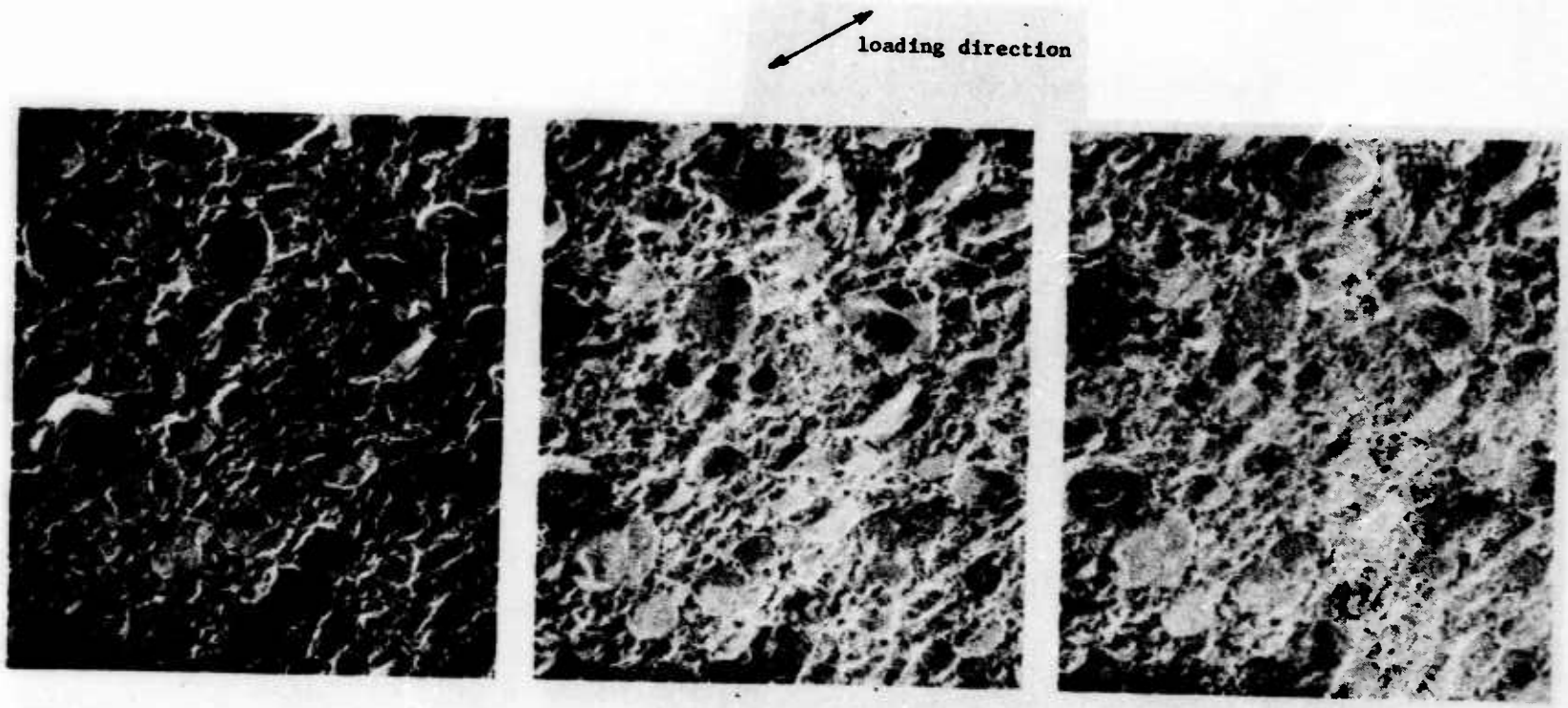

Figure 1a. Thin sheet of ANB 3066 propellant under various amounts of elongation as observed through a scanning electron microscope (100x).

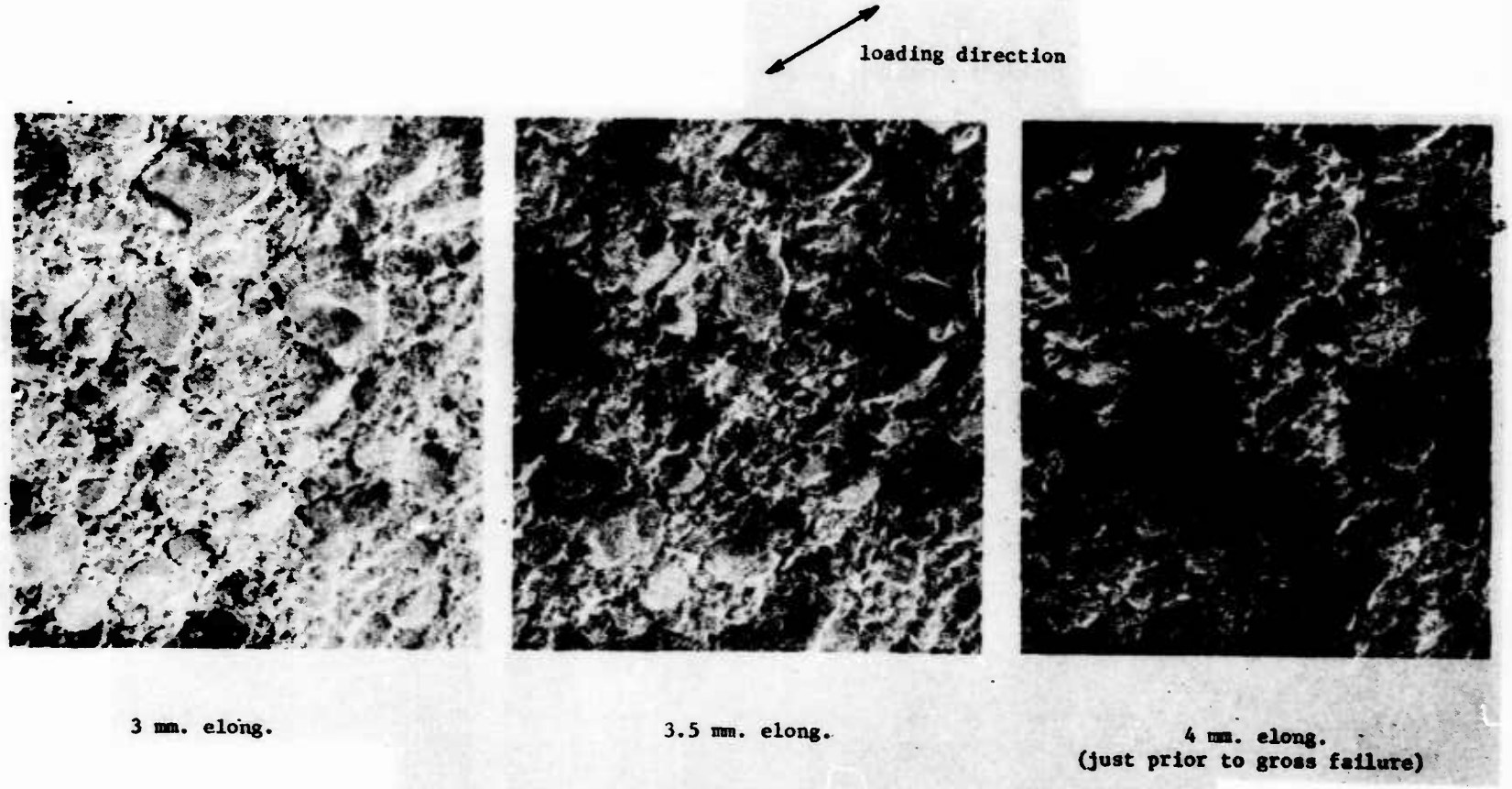

Figure 1b. Thin sheet of ANB 3066 propellant under various amounts of elongation as observed through a scanning electron microscope (100x).

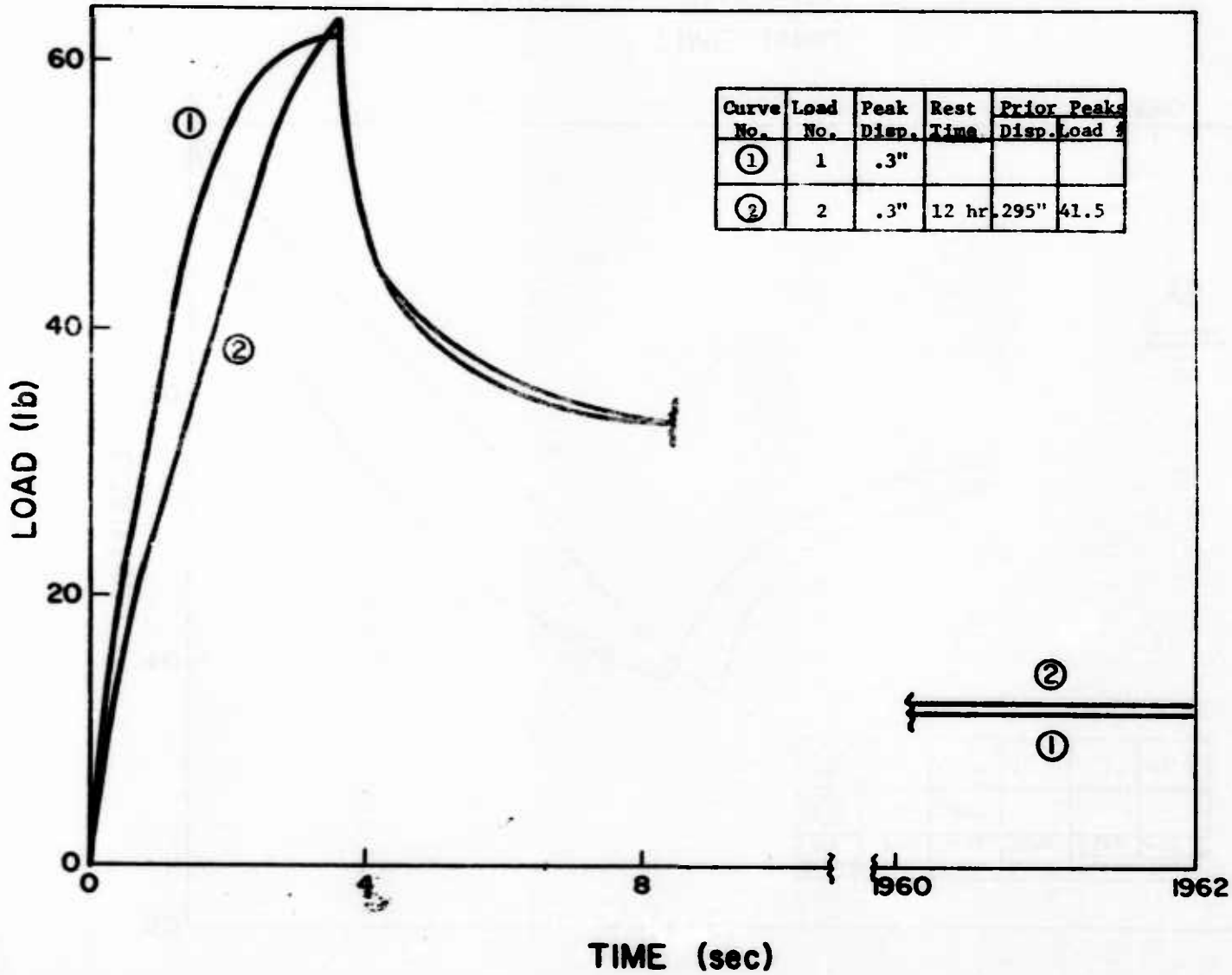

Curve No.	Load No.	Peak Disp.	Rest Time	Prior Peaks Disp.	Prior Peaks Load #
①	1	.3"			
②	2	.3"	12 hr	.295"	41.5

Figure 2. Ramp relaxation test

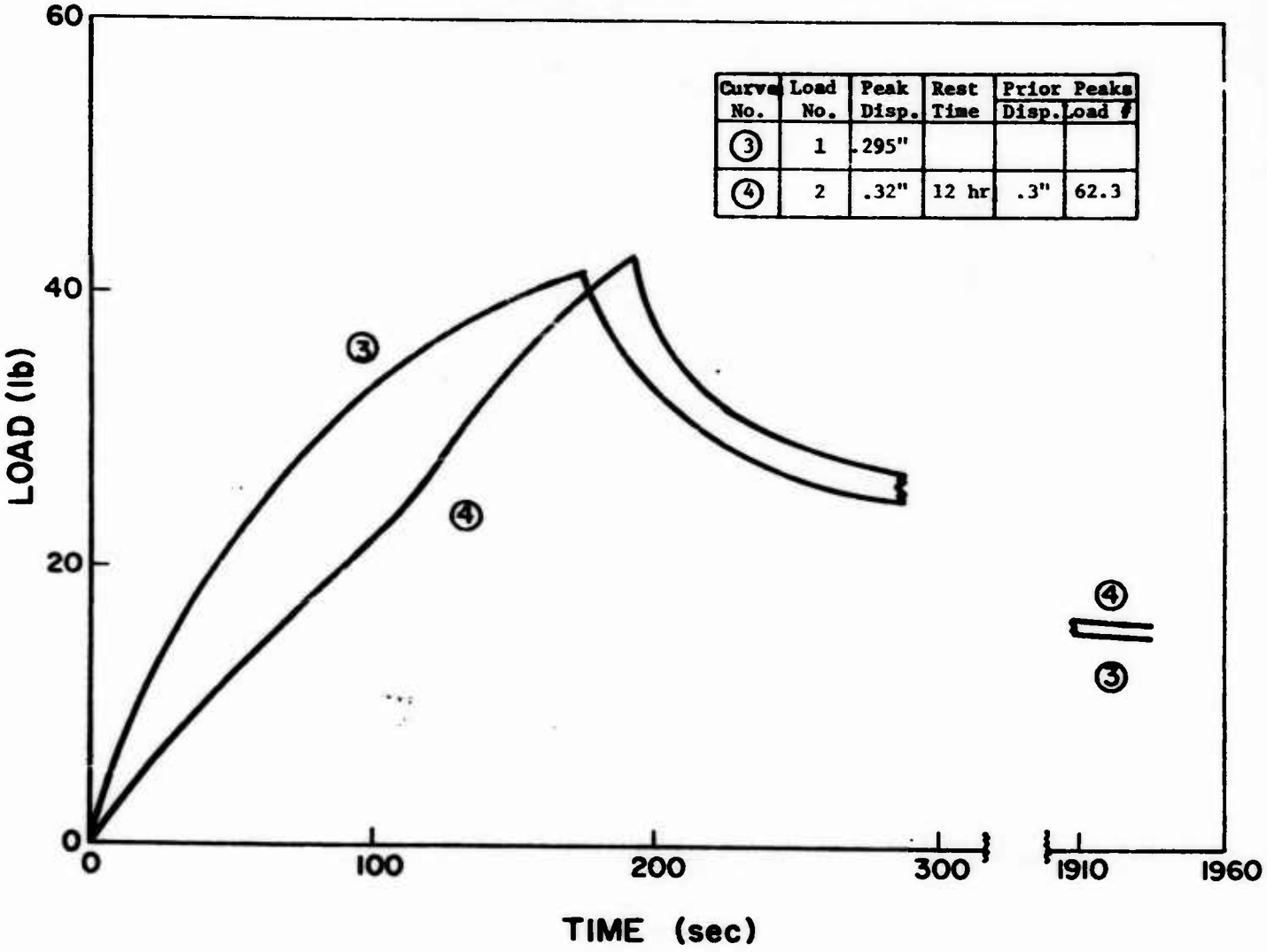

Curve No.	Load No.	Peak Disp.	Rest Time	Prior Peaks Disp.	Prior Peaks Load #
③	1	.295"			
④	2	.32"	12 hr	.3"	62.3

Figure 3. Ramp relaxation test

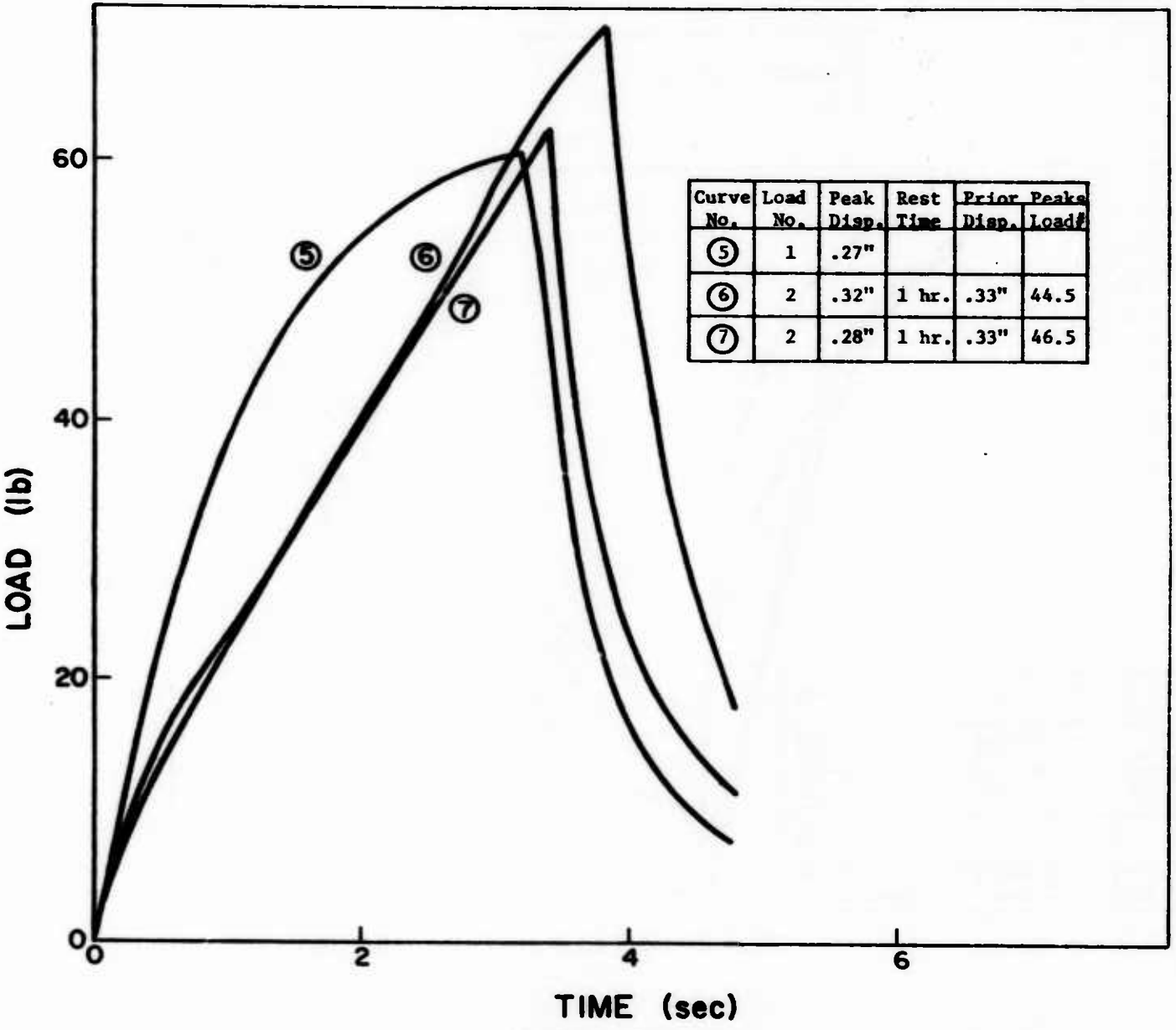

Curve No.	Load No.	Peak Disp.	Rest Time	Prior Peaks Disp.	Prior Peaks Load#
⑤	1	.27"			
⑥	2	.32"	1 hr.	.33"	44.5
⑦	2	.28"	1 hr.	.33"	46.5

Figure 4. Ramp test

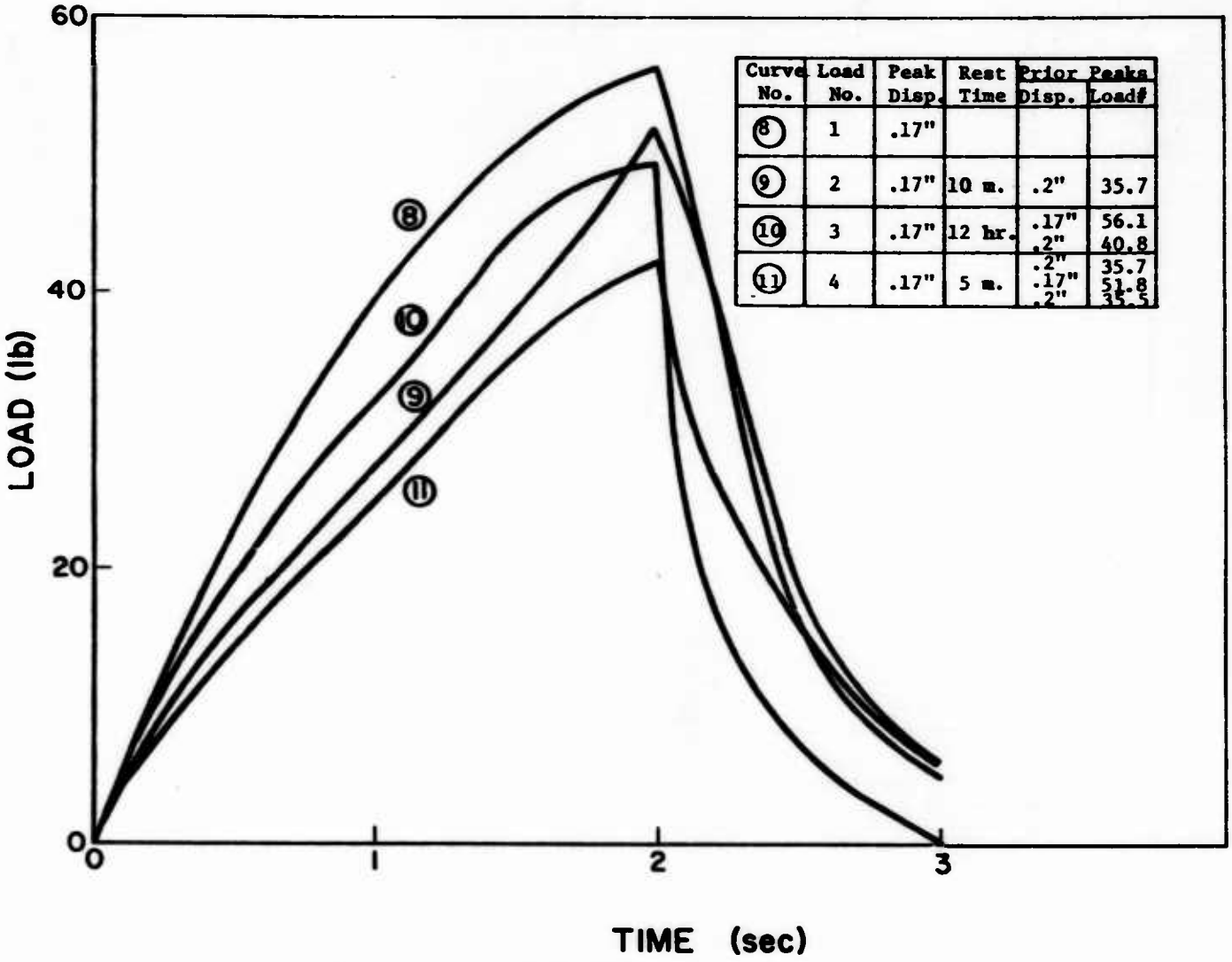

Figure 5. Ramp test with varying rest times

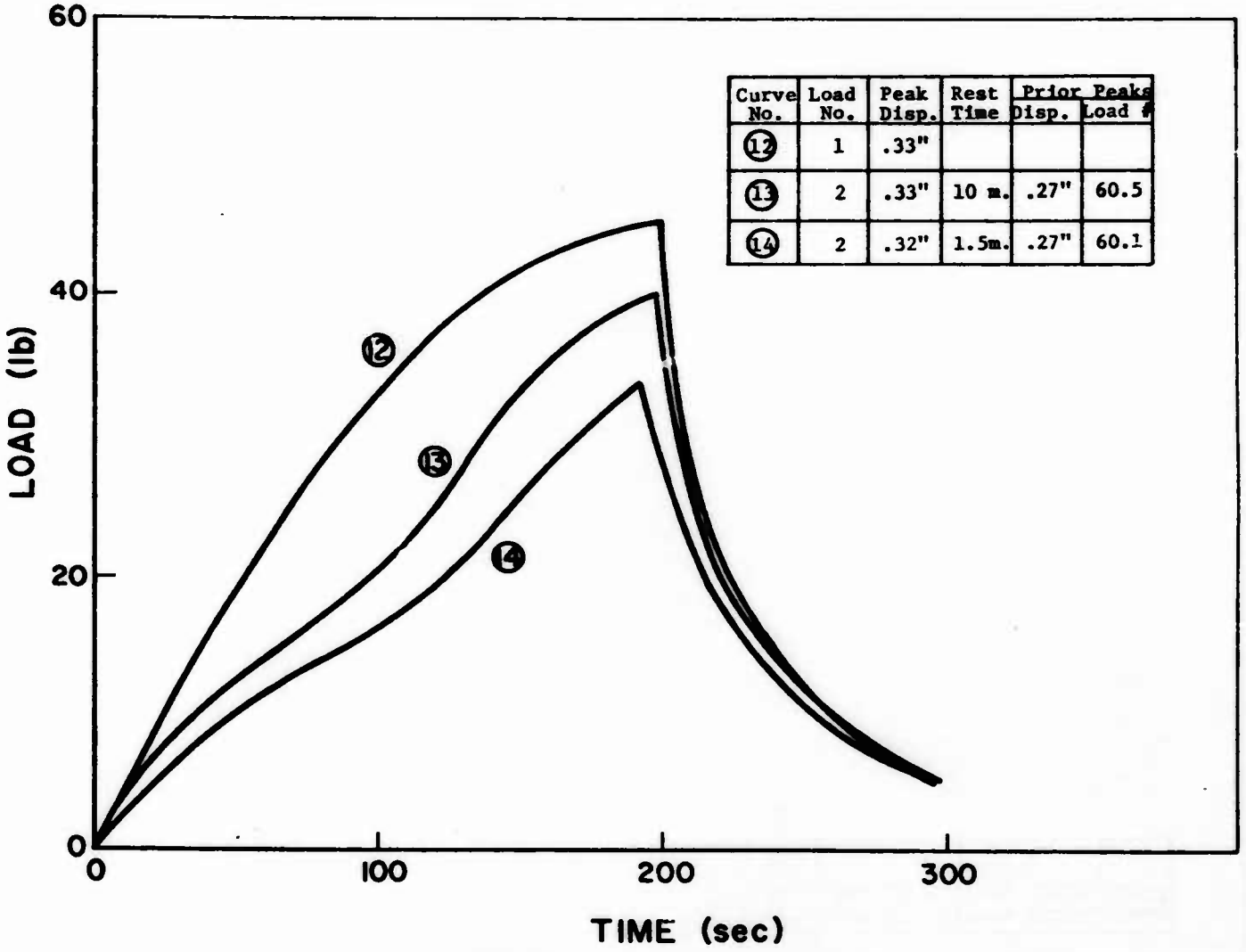

Curve No.	Load No.	Peak Disp.	Rest Time	Prior Peaks Disp.	Prior Peaks Load #
12	1	.33"			
13	2	.33"	10 m.	.27"	60.5
14	2	.32"	1.5m.	.27"	60.1

Figure 6. Ramp test with varying rest times

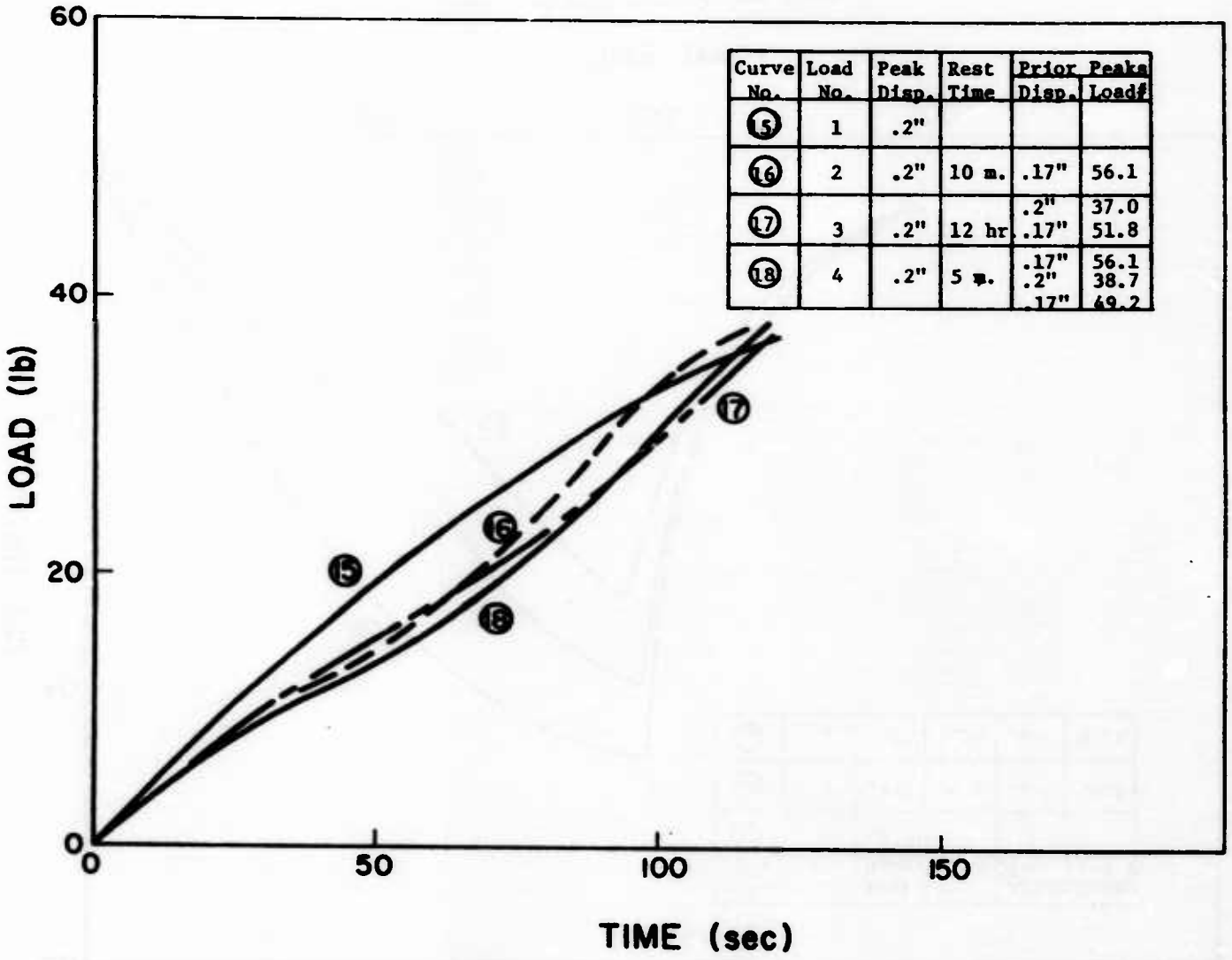

Curve No.	Load No.	Peak Disp.	Rest Time	Prior Peaks Disp.	Prior Peaks Loadf
15	1	.2"			
16	2	.2"	10 m.	.17"	56.1
17	3	.2"	12 hr.	.2" .17"	37.0 51.8
18	4	.2"	5 m.	.17" .2" .17"	56.1 38.7 49.2

Figure 7. Ramp test with varying rest times

APPENDIX B

SA037 - PREPROCESSOR CODE

1. Overview and description

SA037, version 03/01/74, is a small code consisting of a main program and requiring no subroutines to support its operation. Like all the other codes of the materials characterization package it is written entirely in FORTRAN IV. It serves as a data tape processor for the other three codes of the materials characterization package - SA034, SA035, and SA036 (Appendices C, D and E, respectively).

There are three user controlled options available in SA037. These are:

Option 1 - Create a new master data tape

Option 2 - Append additional data to an existing master data tape

Option 3 - Prepare a cataloged printout of the contents of an existing Master Data Tape.

In Option 1 or 2, raw test data is supplied to the code as input. If this is data on a new material, Option 1 is selected to create a new master data dape. IT IS IMPORTANT TO NOTE THAT EACH MATERIAL MUST HAVE ITS OWN MASTER DATA TAPE. This tape then becomes the permanent data reservoir for that material. If, however, the input consists of additional test data on a previously studied material, Option 2 would be chosen to append this new data to the data already residing on the previously created master data tape.

Option 3 is used to obtain a catalog of tests that are currently residing on an existing master data tape. This option is used to find out what specific test data are available for a material that may not have been studied for awhile. In this option the master data tape is the only required input. Figure B-1 shows the relationship between this preprocessor and the other codes of the materials characterization package.

In operation, SA037 initially reads the option card followed by a card specifying the material bulk modulus and volumetric thermal expansion coefficient. The raw data for each test follows with an "END" card as the last card, to signal the end of a run. The code rewinds the assigned master data tape and performs according to the option chosen. If creating or adding data to a tape, Option 1 or 2, a header card precedes the raw test data for each test. The raw data required is temperature, input strain rate, time step, observed stress, and observed volume change, $\Delta V/V_0$. The code next computes the following quantities: strains, corrected dilatation, the three small strain theory invariants, the octahedral shear strain, strain rates, the infinite norm and, if a constant temperature test, the 10th, 20th, 30th, 40th, 50th, and 60th Lebesque norms. These data are then loaded into dummy arrays and written out to the master data tape using unformated FORTRAN write statements. The code then loops back to read the next set of test data. This sequence continues until an "END" card is detected signaling the end of processing. An end-of-file mark is then written, and the tape is rewound.

The only limitations imposed by SA037 are:

a. Each material requires a separate tape.

b. Each test is limited to a maximum of 100 input data points, including the assumed initial, time equals zero, data point.

c. Zero time data points are not input, as all quantities, except temperature, are assumed to be zero at zero time.

There is no limit to the number of tests which may be processed in a single run.

2. Description of Subroutine Required

SA037 requires no additional subroutines, other than those normally available from the FORTRAN Library. The source listing and flow chart are available on request.

3. Usage

This section describes in detail the input required, its format, and the output received from the SA037 preprocessor code. Preceding this, however, is a brief description of the variables appearing in the code.

a. Basic Variables

Following is a list of the variables of SA037. Each variable is described briefly and labeled as either an input or calculator output variable. All input is also saved as output to the master data tape. Any variable which is neither input nor output is merely a working variable used internally usually for intermediate calculations.

A1, A2	Double precision scalar variable used for intermediate calculation
B	Vector used to store all single precision output quantities for output to master data tape
BETA	Volumetric thermal expansion coefficient - INPUT
BULK	Bulk modulus - INPUT
CBRT	FORTRAN supplied cube root function
C1	Single precision scalar used for intermediate calculations
DB	Vector used to store all double precision output quantities for output to master data tape
DIL	Initially, observed dilatation - INPUT. Later on dilatation corrected for temperature and pressure - OUTPUT
DR1, DR2, DR12	Normal and shear calculated strain ratio - OUTPUT
DT	Time step - INPUT
EOCT	Calculated octahedral shear strain - OUTPUT
EPS	Epsilon tolerance tester
E11, E22, E33	Calculated values of normal strain - OUTPUT
E12	Calculated value of shear strain - OUTPUT
IB	Vector used to store all integer output quantities for output to master data tape
ID	Unique test identification made up of six alphanumeric characters - INPUT
INV1	First strain invariant = $E_{11} + E_{22} + E_{33}$ - OUTPUT
INV2	Second strain invariant = $E_{11}E_{22} + E_{22}E_{33} + E_{33}E_{11}$ - OUTPUT
INV3	Third strain invariant = $E_{11}E_{22}E_{33}$ - OUTPUT

IOPT	Run option selector - INPUT: = 1 to create a new master data tape = 2 to append data to an existing tape = 3 to print a catalog of an existing tape
IPG	Page counter
KFAIL	Failure type - INPUT: = 0 for bad failure data = 1 for good failure data
KODE	Test type - INPUT = 1 if a uniaxial test = 2 if a biaxial test = 3 if a shear test
KTEMP	Temperature type - INPUT: = 1 if a constant temperature test = 2 if a variable temperature test
LAST	Indicates last card of raw test data if not blank - INPUT
LINE	Line counter
MATID	Twelve character material identification - INPUT
N	Pointer vector used to position output on unit vectors
NDP	Number of data points in a specific test
NEND	An alphanumeric constant = 'END'
NIN	Number of words of input to tape read vector
NORMF	Infinite Lebesgue norm - OUTPUT
NORM*	*-th Lebesgue norm - OUTPUT
NOUT	Number of words of output from tape unit vector
NU	Tape drive unit number, presently set at 2
PRES	Test pressure - INPUT
RATE	Test input strain rate, observed - INPUT
STRESS	Observed stress - INPUT

STRUE	True stress - OUTPUT
T	Time - OUTPUT
TEMP	Temperature - INPUT

b. Input Required

The card input for SA037 consists of five (5) logical cards, each of which is one physical card, except for card no. 4 which may be up to 99 physical cards long. These cards are described below. The appropriate input formats are shown in parentheses. A description of the variable follows each card.

CARD NO. 1 (I5) IOPT

IOPT is the option selector set to either 1, 2, or 3. Any other value will cause program termination. The options are:

IOPT = 1, create a new master data tape
IOPT = 2, append additional data to an existing master data tape
IOPT = 3, print a catalog of contents of an existing master data type.
NOTE: IF OPTION 3 IS CHOSEN, LOGICAL CARDS NOS. 2 THROUGH 5 ARE NOT REQUIRED.

CARD NO. 2 (2E10.0) BULK, BETA

BULK is the bulk modulus

BETA is the volumetric expansion coefficient

CARD NO. 3 (3A6, E12.0 3I5) ID, MATID, PRES, KODE, KTEMP, KFAIL

This is the header card which precedes the raw test data for each test used. There is one (1) Card No. 3 for each test entered. These header variables are essentially for identification and control.

ID = A six (6) character alphanumeric test identification name.

It is completely arbitrary. However, the following convention has been found convenient for naming tests:

Character	Key
1	U if a uniaxial test
	B if a biaxial test
	S if a shear test
2 & 3	00 = unpressurized test
	11 = pressurized test
4	Test temperature code, key is -
	V = variable
	1 = 150°F
	2 = 110°F
	3 = 77°F
	4 = 40°F
	5 = 20°F
	6 = 0°F
	7 = -20°F
	8 = Not currently assigned
	9 = -40°F
	0 = -65°F
5 & 6	Any two sequence characters desired to make this identification unique.

Example: U002P1 is a uniaxial (U), unpressurized (00), 110°F (2) tests with sequence code P1. This code is completely arbitrary. It should, however, be chosen to allow for quick descriptions of tests from their ID names.

MATID = A twelve character material identification

Example: 'ANB 3335-1'

PRES = Test pressure, assumed constant

KODE = Test type: Uniaxial = 1

Biaxial = 2

Shear = 3

KTEMP = Temperature type: Constant = 1

Variable = 2

KFAIL = Failure type: Bad failure data = 0

Good failure data = 1

By "good" or "bad" failure data is meant whether or not this material failure should be used in a cumulative damage failure characterization.

CARD(S) NO. 4 (5E10.0, I5) TEMP(J), RATE (J), DT(J), STRESS(J), DIL(J), LAST

This is the raw test data, one card per test data point, up to a maximum of 99 (zero time always counts as one point). Here J represents the J-th data point. LAST is always left blank, except on the final data point card when it is set to any convenient non-blank field (11111 has been found to be convenient). Logical cards no. 3 and 4 are repeated once for each test.

CARD NO. 5 (A6) END

After the last data point card (Card No. 4) of the last test, a card with an 'END' in Columns 1-3 is input. This alerts the program to end of data conditions.

In addition to the above card input provision must be made to provide a READ/WRITE tape to be used as the permanent master data tape for this material. Option 1 requires only tape write operations; Option 2 requires tape read and write operations; Option 3 requires tape read only. The tape unit is currently

designated as unit Number 2. This can be easily changed to any desired unit number by changing the value of the variable NU in the beginning of the computer code.

Figure B-2 shows the master data input sheet for SA037. Table B-1 is a listing of the input for an IOPT = 1, master data tape generation run. Figure B-3 illustrates the data reduction of experimental curves to input points.

c. Output Received

The output of SA037 consists of the following printout. An option dependent title stating whether or not this is a "master tape generation run" (IOPT = 1), a "master tape addition run" (IOPT = 2) or a "master tape catalog run" (IOPT = 3). For each test either input, appended, or cataloged the following information is printed regardless of option: MATID, ID, KODE, KTEMP, KFAIL, the number of data points in the test, the test pressure, PRES, the initial test temperature, TEMP(1), BULK, and BETA. Following the last test, the word "END" is printed to indicate all available information was output. Table B-2 is a page of typical output for Option 1.

4. Demonstration Problem

As a demonstration problem, the input of Table B-1 was used to generate the output of Table B-2.

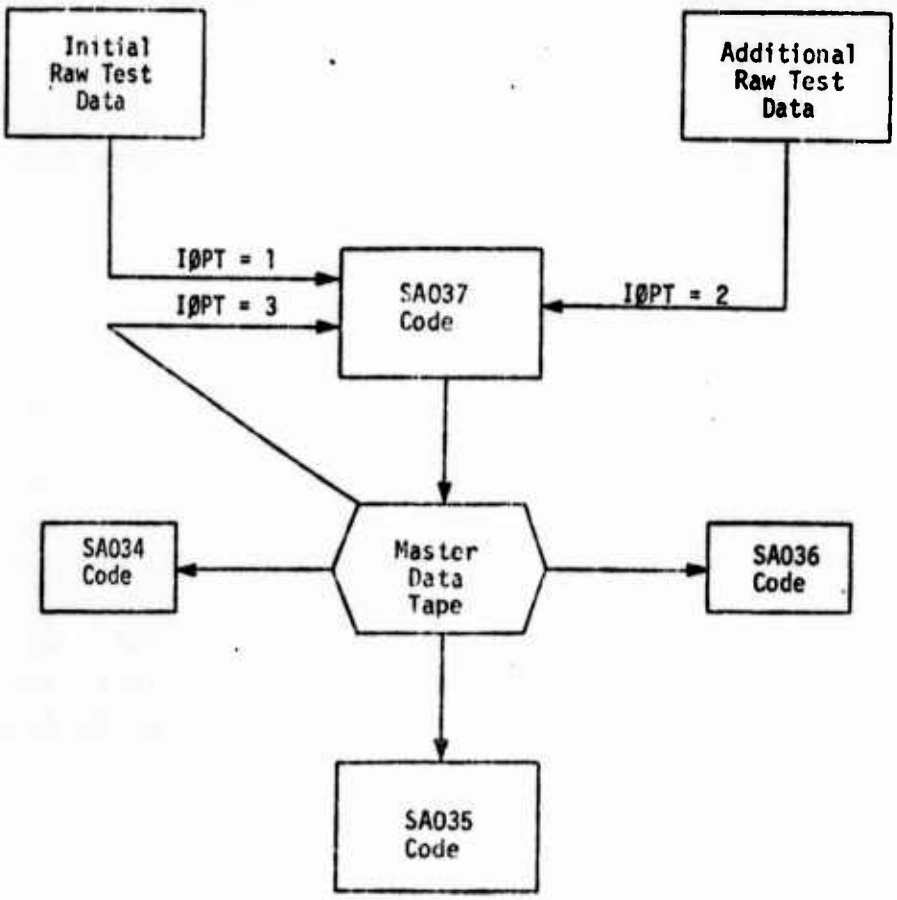

FIGURE B-1

RELATIONSHIP OF SA037 TO

MATERIAL CHARACTERIZATION CODES PACKAGE

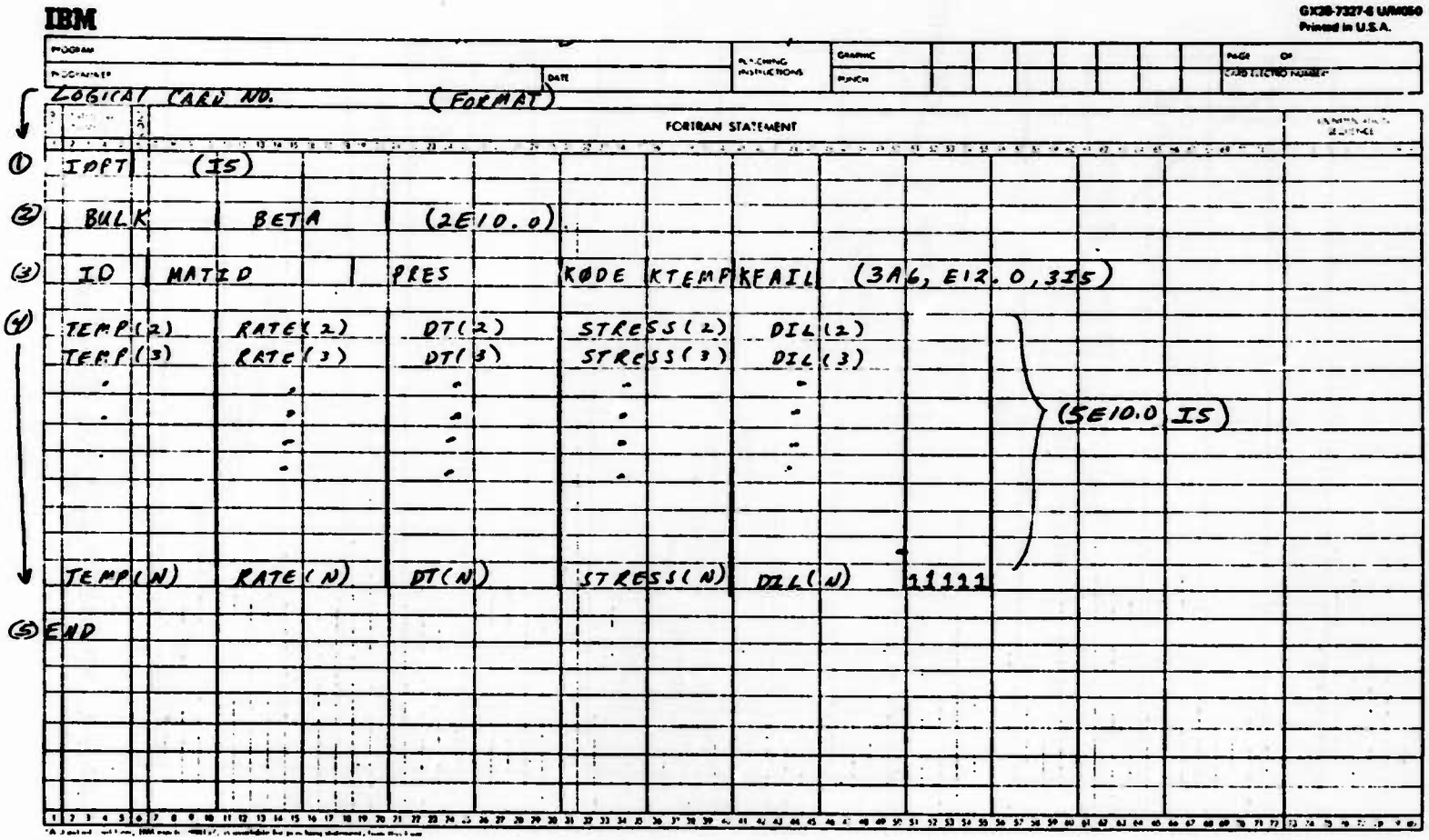

FIGURE B-2. MASTER DATA INPUT SHEET FOR CODE SA037

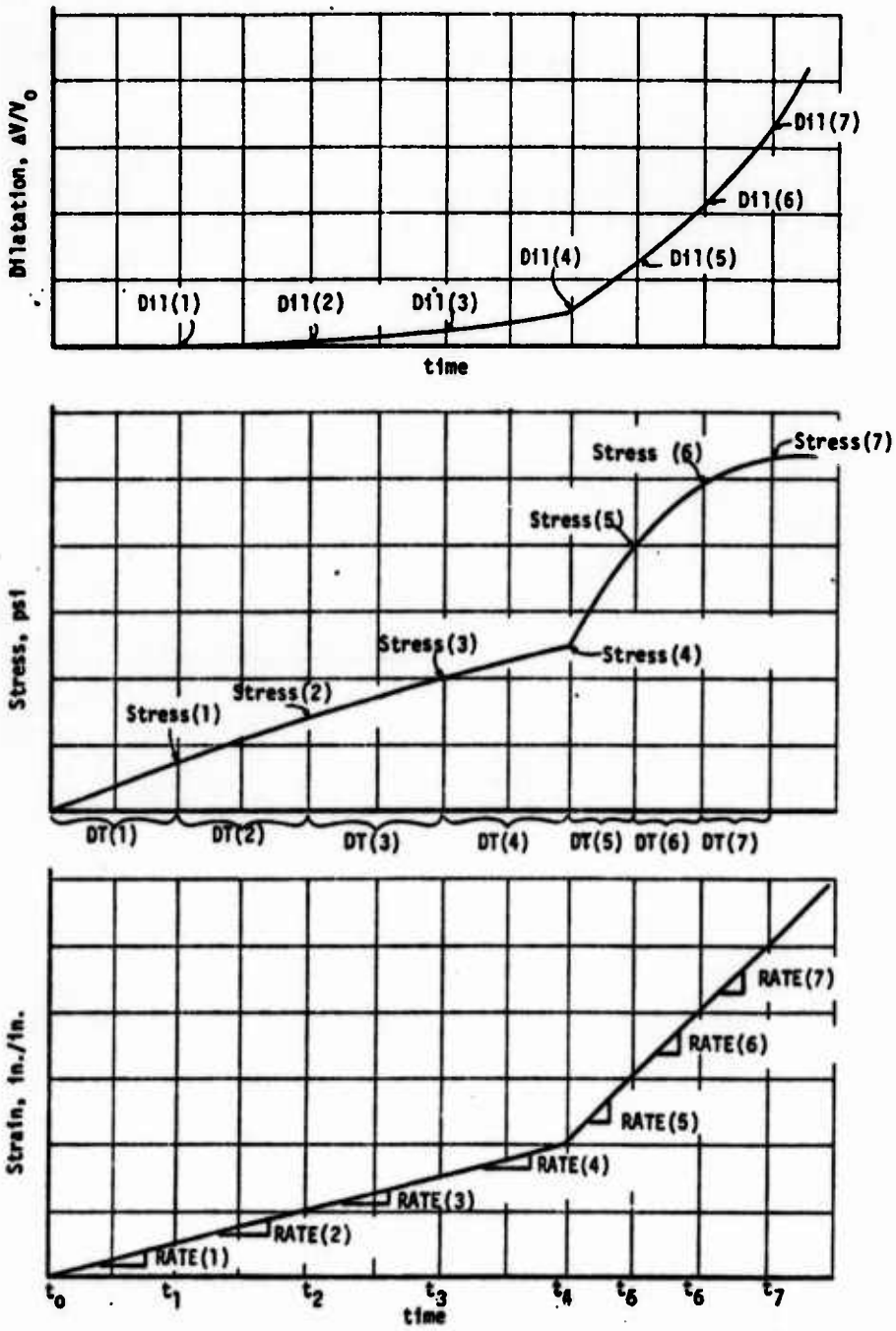

FIGURE B-3. DATA REDUCTION REQUIRED FOR INPUT INTO CODE SA037 FROM STRESS-STRAIN-DILATATION TIME DATA

TABLE B-1

LISTING OF TYPICAL INPUT FOR OPTION 1 OF CODE SA037

```
   1
500000.      4.0E-04
U001S1SOLITHANE113  0.0          1    1    1
150.         0.5        .036     12.5
150.         0.5        .04      24.4
150.         0.5        .04      35.3
150.         0.5        .04      47.5
150.         0.5        .04      57.8
150.         -0.5       .04      47.
150.         -0.5       .04      35.5
150.          -0.5      .02      29.5
150.          0.5       .02      35.0
150.          0.5       .04      46.5
150.          0.5.      .043     58.0
150.           -0.5     .037     47.5
150.           -0.5     .04      36.5
150.           -0.5     .02      30.6                    1111
U001S2SOLITHANE113  0.0          1    1    1
150.          0.5       .013      4.
150.          0.5       .013      8.
150.          0.5         .011    12.
150.          0.5       .013     15.7
150.         0.0        .029     15.8
150.         0.0         .06     15.58
150.         0.0         .06     15.5
150.         0.0          0.4    15.5
150.         0.0         1.0     15.4
150.         0.0         1.0     15.4
150.         0.0            1.6  15.5
150.           0.5       .005     17.5
150.           0.5       .016     22.5
150.           0.5       .018     27.4
150.           0.0       .062     27.4
150.           0.0       .062     27.4
150.           0.0       .062     27.4
150.           0.0        4.      27.4
150.          -0.5        .008    25.
150.          -0.5       .014     20.5
150.          -0.5       .019     15.
150.          -0.5       .016     10.
150.           0.0       .006     10.
150.           0.0         0.6    10.1
150.           0.0        2.0     10.4                    11111

U000S1SOLITHANE113  0.0          1    1    1
-65.         .5         .003     295.
-65.         .5         .003      520.
-65.         .5          .002    660.
-65.         .5          .01     718.
-65.         0.0        .017      680.
-65.         0.0         .06     640.
-65.         0.0        .06      635.
-65.         0.0         .21      618.
-65.         0.0        .52      600.
-65.         0.0         2.0     578.
-65.         0.0         2.2     560.
-65.         .5         .002      700.
-65.         .5          .004    1100.
-65.         .5         .002     1300.
-65.         .5         .002     1460.
-65.         .5         .002      1580.
-65.         .5          .001    1620.
-65.         0.0        .025     1560.
-65.         0.0         .074    1520.
-65.         0.0        .1       1500.
-65.         0.0         .6      1458.
-65.         0.0          1.4    1400.
-65.         0.0          2.2    1360.
-65.         0.0          4.2    1305.                   11111
END
```

TABLE B-2
TYPICAL OUTPUT FOR CODE SA037

S A 0 3 7 MASTER TAPE GENERATION RUN PAGE 1

MATERIAL ID	TEST ID	MODE	KTEMP	KFAIL	NO. PTS.	PRESSURE	TEMPERATURE	BULK	BETA
SOLITHANE113	U001S1	1	1	1	15	0.	150.	.5000+06	.4000-03
SOLITHANE113	U001S2	1	1	1	26	0.	150.	.5000+06	.4000-03
SOLITHANE113	U002S1	1	1	1	28	0.	1.	.5000+06	.4000-03
SOLITHANE113	U003S1	1	1	1	14	0.	77.	.5000+06	.4000-03
SOLITHANE113	U003S2	1	1	1	33	0.	77.	.5000+06	.4000-03
SOLITHANE113	U003S3	1	1	1	31	0.	77.	.5000+06	.4000-03
SOLITHANE113	U005S1	1	1	1	16	0.	16.	.5000+06	.4000-03
SOLITHANE113	U006S1	1	1	1	48	0.	0.	.5000+06	.4000-03
SOLITHANE113	U006S2	1	1	1	30	0.	0.	.5000+06	.4000-03
SOLITHANE113	U007S1	1	1	1	31	0.	-20.	.5000+06	.4000-03
SOLITHANE113	U008S1	1	1	1	49	0.	-40.	.5000+06	.4000-03
SOLITHANE113	U009S1	1	1	1	25	0.	-65.	.5000+06	.4000-03

END

EOIN

APPENDIX C

SA035 - POST PROCESSOR CODE

1. Overview and Description

SA035, version 03/01/74, consists of a main program and two subroutines. It is written entirely in FORTRAN IV. Its sole function is to provide a ready-to-copy summary of selected observed and calculated data stored on the master data tape created by Code SA037. The summary, printed for each test selected by the user, consists of two logical pages, which could be as many as six physical pages. Figure C-1 shows the relationship of SA035 to the other codes of the materials characterization package.

In operation, the user merely supplies the appropriate master data tape and a list of the ID's of the tests desired in the summary to the code as input. The only limitation, other than the rather obvious ones of mounting the correct tape and requesting only tests which actually reside on that tape, is that THE TESTS DESIRED MUST BE SELECTED IN THEIR ORDER OF APPEARANCE ON THE TAPE. If there is any doubt as to their order on the tape, it is strongly recommended that Code SA037 be used to make a catalog run (Option 3), which provides such a listing. An "END" card, E-N-D in Columns 1, 2, and 3, follows the last test request to signify the end of the run.

2. Description of Subroutines Required

SA035 requires only two subroutines which, together with the main program, make up the SA035 code. These are PAG035 and TPRD35. A listing of these subroutines is available on request.

a. Subroutine PAG035

Subroutine PAG035 is merely a page increment routine. It pulls up a new page, numbers it, writes page header information, material date, and test data headers, then returns control to the main program.

b. Subroutine TPRD35

Subroutine TPRD35 searches the master data tape for the requested tests. Upon finding one, it loads selected data from the transfer vectors into the labeled common block, INPUT, and returns control to the main program the summary pages are printed. If a requested test is not found, an error message is printed and execution terminated.

3. Usage

This section describes in detail the input required, its format, and the output received from SA035, the post processor code. Preceding this, however, is a brief description of the variables appearing in the code.

a. Basic Variables

Following is a list of the variables appearing in the main program of the SA035 code. There are no calculations of variable values in SA035. It merely reads selected data from the master data tape and prints it.

BETA	Volumetric thermal expansion coefficient
BULK	Bulk modulus
DIL	Corrected dilatation
EOCT	Octahedral shear strain
E**	Strains, ** = 11,22,33, or 12
I	Data point index

IFAIL	Alpha failure type heading, "GOOD" or "BAD"
IFLAG	Flag to indicate end of run
INV*	Strain invariants, * = 1, 2, or 3
IPG	Page counter
ITEMP	Alpha temperature type heading, "CONSTANT" or "VARIABLE"
ITEST	Identification of desired test
ITYPE	Alpha test type heading, "UNIAXIAL", "BIAXIAL" or "SHEAR"
KFAIL	Failure Code
KODE	Test type code
KTEMP	Temperature code
LINE	Line counter
MATID	Material identification
NDP	Number of data points in test
NU	Tape drive unit number, presently fixed to 2
PRES	Test pressure
RATE	Test input strain rate
STOBS	Observed stress
T	Time
TEMP	Temperature

b. Input Required

The card input for SA035 consists of only two logical cards. Card No. 1 may consist of any number of physical cards. Card No. 2 is an end-of-run card, "END" in columns 1, 2, and 3. These cards are described below, with input formats shown in parentheses, and a description of the input.

CARD(S) NO. 1 (A6) MTEST

MTEST is the six character alphanumeric test identification of the desired test. This card is repeated once for each test desired. There is no limit to how many tests may be selected from a master data tape, it may be one or all.

CARD NO. 2 END (A6)

An end-of-run card consisting of E-N-D in Columns 1, 2, and 3. This card follows last requested test, MTEST, card.

In addition to the above card input, provision must be made to mount the appropriate master data tape in a read only mode. The code currently designates this tape drive as Unit 2. This value is easily changed by resetting the fixed value of the variable NU to any desired value.

Figure C-2 shows the master data input sheet for SA-34. Figure C-3 is the actual input sheet used for the demonstration problem in Appendix B.

c. Output Received

The output from SA035 consists of two logical pages which may be up to three physical pages each. Each page contains the following header information: material identification, bulk modulus, volumetric expansion coefficient, failure type, test type, initial strain rate, test pressure, and temperature type. This header information, together with test identification and page number, is printed at the top of each page, and is followed by several columns of data. For either page, Column 1 contains the data point number, and Column 2 the accumulated time in minutes. On Page 1, the remaining six columns contain temperature, the three normal strains, the shear strain, and the observed stress, respectively. On Page 2, the remaining five columns contain the three strain invariants, the corrected dilatation, and the octahedral strain. Table C-1 contains two pages of a typical run.

4. Demonstration Problem

As a demonstration problem, the input of Figure C-3 was used to generate the output of Table C-1.

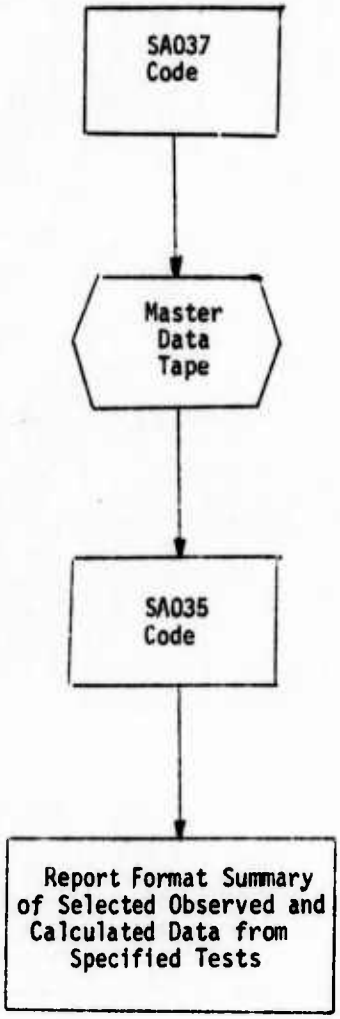

FIGURE C-1

RELATIONSHIP OF SA035 TO
MATERIAL CHARACTERIZATION CODES PACKAGE

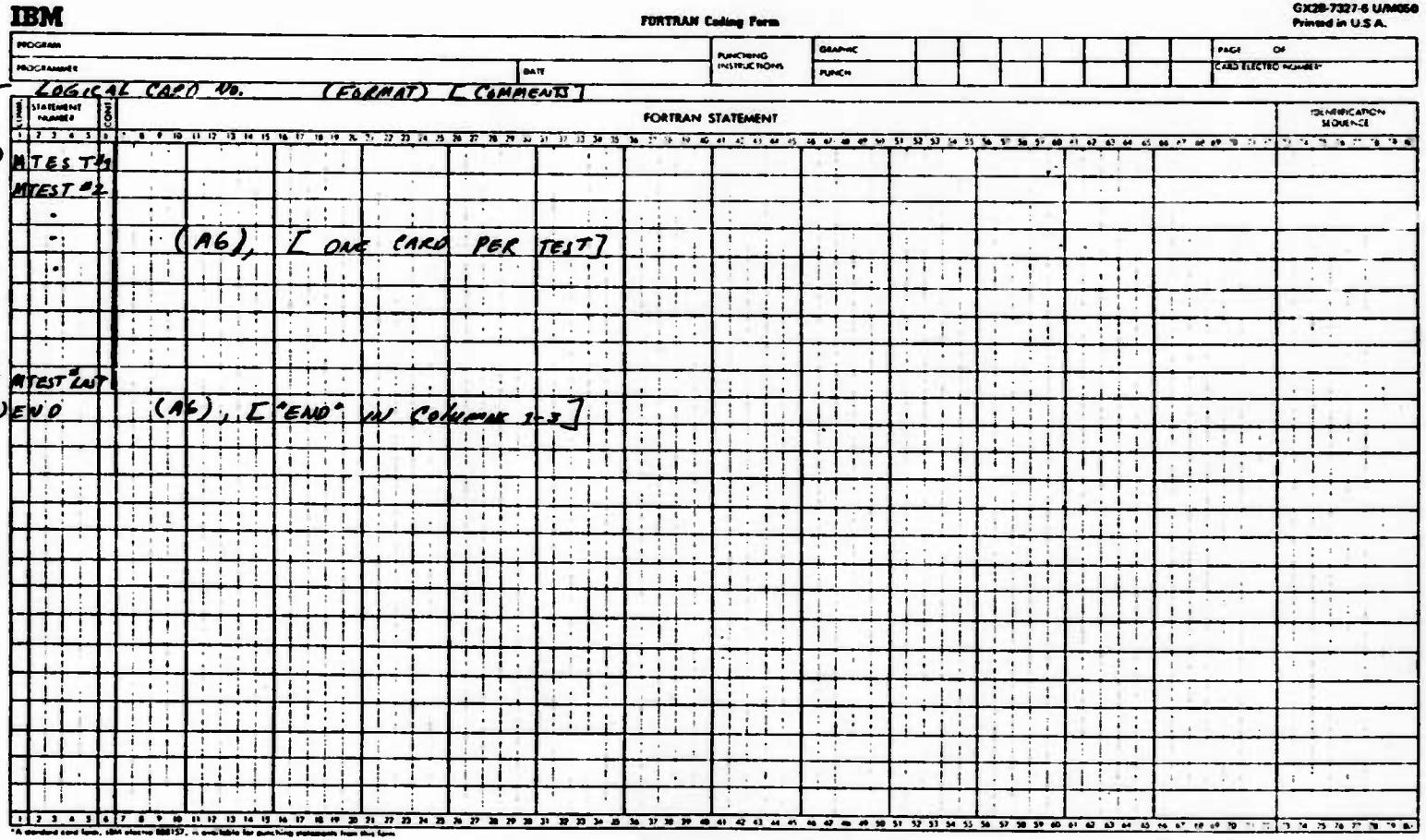

FIGURE C-2. MASTER DATA INPUT SHEET FOR CODE SA035

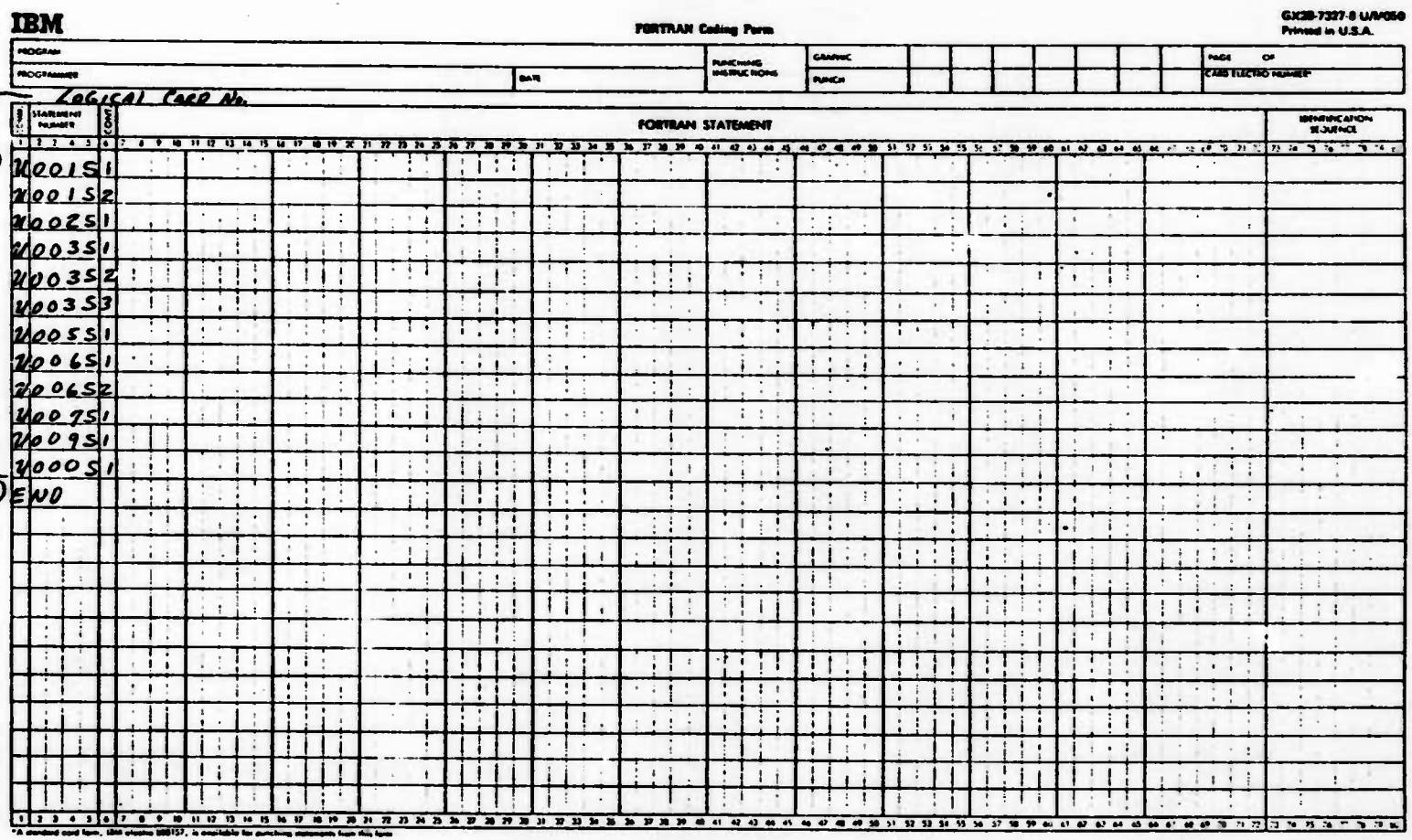

FIGURE C-3. EXAMPLE INPUT FOR SA035

TABLE C-1

EXAMPLE OF THE TWO PAGES OF OUTPUT FROM A SINGLE EXPERIMENT FROM CODE SA035

SUMMARY OF TEST NO. U0652 PAGE U0652 - 2

MATERIAL DATA

MATERIAL IS SOLITHANE113
BULK MODULUS = .5000+06
VOLUMETRIC EXPANSION COEFFICIENT = .4000-03
FAILURE TYPE = GOOD

TEST DATA

TYPE ... UNIAXIAL
INITIAL STRAIN RATE = .5000+00
PRESSURE = 0. PSIG
CONSTANT TEMPERATURE TEST

DATA POINT	TIME MIN.	STRAIN INVARIANTS I1	I2	I3	CORRECTED DILATATION	OCTAHEDRAL STRAIN
1	.000	.0000	.0000	.0000	.0000	.0000
2	.100-01	.1866-04	-.1870-04	.3102-07	.0000	.3531-02
3	.200-01	.7437-04	-.7463-04	.2463-06	.0000	.7054-02
4	.300-01	.1667-03	-.1675-03	.8251-06	.0000	.1057-01
5	.400-01	.2951-03	-.2970-03	.1941-05	.0000	.1407-01
6	.500-01	.4592-03	-.4630-03	.3764-05	.0000	.1757-01
7	.600-01	.6586-03	-.6650-03	.6457-05	.0000	.2106-01
8	.700-01	.8927-03	-.9029-03	.1018-04	.0000	.2454-01
9	.800-01	.1161-02	-.1176-02	.1508-04	.0000	.2801-01
10	.900-01	.1464-02	-.1485-02	.2132-04	.0000	.3147-01
11	.900-01	.1662-02	-.1687-02	.2577-04	.0000	.3355-01
12	.100+00	.1528-02	-.1551-02	.2274-04	.0000	.3217-01
13	.105+00	.1370-02	-.1389-02	.1930-04	.0000	.3044-01
14	.110+00	.1219-02	-.1235-02	.1622-04	.0000	.2870-01
15	.115+00	.1077-02	-.1091-02	.1348-04	.0000	.2697-01
16	.120+00	.9437-03	-.9548-03	.1106-04	.0000	.2523-01
17	.125+00	.8189-03	-.8278-03	.8945-05	.0000	.2350-01
18	.130+00	.7026-03	-.7097-03	.7114-05	.0000	.2175-01
19	.135+00	.5951-03	-.6006-03	.5548-05	.0000	.2001-01
20	.140+00	.4962-03	-.5005-03	.4228-05	.0000	.1827-01
21	.150+00	.3251-03	-.3273-03	.2244-05	.0000	.1477-01
22	.154+00	.3893-03	-.3922-03	.2940-05	.0000	.1617-01
23	.158+00	.4592-03	-.4630-03	.3764-05	.0000	.1757-01
24	.169+00	.6586-03	-.6650-03	.6457-05	.0000	.2106-01
25	.178+00	.8927-03	-.9029-03	.1018-04	.0000	.2454-01
26	.188+00	.1161-02	-.1176-02	.1508-04	.0000	.2801-01
27	.200+00	.1528-02	-.1551-02	.2274-04	.0000	.3217-01
28	.208+00	.1278-02	-.1296-02	.1741-04	.0000	.2940-01
29	.218+00	.9961-03	-.1008-02	.1199-04	.0000	.2593-01
30	.228+00	.7481-03	-.7559-03	.7813-05	.0000	.2245-01

TABLE C-1

EXAMPLE OF THE TWO PAGES OF OUTPUT FROM A SINGLE EXPERIMENT FROM CODE SA035 (Continued)

SUMMARY OF TEST NO. U00652 PAGE U00652 - 1

MATERIAL DATA

MATERIAL IS SOLITHANE113
BULK MODULUS = .5000+06
VOLUMETRIC EXPANSION COEFFICIENT = .4000-03
FAILURE TYPE = GOOD

TEST DATA

TYPE ... UNIAXIAL
INITIAL STRAIN RATE = .5000+00
PRESSURE = 0. PSIG
CONSTANT TEMPERATURE TEST

DATA POINT	TIME MIN.	TEMP. DEG.-F	STRAINS (CALCULATED) E11	E22	E33	E12	CRS. STRESS (S11 - S22)
1	.000	0.	.0000	.0000	.0000	.0000	.0000
2	.100-01	0.	.5000-02	-.2491-02	-.2491-02	.0000	.4700+03
3	.200-01	0.	.1000-01	-.4963-02	-.4963-02	.0000	.8400+03
4	.300-01	0.	.1500-01	-.7417-02	-.7417-02	.0000	.1160+04
5	.400-01	0.	.2000-01	-.9852-02	-.9852-02	.0000	.1420+04
6	.500-01	0.	.2500-01	-.1227-01	-.1227-01	.0000	.1640+04
7	.600-01	0.	.3000-01	-.1467-01	-.1467-01	.0000	.1750+04
8	.700-01	0.	.3500-01	-.1705-01	-.1705-01	.0000	.1910+04
9	.800-01	0.	.4000-01	-.1942-01	-.1942-01	.0000	.1980+04
10	.900-01	0.	.4500-01	-.2177-01	-.2177-01	.0000	.2020+04
11	.960-01	0.	.4800-01	-.2317-01	-.2317-01	.0000	.2050+04
12	.100+00	0.	.4600-01	-.2224-01	-.2224-01	.0000	.1880+04
13	.105+00	0.	.4350-01	-.2107-01	-.2107-01	.0000	.1530+04
14	.110+00	0.	.4100-01	-.1989-01	-.1989-01	.0000	.1260+04
15	.115+00	0.	.3850-01	-.1871-01	-.1871-01	.0000	.1050+04
16	.120+00	0.	.3600-01	-.1753-01	-.1753-01	.0000	.8500+03
17	.125+00	0.	.3350-01	-.1634-01	-.1634-01	.0000	.6600+03
18	.130+00	0.	.3100-01	-.1515-01	-.1515-01	.0000	.5000+03
19	.135+00	0.	.2850-01	-.1395-01	-.1395-01	.0000	.3400+03
20	.140+00	0.	.2600-01	-.1275-01	-.1275-01	.0000	.2000+03
21	.150+00	0.	.2100-01	-.1034-01	-.1034-01	.0000	.0000
22	.154+00	0.	.2300-01	-.1131-01	-.1131-01	.0000	.3200+03
23	.158+00	0.	.2500-01	-.1227-01	-.1227-01	.0000	.4800+03
24	.168+00	0.	.3000-01	-.1467-01	-.1467-01	.0000	.8400+03
25	.178+00	0.	.3500-01	-.1705-01	-.1705-01	.0000	.1150+04
26	.188+00	0.	.4000-01	-.1942-01	-.1942-01	.0000	.1390+04
27	.200+00	0.	.4600-01	-.2224-01	-.2224-01	.0000	.1610+04
28	.208+00	0.	.4200-01	-.2036-01	-.2036-01	.0000	.1180+04
29	.218+00	0.	.3700-01	-.1800-01	-.1800-01	.0000	.7300+03
30	.228+00	0.	.3200-01	-.1563-01	-.1563-01	.0000	.3800+03

APPENDIX D

SA034 - LINEAR VISCOELASTIC CHARACTERIZATION CODE

1. Overview and Description

This code was an added effort to the contract and was undertaken since linear viscoelastic characterization is used so often in the industry. Originally it was decided to use both a Prony series and a Power Law series representation of the relaxation modulus, however only the Prony series representation was completed.

SA034, version 03/01/74, is the linear viscoelastic materials characterization code. It consists of a main program and eleven subroutines, all written in FORTRAN IV. This code calculates the best fit distortional stress-strain relation for mixed uniaxial and biaxial tests having complex deformation histories while simultaneously generating the time-temperature shift function needed to properly characterize these data. There is provision in the code to represent the kernel function of the constitutive equation as a Prony series.

$$G(t') = \sum_{i=1}^{NBETA} B_i \exp(-\beta_i t') \qquad \text{(D-1)}$$

where the reduced time, t', depends on the temperature

$$t' = \int_0^t d\xi / a_T(\xi) \qquad \text{(D-2)}$$

and the stress is calculated from the convolution integral

$$\sigma(t) = \int_0^t G(t'-\xi')\dot{\varepsilon}(\xi)d\xi \qquad \text{(D-3)}$$

A linear term is easily included by setting one of the β_i, say β_1, equal to zero. In SA034 the shift function, a_T, is generated automatically by assigning a set of pivotal temperatures which span the temperature range of interest, with a single coefficient representing the slope of the curve of shift function versus temperature at these pivotal temperatures. The log (a_T) is assumed to vary linearly with temperature between pivotal temperatures. These coefficients are nonlinear and are determined by an iterative method. At each step of the iteration, the linear coefficients of the exponential Prony series terms are also updated to yield the best least squares fit. The method forces the shift function to be unity at $77^{o}F$, and thus $77^{o}F$ must always be included in the set of pivotal temperatures. Additionally, there must be one pivotal temperature greater than each test temperature.

The iterative method employed is controlled entirely by the subroutine TAYLOR, which is common to both this linear code, SA034, and the nonlinear code, SA036. Basically, the procedure is to expand the chosen representation in a TAYLOR series about some set of user supplied initial guesses. These initial values of the coefficients, B_i^0, must be nonzero for the nonlinear shift function coefficients. This results in an nth order symmetric matrix equation for the increment to these initial guesses, the ΔB_i. The order, N, is equal to the number of linear coefficients, i.e., the number of Prony series terms taken, plus the number of nonlinear coefficients, one for each shift function pivotal temperature. The maximum number of a_T pivotal temperatures is currently limited to eight (8) with the maximum value of N being twenty-five (25). The user may specify any of these coefficients to be held fixed throughout the iteration process.

The ΔB_i are solved for using Choleski decomposition and forward/backward substitution, a method which is fast, efficient, and reliable. The ΔB_i are added to the initial B_i^0 and the error function, Φ, recomputed. These ΔB_i are then successively halved to further improve the minimization of the error function. When no further improvement can be obtained, these new B_i become the new "initial values" and a new set of ΔB_i is obtained. This iterative cycle stops when convergence is obtained, i.e., the change in error function is negligible, the maximum number of requested iterations have been performed, or if no improvement to Φ is obtained after ten (10) ΔB_i interval halvings.

In operation, the user supplies the appropriate master data tape, some control information, the initial guesses, B_i^0, the β_i of the Prony series, the pivoted temperatures, ordered cold to hot and including 77°F, and the ID's

of the tests to be used in this characterization. An 'END' card, E-N-D in columns 1, 2 and 3 follows the last test request card. Figure D-1 shows the relationship of SA034 to the other codes of the materials characterization package.

2. Description of Subroutines Required

SA034 requires ten subroutines which, together with the main program, make up the SA034 code. These subroutines are: ATCALC, FLIN, INDATA, PLTN, PRONY, SHIFT, SOLV34, TAYLOR, TPRD34, and WHICH. A listing of all these subroutines is available on request.

a. Subroutine ATCALC

Subroutine ATCALC computes the value of the shift function, a_T, at the I-th data point, using the nonlinear coefficients, B_i, the pivotal temperature set, TTEMP, and the temperature at the I-th data point.

b. Subroutine FLIN

Subroutine FLIN, the "FCODE" of SA034, is called by subroutine TAYLOR to supply it with a calculated value of the normalized distortional stress at the I-th data point. FLIN in turn, calls subroutine SHIFT to set up the arrays of shift function and reduced time used to compute the derivatives of the nonlinear coefficients. FLIN then calls subroutine PRONY to actually evaluate the series at this data point.

c. Subroutine INDATA

Subroutine INDATA, called from the main program, is the primary input routine. It reads all the card input, rewinds the master data tape, and stacks the data from each requested test into the global vectors for use in the regression analysis. It calls IPRD34, which finds the requested tests and passes these data back to INDATA. An echo of the major card input and a list of tests and their header card information is also printed by INDATA before the iteration cycle is begun.

d. Subroutine PLIN

Subroutine PLIN, the "PCODE" of SA034, computes the analytical and numerical derivatives, one per unknown coefficient, at the I-th data point; normalizes them, stores them in a vector, P, and returns them to TAYLOR, from which it is called. TAYLOR then uses these derivatives to form the coefficient matrix, [A] , and the right hand side vector, {G}, in the regression matrix equation, used to solve for the increments to the undetermined coefficients, $\Delta\beta$, such that $[A]\{\Delta\beta\} = \{G\}$

e. Subroutine PRONY

Subroutine PRONY is called by FLIN for the Prony series representation of the kernel function. It evaluates the distortional stress and numerical derivatives vector for the I-th data point based on the current values of the linear and nonlinear coefficients.

f. Subroutine SHIFT

Subroutine SHIFT is called by FLIN each time a new iteration is started. SHIFT then computes the value of the shift function and reduced time for all the data points at once. It then computes the values of shift function and reduced time for all the data points once more for a small perturbation in each of the nonlinear coefficients. These additional values are later used in PRONY to evaluate a vector used

to compute the derivatives with respect to the nonlinear coefficients numerically. SHIFT calls the subroutine ATCALC approximately once for each test or data point depending upon whether the test involves constant or variable temperature.

g. Subroutine SOLV34

Subroutine SOLV34 solves the matrix equation [A] {X} = {Y}. It uses Choleski decomposition and forward/backward substitution. It assumes that the matrix [A] is symmetric. All calculations are performed in double precision. In this method, [A] is decomposed such that

$$[A] = [S]^T[D][S] \qquad \text{(D-4)}$$

where [S] is an upper triangular matrix, $[S]^T$ is the transpose of [S], and [D] is a diagonal matrix. Then defining vector {Z} such that

$$\{Z\} = [D][S]\{X\} \qquad \text{(D-5)}$$

and substituting into the Equation (D-4) yields

$$[S]^T\{Z\} = \{Y\} \qquad \text{(D-6)}$$

Here, since $[S]^T$ is a lower triangular matrix, {Z} may be solved for by forward substitution. Knowing {Z} one can substitute in Equation (D-5) and solve for {X} by backward substitution, [S] being an upper triangular matrix. If a print option is turned on, the matrices [S] and [D] are printed for each solution.

h. Subroutine TAYLOR

Subroutine TAYLOR is the heart of the iterative procedure for determination of the nonlinear, as well as the linear, coefficients. It is called by the main program at the beginning of the iterative loop and retains control until its completion. TAYLOR requires four subroutines, three of which are part of this package. These are FCODE, named FLIN for SA034; PCODE,

named PLIN; SOLV34, and TLEFT. Subroutines FLIN, PLIN, and SOLV34 have already been discussed above. Each computer has available to it a subroutine comparable to TLEFT which will be supplied by the user. This subroutine polls the system clock to determine the amount of run time remaining, and returns this time to TAYLOR. TAYLOR then compares this to some preset time - here 60 seconds - and if less time is left, terminates iteration and returns control to main. Although a description of the function of TAYLOR was previously given, it would be helpful to review its primary structure and logic at this point.

The primary goal of TAYLOR is to minimize the error function, Φ, which is defined through the use of the subroutine FCODE, which for each data point I, returns a value, $\hat{F}$, which is an approximation to the exact (observed) value F. The error function, Φ, is then defined as the difference in the relative error, squared, summed over all the data points, NDP:

$$\Phi = \sum_{I=1}^{NDP} (1-\hat{F}/F)^2 \qquad \text{(D-7)}$$

Upon entering TAYLOR for the first time, a starting value for Φ is determined, Φ_0, based on the initial coefficients, B_i^0. The next step is to determine a set ΔB_i which will further reduce the value of Φ from Φ_0 to some new value. If the ΔB_i result in a larger value of Φ than Φ_0, they are successively halved until no further improvement in Φ is achieved. This last best value of Φ then becomes the new Φ_0 and the process is repeated. The iteration loop is broken by any of the following criteria.

(1) The maximum number of iterations (user input) is exceeded.

(2) The ΔB_i were successively halved more than ten (10) times, with no improvement over Φ_0.

(3) The change in Φ is less than 1.0E-0.7.

(4) The absolute sum of the ΔB_i is less than 1.0E-08.

(5) $|(2 \times \Delta B_i / |B_i + 1.0E\text{-}7|)| \leq 1.0E\text{-}08$

(6) Insufficient time for another iteration (if subroutine TLEFT is used)

Causes (1) and (2) are by far the most common reasons for termination, although the criteria do overlap each other somewhat.

Having determined a new $\bar{\Phi}$, the corresponding set of coefficients, B_i, are used to evaluate the approximation to the observed stress, F and the derivatives of $\bar{\Phi}$ with respect to each coefficient, P_j. These values, F and P_j are used to formulate the matrix equation which is solved for the next set of ΔB_i as follows. Letting y be the exact observed value of stress and $\bar{y}$ the approximation,

$$\bar{\Phi} = \sum_{i=1}^{NDP} (1-\bar{y}/y)^2 \qquad \text{(D-8)}$$

but, at the i-th data point,

$$y \approx y_0 + \Delta B_1 P_1 + \Delta B_2 P_2 + \ldots \qquad \text{(D-9)}$$

where

$$P_k = \frac{\partial \bar{y}_1}{\partial B_k} \qquad \text{(D-10)}$$

Minimizing $\bar{\Phi}$ with respect to the B_k then yields the k-th equation as,

$$\frac{\partial \bar{\Phi}}{\partial B_k} = 0 = 2 \sum_{i=1}^{NDP} \frac{(y-\bar{y})(-P_k^i)}{y^2} \qquad \text{(D-11)}$$

or

$$\sum_{i=1}^{NDP} \frac{(y^i - y_0^i)(P_k^i)}{y^2} = \sum_{i=1}^{NDP} \frac{P_k^i P_1^i \Delta B_1 + P_k^i P_2^i \Delta B_2 + \ldots}{y^2} \qquad \text{(D-12)}$$

or

$$\{G\} = [A]\{\Delta B\} \qquad \text{(D-13)}$$

Equation (D-13) is then solved for the ΔB_i in subroutine SOLV34, and the new and old values of ϕ are compared, the ΔB_i halved if necessary, a new best set of B_k determined, and the loop repeated again.

i. Subroutine TPRD34

Subroutine TPRD34 searches the master data tape for the requested tests and, if found, loads the required data from the transfer vectors into the labeled common block LINPUT for use in subroutine INDATA. If a requested test is not found, an error message is printed and execution terminated.

j. Subroutine WHICH

Subroutine WHICH is an extremely useful utility routine which, given a global data point location, I, returns with the number of the test, IT, and the highest global data point number in that test, KOUNT.

3. Usage

This section describes the input required, its format, and the output received from SA034, the linear viscoelastic material characterization code with automatic shift function generation. Preceding this is a brief description of the variables appearing in the code.

a. Basic Variables

Following is a list of the variables appearing in the main program of the SA034 code. Each is labeled as either an INPUT or OUTPUT variable. Those variables which are input from the master data tape are labeled TAPE. All other variables are used for intermediate storage, calculations, or location indicators. The names of all variables are capitalized.

AT	Calculated value of the shift function - OUTPUT
ATEMP	Shift function pivotal temperatures - INPUT
B	Unknown coefficients - OUTPUT
BETA	Fixed coefficient in the Prony series term, exp(-BETA/AT) - INPUT
BOUND	5% of the absolute value of the maximum observed stress
DEV	Local error - OUTPUT
DEVRAT	Observed strain rate, D(E11-E22)/DT - TAPE
DT	Time step between data points - TAPE
FACTOR	Equals the temperature/volume correction term if used; otherwise equals unity. Defined as FACTOR = [(TEMP + 459.4)/540]* [(1 + VOL)/(1 + STRN1)]
HINT	Contains the values of the hereditary integrals for each data point
I	Usually refers to I=th data point of global set
IB	Subscripts of coefficients held fixed - INPUT
IFF	Equals unity to multiply this term of series by FACTOR; otherwise equals zero - INPUT
IHMAX	Maximum number of times ΔB_i are to be halved - fixed at 10
IP	Number of coefficients which are to be held fixed during iteration - INPUT
IPG	Page counter
IPRINT	Print control, normally equals zero - INPUT

IQUIT	Maximum number of iterations - INPUT
IT	Test number determined by subroutine WHICH
ITYPE	Equals one (1) for a Prony series representation
KODE	Indicates whether test is uniaxial, biaxial, or shear - TAPE
KOUNT	Highest global data point in a given test
KTEMP	Indicates whether a test is constant or variable temperature - TAPE
LINE	Line counter
NBETA	Number of Prony series terms - INPUT
NC	Total number of nonlinear coefficients
NDP	Total number of data points in the global set - currently 500 MAXIMUM
NEXP	Contains number of data points in a test
NT	Number of shift function pivotal temperatures
NTESTS	Number of tests used in this characterization
LAST	Indicates last card of a series if not blank
NTOT	Total number of coefficients, linear and nonlinear, 25 maximum
N77	Subscript of nonlinear coefficient corresponding to 77^{o}F pivotal temperature
STD	Standard deviation - OUTPUT
STRN*	Strain, * = 1, 2 - TAPE
TITLE	80 column alphanumeric title, printed at the top of each page - INPUT
VOL	Dilatation - TAPE
X(I, 1)	Time - TAPE
X(I, 2)	Temperature - TAPE
X(I, 3)	Observed stress - TAPE

XBAR	Average error of all local errors - OUTPUT
XF	Temperature volume correction factor, see FACTOR above
Y	Unity for SA034
YCAL	Local calculated value of stress - OUTPUT

b. Input Required

The card input to SA034 consists of up to ten (10) logical cards, some of which may be more than one physical card. These cards are listed below and show the program variables appearing on each card with the format in parentheses. Descriptive comments follow each card. The cards are numbered in their order of appearance.

CARD NO. 1 (20A4) TITLE

The 80 column title which will appear on each page of the output.

CARD NO. 2 (2I5) IQUIT, IPRNT

IQUIT is the maximum number of iterations desired. IPRNT is a print control, normally equal to zero. If IPRNT is not zero, additional output is received during each iteration. This output includes the error measure and the intermediate parameters during each incremental halving step. This type of additional output is useful in program de-bugging or if convergence problems should occur.

CARD NO. 3 (3I5) ITYPE, IP, NBETA

ITYPE must equal 1 and this results in a Prony series representation to the kernel function. WARNING - THE POWER LAW OPTION HAS NOT BEEN MADE OPERATIONAL. However this could be done at a minimal extra effort.

IP equals the number of coefficients which are to be held fixed. Specifying the first NT coefficients as fixed (IB = 1, 2, 3, ..., NT) eliminates determining a new a_T function.

NBETA equals the number of Prony series terms to be used, including a linear term ($\beta_1 = 0$).

CARD(S) NO. 4 (16I5) IB(1), IB(2), . . . , IB(IP)

IB equals the subscript of the coefficients to be held fixed. NOTE - this card is read only if IP does not equal zero.

CARD NO. 5 (80I1) IFF(1), IFF(2), . . . , IFF(NTOT)

IFF(1) equals 1 to multiply the J-th series term by FACTOR; equals zero otherwise. FACTOR is the temperature/volume correction term defined as,

$$FACTOR = [(TEMP + 459.4)/540] * [(1 + VOL)/(1 + STRN1)]$$

CARD(S) NO. 6 (E10.0, 15) ATEMP, LAST

ATEMP(K) is the K-th shift function pivotal temperature. LAST is blank except on last ATEMP card when it is non-blank, and then 11111 is used. NOTE - these shift function pivotal temperatures are ordered cold to hot, must include 77°F, and the last ATEMP, the hottest one, must be greater than the hottest test temperature.

CARD(S) NO. 7 (8E10.0) B(K), K = 1, NTOT

B(K) are the initial values of the unknown coefficients. The first NT values are for the nonlinear shift function coefficients. The remaining NTOT-NT coefficients are the linear ones. The linear coefficients may be assigned initial values of zero but the nonlinear coefficients, $B_0(1)$ to $B_0(NT)$ must be assigned nonzero initial values. There are NBETA linear coefficients and NT nonlinear coefficients so that NTOT = NT + NBETA.

CARD(S) NO. 8 (8E10.0) BETA(K), K = 1, NBETA

These are the fixed values of β in the K-th Prony series term, $\exp(-\beta t)$. If it is desired to include an elastic term, β_1 should be set to zero. It has been found convenient to input these β_k in either an ascending or descending series.

CARD(S) NO. 9 (A6) MTEST

MTEST is the six alphanumeric character identification of the tests to be included in this characterization. There is one test ID per card.

NOTE - These tests must be requested in their order of appearance on the master data tape. If there is any doubt as to the tape's contents or ordering it is strongly recommended that code SA037, Option 3, be run to obtain a current catalog of the tape.

CARD NO. 10 (A6) END

This is the last card of the input deck. It consists of an E-N-D in columns 1-3.

In addition to the above card input, provision must be made to mount the appropriate master data tape in a "read only" mode. The SA034 code currently assumes tape drive unit Number 2. This value is easily changed by changing the value of NU in the main program to any convenient value.

In using SA034 the following limitations must be observed:

(1) The maximum number of data points allowed is 500.

(2) The maximum number of tests is 100.

(3) The maximum number of shift function pivotal temperatures including 77°F, is eight (8). The number of pivotal temperatures actually used is designated as NT.

(4) The maximum number of Prony series terms then is (25-NT) and equals the number of β values, NBETA.

(5) The maximum number of unknown coefficients is twenty-five (25) and equals NT + NBETA.

Figure D-2 shows the master data input sheet for SA034. Figure D-3 shows the actual data input sheet for a demonstration problem.

c. Output Received

The output from SA034 can be divided into three types: input, iteration, and characterization summary. The input portion of the output consists of a header page identifying the code and version being run, followed by a list of the tests requested from the master data tape, together with their local test numbers, number of data points, test type, temperature type, test pressure and initial temperature. An "END" signifies that all tests requested were found. Following this page is a list of the BETA(I) values for the Prony series terms.

The output from the iteration loop follows next. For each iteration the following data are printed:

(1) The iteration number and the time remaining.

(2) The value of the objective function ("ERROR") and the corresponding coefficient values.

(3) The number of times the ΔB_i were halved, and their sum.

(4) Which $\Delta B_i = 0$, if any (for any coefficient held fixed).

(5) The new ΔB_i as obtained from subroutine SOLV34, i.e., before any halving takes place.

After iteration terminates, a diagnostic message giving the reason for termination is printed.

The characterization portion of the output is a test by test summary giving temperature, time, input strain, volume change, $\Delta V/V_0$, the calculated and observed values of the distortional stress, the percent deviation of the predicted from observed, and values of the NBETA hereditary integrals (and the elastic term, if $\beta_1 = 0.0$). Following the last test the final values of the regression coefficients are listed, followed by the statistical summary which gives the total number of data points, the average deviation, and the value of one standard deviation. The last page of output follows this and contains a tabulation of the calculated shift function versus temperature, followed by a list of the input pivotal temperatures. Table D-1 shows portions of the thirty-nine pages of output corresponding to the input of Figure D-3

4. Demonstration Problem

As a demonstration problem, the input of Figure D-3 was used to generate the output of Table D-1.

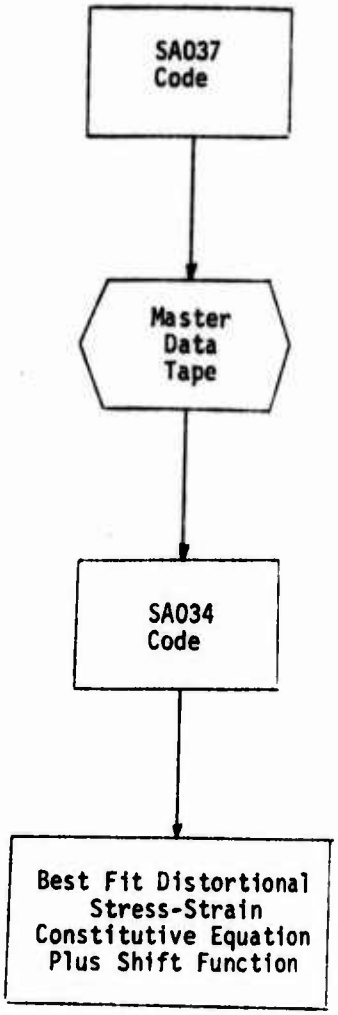

FIGURE D-1

RELATIONSHIP OF SA034 TO

MATERIAL CHARACTERIZATION CODES PACKAGE

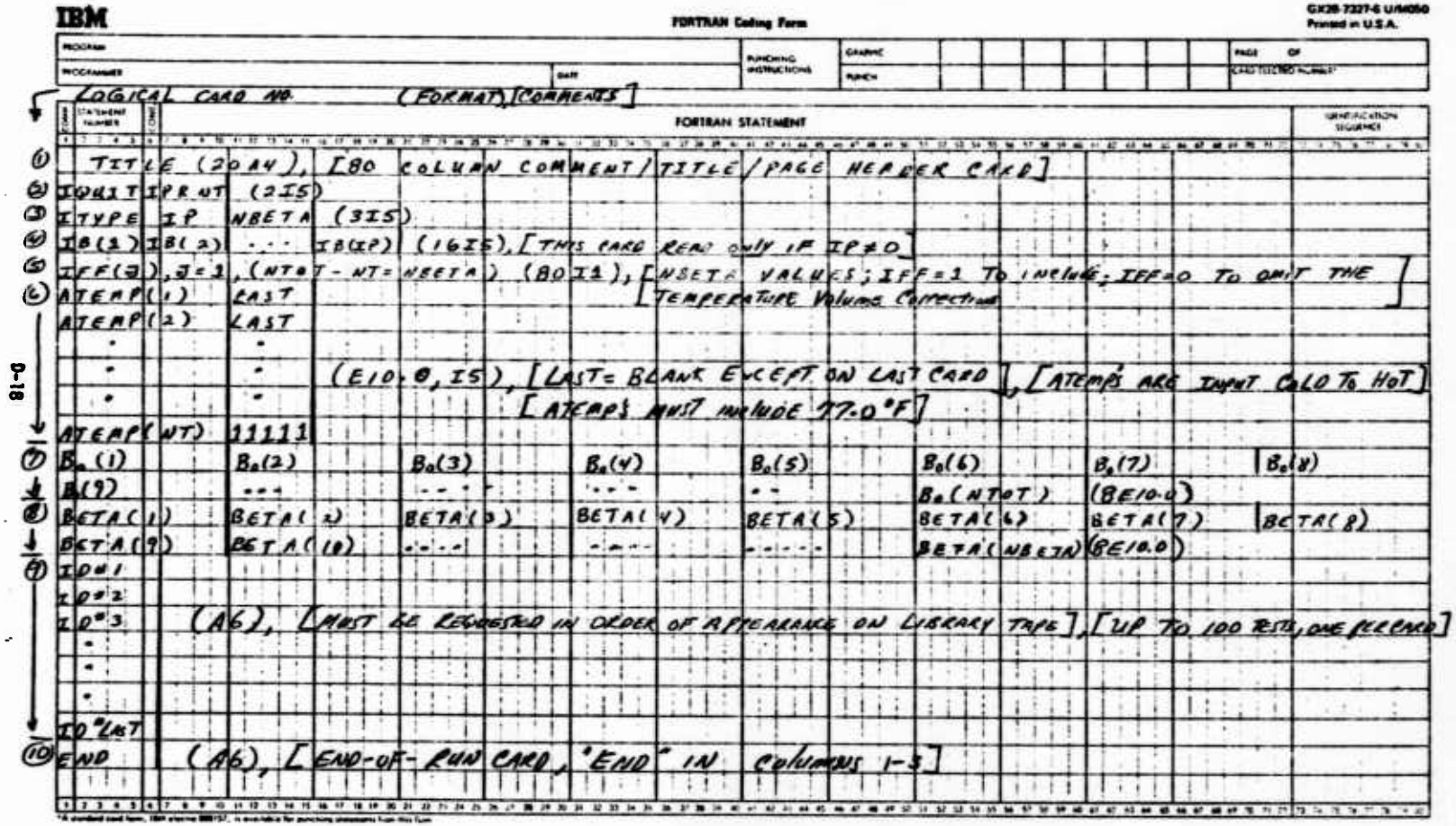

FIGURE D-2. MASTER DATA INPUT SHEET FOR CODE SA034

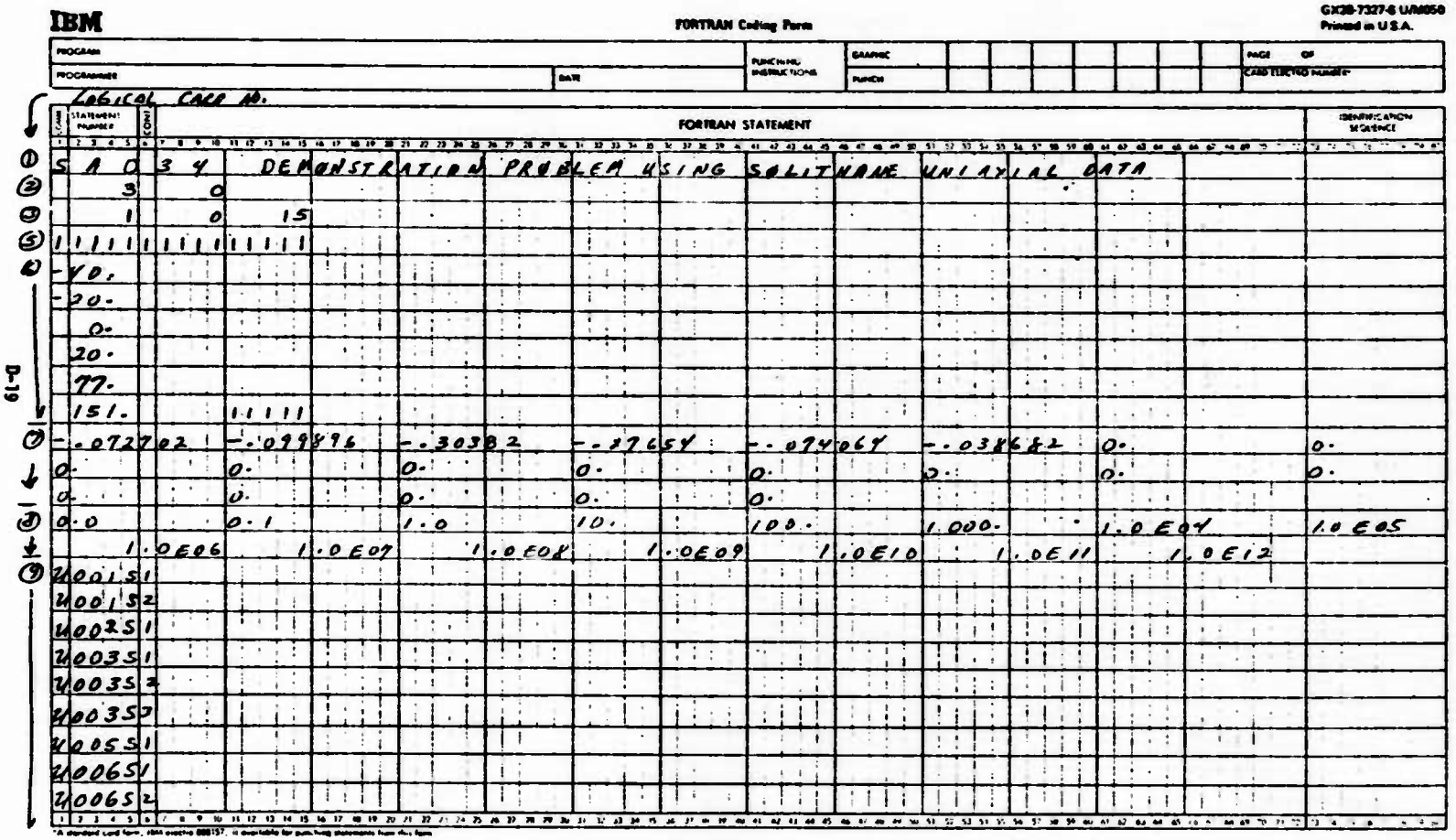

FIGURE D-3. EXAMPLE INPUT SHEET FOR CODE SA034

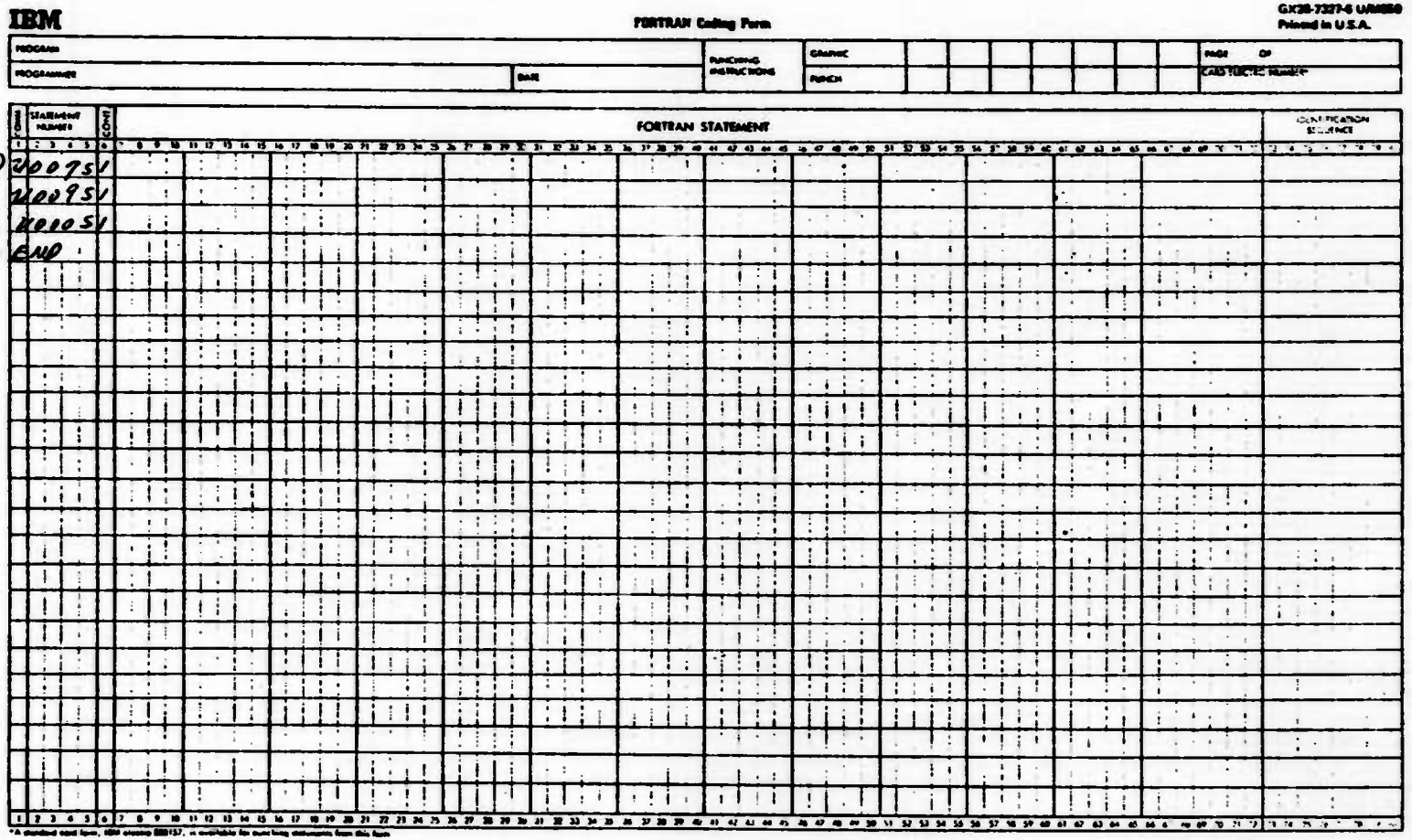

FIGURE D-3. EXAMPLE INPUT SHEET FOR CODE SA034 (Continued)

TABLE D-1

PORTIONS OF OUTPUT FOR LINEAR VISCOELASTIC CHARACTERIZATION

CODE SA034 FOR THE CASE DESCRIBED IN FIGURE D-3

```
LINEAR VISCOELASTIC CHARACTERIZATION CODE
WITH AUTOMATIC SHIFT FUNCTION GENERATION.

THIS IS S A 0 3 4, VERSION 03/01/74.
```

TABLE D-1 (Continued)

LINLAP VISCOELASTIC CHARACTERIZATION CODE

SAMPLE DEMONSTRATION PROBLEM USING ORIGINAL SOLITHANE 113 LINEAR DATA

TEST NO.	TEST ID	NDP	KODE	KTEMP	PRESSURE	TEMP
1	U0U1S1	15	1	1	.00	150.0
2	U0U1S2	26	1	1	.00	150.0
3	U0U2S1	27	1	1	.00	110.0
4	U0U3S1	14	1	1	.00	77.0
5	U0U3S2	33	1	1	.00	77.0
6	U0U3S3	31	1	1	.00	77.0
7	U0U5S1	16	1	1	.00	16.0
8	U0U6S1	48	1	1	.00	.0
9	U0U6S2	30	1	1	.00	.0
10	U0U7S1	31	1	1	.00	-20.0
11	U0U9S	49	1	1	.00	-40.0
12	U0U0S1	25	1	1	.00	-65.0

END

TABLE D-1 (Continued)

LINEAR VISCOELASTIC CHARACTERIZATION CODE

SAMPLE DEMONSTRATION PROBLEM USING ORIGINAL SOLITHANE 113 LINEAR DATA

I	BETA(I)
1	.0000
2	.1000+00
3	.1000+01
4	.1000+02
5	.1000+03
6	.1000+04
7	.1000+05
8	.1000+06
9	.1000+07
10	.1000+08
11	.1000+09
12	.1000+10
13	.1000+11
14	.1000+12
15	.1000+13

TABLE D-1 (Continued)

SAND 34 DEMONSTRATION PROBLEM USING ORIGINAL SOLITHANE 113 LINEAR DATA

```
 ITERATION NO.     1 OF    3, WITH  208 SECONDS TO GO
 E R R O R  =    .324000+03       AND THE B(K) ARE ...      -.727020-01  -.998960-01  -.303820+00  -.276540+00  -.740640-01
                                                            -.386820-01   .000000      .000000      .000000      .000000
                                                             .000000      .000000      .000000      .000000      .000000
                                                             .000000      .000000      .000000      .000000      .000000
                                                              000000
        THE DB(K) WERE HALVED   0 TIMES, AND THEIR SUM WAS  .100000+01

     DB( 1) = 0.0

     DB( 2) = 0.0

     DB( 3) = 0.0

     DB( 4) = 0.0

     DB( 5) = 0.0

     DB( 6) = 0.0

                                NEW DB(K) ARE ...           .000000      .000000      .000000      .000000      .000000
                                                            .000000      .352716+03   .446090+02  -.447858+02   .109083+03
                                                           -.102970+04   .566834+04   .164312+05   .320873+05   .747835+05
                                                            .220151+05   .231726+05   .375638+04   .488930+05  -.666067+04
                                                            .390123+06

 ITERATION NO.     2 OF    3, WITH  231 SECONDS TO GO
 E R R O R  =    .234212+01       AND THE B(K) ARE ...      -.727020-01  -.998960-01  -.303820+00  -.276540+00  -.740640-01
                                                            -.386820-01   .352716+03   .446090+02  -.447858+02   .109083+03
                                                           -.102970+04   .566834+04   .164312+05   .320873+05   .747835+05
                                                            .220151+05   .231726+05   .375638+04   .488930+05  -.666067+04
                                                            .390123+06
        THE DB(K) WERE HALVED   1 TIMES, AND THEIR SUM WAS  .625171+06

                                NEW DB(K) ARE ...          -.211729-01  -.551540-02  -.594022-04   .689864-03  -.138442-02
                                                            .143125-02  -.185837-01  -.382960+00   .872294+00  -.369605+01
                                                            .614930+02  -.433767+03  -.288463+03  -.842275+03  -.294695+04
                                                            .345089+04  -.950716+03   .500725+04  -.239689+05   .172775+06
                                                           -.128698+07

 ITERATION NO.     3 OF    3, WITH  169 SECONDS TO GO
 E R R O R  =    .231424+01       AND THE B(K) ARE ...      -.832884-01  -.102654+00  -.303850+00  -.276195+00  -.747562-01
                                                            -.379664-01   .352707+03   .444175+02  -.443467+02   .107235+03
                                                           -.998449+03   .545246+04   .162869+05   .316662+05   .733101+05
                                                            .237405+05   .226972+05   .626001+04   .369085+05   .797267+05
                                                           -.253369+06
        THE DB(K) WERE HALVED   2 TIMES, AND THEIR SUM WAS  .149771+07

                                NEW DB(K) ARE ...          -.109603-01  -.205749-02   .104670-02   .359257-04  -.113231-03
                                                           -.429048-03  -.857596-02   .175614+00  -.265604+00   .572485+00
```

TABLE D-1 (Continued)

LINEAR VISCOELASTIC CHARACTERIZATION CODE PAGE 1

SAG34 DEMONSTRATION PROBLEM USING ORIGINAL SOLITHANE 113 LINEAR DATA

TEST NO. 1 15 INPUT DATA POINTS

DATA IS FROM A UNIAXIAL TEST

TEMP	TIME	STRN1	VOLUME	SIGCAL	SIG1	% DEV	BETA HEREDITARY INTEGRAL TERMS					
150.	.00000	.00000	.00000	.00	.00	.00	.000	.000	.000	.000	.000	.000
							.000	.000	.000	.000	.000	.000
							.000	.000	.000			
150.	.38000-01	.19000-01	.00000	11.57	12.50	-7.43	.284-01	.184-01	.142-01	.310-02	.310-03	.310-04
							.310-05	.310-06	.310-07	.310-08	.310-09	.310-10
							.310-11	.310-12	.310-13			
150.	.78000-01	.39000-01	.00000	23.18	24.40	-5.02	.579-01	.366-01	.222-01	.310-02	.310-03	.310-04
							.310-05	.310-06	.310-07	.310-08	.310-09	.310-10
							.310-11	.310-12	.310-13			
150.	.11800+00	.59000-01	.00000	34.36	36.30	-5.33	.873-01	.537-01	.264-01	.310-02	.310-03	.310-04
							.310-05	.310-06	.310-07	.310-08	.310-09	.310-10
							.310-11	.310-12	.310-13			
150.	.15800+00	.79000-01	.00000	45.09	47.50	-5.08	.116+00	.697-01	.286-01	.310-02	.310-03	.310-04
							.310-05	.310-06	.310-07	.310-08	.310-09	.310-10
							.310-11	.310-12	.310-13			
150.	.19800+00	.99000-01	.00000	55.33	57.80	-4.27	.145+00	.848-01	.298-01	.310-02	.310-03	.310-04
							.310-05	.310-06	.310-07	.310-08	.310-09	.310-10
							.310-11	.310-12	.310-13			
150.	.23800+00	.79000-01	.00000	45.39	47.00	-3.42	.116+00	.601-01	.881-02	-.310-02	-.310-03	-.310-04
							-.310-05	-.310-06	-.310-07	-.310-08	-.310-09	-.310-10
							-.310-11	-.310-12	-.310-13			
150.	.27800+00	.59000-01	.00000	34.95	35.50	-1.54	.873-01	.370-01	-.143-01	-.310-02	-.310-03	-.310-04
							-.310-05	-.310-06	-.310-07	-.310-08	-.310-09	-.310-10
							-.310-11	-.310-12	-.310-13			
150.	.29800+00	.49000-01	.00000	29.43	29.50	-.23	.726-01	.260-01	-.189-01	-.310-02	-.310-03	-.310-04
							-.310-05	-.310-06	-.310-07	-.310-08	-.310-09	-.310-10
							-.310-11	-.310-12	-.310-13			
150.	.31800+00	.59000-01	.00000	34.94	35.00	-.16	.873-01	.350-01	-.514-02	.286-02	.310-03	.310-04
							.310-05	.310-06	.310-07	.310-08	.310-09	.310-10
							.310-11	.310-12	.310-13			
150.	.35800+00	.79000-01	.00000	45.04	46.50	-3.14	.116+00	.522-01	.120-01	.310-02	.310-03	.310-04
							.310-05	.310-06	.310-07	.310-08	.310-09	.310-10
							.310-11	.310-12	.310-13			
150.	.40100+00	.10050+00	.00000	55.71	58.00	-3.95	.147+00	.695-01	.215-01	.310-02	.310-03	.310-04
							.310-05	.310-06	.310-07	.310-08	.310-09	.310-10
							.310-11	.310-12	.310-13			

TABLE D-1 (Continued)

LINEAR VISCOELASTIC CHARACTERIZATION CODE PAGE 17

SAND34 DEMONSTRATION PROBLEM USING ORIGINAL SOLITHANE 113 LINEAR DATA

TEST NO. 7 16 INPUT DATA POINTS

DATA IS FROM A UNIAXIAL TEST

TEMP	TIME	STRAIN	VOLUME	SIGCAL	SIGI	% DEV	BETA HEREDITARY INTEGRAL TERMS					
16.	.00000	.00000	.00000	.00	.00	.00	.000	.000	.000	.000	.000	.000
							.000	.000	.000	.000	.000	.000
							.000	.000	.000			
16.	.35000-02	.17500-02	.00000	61.93	40.00	54.83	.262-02	.176-02	.175-02	.175-02	.175-02	.174-02
							.161-02	.862-03	.107-03	.107-04	.107-05	.107-06
							.107-07	.107-08	.107-09			
16.	.70000-02	.35000-02	.00000	93.64	80.00	17.05	.525-02	.350-02	.350-02	.350-02	.349-02	.348-02
							.299-02	.103-02	.107-03	.107-04	.107-05	.107-06
							.107-07	.107-08	.107-09			
16.	.11000-01	.55000-02	.00000	121.63	120.00	1.36	.824-02	.551-02	.550-02	.550-02	.549-02	.536-02
							.430-02	.107-02	.107-03	.107-04	.107-05	.107-06
							.107-07	.107-08	.107-09			
16.	.13000-01	.65000-02	.00000	133.92	140.00	-4.34	.973-02	.651-02	.650-02	.650-02	.648-02	.631-02
							.487-02	.107-02	.107-03	.107-04	.107-05	.107-06
							.107-07	.107-08	.107-09			
16.	.17000-01	.65000-02	.00000	89.44	112.00	-20.14	.973-02	.650-02	.650-02	.650-02	.647-02	.619-02
							.404-02	.165-03	.848-12	.000	.000	.000
							.000	.000	.000			
16.	.19000-01	.65000-02	.00000	81.28	90.00	-9.69	.973-02	.650-02	.650-02	.650-02	.646-02	.617-02
							.368-02	.650-04	.744-16	.000	.000	.000
							.000	.000	.000			
16.	.23000-01	.65000-02	.00000	70.32	76.00	-7.47	.973-02	.650-02	.650-02	.648-02	.645-02	.609-02
							.306-02	.101-04	.583-24	.000	.000	.000
							.000	.000	.000			
16.	.33000-01	.65000-02	.00000	52.59	54.00	-2.61	.973-02	.650-02	.650-02	.648-02	.642-02	.574-02
							.192-02	.947-07	.000	.000	.000	.000
							.000	.000	.000			
16.	.43000-01	.65000-02	.00000	41.22	42.00	-1.85	.973-02	.650-02	.650-02	.649-02	.639-02	.548-02
							.120-02	.891-09	.000	.000	.000	.000
							.000	.000	.000			
16.	.53000-01	.65000-02	.00000	33.70	36.00	-6.40	.973-02	.650-02	.650-02	.648-02	.636-02	.523-02
							.754-03	.838-11	.000	.000	.000	.000
							.000	.000	.000			
16.	.75000-01	.65000-02	.00000	24.45	26.00	-5.95	.973-02	.650-02	.650-02	.648-02	.630-02	.472-02
							.270-03	.292-15	.000	.000	.000	.000
							.000	.000	.000			

TABLE D-1 (Continued)

LINEAR VISCOELASTIC CHARACTERIZATION CODE PAGE 34

SAND84 DEMONSTRATION PROBLEM USING ORIGINAL SOLITHANE 113 LINEAR DATA

TEST NO. 12 25 INPUT DATA POINTS

DATA IS FROM A UNIAXIAL TEST

TEMP	TIME	STRN1	VOLUME	SIGCAL	SIG1	% DEV	NBETA HEREDITARY INTEGRAL TERMS					
-65.	.00000	.00000	.00000	.00	.00	.00	.000	.000	.000	.000	.000	.000
							.000	.000	.000	.000	.000	.000
							.000	.000	.000			
-65.	.30000-02	.15000-02	.00000	280.34	295.00	-4.97	.225-02	.225-02	.225-02	.225-02	.225-02	.225-02
							.155-02	.152-02	.150-02	.150-02	.150-02	.150-02
							.146-02	.114-02	.260-03			
-65.	.60000-02	.30000-02	.00000	527.79	520.00	1.50	.450-02	.450-02	.450-02	.450-02	.450-02	.450-02
							.291-02	.301-02	.300-02	.300-02	.300-02	.298-02
							.203-02	.178-02	.261-03			
-65.	.80000-02	.40000-02	.00000	692.12	660.00	4.87	.599-02	.599-02	.599-02	.599-02	.599-02	.599-02
							.427-02	.402-02	.400-02	.400-02	.400-02	.397-02
							.371-02	.205-02	.261-03			
-65.	.90000-02	.45000-02	.00000	768.36	718.00	7.00	.674-02	.674-02	.674-02	.674-02	.674-02	.674-02
							.466-02	.451-02	.450-02	.450-02	.450-02	.446-02
							.413-02	.214-02	.261-03			
-65.	.26000-01	.45000-02	.00000	663.99	660.00	.59	.674-02	.674-02	.674-02	.674-02	.674-02	.674-02
							.447-02	.449-02	.450-02	.450-02	.448-02	.432-02
							.298-02	.823-04	.182-17			
-65.	.86000-01	.45000-02	.00000	610.74	640.00	-4.57	.674-02	.674-02	.674-02	.674-02	.674-02	.674-02
							.447-02	.449-02	.450-02	.449-02	.443-02	.385-02
							.944-03	.830-09	.000			
-65.	.14600+00	.45000-02	.00000	592.92	635.00	-6.63	.674-02	.674-02	.674-02	.674-02	.674-02	.674-02
							.447-02	.449-02	.450-02	.449-02	.438-02	.343-02
							.299-03	.837-14	.000			
-65.	.35600+00	.45000-02	.00000	578.38	618.00	-6.41	.674-02	.674-02	.674-02	.674-02	.674-02	.674-02
							.447-02	.451-02	.450-02	.447-02	.421-02	.229-02
							.533-05	.272-31	.000			
-65.	.87600+00	.45000-02	.00000	563.98	600.00	-6.00	.674-02	.674-02	.674-02	.674-02	.674-02	.674-02
							.447-02	.449-02	.449-02	.443-02	.381-02	.846-03
							.249-09	.000	.000			
-65.	.28760+01	.45000-02	.00000	536.46	578.00	-7.19	.674-02	.674-02	.674-02	.674-02	.674-02	.674-02
							.447-02	.451-02	.447-02	.426-02	.259-02	.183-04
							.552-26	.000	.000			
-65.	.50760+01	.45000-02	.00000	517.26	560.00	-7.63	.674-02	.674-02	.674-02	.674-02	.674-02	.674-02
							.447-02	.451-02	.446-02	.408-02	.170-02	.269-06
							.000	.000	.000			

TABLE D-1 (Continued)

S A 0 3 4 DEMONSTRATION PROBLEM USING ORIGINAL SOLITHANE 113 LINEAR DATA

TEST NO. 12 25 INPUT DATA POINTS

DATA IS FROM A U N I A X I A L TEST

TEMP	TIME	STRN1	VOLUME	SIGCAL	SIG1	% DEV	NPETA HEREDITARY INTEGRAL TERMS					
-65.	.56780+01	.55000-02	.00000	710.31	700.00	1.47	.824-02	.824-02	.824-02	.824-02	.824-02	.824-02
							.563-02	.550-02	.546-02	.508-02	.270-02	.998-03
							.981-03	.831-03	.255-03			
-65.	.50820+01	.75000-02	.00000	1040.73	1100.00	-5.39	.112-01	.112-01	.112-01	.112-01	.112-01	.112-01
							.738-02	.750-02	.746-02	.708-02	.470-02	.298-02
							.283-02	.178-02	.261-03			
-65.	.50840+01	.85000-02	.00000	1203.68	1300.00	-7.41	.127-01	.127-01	.127-01	.127-01	.127-01	.127-01
							.874-02	.851-02	.846-02	.808-02	.570-02	.397-02
							.371-02	.205-02	.261-03			
-65.	.50860+01	.95000-02	.00000	1358.35	1460.00	-6.96	.142-01	.142-01	.142-01	.142-01	.142-01	.142-01
							.971-02	.952-02	.946-02	.908-02	.669-02	.495-02
							.455-02	.222-02	.261-03			
-65.	.50880+01	.10500-01	.00000	1512.08	1580.00	-4.30	.157-01	.157-01	.157-01	.157-01	.157-01	.157-01
							.109-01	.105-01	.105-01	.101-01	.769-02	.593-02
							.536-02	.235-02	.261-03			
-65.	.50890+01	.11000-01	.00000	1583.51	1620.00	-2.25	.165-01	.165-01	.165-01	.165-01	.165-01	.165-01
							.111-01	.110-01	.110-01	.106-01	.815-02	.642-02
							.575-02	.239-02	.261-03			
-65.	.51140+01	.11000-01	.00000	1447.53	1560.00	-7.21	.165-01	.165-01	.165-01	.165-01	.165-01	.165-01
							.111-01	.110-01	.110-01	.106-01	.815-02	.612-02
							.356-02	.198-04	.396-24			
-65.	.51180+01	.11000-01	.00000	1375.38	1520.00	-9.51	.165-01	.165-01	.165-01	.165-01	.165-01	.165-01
							.109-01	.110-01	.110-01	.104-01	.804-02	.531-02
							.062-03	.136-10	.000			
-65.	.52680+01	.11000-01	.00000	1354.11	1500.00	-9.73	.165-01	.165-01	.165-01	.165-01	.165-01	.165-01
							.111-01	.110-01	.110-01	.105-01	.788-02	.438-02
							.127-03	.642-14	.000			
-65.	.58080+01	.11000-01	.00000	1321.43	1458.00	-9.37	.165-01	.165-01	.165-01	.165-01	.165-01	.165-01
							.111-01	.110-01	.109-01	.104-01	.703-02	.139-02
							.128-08	.000	.000			
-65.	.72680+01	.11000-01	.00000	1281.97	1400.00	-8.44	.165-01	.165-01	.165-01	.165-01	.165-01	.165-01
							.111-01	.110-01	.109-01	.101-01	.537-02	.947-04
							.281-20	.000	.000			
-65.	.94680+01	.11000-01	.00000	1240.30	1360.00	-8.80	.165-01	.165-01	.165-01	.165-01	.165-01	.165-01
							.111-01	.110-01	.109-01	.973-02	.352-02	.139-05
							.000	.000	.000			

TABLE D-1 (Continued)

S A 0 3 4 DEMONSTRATION PROBLEM USING ORIGINAL SOLITHANE 113 LINEAR DATA

REGRESSION COEFFICIENTS ...

I	D(I)
1	-.88769-01
2	-.10368+00
3	-.30333+00
4	-.27618+00
5	-.74813-01
6	-.38181-01
7	.35270+03
8	.44505+02
9	-.44442+02
10	.10752+03
11	-.99876+03
12	.54486+04
13	.16227+05
14	.31695+05
15	.73105+05
16	.23856+05
17	.23327+05
18	.57731+04
19	.32206+05
20	.41328+05
21	.65353+05

THERE WERE 345 EXPERIMENTAL TEST POINTS

THE AVERAGE DEVIATION = -.736 PERCENT, AND
THE STANDARD DEVIATION = 8.125 PERCENT.

TABLE D-1 (Continued)

SAMPLE PROBLEM USING ORIGINAL SOLITHANE 113 LINEAR DATA

SHIFT FUNCTION	TEMPERATURE - F
.2129+10	-80.
.3807+09	-60.
.6110+08	-40.
.7682+07	-20.
.1782+07	0.
.7112+06	20.
.1593+06	40.
.3567+05	60.
.8918+04	80.
.4155+04	100.
.1936+04	120.
.9023-01	140.
.4205-01	160.
.1959-01	180.
.9129-02	200.

ATEMPS USED
-40.
-20.
0.
20.
77.
151.

GFREE 2.

GFIN

APPENDIX E

SA036 - NONLINEAR VISCOELASTIC CHARACTERIZATION CODE

1. Overview and Description

SA036, version 03/01/74, is the nonlinear viscoelastic materials characterization code. It consists of a main program and seventeen subroutines, all written in FORTRAN IV. It is a user oriented tool, capable of characterizing nonlinear, viscoelastic, propellant-like materials. This code can handle large masses of data, and completely determines all unknown coefficients, linear and nonlinear, in the constitutive equation, including the time-temperature shift function. SA036 will, at the user's option, perform a characterization of the bulk, as well as the distortional stress-strain relationship. In addition to these response characterizations, the code can also perform a failure characterization based on a nonlinear cumulative damage theory. Just as in the previous code, any of the variables can be specified as being constant and these will not be varied. This feature more than satisfies the requirement that the a_T function be determined as a user option.

The form of the distortional stress-strain relationship is

$$\sigma'_y(t) = \exp[B_{NC+1} I_\gamma + (B_{NC+2} I_d)/I_\gamma] \left\{ B_{NC+5} \dot{\varepsilon}'_{ij}(t) + B_{NC+6} \left(\frac{I_\gamma}{\| I_\gamma \|_{B_{NT+1}}} \right)^{B_{NC+3}} \varepsilon_{ij}(t) + B_{NC+7} \left(1 - \frac{I_\gamma}{\| I_\gamma \|_\infty} \right)^{B_{NC+4}} \int_0^t (t'-\xi')^{B_{NC}} \dot{\varepsilon}_{ij}(\xi) d\xi \right\} \quad \text{(E-1)}$$

where σ'_y = distortional stress

ε'_{ij} = distortional strain

I_γ = octahedral shear strain

I_d = volumetric dilatation, $\Delta V/V_o$

and the total stress and strain state is defined by

$$\sigma_{ij} = \delta_{ij}\bar{\sigma} + \sigma'_{ij} \qquad \text{where } \bar{\sigma} = \text{mean pressure} = \frac{\sigma_{11}+\sigma_{22}+\sigma_{33}}{3} \tag{E-2}$$

$$\varepsilon_{ij} = \delta_{ij}\bar{\varepsilon} + \varepsilon'_{ij} \qquad \text{where } \bar{\varepsilon} = \frac{\varepsilon_{11}+\varepsilon_{22}+\varepsilon_{33}}{3} = I_1/3 \tag{E-3}$$

The distortional stresses and strains can be obtained from the characterization experiments simply by subtracting principle values. Equation (E-1) is a minor simplification of the constitutive equation proposed at the end of the previous contract (E-1) and the uniaxial and biaxial stress states are converted to distortional values automatically by computer code SA036. The definitions of the norms and the reduced times are:

$$t'-\xi' = \int_{\xi}^{t} d\xi/a_T(\xi) \tag{E-4}$$

$$\|I_\gamma\|_p = \left\{\int_0^t \left(|I_\gamma(\xi)|^p/a_T(\xi)\right)\, d\xi\right\}^{1/P} \tag{E-5}$$

The B_i in Equation (E-1) represent the unknown coefficients to be determined. Coefficients B_1 through B_{NT} correspond to the NT values of pivotal temperatures used to generate the shift function, a_T, as discussed previously. Here, B_{NT+1} represents the order of the Lebesgue norm, NC equals NT + 2 and the total number of coefficients is NC + 7. The following limitations have been placed on certain of these coefficients:

$$0<B_{NT+1} < 100$$

$$-1<B_{NC} < 0$$

$$0<B_{NC+3} < 20$$

$$0<B_{NC+4} < 20$$

The characterization for the dilatation, $\Delta V/V_o$, is given by,

$$I_d = \Delta V/V_o = B_6\bar{\sigma}_B \left\{\exp\left[[B_1 + B_2\,(T-77)]\,\bar{\sigma}_B\right] - 1.0\right\} + B_1(I_\gamma)^{B_3} \exp\left[[B_4 + B_5(T-77)]\,\bar{\sigma}\right] \qquad \text{(E-6)}$$

where $\bar{\sigma}$ is the calculated value of the bulk stress and T is the temperature in degrees Fahrenheit.

For the cumulative damage failure characterization, the following representation, utilizing only nine coefficients, is used:

$$D(t) = B_8 \left\{||\exp\{[B_1 + B_2(T-77)]\,\bar{\sigma}_B\}\,\sigma_{oct}||_\infty\right\}^{B_6} + B_9 \left\{||\exp\{[B_3 + B_4(T-77)]\,\bar{\sigma}_B\}\,\sigma_{oct}||_{B_5}\right\}^{B_7} \qquad \text{(E-7)}$$

where $\bar{\sigma}$ is the calculated value of the bulk stress, and σ_{oct} is the calculated value of the octahedral stress. Coefficient B_5 represents the order of the Lebesgue norm.

For each characterization, distortional, dilatational, and failure, an iterative process is used to determine the unknown coefficients. The method of iteration is similar to that used in Code SA034, the only difference being in the number of nonlinear coefficients to be determined.

In operation, SA036 is again quite similar to the linear Code SA034. The user supplies the appropriate master data tape (created by Code SA037), some control and limit variables, a set of shift function pivotal temperatures, a set of initial guesses for all of the nonlinear

coefficients in the characterization chosen, and the ID's of the tests from the master data tape to be included in this run. Figure E-1 shows the relationship of SA036 to the other codes of the materials characterization package.

2. Description of Subroutines Required

SA036 requires seventeen subroutines which, together with the main program, make up the SA036 code. These subroutines are: ATCALC, BULK, DLTATN, DVTORC, FAILUR, FBULK, FCODNL, FFAIL, PBULK, PCODNL, PFAIL, SHIFT, SOLVDP, SUB1, TAYLOR, TPRD36, and WHICH. Some of these are similar in name and operation to subroutines making up the SA034 code. A source listing of all subroutines is available on request.

a. Subroutine ATCALC

Subroutine ATCALC computes the value of the shift function, a_T, at a specific data point, using the current set of coefficients, B_i, the data point temperature and the set of shift function pivotal temperatures, TTEMP.

b. Subroutine BULK

Subroutine BULK computes the value of the bulk stress, using the final set of deviatoric coefficients, reduced time matrix, Lebesgue norm matrix, and the calculated value of the first strain invariant. These values of bulk stress, σ_B, are then used in the mathematical characterization of dilatation and cumulative damage failure; see Equations (E-6) and (E-7).

c. Subroutine DLTATN

Subroutine DLTATN is the controlling program for the segment of SA036 which performs the dilatational characterization. After receiving the data from the master data tape and the

calculated values of the bulk stress from the mean program, DLTATN reads the dilatation input, logical input cards number 8, 9, and 10. Control is then transferred to TAYLOR which solves for the B_i required in the dilatational characterization, Equation (E-6). After returning from TAYLOR, a summary page for each test is output, calculated and observed values of dilatation and a percent difference, as well as the values of the octahedral strain, calculated bulk stress (based on the best-fit distortional characterization), temperature, time, and values of the two terms multiplied by the linear coefficients for each data point. The statistical quality of the fit is shown after the last summary page in the first of the overage deviation and one standard deviation.

d. Subroutine DVTORC

Subroutine DVTORC is the controlling program for the segment of SA036 which performs the distortional stress characterization. It is quite analogous to DLTATN discussed above. The major difference is that all the logical input cards are read in the main program instead of this subroutine, since most of this input is common to any characterization. On output the summary page for each test contains the time, temperature, input strain, corrected dilatation, calculated and observed values of distortional stress, the percent difference, and the two "divatoric terms", the first of which is the observed distortional strain, $(\varepsilon_{11}-\varepsilon_{22})$, and the second of which is the value of the hereditary integral. The average and first standard deviation follows the last summary page.

e. Subroutine FAILUR

Subroutine FAILUR is analogous to subroutines DLTATN and DVTORC discussed above; it is the controlling program for the segment of SA036 which performs the cumulative damage failure characterization. It receives all required test data through its common blocks

and reads logical input cards number 11, 12, and 13. Before beginning the iteration loop to determine the nine coefficients used for the characterization, however, FAILUR calculates the octahedral shear stress and reduced time vector. Each test requested from the master data tape is then checked to see if it is to be used in the characterization. Only those tests possessing good failure data will be used. On output, the time, temperature, calculated octahedral shear stress, calculated bulk stress, calculated cumulative damage, D(t), the Lebesque norm term, and the infinite norm term are printed for each data point of each test including those not included in the failure characterization.

Unlike the deviatoric and dilatational characterizations which provide one regression point for each data point, the failure characterization received only one regression point per test, the last one. Thus, for a given number of tests, the statistical sample is not nearly as good for the failure analyses as for the deviatoric and dilatational analyses. This point should be borne in mind when evaluating the average and first standard deviation printed after the summary page for the last test.

f. Subroutine FBULK

Subroutine FBULK is the "FCODE" subroutine for the dilatational characterization. It is called by TAYLOR to evaluate the objective error function, Φ, at a given data point. For a given set of coefficients, B_i, then, FBULK computes the dilatation per Equation (E-6).

g. Subroutine FCODNL

Subroutine FCODNL is the "FCODE" subroutine for the deviatoric stress characterization. When called by subroutine TAYLOR,

it computes the distortional stress at a specific data point for a given set of B_i per Equation (E-1). Additionally, it checks to make certain all bounded coefficients are indeed within bounds immediately after each update by subroutine TAYLOR. FCODNL also, for each unique set of B_i, recomputes the shift function, reduced time, and Lebesgue norm matrices for subsequent use in evaluating the objective function and its derivatives.

h. Subroutine FFAIL

Subroutine FFAIL is the "FCODE" subroutine for the cumulative damage failure characterization. It is quite similar in function to FCODNL in that it ensures that all bounded coefficients are within their limits, and re-evaluates the Lebesgue norm matrices for each unique set of B_i generated by subroutine TAYLOR during the iteration process. These matrices are used later to evaluate the objective function and its derivatives. Due to the numerics involved in evaluating high order Lebesgue norms, FFAIL contains considerably more double precision arithmetic than the other "FCODE" subroutines.

i. Subroutine PBULK

Subroutine PBULK is the "PCODE" subroutine for the dilatational characterization. At each data point of the regression, PBULK computes $\partial\phi/\partial B_i$ for each of the B_i. For the bulk characterization all seven derivatives are computed analytically, due to the simplicity of the expressions involved.

j. Subroutine PCODNL

Subroutine PCODNL is the "PCODE" subroutine for the deviatoric characterization. It evaluates $\partial\phi/\partial B_i$ for each data point for each coefficient B_i. All derivatives with respect to the

first NC nonlinear coefficients, those associated with the shift function, Lebesgue norm, and power of the kernel in the hereditary integral term, are evaluated numerically. The remaining nonlinear, and all the linear, coefficients are evaluated analytically. A "factor" is computed which weights each derivative by the number of times it is nonzero in the regression. Thus, all derivatives will have an equal influence on the coefficient increment. Specifically, those derivatives associated with the hereditary integral, P_{NC}, P_{NC+4}, and P_{NC+7}, are nonzero only during unloading strain histories. To apply effective changes to the corresponding coefficients, B_{NC}, B_{NC+4}, and B_{NC+7}, they are multiplied by a factor which is the ratio of the total number of data points to the number of times their derivatives are nonzero.

k. Subroutine PFAIL

Subroutine PFAIL is the "PCODE" subroutine for the cumulative damage failure characterization. It supplies a set of partial derivatives, P_k of the objective error function, Φ, with respect to each of the unknown coefficients, B_k, for each test. These derivatives are always zero, except at the last point of the test, where it is assumed failure occurred. The derivatives of the nonlinear coefficients B_1 through B_5 are computed numerically. The remainder of the derivatives, P_6 through P_9, are computed analytically.

l. Subroutine SHIFT

Subroutine SHIFT is called by subroutine FCODNL to compute the shift function, reduced time, and Lebesgue norm matrices. The first column of each of these matrices contains the values of shift function, reduced time, and Lebesgue norm associated with the current values of the unknown coefficients, B_k, for each data point, i.e., the column size is equal to the number of data points. The remaining

columns of these matrices contain the values associated with perturbations to each of the coefficients whose derivatives are computed numerically. SHIFT is called only once for each unique set of coefficients, B_k, regardless of the number of data points involved.

m. Subroutine SOLVDP

Subroutine SOLVDP solves the matrix equation $[A]\{\Delta B\} = \{G\}$. It is identical to subroutine SOLV34 discussed in Appendix D. The only difference is that the sizes of the array have been made compatible with the SA036 code requirements.

n. Subroutine SUB1

Subroutine SUB1 exists solely for overlay purposes. It allows for a more convenient overlay structure if subroutines DVTORC and BULK are grouped under the labeled common block, BLK1. If the overlay structure is not desired, replace the call to SUB1 in the main program by a call to DVTORC, and the call to SUB2 by a call to BULK. The labeled common area would then have to be included in the main program data bank.

o. Subroutine TAYLOR

Subroutine TAYLOR controls the iteration loop to determine the unknown coefficients in any of the three types of regression analysis. It is the same subroutine used by the SA034 linear viscoelastic code (see Appendix D).

p. Subroutine TPRD36

Subroutine TPRD36 is the master data tape search/read routine for the SA036 code. It searches the master data tape for the tests requested to be included on logical input card No. 7.

If a test is not found an error message is written and execution terminated. When the requested test is found the required data from the master data tape is loaded into the appropriate locations in labeled common block NLINPT for use throughout the rest of the code. It is completely analogous to subroutines TPRD34,and TPRD35; pages D-9 and C-3, respectively.

q. Subroutine WHICH

Subroutine WHICH is a utility subroutine which when given a global data point number, I, returns with the number of the test it is from, IT, and the number of the highest data point in that test in KOUNT. It is used also in Code SA034 (see Appendix D, page D-10).

3. Usage

This section describes the more important variables found in SA036, the input required, its format, and the output received.

a. Basic Variables

This section presents a list of the basic variables appearing in the SA036 code. Card input variables are labeled as INPUT, data read from the master data tape are labeled as TAPE, output variables are labeled as OUTPUT. All other variables are used for intermediate calculations, temporary storage, dummy arrays, or as points and indices. The variables are related to the subroutines in which they first appear. The basic variables appearing in the main program are defined as follows:

ATEMP	Shift function pivotal temperature - INPUT
B	Always the unknown coefficients in the characterization - OUTPUT
BOUND	5% of the maximum value of absolute value of the observed stress in that test. Stresses whose magnitude are less than BOUND are not used in the characterization.

DEL	Increment to B_i's used to compute numerical partial derivatives - INPUT
DEVRAT	Observed strain rate, $D(E_{11}-E_{22})/DT$ - TAPE
DIL	Local values of dilatation - TAPE
DR*	Strain rate, DE*/DT, * = 1, 2 - TAPE
EMAX	Maximum value of strain to be included in this characterization - INPUT
EOCT	Global vector of octahedral shear strain; the union of the set of the OCT vectors
E**	Local strain vectors,** - 11, 22 - TAPE
HINT	An array used to store numerical values of certain portions of the series representation - OUTPUT
IB	Index of coefficients to be held fixed during the iteration loop - INPUT
IF*	Characterization selection option, * = 1, 2 or 3 - INPUT
IHMAX	Maximum number of interval halvings accepted before iteration loop is terminated - INPUT
IP	Total number of coefficients to be held fixed during a characterization - INPUT
IPG	Page counter
IPRNT	Print control, equal zero for normal run - INPUT
IQUIT	Maximum number of iterations - INPUT
ITEST	Test ID read from master data tape - TAPE
ITYPE	Normalization option, equals unity (1) for a normalized regression - INPUT for dilatational characterization only
KEEP	Flag vector indicating type of failure data; the union of the KFAIL flags
KFAIL	Type of local failure data, 0 = bad, 1 = good - TAPE
KOD	Local test type; 1 = uniaxial, 2 = biaxial, 3 = shear - TAPE
KODE	Union of the KOD flags

KTEM	Local temperature type; 1 = constant, 2 = variable - TAPE
KTEMP	Union of the KTEM flags
LAST	Flag indicating last card of ATEMP set; is blank except on last card - INPUT
LINE	Output line counter
NC	Number of coefficients whose derivatives are to be determined numerically
NDP	Total number of data points in the characterization, 1000 maximum for version 03/01/74
NEXP	Global vector containing the number of experimental data points in each test
NORMF	Infinite Lebesgue norm - TAPE
NT	Number of shift function pivotal temperatures
NTESTS	Number of tests used in the characterization, 100 maximum
NTOT	Total number of regression coefficients
NU	Tape drive unit number, currently fixed at 2
OCT	Local vector of octahedral shear strain - TAPE
P	Global vector of test pressures, union of PRES values
PRES	Local test pressures - TAPE
STRN*	Union of local strain vectors, E**, E = 0, 1, 2
T	Local time vector - TAPE
TEMP	Local temperature vector - TAPE
TITLE	80-column title printed at the top of each page - OUTPUT
VAR1	First strain invariant
VMIN	Minimum value of dilatation to be included in this characterization - INPUT
VOL	Union of the DIL vectors - OUTPUT
X	A working global array containing time in the first column, temperature in the second column and visually, stress in the third column

XINF	Union of NORMF vectors
XORM	Matrix of values of p-th Lebesgue norm
Y	Working storage vector

b. Input Required

The input to SA036 consists of the appropriate master data tape, mounted in a "read only" mode, and up to thirteen (13) logical input cards. Each logical input card may be more than one physical card long. These cards are listed below with the format appearing in parentheses after each card number, and show the program variables appearing on each card. This is followed by any necessary descriptive comments. All FORTRAN names are capitalized. Card numbers are their logical numbers. All logical input cards and their sequence are clearly labeled in the code source listing.

CARD NO. 1 (20A4) TITLE

An 80-column alphanumeric title which will appear on each page of output.

CARD NO. 2 (3E10.0) DEL, EMAX, VMIN

DEL is the numerical increment to the coefficients, used to compute the partial derivatives numerically.

EMAX is the maximum value of strain to be included in this characterization. Data points having strains greater than EMAX are not used in the characterization.

VMIN is the minimum dilatation, $\Delta V/V_0$, to be included in the characterization. Data points having dilatation values less than VMIN are not used in the characterization.

CARD NO. 3 (7I5) IQUIT, IHMAX, IPRNT, IF1, IF2, IF3, IP

IQUIT is the maximum number of iterations for the deviatoric characterization.

IHMAX is the maximum number of halvings of the coefficient interval, ΔB_i, before iteration is terminated.

IPRNT is a print control equal to zero except for debugging. If IPRNT is not zero, additional output is received during each iteration. This output includes the error measure and the intermediate parameters during each incremental halving step. This type of additional output is useful in program debugging or if convergence problems should occur.

IF1 is set to 1 for a distortional characterization and set to zero otherwise. If set to zero, a single pass is made through the distortional segment to generate shift function, reduced time, and Lebesgue norm matrices for use by the other characterizations.

IF2 is set to 1 for the dilatational characterization and set to zero otherwise.

IF3 is set to 1 for the failure characterization and set to zero otherwise.

IP is the number of coefficients in the distortional representation which are to be held fixed throughout the characterization.

CARD(S) NO. 4 (E10.0I5) ATEMP, LAST

ATEMP is the shift function pivotal temperature. These temperatures are ordered sequentially from cold to hot and must be selected to span the range of test temperatures such that the "coldest" ATEMP, the first one, is hotter than the coldest test temperature and the "hottest" ATEMP, the last or NT-th one, is "hotter" than the hottest test temperature. Additionally, the ATEMP sequence must include 77°F.

LAST is blank except on the last card when it is set to 11111.

CARD(S) NO. 5 (8E10.0) (B_0(K), K = 1, NTOT)

B_0(K) is the initial value of the K-th coefficient. Nonzero values must be entered for all nonlinear coefficients. The initial values for the linear coefficients may be entered as zero and cause no problems.

CARD NO. 6 (15I5) (IB(J), J = 1, IP)

IB is the vector of the indices of the coefficients which are to be held fixed at their initial values during the deviatoric characterization. Specifying the first NT coefficients as fixed (IB = 1, 2, 3, . . ., NT) eliminates determining a new a_T function. NOTE: This card is read only if IP $\neq$ 0.

CARD(S) NO. 7 (A6) MTEST

MTEST is the six-character alphanumeric ID of the test(s) desired from this master data tape. There is one card for each test. The last test ID is followed by a card with E-N-D in columns 1-3.

NOTE: The tests must be requested in their order of appearance on the master data tape. If there is any doubt as to the tape's contents or sequence it is strongly recommended that an SA037 Option 3 run be made to obtain a current tape catalog.

Logical cards number 8 through 10 are read only if it is desired to do a dilatational characterization, i.e. IF2 = 1.

CARD NO. 8 (4I5) ITYPE, IP, IQUIT, IHMAX

ITYPE is the normalization option selector. It is equal to unity (1) for a normalized regression and equal to 2 for a non-normalized analysis.

IP is the number of coefficients in the dilatational representation which are to be held fixed throughout the characterization.

IQUIT is the maximum number of iterations allowed for the dilatational characterization. If left blank, the value input on Card No. 3 is used.

IHMAX is the maximum number of halvings of the coefficient interval, B_i, before iteration is terminated. If left blank, the value input on Card No. 3 is used.

CARD NO. 9 (7E10.0) ($B_0(K)$, K = 1, 7)

The $B_0(K)$ are the initial values of the dilatational coefficients. The first five coefficients must have nonzero initial values. The last two coefficients may be entered as zero.

CARD NO. 10 (7I5)(IB(J), J = 1, IP)

IB is the vector of indices of the coefficients which are to be held fixed at their initial values throughout the dilatational characterization.

NOTE: This card is read only if the value of IP on card No. 8 is nonzero.

Logical cards number 11 through 13 are read only if it is desired to do a failure characterization, i.e. IF3 = 1.

CARD NO. 11 (3I5) IP, IQUIT, IHMAX

IP is the number of coefficients in the failure representation which are to be held fixed throughout the characterization.

IQUIT is the maximum number of iterations allowed for the failure characterization. If left blank, the value input on Card No. 3 is used.

IHMAX is the maximum number of times the coefficient interval, B_1, may be halved before iteration is terminated. If left blank, the value input on Card No. 3 is used.

CARD(S) NO. 12 (8E10.0) ($B_0(K)$, K = 1, 9)

$B_0(K)$ is the initial value of the K-th coefficient. Nonzero values must be entered for the nonlinear coefficients, $B_0(1)$ through $B_0(7)$. The initial values for the linear coefficients may be entered as zero.

CARD NO. 13 (9I5) (IB(J), J = 1, IP)

IB is the vector of the indices of the coefficients which are to be held fixed at their initial values throughout the failure characterization.

NOTE: This card is read only if the value of IP on Card No. 11 is nonzero.

SA036, version 03/01/74, assumes the master data input tape is on Unit 2. This specification is easily changed by setting the value of the variable NU in the main program to any desired number.

In using SA036 the following limitations should be observed:

(1) The maximum number of data points allowed is 1000.

(2) The maximum number of tests is 100.

(3) The maximum number of shift function pivotal temperatures is 6.

(4) The shift function pivotal temperatures must include $77^{o}F$.

(5) The shift function pivotal temperatures must be ordered cold to hot, with the coldest and hottest pivotal temperatures being hotter than the coldest and hottest test temperatures.

(6) The maximum number of distortional coefficients is 9 + NT where NT is the number of shift function pivotal temperatures.

(7) The number of coefficients involved in the dilatation and failure characterization is fixed at seven and nine respectively.

(8) Only one material may be characterized per run.

Figure E-2 shows the master data input sheet for Code SA036. Figure E-3 shows the actual data input sheet for a demonstration problem.

c. Output Received

The order of the characterizations performed by SA036, assuming all three are run at the same time, is deviatoric, dilatational, and failure. The output for each type of characterization is independent of the others and is presented separately. Within each characterization the output can be loosely grouped into three types: input, iteration, and characterization summary.

The initial page of output is a heading identifying the code and version being executed. The second page is a brief summary of current program size limitations. The first page of unique output is labeled page 1, and is a list of the tests requested from the master data tape, their SA036 sequence number, their ID's, number of points in each, then KODE, KTEMP, and KFAIL values, followed

by the initial test temperature and pressure. These data are printed regardless of the type of characterization performed.

Page 2 of the output comes from the distortional segment of the code. It lists the following parameters:

(1) Number of tests, NTESTS
(2) Number of data points, NDP
(3) Maximum number of iterations allowed, IQUIT
(4) Maximum number of interval halvings allowed, IMMAX
(5) The numerical derivative increment, DEL
(6) The print flag, IPRNT
(7) The upper bound on included strains, EMAX
(8) The number of shift function temperatures, NT
(9) The total number of coefficients, NTOT

This is followed by a list of the initial values of the coefficients, $B_0(K)$; a list of the coefficients held constant, if any; and a list of the shift function pivotal temperatures.

The next section of output comes from subroutine TAYLOR which controls the iteration loop. For each iteration the following data are printed:

(1) The iteration number and time remaining.
(2) The value of the objective function, called "ERROR", and the corresponding coefficient values.
(3) The number of times the ΔB_i were halved and their sum.
(4) Which $\Delta B_i = 0$, if any, for those coefficients held fixed.
(5) The new ΔB_i obtained for solving $[A]\{\Delta B\} = \{G\}$, i.e., the new ΔB_i before any interval halving.

After iteration terminates, a diagnostic message is printed giving the reason for termination. Control is then transferred back to the deviatoric segment of the code, subroutine DVTORC, where the third portion of the output, the characterization summary, is printed.

The deviatoric characterization summary presents the following information for each of the tests included in the characterization. At the top of each page the title is printed, followed immediately by the run test number, the number of data points in the test, and the type of test. This is followed by values of temperature, input strain, dilatation, calculated and observed distortional stress, their percent difference, an omitted points flag (any data point followed by an asterisk was not included in the characterization), and deviatoric terms, all versus time. Of the two numbers listed as deviatoric terms, the first is the distortional strain, $E_{11}-E_{22}$, and the second is the hereditary integral term of Equation (E-1), i.e. everything which is multiplied by B_{NC+7}, but not including B_{NC+7} itself.

Following the last test, the final regression coefficients are printed, followed by a brief statistical summary containing the number of data points used, the average deviation, and one standard deviation, thus giving the user some measure of the adequacy of the distortional fit. This is followed, on the next page, by the tabulated values of shift function versus temperature generated by using the final coefficients. The shift function pivotal temperatures used as input are reprinted here for convenience. If no dilatational nor failure characterization is requested (IF2 = 0 and IF3 = 0), this is the last page of output.

Assuming, however, that a dilatational characterization was also requested, the next page of output would be a list of the following input parameters:

(1) The number of tests, NTESTS
(2) The total number of data points, NDP

(3) The maximum number of iterations allowed, IQUIT

(4) The maximum number of interval halvings, IHMAX

(5) The numerical derivative increment, DEL

(6) Print parameter value, IPRNT

(7) The largest value of dilatation to be ignored, VMIN

(8) The total number of coefficients in the bulk characterization, currently fixed at 7

This is followed by a list of the seven initial values of the $B_0(K)$, and the indices of those coefficients, to be held fixed, if any. Control is then transferred from the dilatational segment of SA036 to the iteration segment, subroutine TAYLOR, and the output from the iteration loop is the same as discussed above for the distortional case.

The third portion of the output, the dilatational characterization summary, presents values of temperature, octahedral shear strain, calculated bulk stress, calculated and observed values of the dilatation and their percent difference, the omitted points flag, and the two bulk terms, all versus time. Here the two "bulk terms" numbers are the values of the quantities of Equation (E-6), multiplied by B_6 and B_7 respectively. Following the last test are the final values of the seven dilatational coefficients and the statistical summary listing average and standard deviations. If a failure characterization has not been requested (IF3 = 0), this is the last page of output.

If a failure characterization is requested (IF3 = 1), the next page of output contains a list of the nine (9) initial coefficients, the indices of those coefficients to be held fixed, if any, and the sequence numbers of those tests which contained good failure data and were included in the characterization. A zero is printed instead of the number of an omitted test. This is followed

by the usual iteration output as discussed above. The third portion of the output, from the failure characterization segment of the code, subroutine FAILUR, presents a summary page for each test, including those not used in the failure analysis, containing values of temperature, calculated octahedral shear stress, calculated bulk stress, the damage, D(t), the value of the final Lebesgue norm, and the infinite norm, all versus time. After the last test summary is the list of the final nine (9) failure coefficients, the number of failure "data points", and the average and standard deviation values. Table E-1 shows a few of the forty pages of output corresponding to the input of Figure E-3.

4. Demonstration Problem

As a demonstration problem of SA036, the input of Figure E-3 was used to generate the output shown as Table E-1.

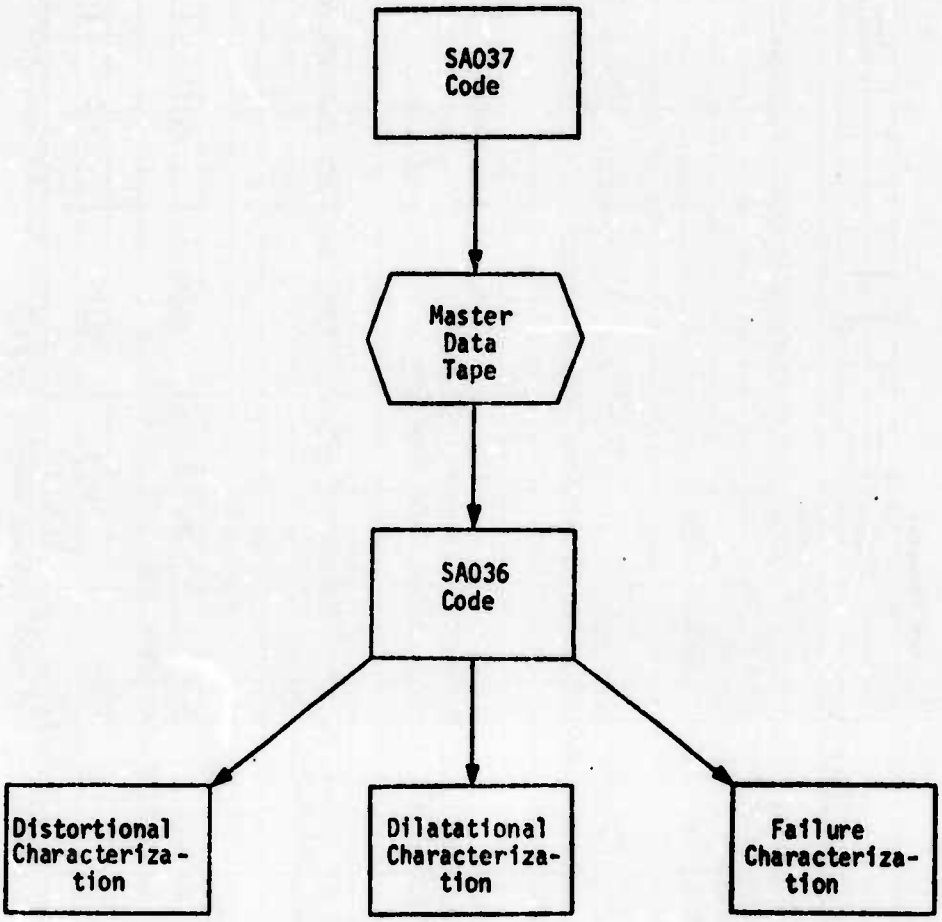

FIGURE E-1

RELATIONSHIP OF SA036 TO
MATERIAL CHARACTERIZATION CODES PACKAGE

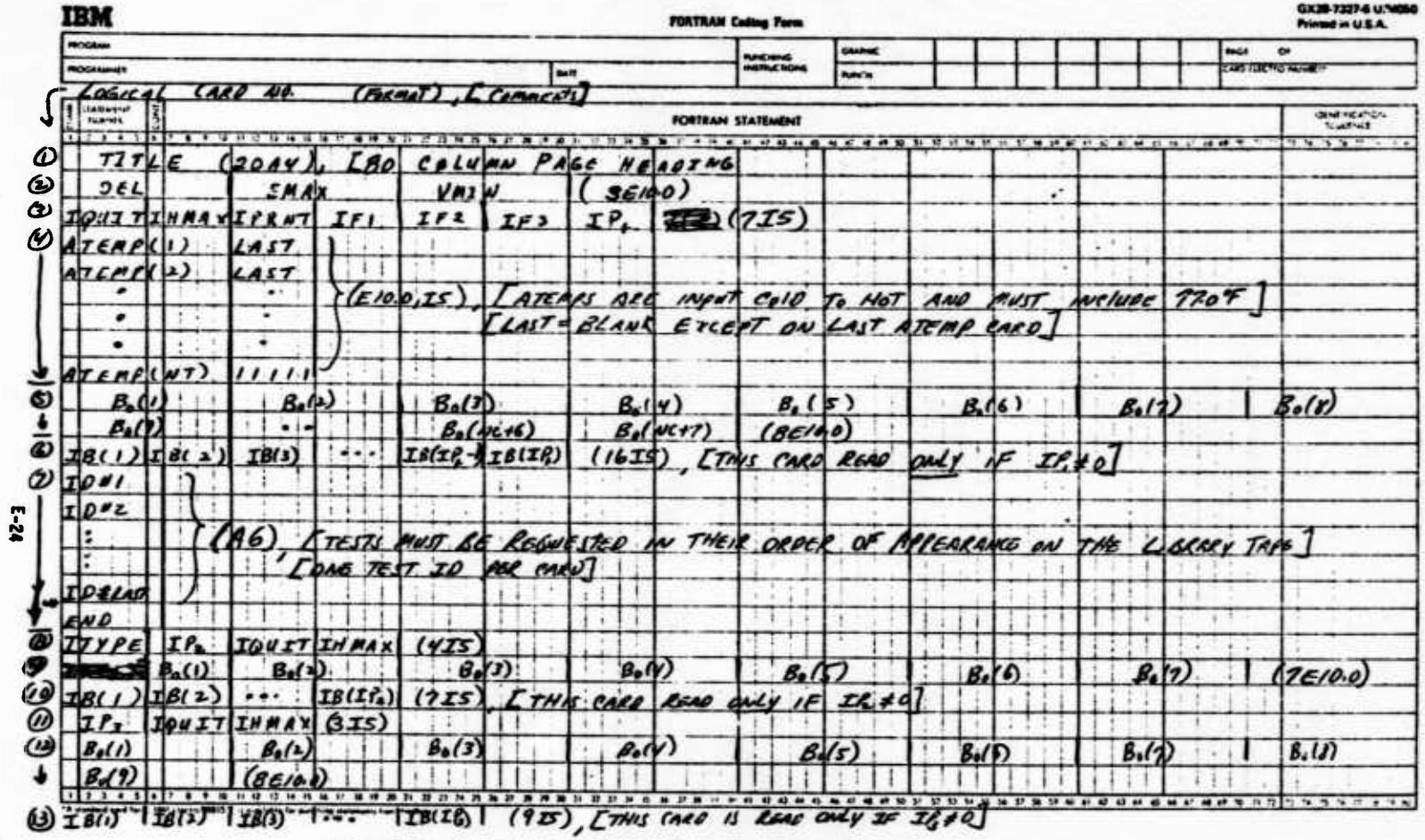

FIGURE E-2. MASTER DATA INPUT SHEET FOR THE NONLINEAR CHARACTERIZATION CODE SA036

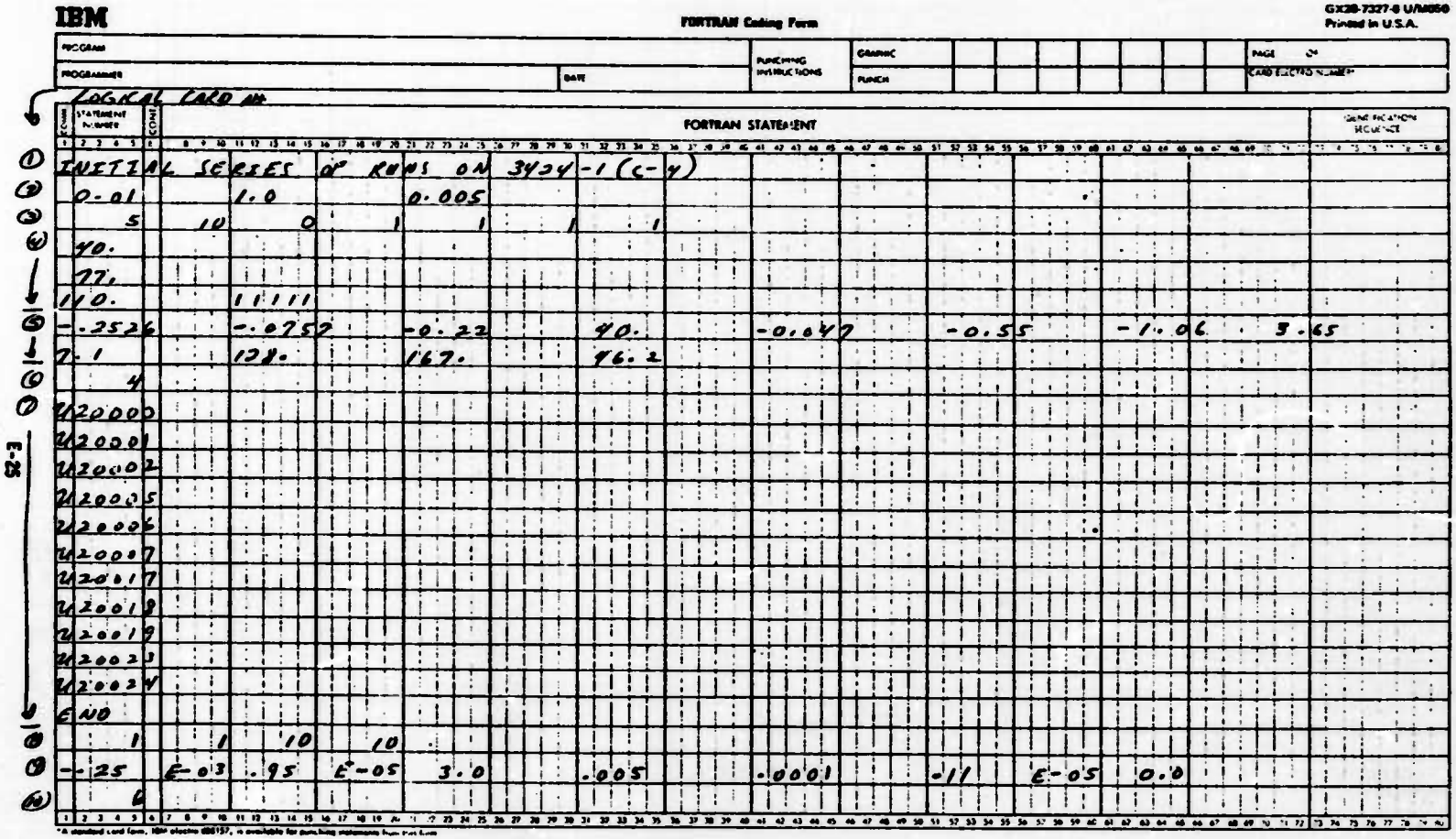

FIGURE E-3. EXAMPLE INPUT FOR THE NONLINEAR CHARACTERIZATION CODE SA036

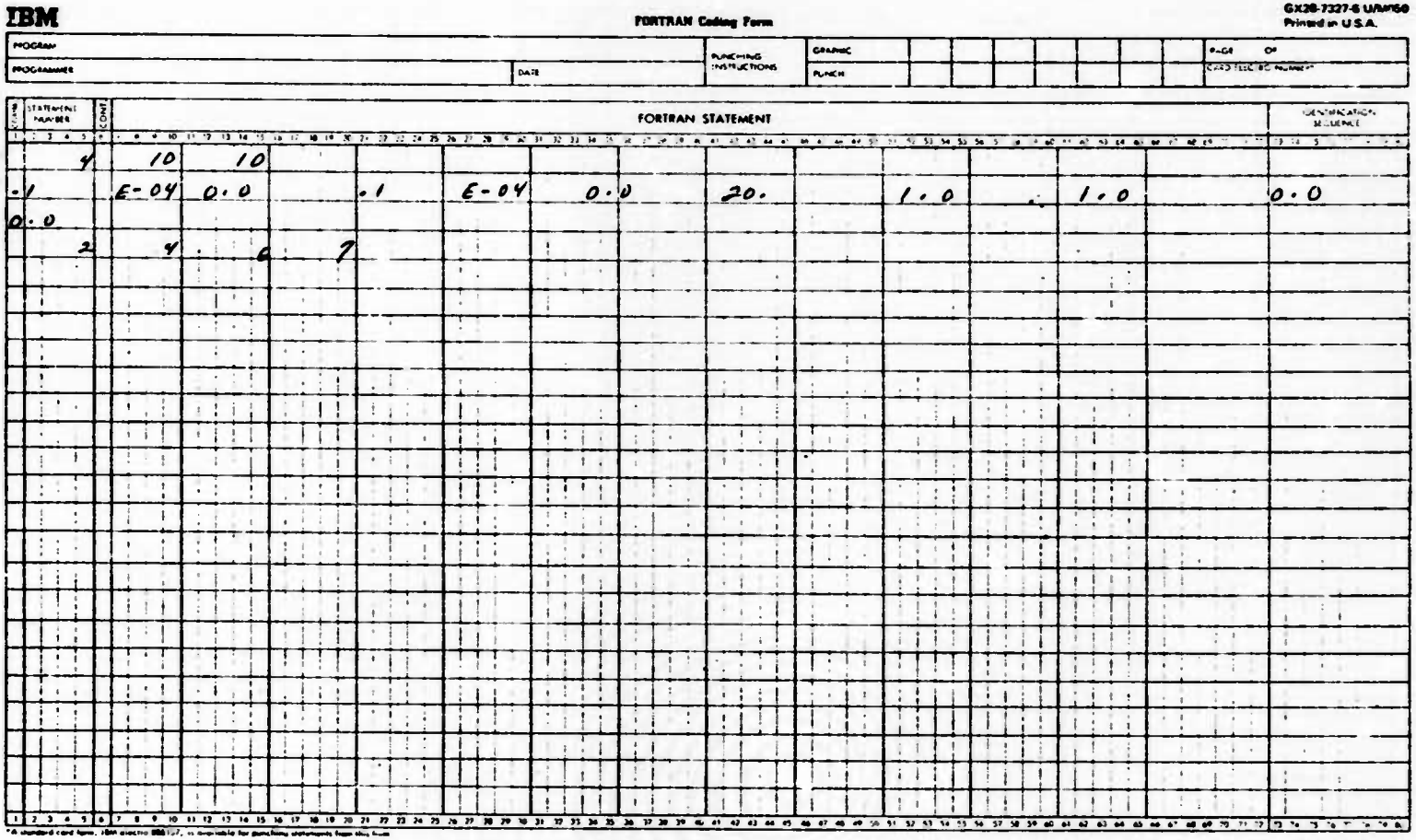

FIGURE E-3. EXAMPLE INPUT FOR THE NONLINEAR CHARACTERIZATION CODE SA036 (Continued)

TABLE E-1

PORTIONS OF THE OUTPUT FROM THE NONLINEAR CHARACTERIZATION CODE SA036 FOR THE EXAMPLE DESCRIBED IN FIGURE E-3

```
      CURRENT PROGRAM SIZE LIMITATIONS

   MAX TOTAL NO. OF DATA POINTS = 1000
   MAX NO. OF TESTS = 100
   MAX NO. DATA POINTS IN ANY ONE TEST = 100
   MAX NO. OF SHIFT FUNCTION COEFFICIENTS = 6
```

TABLE E-1 (Continued)

NONLINEAR THERMOVISCOELASTIC CHARACTERIZATION CODE PAGE 1

INITIAL SERIES OF RUNS ON 3424-1 (C-4)

TEST NO.	TEST ID.	NO. PTS.	KCODE	KTEMP	KFAIL	INITIAL TEMP.	PRESSURE
1	U20000	37	1	1	1	110.	0.
2	U20001	39	1	1	1	110.	0.
3	U20002	10	1	1	1	110.	0.
4	U20005	47	1	1	1	77.	0.
5	U20006	10	1	1	1	74.	0.
6	U20007	10	1	1	1	75.	0.
7	U20017	41	1	1	1	40.	0.
8	U20018	42	1	1	1	40.	0.
9	U20019	13	1	1	1	40.	0.
10	U20023	12	1	1	1	0.	0.
11	U20024	45	1	1	1	0.	0.

END

TABLE E-1 (Continued)

INITIAL SERIES OF RUNS ON 3424-1 (C-4)

... INPUT PARAMETERS ...

NO. OF TESTS = 11
NO. OF DATA POINTS = 306
MAX NO. OF ITERATIONS = 5
MAX NO. OF INTERVAL HALVINGS = 10
NUMERICAL DERIVATIVE INCREMENT = .1000-01
PRINT PARAMETER(S) = 0
STRAINS GREATER THAN .1000+01 WERE IGNORED.
NO. OF SHIFT FUNCTION COEFFICIENTS = 3
TOTAL NUMBER OF SHEAR COEFFICIENTS = 12

THE INITIAL COEFFICIENTS

K	B(K)
1	-.252600+00
2	-.757000-01
3	-.220000+00
4	.400000+02
5	-.470000-01
6	-.550000+00
7	-.106000+01
8	.365000+01
9	.710000+01
10	.120000+03
11	.167000+03
12	.460000+02

THE FOLLOWING 1 COEFFICIENTS WERE HELD CONSTANT: 4

K	ATEMP(K)
1	40.
2	77.
3	120.

TABLE E-1 (Continued)

INITIAL SERIES OF RUNS ON 3424-1 (C-4)

```
 ITERATION NO.     1 OF    5, WITH  171 SECONDS TO GO
 ERROR  =    .420266+01        AND THE B(K) ARE ...      -.252600+00  -.757000-01  -.220000+00   .400000+02  -.470000-01
                                                         -.550000+00  -.106000+01   .365000+01   .710000+01   .128000+03
                                                          .167000+03   .460000+02
        THE DB(K) WERE HALVED   0 TIMES, AND THEIR SUM WAS  .100000+01

             *** FACTOR =   .231818+01

     DB( 4) = 0.0

                              NEW DB(K) ARE ...           .237167-01  -.197151-01   .101478-01   .000000   -.443356-01
                                                         -.117032+01   .498122+00   .111273+01  -.307857+01   .648600+02
                                                         -.643323+02  -.469628+01
 ITERATION NO.     2 OF    5, WITH  157 SECONDS TO GO
 ERROR  =    .262888+01        AND THE B(K) ARE ...      -.210742+00  -.855875-01  -.214926+00   .400000+02  -.691678-01
                                                         -.113516+01  -.810939+00   .420637+01   .516074+01   .160430+03
                                                          .134834+03   .436519+02
        THE DB(K) WERE HALVED   2 TIMES, AND THEIR SUM WAS  .140706+03

             *** FACTOR =   .231818+01

     DB( 4) = 0.0

                              NEW DB(K) ARE ...           .155720-01  -.141050-01   .155203-01   .000000   -.137104-01
                                                         -.641026+00   .254527+00  -.926990-01  -.509443+01  -.477539+01
                                                          .607366+01   .122422+02
 ITERATION NO.     3 OF    5, WITH  144 SECONDS TO GO
 ERROR  =    .237969+01        AND THE B(K) ARE ...      -.202956+00  -.926100-01  -.207166+00   .400000+02  -.760230-01
                                                         -.145568+01  -.603675+00   .416002+01   .261352+01   .158042+03
                                                          .137871+03   .497080+02
        THE DB(K) WERE HALVED   2 TIMES, AND THEIR SUM WAS  .292629+02

             *** FACTOR =   .231818+01

     DB( 4) = 0.0

                              NEW DB(K) ARE ...          -.945901-04  -.752322-02   .148074-01   .000000   -.357671-03
                                                         -.328856+00   .126567+00  -.373009+00  -.239111+01  -.185281+02
                                                          .186140+02   .309634+02
 ITERATION NO.     4 OF    5, WITH  130 SECONDS TO GO
 ERROR  =    .233659+01        AND THE B(K) ARE ...      -.202979+00  -.944909-01  -.207464+00   .400000+02  -.761125-01
                                                         -.153789+01  -.682034+00   .406676+01   .201574+01   .153408+03
                                                          .142524+03   .575988+02
        THE DB(K) WERE HALVED   3 TIMES, AND THEIR SUM WAS  .717578+02

             *** FACTOR =   .231818+01
```

TABLE E-1 (Continued)

NONLINEAR THERMOVISCOELASTIC CHARACTERIZATION CODE PAGE 9

INITIAL SERIES OF RUNS ON 3424-1 (C-4)

TEST NO. 4 47 INPUT DATA POINTS

DATA IS FROM A U N I A X I A L TEST

TEMP.	TIME	STRAIN	DILATATION	S1-CALC.	S1-OBS.	% DEV.	OMITTED POINTS	DEVIATORIC TERMS	
77.	.000	.0000	.0000	.00	.00	.00		.0000	.0000
77.	.074	.4958-01	.0000	29.51	27.00	9.29		.7348-01	.0000
77.	.084	.4958-01	.0000	26.24	26.00	.91		.7348-01	.0000
77.	.104	.4958-01	.0000	24.74	25.50	-2.99		.7348-01	.0000
77.	.154	.4958-01	.0000	23.44	24.00	-2.34		.7348-01	.0000
77.	.254	.4958-01	.0000	22.43	23.00	-2.47		.7348-01	.0000
77.	.354	.4958-01	.0000	21.91	22.50	-2.62		.7348-01	.0000
77.	.554	.4958-01	.0000	20.78	21.00	-1.04		.7348-01	.0000
77.	1.854	.4958-01	.0000	19.95	20.00	-.26		.7348-01	.0000
77.	3.854	.4958-01	.0000	19.24	19.00	1.29		.7348-01	.0000
77.	11.354	.4958-01	.0000	18.31	18.00	1.72		.7348-01	.0000
77.	11.384	.6968-01	.1000-03	39.36	30.00	31.21		.1028+00	.0000
77.	11.404	.8308-01	.3000-03	45.46	40.00	13.65		.1231+00	.0000
77.	11.454	.1166+00	.1300-02	59.18	60.00	-1.37		.1696+00	.0000
77.	11.484	.1367+00	.3300-02	65.79	70.00	-6.01		.1972+00	.0000
77.	11.504	.1367+00	.3500-02	59.68	64.00	-6.74		.1971+00	.2112+00
77.	11.554	.1367+00	.3600-02	56.01	60.00	-6.64		.1970+00	.2052+00
77.	11.654	.1367+00	.3800-02	53.36	56.50	-5.57		.1969+00	.1986+00
77.	11.854	.1367+00	.3900-02	51.20	54.00	-5.18		.1969+00	.1924+00
77.	12.354	.1367+00	.4100-02	48.93	50.50	-3.10		.1968+00	.1846+00
77.	13.354	.1367+00	.4200-02	47.05	48.00	-1.99		.1967+00	.1774+00
77.	15.354	.1367+00	.4500-02	45.37	45.50	-.28		.1966+00	.1710+00
77.	18.354	.1367+00	.4500-02	44.21	43.50	1.63		.1966+00	.1656+00
77.	21.854	.1367+00	.4500-02	43.41	42.00	3.36		.1966+00	.1616+00
77.	21.859	.1400+00	.4600-02	46.18	47.50	-2.78		.2013+00	.0000
77.	21.864	.1434+00	.4700-02	49.19	52.00	-5.39		.2060+00	.0000
77.	21.884	.1568+00	.4950-02	62.62	64.00	-2.16		.2243+00	.0000
77.	21.904	.1702+00	.5200-02	74.24	72.00	3.12		.2424+00	.0000
77.	21.916	.1782+00	.5500-02	77.45	76.00	1.91		.2530+00	.0000
77.	21.924	.1782+00	.5700-02	73.93	72.00	2.69		.2530+00	.2341+00
77.	21.944	.1782+00	.5900-02	70.29	68.50	2.61		.2529+00	.2319+00
77.	21.974	.1782+00	.6000-02	67.82	66.50	1.99		.2528+00	.2289+00
77.	22.014	.1782+00	.6100-02	65.99	65.00	1.53		.2528+00	.2269+00
77.	22.104	.1782+00	.6250-02	63.68	63.00	1.08		.2527+00	.2241+00
77.	22.604	.1782+00	.6750-02	59.43	59.00	.73		.2525+00	.2181+00

TABLE E-1 (Continued)

INITIAL SERIES OF RUNS ON 3424-1 (C-4)

TEST NO. 4 47 INPUT DATA POINTS

DATA IS FROM A UNIAXIAL TEST

TEMP.	TIME	STRAIN	DILATATION	S1-CALC.	S1-OBS.	% DEV.	OMITTED POINTS	DEVIATORIC TERMS	
77.	23.604	.1782+00	.1000-01	56.77	56.00	1.38		.2524+00	.2134+00
77.	25.604	.1782+00	.1010-01	54.62	53.50	2.21		.2524+00	.2090+00
77.	30.104	.1782+00	.1000-01	52.78	51.00	3.50		.2524+00	.2036+00
77.	32.104	.1782+00	.9900-02	52.32	50.00	4.63		.2524+00	.2014+00
77.	32.304	.1782+00	.9900-02	52.27	50.00	4.54		.2524+00	.2013+00
77.	32.312	.1836+00	.1050-01	56.14	59.00	-4.84		.2596+00	.0000
77.	32.332	.1970+00	.1230-01	67.15	72.00	-6.74		.2774+00	.0000
77.	32.352	.2104+00	.1450-01	78.91	79.50	-.75		.2949+00	.0000
77.	32.382	.2305+00	.1880-01	88.55	86.00	2.96		.3206+00	.0000
77.	32.412	.2506+00	.2430-01	92.06	90.00	2.29		.3456+00	.0000
77.	32.452	.2774+00	.3250-01	95.54	95.00	.56		.3782+00	.0000
77.	32.482	.2975+00	.4030-01	97.47	96.00	1.53		.4021+00	.0000

TABLE E-1 (Continued)

NONLINEAR THERMOVISCOELASTIC CHARACTERIZATION CODE PAGE 21

INITIAL SERIES OF RUNS ON 3424-1 (C-4)

REGRESSION COEFFICIENTS ...

I	A(I)
1	-.2032E+00
2	-.9661E-01
3	-.1974E+00
4	.4006E+02
5	-.7456E-01
6	-.1645E+01
7	-.6106E+00
8	.3916E+01
9	.1422E+01
10	.1445E+03
11	.1511E+02
12	.7600E+02

THERE WERE 295 EXPERIMENTAL TEST POINTS

THE AVERAGE DEVIATION = -.966 PERCENT, AND
THE STANDARD DEVIATION = 8.583 PERCENT.

TABLE E-1 (Continued)

NONLINEAR THERMOVISCOELASTIC CHARACTERIZATION CODE

INITIAL SERIES OF RUNS ON 3424-1 (C-4)

SHIFT FUNCTION	TEMPERATURE - F
.1595+13	-80.
.2895+11	-60.
.5111+09	-40.
.7056+07	-20.
.1211+06	0.
.2079+04	20.
.3566+02	40.
.5167+01	60.
.5530+00	80.
.1066-01	100.
.2659-03	120.
.5962-05	140.
.7639-07	160.
.1473-08	180.
.2039-10	200.

ATEMPS USED
40.
77.
120.

TABLE E-1 (Continued)

INITIAL SERIES OF RUNS ON 3424-1 (C-4)

. . . INPUT PARAMETERS . . .

NO. OF TESTS = 11
NO. OF DATA POINTS = 306
MAX NO. OF ITERATIONS = 10
MAX NO. OF INTERVAL HALVINGS = 10
NUMERICAL DERIVATIVE INCREMENT = .1000-01
PRINT PARAMETER(S) = 0
DILATATIONS LESS THAN .5000-02 WERE IGNORED.
TOTAL NUMBER OF BULK COEFFICIENTS = 7

THE INITIAL COEFFICIENTS

K	D(K)
1	-.250000-03
2	.950000-05
3	.300000+01
4	.500000-02
5	-.100000-03
6	.110000-05
7	.000000

THE FOLLOWING 1 COEFFICIENTS WERE HELD CONSTANT: 6

TABLE E-1 (Continued)

INITIAL SERIES OF RUNS Cn 3424-1 (C-4)

```
 VLIMIT =  .1000+00     GLIMIT =  .1575-01     SMAX =  .6705+02     TMIN = -.7700+02

 ITERATION NO.     1 OF   10, WITH   94 SECONDS TO GO
 E R R O R  =   .137708+00      AND THE A(K) ARE ...      -.250000-03  .950000-06  .300000+01  .500000-02  -.100000-03
                                                          .110000-05  .000000
       THE DA(K) WERE HALVED   0 TIMES, AND THEIR SUM WAS  .100000+01

    DA( 3) = 0.0

    DA( 4) = 0.0

    DA( 5) = 0.0

    DA( 6) = 0.0

                               NEW DA(K) ARE ...         -.366193+01  -.811349-01  .000000     .000000     .000000
                                                          .000000      .597391+01
 ITERATION NO.     2 OF   10, WITH   93 SECONDS TO GO
 E R R O R  =   .117231+00      AND THE A(K) ARE ...      -.597899-02  -.930154-03  .300000+01  .500000-02  -.100000-03
                                                          .110000-05  .373969+00
       THE DA(K) WERE HALVED   5 TIMES, AND THEIR SUM WAS  .971697+01

    DA( 6) = 0.0

                               NEW DA(K) ARE ...          .165156+01  .218116-01  -.264351+01  .531599-01  -.996287-03
                                                          .000000     .246043+01
 ITERATION NO.     3 OF   10, WITH   93 SECONDS TO GO
 E R R O R  =   .609655-01      AND THE A(K) ARE ...      .602570-02  .105743-02  .266956+01  .116450-01  -.224536-03
                                                          .110000-05  .680923+00
       THE DA(K) WERE HALVED   4 TIMES, AND THEIR SUM WAS  .683147+01

    DA( 6) = 0.0

                               NEW DA(K) ARE ...         -.252442+01  -.289662-01  .135546+00  -.114584-01  .305425-03
                                                          .000000     .241769+01
 ITERATION NO.     4 OF   10, WITH   92 SECONDS TO GO
 E R R O R  =   .473511-01      AND THE A(K) ARE ...      -.601329-02  -.866800-03  .268650+01  .102077-01  -.186358-03
                                                          .110000-05  .983134+00
       THE DA(K) WERE HALVED   4 TIMES, AND THEIR SUM WAS  .511843+01

    DA( 6) = 0.0

                               NEW DA(K) ARE ...          .202312+01  .266627-01  .343316+00  -.172356-01  .543367-05
                                                          .000000     .251960+01
```

TABLE E-1 (Continued)

INITIAL SERIES OF RUNS ON 3424-1 (C-4)

TEST NO. 4 47 INPUT DATA POINTS

DATA IS FROM A UNIAXIAL TEST

SUMMARY OF RESULTS FOR BULK STRESS TERM

TEMP	TIME	FOCT	SD-CALC	DIL-CALC	DIL.	% DEV.	OMITTED POINTS	BULK TERMS	
77.0	.000	.0000	.0000	.0000	.0000	.0	*	.0000	.0000
77.0	.074	.3464-01	.8582+01	.1966-03	.0000	.0	*	.1066+02	.7534-04
77.0	.084	.3464-01	.8627+01	.1967-03	.0000	.0	*	.1073+02	.7536-04
77.0	.104	.3464-01	.8627+01	.1967-03	.0000	.0	*	.1073+02	.7535-04
77.0	.154	.3464-01	.8093+01	.1954-03	.0000	.0	*	.9932+01	.7518-04
77.0	.254	.3464-01	.7761+01	.1945-03	.0000	.0	*	.9445+01	.7507-04
77.0	.354	.3464-01	.7598+01	.1942-03	.0000	.0	*	.9208+01	.7501-04
77.0	.854	.3464-01	.7036+01	.1928-03	.0000	.0	*	.8407+01	.7483-04
77.0	1.054	.3464-01	.6675+01	.1920-03	.0000	.0	*	.7903+01	.7471-04
77.0	3.854	.3464-01	.6293+01	.1911-03	.0000	.0	*	.7378+01	.7458-04
77.0	11.354	.3464-01	.5948+01	.1903-03	.0000	.0	*	.6914+01	.7447-04
77.0	11.384	.4844-01	.8440+01	.4892-03	.1000-03	389.2	*	.1045+02	.1547-03
77.0	11.404	.5754-01	.1242+02	.8108-03	.3000-03	170.3	*	.1701+02	.3229-03
77.0	11.454	.7995-01	.2014+02	.2120-02	.1300-02	63.0	*	.3351+02	.8489-03
77.0	11.484	.9295-01	.2403+02	.3296-02	.3300-02	-.1	*	.4413+02	.1324-02
77.0	11.504	.9291-01	.1981+02	.3219-02	.3500-02	-8.0	*	.3269+02	.1297-02
77.0	11.554	.9289-01	.1849+02	.3195-02	.3600-02	-11.3	*	.2951+02	.1289-02
77.0	11.654	.9284-01	.1725+02	.3170-02	.3800-02	-16.6	*	.2669+02	.1280-02
77.0	11.854	.9282-01	.1643+02	.3155-02	.3900-02	-19.1	*	.2489+02	.1275-02
77.0	12.354	.9278-01	.1518+02	.3130-02	.4100-02	-23.7	*	.2221+02	.1266-02
77.0	13.354	.9273-01	.1428+02	.3112-02	.4300-02	-27.6	*	.2050+02	.1259-02
77.0	15.354	.9269-01	.1339+02	.3094-02	.4500-02	-31.3	*	.1878+02	.1253-02
77.0	18.354	.9269-01	.1264+02	.3082-02	.4500-02	-31.5	*	.1740+02	.1248-02
77.0	21.854	.9269-01	.1206+02	.3073-02	.4500-02	-31.7	*	.1637+02	.1245-02
77.0	21.859	.9490-01	.1605+02	.3351-02	.4600-02	-27.2	*	.2409+02	.1355-02
77.0	21.864	.9710-01	.1780+02	.3606-02	.4700-02	-23.3	*	.2792+02	.1457-02
77.0	21.884	.1057+00	.2156+02	.4669-02	.5850-02	-20.2		.3720+02	.1886-02
77.0	21.904	.1143+00	.2363+02	.5066-02	.7300-02	-19.6		.4294+02	.2372-02
77.0	21.916	.1193+00	.2509+02	.6669-02	.8500-02	-21.5		.4732+02	.2697-02
77.0	21.924	.1192+00	.2135+02	.6541-02	.8700-02	-24.8		.3663+02	.2650-02
77.0	21.944	.1192+00	.2024+02	.6500-02	.8900-02	-27.0		.3376+02	.2634-02
77.0	21.974	.1192+00	.1967+02	.6479-02	.9000-02	-28.0		.3235+02	.2626-02
77.0	22.014	.1192+00	.1925+02	.6462-02	.9100-02	-29.0		.3132+02	.2620-02
77.0	22.104	.1191+00	.1867+02	.6436-02	.9350-02	-31.2		.2992+02	.2610-02
77.0	22.304	.1190+00	.1784+02	.6385-02	.9750-02	-34.5		.2710+02	.2590-02

TABLE E-1 (Continued)

INITIAL SERIES OF RUNS ON 3424-1 (C-4)

TEST NO. 4 47 INPUT DATA POINTS

DATA IS FROM A U N I A X I A L TEST

SUMMARY OF RESULTS FOR BULK STRESS TERM

TEMP	TIME	EOCT	SR-CALC	DIL-CALC	DIL.	% DEV.	OMITTED POINTS	BULK TERMS	
77.0	23.604	.1190+00	.1643+02	.6346-02	.1000-01	-36.5		.2490+02	.2576-03
77.0	25.604	.1189+00	.1558+02	.6317-02	.1010-01	-37.5		.2309+02	.2569-03
77.0	30.104	.1190+00	.1470+02	.6294-02	.1000-01	-37.1		.2131+02	.2556-03
77.0	32.104	.1190+00	.1429+02	.6285-02	.9900-02	-36.5		.2051+02	.2553-03
77.0	32.304	.1190+00	.1430+02	.6285-02	.9900-02	-36.5		.2053+02	.2553-03
77.0	32.312	.1224+00	.2014+02	.6996-02	.1050-01	-33.4		.3352+02	.2827-03
77.0	32.332	.1307+00	.2481+02	.8622-02	.1230-01	-29.9		.4646+02	.3494-03
77.0	32.352	.1390+00	.2660+02	.1033-01	.1450-01	-28.7		.5212+02	.4188-03
77.0	32.372	.1511+00	.2824+02	.1318-01	.1880-01	-29.9		.5768+02	.5346-03
77.0	32.412	.1629+00	.2966+02	.1640-01	.2430-01	-32.5		.6278+02	.6657-03
77.0	32.452	.1783+00	.3158+02	.2135-01	.3280-01	-34.9		.7017+02	.8671-03
77.0	32.482	.1895+00	.3176+02	.2500-01	.4030-01	-37.0		.7088+02	.1032-01

TABLE E-1 (Continued)

INITIAL SERIES OF RUNS ON 3424-1 (C-4)

REGRESSION COEFFICIENTS ...

I	B(I)
1	.252A7-01
2	.A3146-02
3	.20345+01
4	.44206-02
5	-.172A8-03
6	.11000-05
7	.24533+01

THERE WERE 110 EXPERIMENTAL TEST POINTS

THE AVERAGE DEVIATION = -8.503 PERCENT, AND
THE STANDARD DEVIATION = 32.603 PERCENT.

TABLE E-1 (Continued)

NONLINEAR THERMOVISCOELASTIC CHARACTERIZATION CODE PAGE 43

INITIAL SERIES OF RUNS ON 3424-1 (C-4)

FAILURE ANALYSIS

THE INITIAL COEFFICIENTS ...

K	P(K)
1	.100000-04
2	.000000
3	.100000-04
4	.000000
5	.290000+02
6	.100000+01
7	.100000+01
8	.000000
9	.000000

E-40

THE FOLLOWING 4 COEFFICIENTS WERE HELD CONSTANT: 2 4 6 7

THE FOLLOWING 11 TESTS WERE USED IN THE FAILURE CHARACTERIZATION ...

1 2 3 4 5 6 7 8 9 10 11

TABLE E-1 (Continued)

INITIAL SERIES OF RUNS ON 3424-1 (C-4)

```
 ITERATION NO.     1 OF   10, WITH   82 SECONDS TO GO
ERROR  =    .110000+02      AND THE A(K) ARE ...        .100000-04  .000000     .100000-04  .000000     .200000+02
                                                        .100000+01  .100000+01  .000000     .000000
      THE DA(K) WERE HALVED   0 TIMES, AND THEIR SUM WAS .100000+01

     DA( 1) = 0.0

     DA( 2) = 0.0

     DA( 3) = 0.0

     DA( 4) = 0.0

     DB( 5) = 0.0

     DA( 6) = 0.0

     DB( 7) = 0.0

                              NEW DA(K) ARE ...          .000000     .000000     .000000     .000000     .000000
                                                        .000000     .000000    -.822177-03  .255691-01
 ITERATION NO.     2 OF   10, WITH   78 SECONDS TO GO
ERROR  =    .184475-01      AND THE A(K) ARE ...        .100000-04  .000000     .100000-04  .000000     .200000+02
                                                        .100000+01  .100000+01  -.822177-03  .255691-01
      THE DA(K) WERE HALVED   1 TIMES, AND THEIR SUM WAS .263913-01

     DA( 2) = 0.0

     DB( 4) = 0.0

     DA( 6) = 0.0

     DB( 7) = 0.0

                              NEW DA(K) ARE ...         -.581345-01  .000000    -.775869-03  .000000     .163969+02
                                                        .000000     .000000    -.211199-01  .213480-01
 ITERATION NO.     3 OF   10, WITH   70 SECONDS TO GO
ERROR  =    .183505-01      AND THE A(K) ARE ...       -.491804-05  .000000    -.212295-05  .000000     .202562+02
                                                        .100000+01  .100000+01  -.115218-02  .259027-01
      THE DA(K) WERE HALVED   7 TIMES, AND THEIR SUM WAS .164983+02

     DA( 2) = 0.0

     DB( 4) = 0.0

     DA( 6) = 0.0

     DB( 7) = 0.0
```

TABLE E-1 (Continued)

NONLINEAR THERMOVISCOELASTIC CHARACTERIZATION CODE PAGE 58

INITIAL SERIES OF RUNS ON 3424-1 (C-4)

FAILURE SUMMARY OF TEST NO. 4, CONTAINING 47 DATA POINTS.

TEMP	TIME-T	OCTAHEDRAL SHEAR STRESS CALC.	BULK STRESS - CALC.	D(T) -CALC.	L-P NORM P = P(5)	INFINITE NORM
77.0	.0000	.0000	.0000	.0000	.0000	.0000
77.0	.7400-01	.1341+02	.8582+01	.2564+00	.1052+02	.1391+02
77.0	.8400-01	.1237+02	.8627+01	.2667+00	.1092+02	.1391+02
77.0	.1040+00	.1106+02	.8627+01	.2686+00	.1099+02	.1391+02
77.0	.1540+00	.1105+02	.8093+01	.2700+00	.1104+02	.1391+02
77.0	.2540+00	.1067+02	.7761+01	.2709+00	.1108+02	.1391+02
77.0	.3540+00	.1042+02	.7548+01	.2713+00	.1110+02	.1391+02
77.0	.4540+00	.9746+01	.7036+01	.2723+00	.1113+02	.1391+02
77.0	.1034+01	.9404+01	.6675+01	.2730+00	.1116+02	.1391+02
77.0	.3854+01	.9072+01	.6293+01	.2736+00	.1119+02	.1391+02
77.0	.1135+02	.8691+01	.5948+01	.2746+00	.1122+02	.1391+02
77.0	.1138+02	.1846+02	.8440+01	.3373+00	.1385+02	.1855+02
77.0	.1140+02	.2143+02	.1242+02	.4092+00	.1676+02	.2143+02
77.0	.1145+02	.2790+02	.2014+02	.5438+00	.2224+02	.2789+02
77.0	.1148+02	.3162+02	.2403+02	.6143+00	.2510+02	.3101+02
77.0	.1150+02	.3414+02	.1981+02	.6305+00	.2572+02	.3101+02
77.0	.1155+02	.2641+02	.1849+02	.6358+00	.2593+02	.3101+02
77.0	.1165+02	.2515+02	.1725+02	.6387+00	.2604+02	.3101+02
77.0	.1185+02	.2414+02	.1643+02	.6409+00	.2613+02	.3101+02
77.0	.1235+02	.2307+02	.1514+02	.6430+00	.2621+02	.3101+02
77.0	.1335+02	.2218+02	.1428+02	.6447+00	.2627+02	.3101+02
77.0	.1535+02	.2139+02	.1339+02	.6462+00	.2633+02	.3101+02
77.0	.1835+02	.2084+02	.1264+02	.6473+00	.2638+02	.3101+02
77.0	.2185+02	.2046+02	.1206+02	.6482+00	.2641+02	.3101+02
77.0	.2186+02	.2177+02	.1605+02	.6482+00	.2641+02	.3101+02
77.0	.2186+02	.2319+02	.1780+02	.6482+00	.2641+02	.3101+02
77.0	.2188+02	.2962+02	.2156+02	.6495+00	.2646+02	.3101+02
77.0	.2190+02	.3500+02	.2363+02	.6792+00	.2775+02	.3499+02
77.0	.2192+02	.3661+02	.2509+02	.7181+00	.2936+02	.3651+02
77.0	.2192+02	.3485+02	.2135+02	.7318+00	.2988+02	.3651+02
77.0	.2194+02	.3313+02	.2024+02	.7414+00	.3025+02	.3651+02
77.0	.2197+02	.3197+02	.1967+02	.7463+00	.3044+02	.3651+02
77.0	.2201+02	.3111+02	.1925+02	.7494+00	.3056+02	.3651+02
77.0	.2210+02	.3002+02	.1867+02	.7528+00	.3069+02	.3651+02
77.0	.2260+02	.2802+02	.1744+02	.7591+00	.3094+02	.3651+02

TABLE E-1 (Continued)

NONLINEAR THERMOVISCOELASTIC CHARACTERIZATION CODE PAGE 51

INITIAL SERIES OF RUNS ON 3424-1 (C-4)

FAILURE SUMMARY OF TEST NO. 4, CONTAINING 47 DATA POINTS.

TEMP	TIME-T	OCTAHEDRAL SHEAR STRESS CALC.	BULK STRESS - CALC.	D(T) -CALC.	L-P NORM P = P(S)	INFINITE NORM
77.0	.3360+02	.2676+02	.1643+02	.7624+00	.3107+02	.3651+02
77.0	.2560+02	.2578+02	.1558+02	.7651+00	.3117+02	.3651+02
77.0	.3010+02	.2488+02	.1470+02	.7677+00	.3127+02	.3651+02
77.0	.3210+02	.2466+02	.1429+02	.7684+00	.3130+02	.3651+02
77.0	.3230+02	.2464+02	.1430+02	.7685+00	.3130+02	.3651+02
77.0	.3231+02	.2647+02	.2014+02	.7685+00	.3130+02	.3651+02
77.0	.3233+02	.3165+02	.2481+02	.7688+00	.3131+02	.3651+02
77.0	.3235+02	.3720+02	.2660+02	.7753+00	.3159+02	.3719+02
77.0	.3230+02	.4174+02	.2824+02	.8316+00	.3397+02	.4174+02
77.0	.3241+02	.4340+02	.2966+02	.8917+00	.3636+02	.4339+02
77.0	.3245+02	.4504+02	.3158+02	.9447+00	.3848+02	.4504+02
77.0	.3248+02	.4595+02	.3176+02	.9756+00	.3972+02	.4594+02

E-49

TABLE E-1 (Continued)

INITIAL SERIES OF RUNS ON 3424-1 (C-4)

FINAL FAILURE COEFFICIENTS ...

I	B(I)
1	-.588746-05
2	.000000
3	-.212556-05
4	.000500
5	.2027D4402
6	.1000C+01
7	.100000401
8	-.117321-02
9	.259221-01

THERE WERE 11 FAILURE DATA POINTS.

THE AVERAGE DEVIATION = -.35E PERCENT, AND
THE STANDARD DEVIATION = 4.26A PERCENT.

REFERENCES FOR APPENDIX E

E-1. Farris, R. J., and Schapery, R. A., "Development of a Solid Rocket Propellant Nonlinear Constitutive Theory", Report No. AFRPL-TR-73-50, June 1973.

APPENDIX F

FINITE ELEMENT COMPUTER CODE

This Appendix is divided into three major sections: (1) Description of input; (2) explanatory comments concerning the runs; and (3) demonstration problems.

I. DESCRIPTION OF INPUT

The input to the program is supplied by means of a "TITLE CARD" followed by nine blocks of data. In the following pages these blocks are denoted as [1], [2], etc. Each block must be preceded by a card with the block number punched in Column 1. For a particular problem it may not be necessary to supply the information appropriate to one or more of these blocks; in such a case the appropriate blocks are omitted.

TITLE CARD (12A6) - Columns 1 to 72 - Any information that is to be printed as a title for the problem.

[1] A card with 1 punched in Column 1 followed by:

a. GENERAL CONTROL CARD (I5, 2E10.5, 2I5)

Col. 2	NO	- Number of quadrature points to be used in each direction in the numerical integration for the isoparametric stress elements. Values of 3 or 5 are permitted; if any other value is specified the program defaults to the value of 3.

Col. 5	IPSC	= 1 Axisymmetric Analysis 2 Plane Strain Analysis ($\varepsilon_t = 0$) 3 Generalized Plane Strain Analysis ($\varepsilon_t = \varepsilon_{t_o} \neq 0$) 4 Generalized Plane Stress Analysis ($\sigma_t = \sigma_{t_o}$)	
9-10	ITYPE	= 1 Linear elastic analysis with linear measure of volume change. 1 Linear elastic analysis with nonlinear measure of volume change. 2 Linear viscoelastic analysis with linear measure of volume change. -2 Linear viscoelastic analysis with nonlinear measure of volume change. 3 Nonlinear viscoelastic analysis with nonlinear measure of volume change.	1*
11-20	TER	= Stress free temperature	2*
27-30	SZV	= ε_{t_o} when IPSC = 3, σ_{t_o} when IPSC = 4	
31-35	NPRAQF	= Number of the "time function" associated with specified value of SZV.	3*

* The numbers in the right-hand column refer to explanatory comments given in Part II of this Appendix.

Col. 36-40	NBFUN	= Number of "time function" associated with the body force history	3*
41-50	RELAX	= Iteration factor to be used in nonlinear analysis (default value = 1.0)	4*
51-60	SCALE	= Scale factor used in calculation of Lebesgue norms (should be selected so that SCALE $*\varepsilon_{max} \tilde{\sim} 1.0$) (default value = 10.0)	4*
61-70 71-80	ERAVGS ERMAXS	Average and maximum error criterion used to define convergence of nonlinear analysis (default values are .01 and .05 respectively).	4*

b. MATERIAL CARDS - for each material type the following information must be specified (the thermal conductivity properties are defined in input block [5]). 5*

(1) 1st card (1X, I4, I5, 5E10.3, 2I5)

Col. 5		Material Number	
10	ITYP	1 Linear elastic material (continuum) 2 Linear viscoelastic material (continuum) 3 Nonlinear viscoelastic material (continuum) 4 Isotropic elastic shell 5 Anisotropic elastic shell	6*

Col.	ITYP=1	ITYP=2	ITYP=3	ITYP=4	ITYP=5
11-20	μ_o	μ_o	μ_o	E	C_{11}
21-30	K	K	K	ν	C_{12}
31-40	α	α	α	α	C_{22}
41-50	B_r	B_r	B_r	h_m	$\bar{N}_x$
51-60	B_z	B_z	B_z	h_b	$\bar{N}_y$
61-65		ML	ML		
66-70		NS	NS		

If ITYP = 1 or ITYP = 4 This completes the specification.
If ITYP = 5 go to (4).

(2) For ITYP 2 and 3

If ML>0 then the preceeding card is immediately followed by as many cards (8E10.3) as necessary to specify the ML pairs of values of α_1, B_1. The first card contains α_1, B_1, α_2, B_2, ... B_4, the second (if needed) α_5, B_5, α_6, ... etc.

If NS>0 (NS = 0 denotes a material whose properties are temperature independent) then the preceeding card is immediately followed by as many cards (8E10.3) as necessary to specify the NS pairs of values of F_1, T_1. The first card contains F_1, T_1, F_2, T_2, ... , T_4, the second (if needed) F_5, T_5, F_6, ... etc.

If ITYP = 2 This completes the specification.

(3) For ITYP = 3 The previous card is immediately followed by five cards (8E10.3).

	Col.		
i)	1-10	A_1	Nonlinear viscoelastic properties defined in Note 6*.
	11-20	A_2	
	21-30	P_1	
	31-40	q_1	
	41-50	n_1	
	51-60	A_3	
	61-70	P_2	
	71-80	q_2	
ii)	1-10	n_2	
	11-20	A_4	
	21-30	P_3	
	31-40	q_3	
	41 50	n_3	
	51-60	C_{3_1}	
	61-70	C_{4_1}	
	71-80	C_1	
iii)	1-10	C_2	
	11-20	C_{3_2}	
	21-30	C_{4_2}	
	31-40	T	
	41-50	n_1	
	51-60	n_2	
	61-70	n_3	
	71-80	n_4	

	Col.		
iv)	1-10	n_5	Nonlinear viscoelastic properties defined in Note 6*.
	11-20	n_6	
	21-30	D_1	
	31-40	D_2	
	41-50	D_3	
	51-60	D_4	
	61-70	D_5	
	71-80	D_6	
v)	1-10	D_7	
	11-20	D_8	
	21-30	D_9	
	31-40	D_{10}	

If ITYP = 3 This completes the specifications.

(4) For ITYP = 5 The card of (1) is immediately followed by

Col.		
1-10	D_{11}	Anisotropic shell properties defined in Note 6*.
11-20	D_{12}	
21-30	D_{22}	
31-40	$\bar{M}_x$	
41-50	$\bar{M}_y$	
51-60	h_m	

The notation used in the above section is defined in Note 6*.

[2] A card with 2 punched in column 1, followed by: as many cards as needed to describe the 3*

TIME FUNCTION ARRAYS: For each function the following cards are required:

a. One card (2I5)

Col.

1-5	I - Function number
6-10	N - Number of points defining the function.

b. As many cards (8E10.3) as needed to specify the N pairs of values F_1, t_1. The first card contains F_1, t_1, F_2, t_2.... t_4, the second (if needed) F_5, t_5,..... etc.

[3] A card with 3 punched in column 1, followed by: 7*

TIME STEP ARRAY (1X, I4, 2E10.3) As many cards as necessary to specify the times which define the ends of the time steps used in the analysis (Note: $T_0 = 0.0$).

Col.

2-5	N - Time step number	7*
6-15	T - Time at end of step N	
16-25	D - Spacing ratio used in time step generation option	

[4] A card with 4 punched in column 1, followed by:

NODE POINT ARRAY - (1X, I4, 2E10.3, I5, 3E10.3) — 8*, 5*

Col.

2-5	N - Node point number		9*,10*, 12*
6-15	r - Coordinate		
16-25	z - Coordinate		
26-30	INC-Numbering Increment	Quantities associated with curved or straight line generation option	
31-40	D - Spacing Ratio		
41-50	r_c Coordinates of point interior to circular arc		11*
51-60	z_c		

[5] A card with 5 punched in column 1, followed by:

ELEMENT ARRAY - (1X, I4, 8I5) — 8*,5*

Col.

2-5, 6-10, 11-15, 16-20	The numbers of the four node points which describe the element (reading counterclockwise around the element). For a shell element the third and fourth numbers are left blank.	15*
21-25	MN -Material number (corresponding to the material descriptions in block [11]).	13*

Col.				
26-30	NMIS	- Number of additional elements in the sequence	Quantities associated with the data generation option	14*
31-35	INC	- Numbering increment		
36-40	NMISP	- Number of additional layers		
41-45	INCP	- Numbering increment for the layers		

The order of the element cards need bear no relationship to the locations of the elements in the body except that all shell elements must follow the continuum elements.

[6] A card with 6 punched in Column 1, followed by: 23*

THERMAL ANALYSIS INFORMATION

a. Control Card (1X, I4, 3I5, E10.3)

Col.		
2-5	NMAT	- Number of materials with different thermal properties ($\leq$ 10)
6-10	NNBC	- Number of nodal point boundary conditions (temperatures or heat fluxes)
11-15	NCBC	- Number of convection boundary conditions ($\leq$ 65)
16-20	KAT	- KAT = 0 Axisymmetric Analysis KAT $\neq$ 0 Planar Analysis
21-30	TZ	- Temperature of the body at time zero (°F) (stress free temperature)

b. Material Cards (I10, 6F10.0).

Col.		
1-10	N	- Material number
11-20	XCOND(N)	- Conductivity: K_{rr}, (Btu) $(T)^{-1}(L)^{-2}$ $(°F/L)^{-1}$
21-30	YCOND(N)	- Conductivity: K_{zz}
31-40	XYCOND(N)	-Conductivity: K_{rz}
41-50	SPHT(N)	- Specific heat, (Btu) $(F)^{-1}(°F)^{-1}$
51-60	DENS(N)	- Weight density, (F) $(L)^{-3}$
61-70	QX(N)	- Heat generated per unit volume, (Btu) $(T)^{-1}$ $(L)^{-3}$

24*

Use one card for each different material number assigned in the element array; NMAT cards must be prepared in this section - order is not important.

c. Nodal Point Boundary Conditions (2I5, F10.0, I5)

Skip this section if NNBC = 0

Col.		
1-5	N	- Node number
6-10	KODE(N)	- Boundary condition type = 0, externally supplied heat flux = 1, prescribed node temperature
11-20	T(N)	- Boundary value amplitude = Heat flux (KODE(N) = 0), (Btu) $(T)^{-1}(R)$ = Temperature (KODE(N) = 1), (°F)

Col.			
21-25	NFN(N)	- Function number { A function number equal to zero (or blank) means that the prescribed boundary condition is applied at time zero and remains constant for all time, t > 0.	

All nodal points not specified in this section are assumed to have externally supplied heat flux of zero for all values of time.

d. Convection Boundary Conditions (NCBC Cards, 2I5, 2F10.0, I5)

Skip this section if NCBC = 0

Col.			
1-5	I(N)	- Node number i	
6-10	J(N)	- Node number j	
11-20	H(N)	- Heat transfer coefficient, h: (BTU) $(T)^{-1}(L)^{-2}(°F)^{-1}$; $q = h\,(T - T_o)$	
21-30	TE(N)	- Environmental temperature amplitude, T_o	
31-35	NFCV(N)	- Function number { If the environment does not change temperature with time, then NFCV(N) = 0 and $T_o = T_o$, constant for t > 0.	3*

e. Printing Control for Temperatures

At least one card in this section	22*

Card 1

Col.		
1-5	NO(1)	- Output interval
6-10	NPR(1)	- Number of print operations at this interval
11-15	NO(2)	- Output interval
16-20	NPR(2)	- Number of print operations at this interval
	.....	
71-75	NO(8)	- Output interval
76-80	NPR(8)	- Number of print operations at this interval

Card 2 (If Required)

Col.		
1-5	NO(9)	- Output interval
6-10	NPR(9)	- Number of print operations at this interval
11-15	NO(10)	- Output interval
16-20	NPR(10)	- Number of print operations at this interval

This information is used to control the amount of printed output produced by the program in the temperature section.

7 A card with 7 punched in Column 1, followed by: 5*

BOUNDARY ARRAY (1X, I4, I3, I2, E10.5, I3, I2, 2E10.5, 2I5, 2E10.3). As many cards as necessary to specify displacement or non-zero stress boundary conditions.

Col.			
2-5	N	- Node point number	
6-8	NFUNI	- Time function no. for condition 1	3*
10	IF_1	= $\{0\}_{1}$ indicates $\{$Force / Displacement$\}$ specified in 1 direction	16*, 17*
11-20	V_1	= Value of $\{$Force / Displacement$\}$	
21-23	NFUN2	= Time function no. for condition 2	3*
25	IF_2	= $\{0\}_{1}$ indicates $\{$Force / Displacement$\}$ specified in 2 directions	
26-35	V_2	= Value of $\{$Force / Displacement$\}$ specified in 2 directions	
36-45	Θ	- angle (in degrees) between x_1-axis and r-axis (see Figure F-1)	18*
46-50	N'	- Final point in sequence } Quantities associated with boundary condition generation option	19*
51-55	INC	- Numbering increment } Quantities associated with boundary condition generation option	19*
56-65	P_N	Pressure magnitudes at points N and N' respectively (Note NFUN1 = NFUN2 = time function number for the pressure)	20*
66-75	$P_{N'}$	Pressure magnitudes at points N and N' respectively (Note NFUN1 = NFUN2 = time function number for the pressure)	20*

[8] A card with 8 punched in Column 1, followed by: 21*

PRINT INFORMATION FOR STRESS ANALYSES

Col.			
5	ITYP	=	1 Time point number print information 2 Node point number print information 3 Element number stress and strain print information 4 Element number "damage" print information
6-10	N	-	Number
11-15	NMIS	-	Number of additional numbers for which it is desired to generate same information
16-20	INC	-	Value by which successive numbers in the generation sequence differ

21*

[9] FINAL CARD - Card with 9 punched in Column 1.

The above sequence of cards is repeated for the next analysis, etc.

II. EXPLANATORY COMMENTS CONCERNING THE INPUT

The input is divided into sections each preceded by a card denoting the section number. To run only certain parts of the program only the data necessary to that portion is input. Thus, in running the program to find the thermal history alone only blocks [2], [3], [4], [5] and [6] should be input. To run for stress alone (isothermal) input block [6] is omitted.

Specific comments on the various input sections follows:

1*. The exact forms of the linear and nonlinear viscoelastic characterizations used in the program are described in Note 6*. The "linear volume change measure" is the usual small deformation measure while the "non-linear measure" is exact for all magnitudes of deformations. No other large deformation effects are accounted for in the analysis.

2*. At time T = 0 the complete structure is assumed to be at temperature TER (and to be stress free).

3*. The time dependence of various input quantities (e.g., boundary conditions, body forces, etc.) are described by multiplying their prescribed values by an appropriate time function illustrated in Figure F-2. A given function can be used to describe the time variations of any number of different quantities. If a time function is not prescribed for a given quantity it is assumed to be a step function at T = 0. For solution times which exceed T_N, the last segment of the curve is extended with a constant slope.

4*. These items need only be prescribed for a nonlinear analysis. For a discussion of the selection of RELAX, see Reference (1).

5*. The upper bounds on the dimensions are checked by the program and an error message is given if any are violated. These bounds are specified at the beginning of PREP. The definition of these bounds are as follows:

LMTN1	The number of different materials (N MAT)
LMTN2	The value of NS (input block [1]-b).
LMTN3	Such that NEmax <3(LMTN3) (see comment 8* for NEmax)
LMTN4	The total number of elements (NELEMT)
LMTN5	The maximum node point number (NPT)
LMTN6	The number of boundary condition specifications (NBPCT) plus three
LMTN7	The number of time steps
LMTN8	The value of ML (input block [1]-b)
LMTN9	Twice the sum of the hereditary exponential terms for all materials meeting at each node point.
LMTN10	One plus the sum of different materials coming into each node point.
LMTN11	The number of time input cards (input block [3])
LMTN12	The number of values NO and NPR input as instructions for printing (input block [6]-e)
LMTN13	The number of convection boundary conditions NCBC (input block [6]-a)
LMTN14	The number of time functions specified (input block [2])
LMTN15	The number of time values at which each time function is specified (input block [2])

(5*. Continued)

When changing the dimensions of the program, one must change the dimensions in the Common Blocks and in the Dimension Statements, and also the values of the upper limits LMTN1-LMTN15 specified at the beginning of PREP.

The array dimensions which are related to the size of the problem are indicated below. They are listed by their Common Block followed by the routines in which the blocks appear, or by the routine in which they appear in a dimension statement. In this listing L stands for LMTN.

COMMON/XGRID/R(L5), Z(L5), NOD(5, L5) (MAIN, PREP, DMAGE, STIFNS, HEET)

COMMON/SOLTME/NTI(L11), DTI(L11), CCC(L11) (MAIN, PREP, HEET)

COMMON/PROP/FS(L1, L2), FST(L1, L2) (MAIN, PREP, INTP1)

COMMON/SYMSOL/S(2 x L5 + L4, L3), SL (2 x L5 + L4)(MAIN, PREP, SYSOL, HEET)

COMMON/BLK2/PIPS (L4, 3, 2), PT1S(L4), PT2S(L4), XKVS (L4) PIPSD (L4, 2),
DEZ (L4) (MAIN, DMAGE, STIFNS)

COMMON/BLK3/FUN (L15, L14), FUNT (L15, L14), NPTS (L14)
(MAIN, PREP, INTP2, HEET, INTFN)

COMMON/PREPCO/NON(L1), AP(L1, L8), BP(L1, L8), IFUN(3) IIFLG (3), BIV(L6,5),
APO(L1), NQ(L5 + 1), PROP(L1, 36), ITY (L1), BF(L1,2), ALP(L1), XK(L1),
NOPT(L10), NPRNT(L7)
(MAIN, PREP, DMAGE, STIFNS)

(5*. Continued)

CϕMMϕN/CVNBC/II(L13), JJ(L13), H(L13),TE(L13),NFCU(L13),NCBC (INHEAT, HEET)

CϕMMϕN/TMPBC/NNBC, KϕDE(L5), T(L5), NFN(L5) (INHEAT, HEET)

CϕMMϕN/TMATS/XCϕND(L1), YCϕND(L1), XYCϕND(L1), SPHT(L1), DENS(L1), QX(L1), MNAT, KAT (INHEAT, HEET)

CϕMMON/TMPϕUT/Nϕ(L12), NPR(L12) (INHEAT, HEET)

MAIN - DIMENSIϕN GQTS(3), TEMFA(L4), TEMBA(L4) , EP(L4, 4), CC(L9), SCS(L4,3), XMUA(L4), GQT(2),US(L5), WS(L5), DSL(2 x L5 + L4), DXMUA(L4), XLN(L5,3), XLNP(L5, 3), PSIP(4)

CASE - DIMENSIϕN AP(L1, L8)

HEET - DIMENSIϕN TSAVE(L5), BSAVE(L5), ASAVE(L5 ,L3), B(L5), D(L5, L3)

6*. <u>ITYPE = 1 Linear Elastic Continuum Material</u>

$$S_{ij} = 2\mu_o e_{ij}$$

$$\bar{\sigma} = K(\Delta V - 3\alpha\Delta T)$$

<u>ITYPE = 2 Linear Viscoelastic Continuum Material</u>

$$S_{ij} = 2\left(\mu_o + \int_0^t \left[\sum_{n=1}^{ML} \alpha_n e^{-\beta_n(\xi-\xi')} \right] \dot{e}_{ij} dt' \right)$$

$$\bar{\sigma} = K(\Delta V - 3\alpha\Delta T)$$

(6*. Continued)

ITYPE = 3 Nonlinear Viscoelastic Continuum Material

$$S_{ij} = 2G \left\{ \mu_o e_{ij} + A_3 \left(\frac{||f||_{q_1}}{||f||_{p_1}} \right)^{n_1} e_{ij} + A_4 \left(\frac{||f||_{q_2}}{||f||_{p_2}} \right)^{n_2} e_{ij} \right.$$

$$\left. + \left[1 - \left(\frac{||f||_{q_3}}{||f||_{p_3}} \right)^{n_3} \right] \int_0^t \left[\sum_{n=1}^{ML} \alpha_n e^{-\beta_n (\xi - \xi')} \right] \dot{e}_{ij} dt' \right\}$$

$$G = e^{(A_1 I_\gamma + A_2 I_d / I_\gamma)}$$

$$I_d = \frac{1}{K} e^{(C_{3_1} + C_{4_1} (T-\bar{T}))\bar{\sigma}} + C_1 e^{(C_{3_2} + C_{4_2} (T-\bar{T}))\bar{\sigma}} (I_\gamma)^{C_2} + 3\alpha\Delta T$$

$$F = \eta_1 I_1 + \eta_2 I_1^2 + \eta_3 I_2 + \eta_4 I_1^3 + \eta_5 I_1 I_2 + \eta_6 I_3$$

Where Damage "D(t)" is calculated by

$$D(t) = D_1 \left(||e^{[D_3 + D_5 (T - \bar{T})]\bar{\sigma}} \sigma_{oct} ||_{D_7} \right)^{D_9}$$

$$+ D_2 \left(||e^{[D_4 + D_6 (T - \bar{T})]\bar{\sigma}} \sigma_{oct} ||_{D_8} \right)^{D_{10}}$$

The reduced time is ξ is defined as

$$\xi = \int_0^t e^{-F(T)} dt'$$

(6*. Continued)

Where F(T) is defined by NS points e.

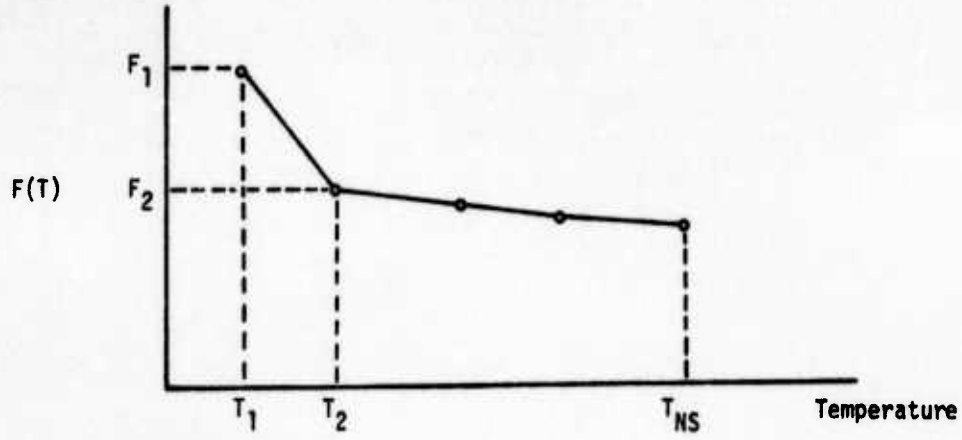

In addition,

B_r = radial body force

B_z = axial body force

ITYPE = 4 Isotropic shell

E = Young's modulus
ν = Poisson's ratio
α = thermal coefficient of expansion
h_m = shell thickness for membrane considerations
h_b = shell thickness for bending considerations

Normally $h_m = h_b$ unless you wish to consider only membrane behavior in which case set $h_b = 0$

(6*. Continued)

ITYPE = 5 Anisotropic Shell

$$\begin{pmatrix} N_x \\ N_y \end{pmatrix} = \begin{pmatrix} C_{11} & C_{12} \\ C_{12} & C_{22} \end{pmatrix} \begin{pmatrix} \bar{\epsilon}_x \\ \bar{\epsilon}_y \end{pmatrix} + \begin{pmatrix} \bar{N}_x \\ \bar{N}_y \end{pmatrix} e_T, \quad e_T = \frac{1}{h} \int \Delta T dz$$

$$\begin{pmatrix} M_x \\ M_y \end{pmatrix} = \begin{pmatrix} D_{11} & D_{12} \\ D_{12} & D_{22} \end{pmatrix} \begin{pmatrix} X_x \\ X_y \end{pmatrix} + \begin{pmatrix} \bar{M}_x \\ \bar{M}_y \end{pmatrix} X_T, \quad X_T = \frac{1^2}{h^3} \int \Delta T z dz$$

7*. The times for those steps not specifically specified in block [3] are generated in identical fashion to the straight line grid generation procedure described in comment 11*.

Note that a time step length of 0.0 is acceptable (i.e. may consider step function loads, etc.).

This method of specifying the solution time points to be used automatically produces small time steps at the beginning of the region while continuously widening the time steps toward the end of the region. As an example, if 50 solution time points are specified over a 24 hour period with D = 1.1 the first solution time point will occur at .0206 hrs (1.24 minutes) and the last solution step ($t_{50} - t_{49}$) will be 2.19 hours (132 Minutes).

It is important to choose D such that the final time set is not excessively large. The following equations may be used to find these values:

$$\frac{\Delta T_1}{T_f} = \frac{D-1}{D^N-1} \qquad \frac{\Delta T_N}{T_f} = \frac{D^{N-1}(D-1)}{D^N-1}$$

(7*. Continued)

where

D = time increment ratio
ΔT_1 = initial solution time step
N = total number of solution time points
ΔT_N = final time step
T_f = final value of time ($T_o = 0$)

8*. These two equations are plotted for various values of D in Figures F-3 and F-4, respectively.

The cross-section of the body is assumed to lie in the r-z plane for axisymmetric analyses and in the x-y plane for plane analyses. For plane analyses the direction perpendicular to the x-y plane is denoted by t. In the application of the analysis the two-dimensional body is described by a series of quadrilateral elements of arbitrary shapes. The numbering of the nodes for a simple element representation is shown in Figure F-1. In addition shell elements (two node elements) are available for modeling thin shell protions of the structure. For example, in the instance of a motor case of a solid propellant motor, shell elements may be prescribed to exist between any two nodes in the system.

Considering any two of the two or four nodes which describe an element, denote the difference in their node numbers as N_i. For a given element deonte the maximum value of N_i as NE_j. Considering all elements in the system denote the maximum value of NE_j as NE_{max}. For a minimization of computational cost, for a given analysis, it is important that the node points be numbered so as to minimize the value of NE_{max} (the numbering used in Figure F-1 gives a value of $NE_{max} = 5$; if the numbering had instead proceeded from left to right a value of $NE_{max} = 10$ would have been obtained).

(8*. Continued)

The program checks the area of each of the quadrilateral elements, if any one of these values should be non-positive, an error message ("data error in element n") is printed. This error is normally a result of one of the following: (1) the nodes describing the element were entered in a clockwise manner instead of counterclockwise; (2) one of the node numbers describing the element was entered incorrectly, or (3) the coordinates of one of the nodes describing the element was entered incorrectly.

9*. Not all numbers between 1 and the maximum node number need correspond to actual nodes in the body, e.g., the grid shown in Figure F-5 is permissible; coordinates may or may not be specified for the non-existent nodes 15 and 21. This feature facilitates the use of the various data generation options (e.g., see comment 11*).

10*. The program has available two generation procedures to assist the user in describing the location of the node points. These generation options are described in the following two "comments". The use of these options can, for instance, permit one to describe the location of the nodes for an arbitrarily large grid by as few as five cards.

11*. The "circular arc (or straight line) coordinate generation option" may be used whenever several sequential points lie along a circular arc or a straight line. For such points it is only necessary to enter data for the end points (denoted as N and N') of the sequence and values of INC and D. INC is the difference between any two successive node numbers in the sequence and D is the ratio of the distances between any two successive pairs of points.

(11*. Continued)

When for a point N, INC≠ 0, then intermediate node points are generated along a straight line ($r_c = z_c = 0$) or a circular arc ($r_c \neq 0$ and/or $z_c \neq 0$) between N and the point described on the previous node card (N'). That is points N' + INC, N' +2·INC, ..., N-INC are generated. Circular arcs are defined as passing through the end points N and N', and some intermediate point (not necessarily one of the nodes) whose coordinates are (r_c, z_c).

The end points of the segment may be entered in any order, i.e. the segments shown in Figure F-6 may be defined by specifying the end-points in order 7 → 22 or 22 → 7. The spacing of the intermediate points is controlled by the value of the spacing ratio D. D is equal to the ratio of the lenghths of the successive segments defined by the intermediate points. A value of D = 1.0 gives equally spaced points. The locations of the inter-medicate points 12 and 17 (see Figure 70) could be generated by either specify-ing points 7 → 22 and D = 2.0 (Note: D = 2.0/1.0 or 22→7 and D = 0.5): the value of INC would be 5. See Note 8* for more discussion related to the factor D.

For the grid shown in Figure F-1 the coordinates could be generated for the points lying between 1-4, 5-8, 9-12, etc., or between 1-29, 2-18, 18-30, 3-31, etc. Note that the line 3-31 cannot be extended to point 33 as the value of INC changes at point 31, however, if nodes 33 and 34 had been instead numbered 35 and 36 (there would then have been no nodes numbered 33 and 34, see comment 9*') it would be possible to generate all the nodes along the line at one time.

12*. The "interior node point generation option" locates all nodes interior to the body whose coordinates have not been specifically specified by the user (i.e. all points not specifically treated in input block [4]. The location of the interior nodes is accomplished by the so-called "Laplacian generation scheme", i.e. the coordinates of an interior node point are selected so that they are equal to the average of the coordinates of the

(12*. Continued)

neighboring nodes. Note that all nodes on the boundaries of the body must be either directly specified or generated by means of the straight line generation scheme (described in comment 11*). Figure F-7 illustrates two grids which have been prepared with the aid of this generation scheme. Grid 1 was prepared by specifying the locations of the exterior nodes by means of the straight line generation scheme; the interior nodes were left unspecified and hence were "generated" as described above. Grid 2 was prepared in a similar way with the exception that the interior sequence of nodes lying on the line 3-21 were generated with the "straight line generated scheme".

13*. When the value of MN remains constant for a number of sequential element cards, it is only necessary to specify MN for the first card in the group (the appropriate columns are left blank for the remainder of the cards in the group).

14*. If the body is divided into layers of elements, and the quantitiy MN remains the same for a number of elements within a layer (and possibly the same for a number of layers), the node numbers for these elements may be simply specified by using the "element data generation option". To use this generation option for the elements in a single layer the data is supplied for the first element in the layer and the appropriate values are specified for NMIS and INC. The quantity NMIS indicates the number of additional elements in the sequence. The quantity INC indicates the amount by which the corresponding node numbers of succesive elements differ.

For example, the bottom row of elements in Figure F-1 could be specified by giving the node numbers for element "a" and the values NMIS = 6 and INC = 4 or the information for element "b" and the values NMIS = 6 and INC = -4 (in order to use this option all the elements from a→ b must, however, have the same value of MN). Alternatively if one wished to generate the element information for the elements in the left hand column (all these elements would need to have the same value of MN), one could do this by giving the node numbers for element "a" and the values NMIS = 2 and INC = 1, etc.

(14*. Continued)

In addition, if the value of MN remains unchanged for a number of layers the data information for all the elements in these layers may be generated with a single card by supplying, in addition to the values of NMIS and INC (for the first layer), the values of NMISP and INCP. NMISP denotes the number of additional layers for which the element data is to be generated and INCP indicates the difference between the node numbers of the successive layers. For example, if the bottom two layers of elements in Figure F-1 all had identical values of MN the data for <u>all</u> these elements could be generated by giving the appropriate data for element "a" and the values.

NMIS = 6
INC = 4
NMISP = 1
INCP = 1

or alternatively

NMIS = 1
INC = 1
NMISP = 6
INCP = 4

As a second example if the elements of Grid 1 of Figure F-7 all had identical values of MN they all could be described by giving the appropriate data for the lower left element and

MNIS = 3
INC = 1
NMISP = 4
INCP = 5

15*. A bending (and stretching) element (shell element for axisymmetry, strip plate element for plane strain, beam element for plane stress) may be placed between any two nodes in the system. If two or more bending elements intersect at a node the connection between them is treated as rigid. Curved members may be approximated by a series of straight elements. In the element array shell elements are designed by leaving their third and fourth node numbers blank.

16*. For each of the two coordinate directions (see comments 8* and 18*) one either specifies the displacement by setting "IF" equal to one, "V" equal to the specified displacement or adds in the "boundary load" by leaving "IF" blank and setting "V" equal to the boundary load (i.e., resultant of specified boundary stress). Boundary displacements and forces are positive when they have the same sense as the positive coordinate direction. If a boundary point is not constrained and has no load applied to it, it is not neccessary and in fact economically not desirable to include the point in the boundary array.

<u>In an axisymmetric analysis the applied force is in terms of force per-unit radian of circumference</u> (note a concentrated load applied at R = 0 must have its value divided by 2π in order to make it a force per unit radian). The fact that the radial displacements along the axis of revolution are zero is recognized within the program and need not be specified by the user.

A point load may be applied at any node point within the structure by treating it as a boundary point.

17*. Slope boundary conditions for bending elements are specified automatically by the program as follows: If no displacement boundary conditions are specified for a node at the end of a bending member the moment at the end of the bending member is taken to be zero; if one or both of the displacements are specified the slope of the bending element is set equal to zero.

18*. If $\theta = 0$ the subscripts 1 and 2 refer to r and z, if $\theta \neq 0$ (see Figure F-1) they refer to x_1 and x_2, (i.e., $IF_1 = IFx_1$, etc.).

19*. If several sequential points have identical boundary conditions, they may all be considered with a single card by supplying the proper values for the quantities N' and INC. The quantity N' denotes the number of the last point in the sequence. The quantity INC specifies the difference between the node numbers of successive points.

If for example the points 1 → 21 on the bottom boundary of the structure shown in Figure F-1 all had the same boundary condition specifications, this could be accomplished by specifying the appropriate boundary conditions and N = 1, N' = 21, INC = 4.

20*. Uniform or linearly varying pressure may be applied to a straight or curved boundary by using the boundary condition generation option (see comment 19* - leaving the spaces for IF_1, IF_2, V_1, V_2 and TH blank) for the points involved and specifying appropriate values for P_N and $P_{N'}$ (if the pressure is uniform $P_N = P_{N'}$). For example, for the boundary shown in Figure F-8, one would specify:

$$\begin{aligned} N &= 11 \\ N' &= 2 \\ INC &= -3 \\ P_N &= 100 \\ P_{N'} &= 50 \end{aligned}$$

The points N → N' must be specified in a counterclockwise order as one proceeds along an external boundary and clockwise along internal boundaries (i.e., inside holes in the body). Pressure specification cards must precede all others in the "Boundary Condition Array".

21*. In the "Print Information" section, the following information must be specified.

(i) The time increment numbers for which it is desired to have all node point displacements and element stresses and strains printed regardless of specification in "ii" and "iii" below.

(ii) Those node points for which it is desired to suppress printing of displacements (with the exception noted in "i" above).

(iii) Those elements for which it is desired to suppress printing of stresses and strains (with the exception noted in "i" above).

(iv) Those elements where it is desired to compute and print damage information (for these elements stresses and strain are also printed regardless of specification in "iii").

NOTE: Damage calculations can only take place if the material in the element is Type 3.

22*. In preparing the data for part e of block [6], the following condition must be observed:

NO(1)*NPR(1) + NO(2)*NPR(2) + ...= Number of time steps

That is to say that the printing range must cover the solution period.

Suppose that temperature output is required at time points 2, 4, 7 and 8. In this case one card would be input in this section:

Card 1: 2,2,3,1,1,1; [2(2) + 3(1) + 1(1) = 8]

(22*. Continued)

If temperatures at all 8 points are requested, then

Card 1: 1, 8; [1(8) = 8]

23*. The heat transfer portion of the program does not include case elements. If the motor case is compared with the adjacent propellant liner elements, and the thermal conductivity of the case is not significantly differerent from the propellant, then neglecting the case is a reasonable assumption. If, on the other hand, the case has significantly different thermal properties than the propellant, the elements adjacent to the propellant should be assigned anisotropic properties which will account for the presence of the case.

For example, if the element adjacent to the case is rectangular with a radial thickness t_E and a thermal conductivity K_E, and the case has a thickness t_c and a conductivity K_c then the conductivities of the element should be replaced with

$$K_{RR} = K_E K_c (t_E + t_c)/(T_E K_c + t_c K_E) \text{ and}$$

$$K_{zz} = (t_E K_E + t_c K_c)/(T_E + t_c)$$

which will account for the presence of the case.

24*. If the thermal conductivity of a material is independent of direction, then

$$K_{rr} = K_{zz} = K$$

$$K_{rz} = 0$$

The heat generated per unit volume is assumed to be constant with time.

III. DEMONSTRATION PROBLEMS

Three test cases were prepared to illustrate the input and output features of the program. These examples are not intended to cover all possible cases, but to give an indication of the form of the input and the extreme flexibility of the program and its input options.

EXAMPLE 1

The first example chosen was the solution of an elastic plate with a centrally located hole and subjected to an axial pull. This is a plane stress problem and is illustrative of the relative ease with which a complicated grid can be generated. The grid generated for this example is that shown in Figure 46 of the text. Because of symmetry, the grid representation may be limited to one-fourth of the actual plate.

The computer input sheets have numbers in the far left column that correspond to the block numbers in the program description. For this example, blocks [2], [3], [6] and [8] were omitted because they were not needed, see input data sheet, Table F-1.

When inputting the data, the first card in block [1] tells the program to solve a plane stress linear elastic problem (see Column 1 of Table F-1). The second card gives the material properties. Block [4] gives the node point array. Only certain points on the boundary are specified and the generation option is used for the remaining boundary points. Interior node points are automatically generated in the program. Block [5] describes the element array which tells how the elements and nodes are to be labeled. Block [7] describes the boundary conditions. Here again a very small number of cards are required for a complete description of all the conditions in the boundary.

The output of this example, Table F-2, contains first, the label which was input as the first data card. Following this are descriptions of the type of problem being solved and the material properties. Next comes the complete geometry of the grid followed by the element information, the element areas and the complete boundary conditions. Note that all this output information is in considerable detail in that it contains the results of the internal generation options.

The next output contains the displacements of each node, and the stresses and strains in each element.

EXAMPLE 2

This example was chosen to show the solution of a nonlinear viscoelastic problem. The problem is an axisymmetric analysis of a five element representation of a segment of a rocket motor. The material properties were those found for the Aerojet propellant ANB-3124.

The input to this example is given in Table F-3. As may be seen in Table F-3, block [1] is longer than that for Example 1 because the material properties require the more complex nonlinear viscoelastic descriptions. Block [2] has been added to describe the time function array which for this problem is simply a linearly increasing function of time. Block [3] is the time step array which describes the times of which the analysis will be performed. Other input blocks are similar to those previously described.

The output for Example 2 is given in Table F-4. As can be seen, the main difference between the output for this example and that for Example 1 is that the node point displacements and the element stresses and strains are output for each of the time increments specified by the input.

EXAMPLE 3

This example illustrates the input and output for a thermal analysis problem. The analysis is of a Minuteman rocket motor which has a prescribed internal and external temperature histories. The motor is comprised of five different materials (propellant, liner, insulators, and case).

The input to this example is given in Table F-5. Block [2] of the input gives the two time histories. For instance, the first history provides that at time 0 we have a temperature of 60°F and at time 4 seconds the temperature has dropped to 55°F, etc. Block [3] gives the time step array, and [4] and [5] are similar to those blocks previously discussed.

Block [6] contains the thermal analysis information. The first card in block [6] describes the type of problem to be solved, while the next five cards describe the thermal properties in each of the five different materials, and the next four cards tell the four nodes at which the temperature is prescribed. The last card in block [6] is a print control for the temperatures. It tells the program to print the temperature at every 20th time step.

When running both the thermal and stress analysis parts of the program, the temperatures are output on an auxilliary unit (tape or disk) and read back in for the stress analysis portion. When running the thermal analysis program alone the omission of input block [1] tells the program not to generate the auxilliary tape or disk information. If the program is to be run with both thermal and stress portions a scratch tape or disk labeled 1 is called for.

The initial output of Example 3, Table F-6, repeats the input information in the order that it was originally given. Hence, the two time functions are output first, followed by the time step information, node point geometry, and the element information. These are followed by transient heat transfer information which describes the thermal problem being solved. Next comes a material table which lists the thermal properties for each of the five materials. This is followed by the nodal point boundary conditions which references the node where applied, the type of condition, the function amplitude, and the function number (the function number refers to one of the two time functions listed at the beginning of the output section). This is followed by a statement of the print control.

Finally, the solution is output, Table F-6. This consists of the time at which the temperatures are calculated, followed by the temperatures at each node. For this example, there were 64 nodes; hence, at each time step 64 temperatures are printed. For example, at a time of 8 sec. the temperature at the 45th node is 57.7°F.

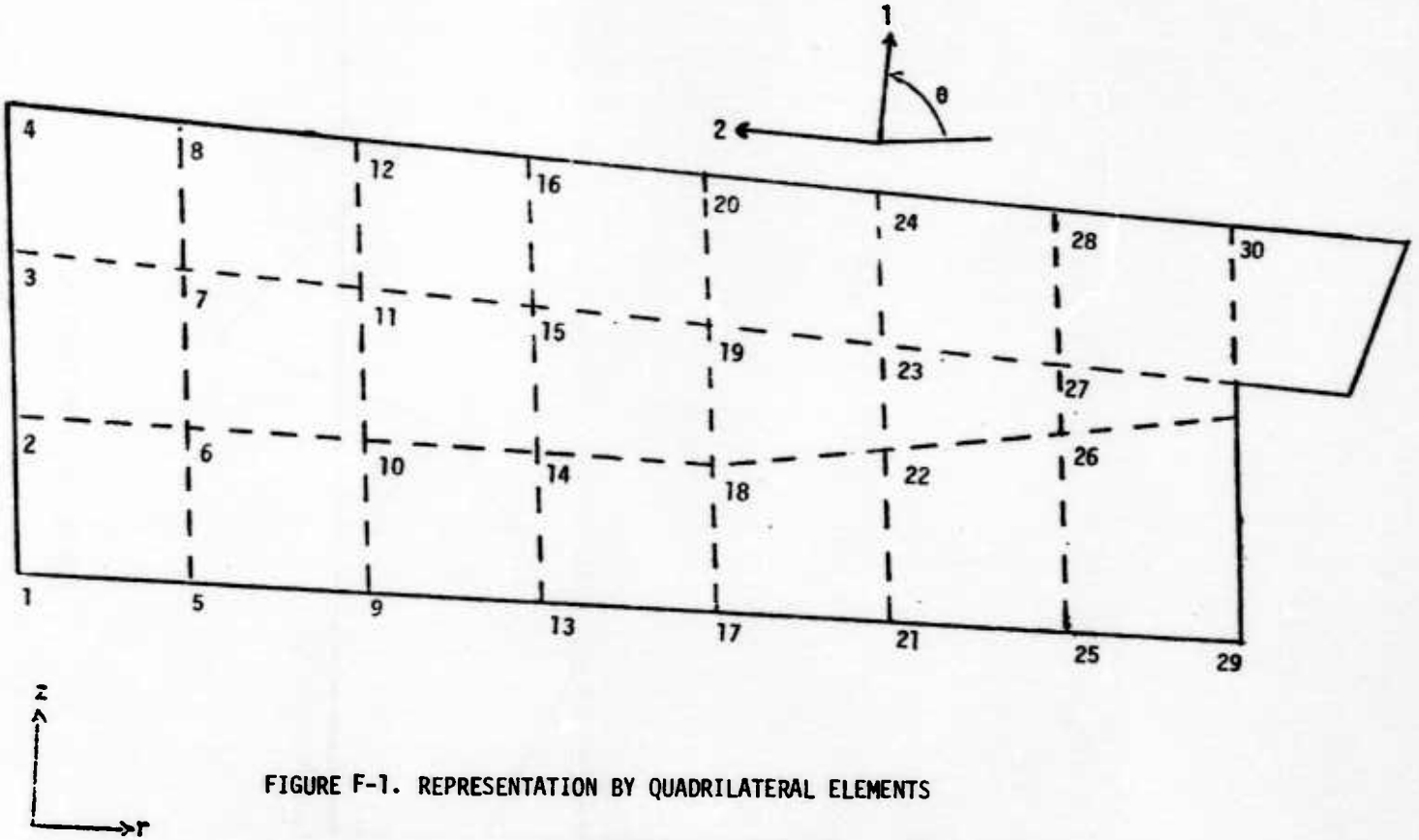

FIGURE F-1. REPRESENTATION BY QUADRILATERAL ELEMENTS

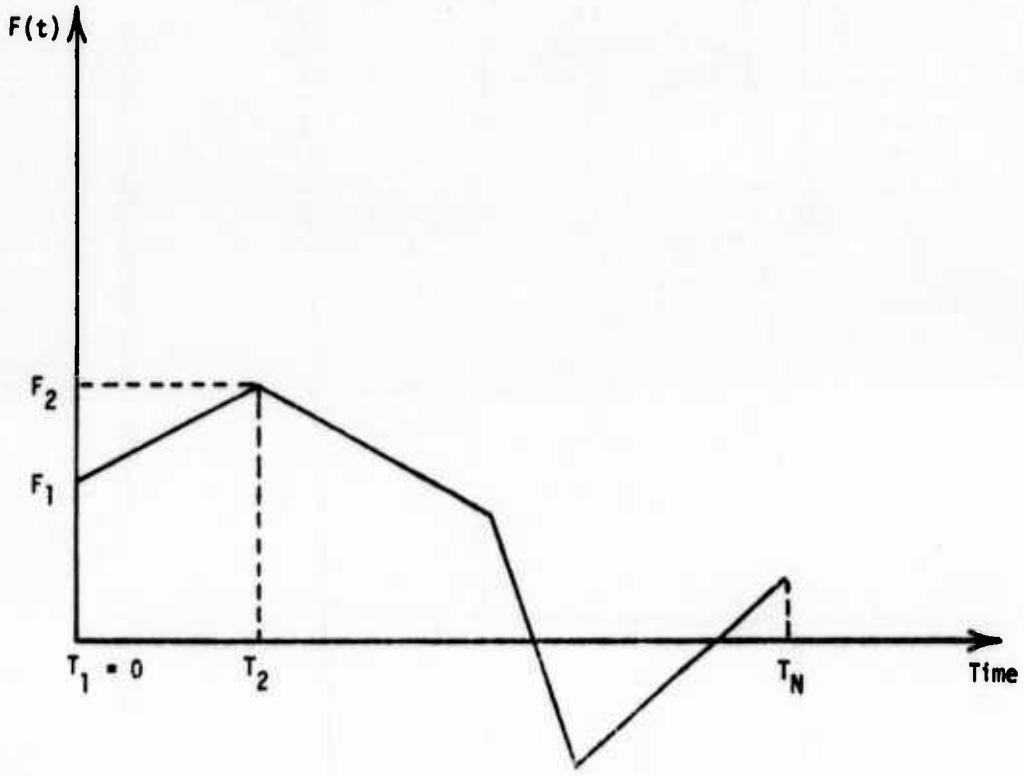

FIGURE F-2. TIME FUNCTION

INITIAL SOLUTION TIME INCREMENT

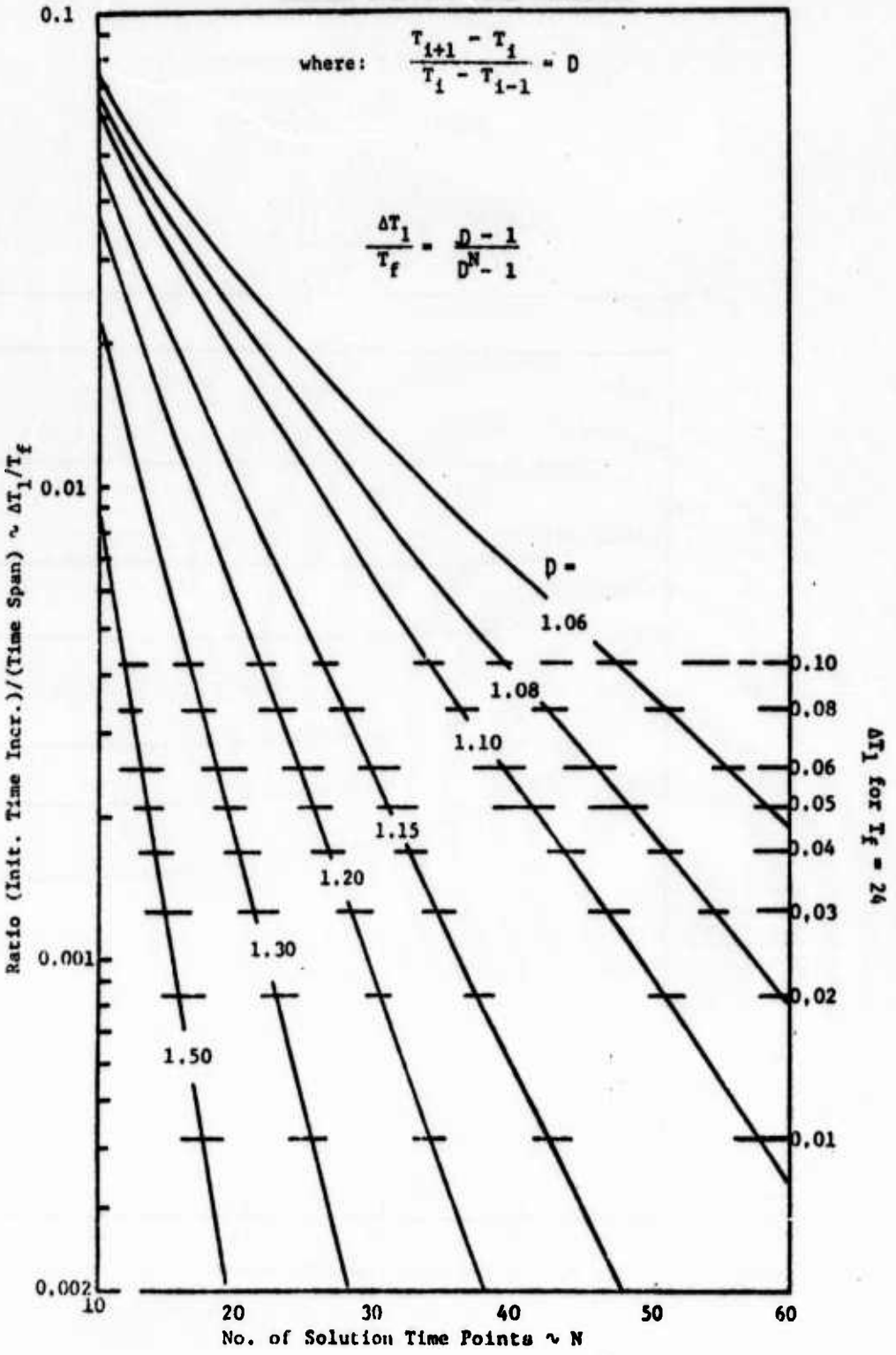

FINAL SOLUTION TIME INCREMENT

where: $\dfrac{T_{i+1} - T_i}{T_i - T_{i-1}} = D$

$$\frac{\Delta T_N}{T_f} = \frac{D^{N-1}(D-1)}{D^N - 1}$$

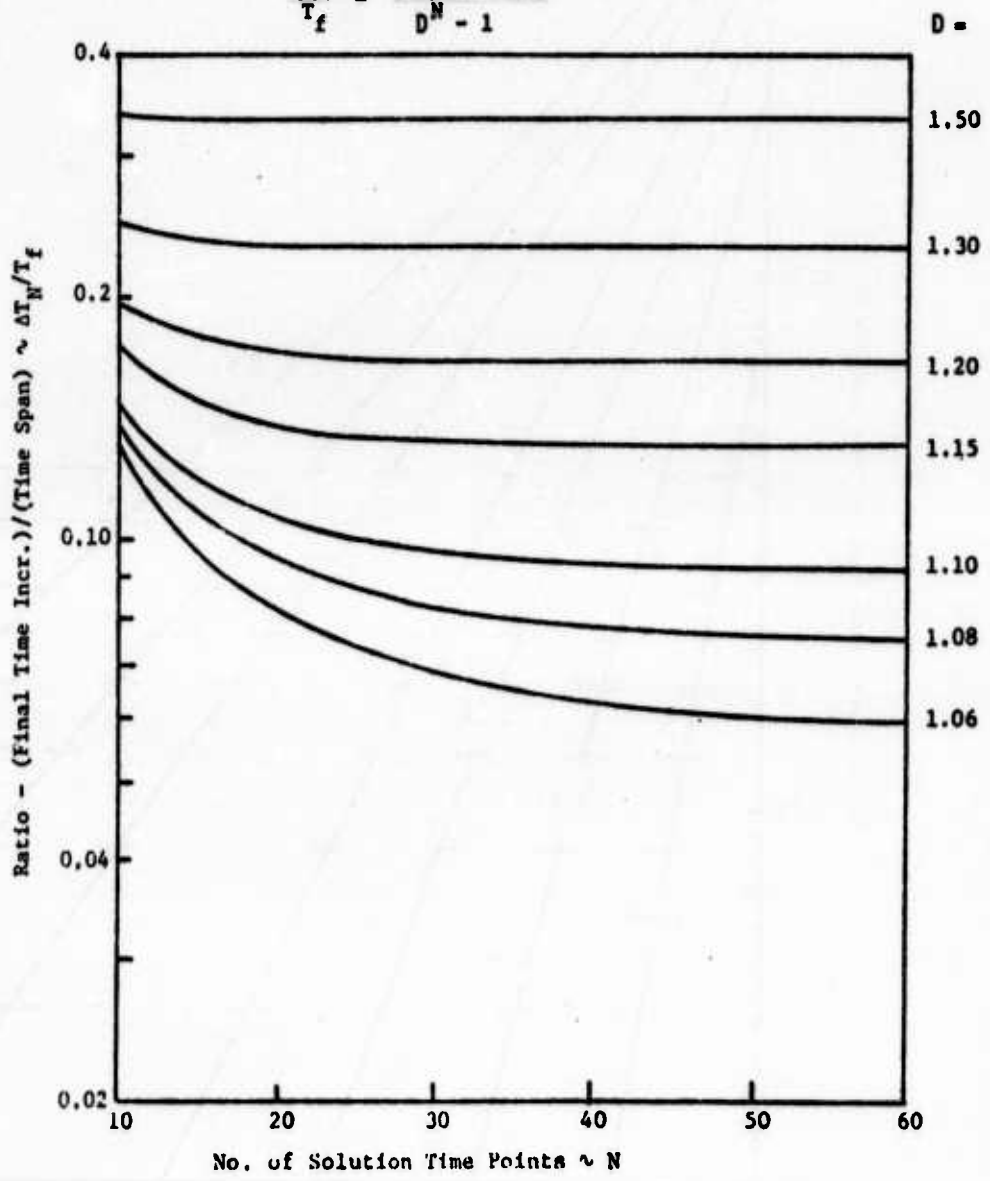

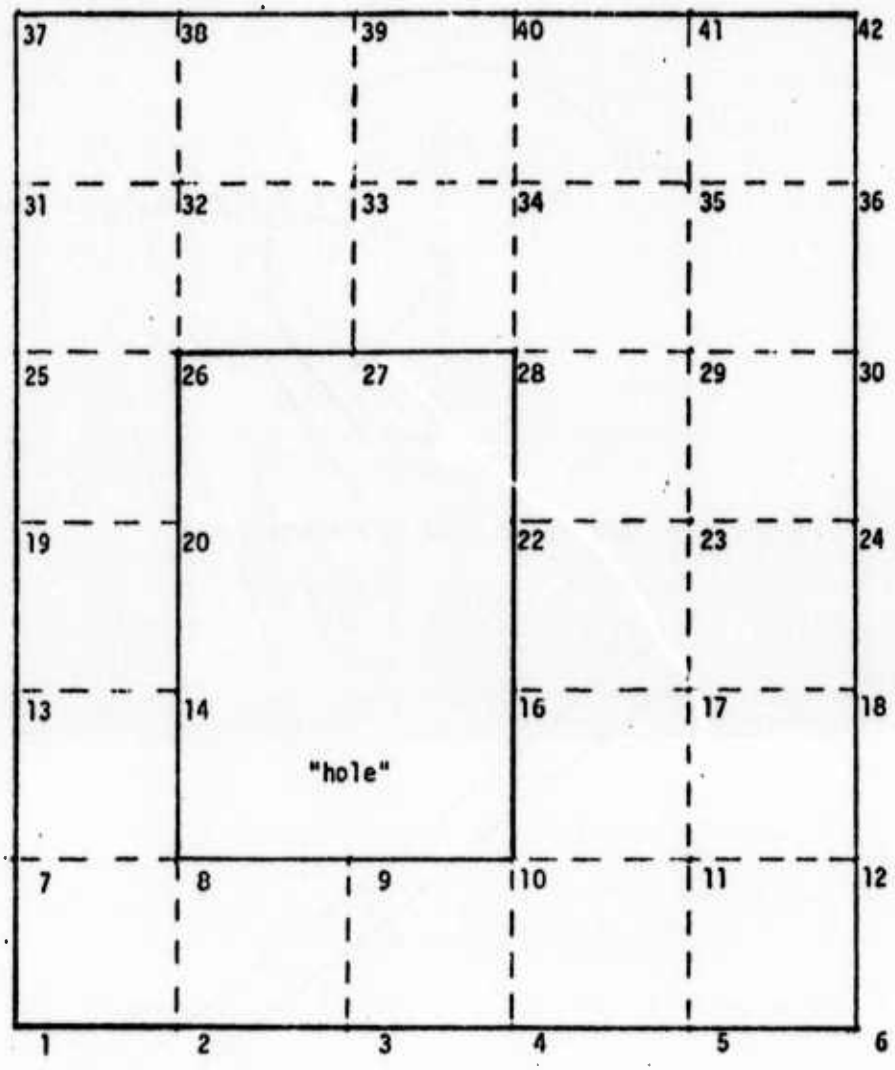

FIGURE F-5. EXAMPLE OF GRID WITH MISSING NODE NUMBERS

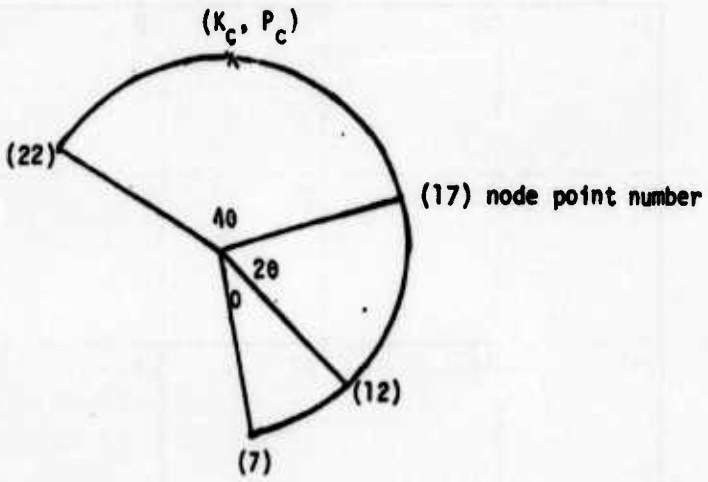

FIGURE F-6a. NODE POINTS LYING ON A CIRCULAR ARC

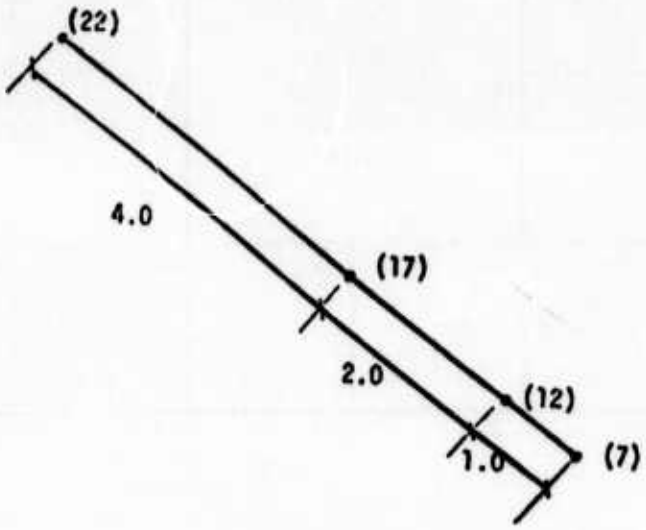

FIGURE F-6b. NODE POINTS LYING ON STRAIGHT LINE

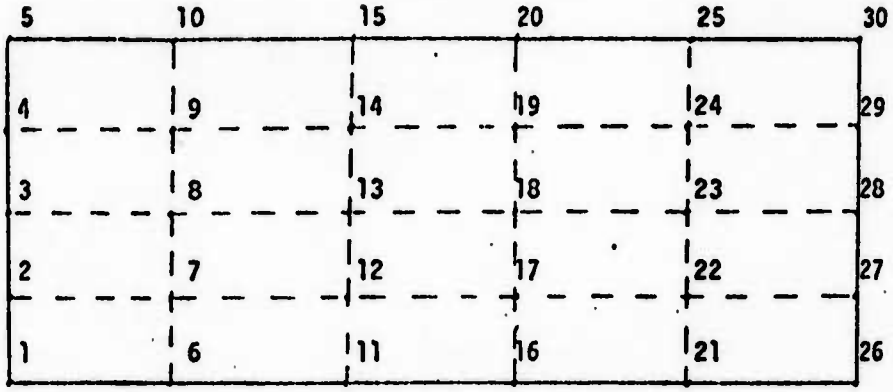

Grid 1

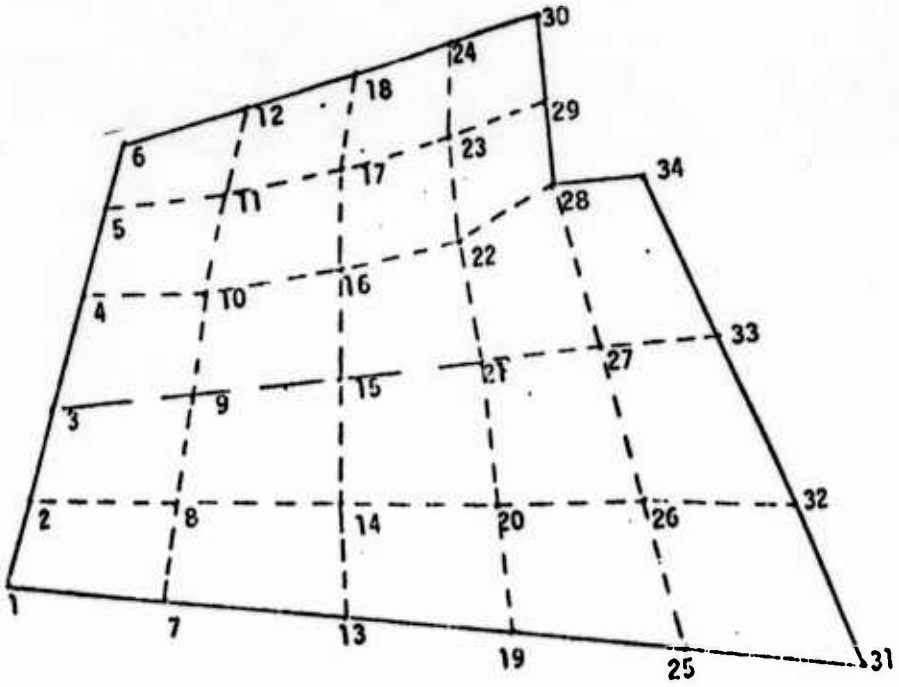

Grid 2

FIGURE F-7. GRIDS PREPARED WITH THE AID OF THE GENERATION OPTIONS

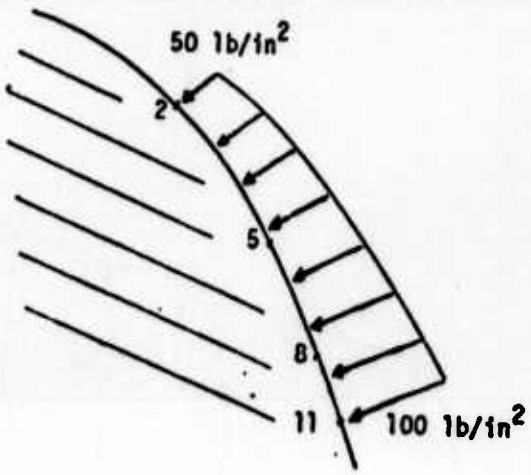

FIGURE F-8. PRESSURIZED BOUNDARY

TABLE F 1
INPUT FOR EXAMPLE 1 OF THE FINITE ELEMENT COMPUTER CODE

```
ELASTIC  PLATE  WITH  HOLE - PLANE  STRESS
[1]
  4    1
  1    1 11538462. 25000000.
[2]
  1        0.0        0.0
  6        0.5        0.0    1        1.0
  7        0.8        0.1
 49        0.8        0.8    6        1.0
 12        0.5        0.1
 48        0.5        0.8    6        1.0
 66        0.5       0.95
 84        0.5        1.1    6        1.0
 88       0.25        1.1
 83        0.0        1.1    1        1.0
 55        0.0        0.9
 79        0.2        1.1    6        1.0      0.12      0.24
[5]
  1    2    8    7    1    4    1   12    6
[7]
  1    1              1      0.001              6    1
 79    0              1                        84    1
  7    1              0                        55    6
[9]
```

[ ] - The block enclosing the number was added to indicate the applicable input block.
The actual card merely contains the number punched in Column 1.

TABLE F-2

OUTPUT FOR EXAMPLE 1 OF THE FINITE ELEMENT COMPUTER CODE

```
          ELASTIC  PLATE  WITH  HOLE - PLANE  STRESS

     GENERALIZED PLANE STRESS ANALYSIS-X=R Y=Z
       AXIAL STRESS= 0.

  REF. TEMP.= 0.                    0   0   0.          0.          0.          0.
PROPERTIES FOR MAT    1
EQIV. SHEAR MODULUS=     1.15385E+07
BULK MODULUS=     2.50000E+07
COEFF. OF EXPANSION=     0.
R BODY FORCE=     0.
Z BODY FORCE=     0.
TEMPERATURE INDEPENDENT MATERIAL
```

TABLE F-2 (Continued)

*****GEOMETRY*****

NODAL POINT	R-Z COORDINATES	
1	0.	0.
2	1.00E-01	0.
3	2.00E-01	0.
4	3.00E-01	0.
5	4.00E-01	0.
6	5.00E-01	0.
7	0.	1.00E-01
8	1.00E-01	9.98E-02
9	2.00E-01	9.97E-02
10	3.00E-01	9.97E-02
11	4.00E-01	9.98E-02
12	5.00E-01	1.00E-01
13	0.	2.00E-01
14	1.00E-01	2.00E-01
15	2.00E-01	1.99E-01
16	3.00E-01	1.99E-01
17	4.00E-01	2.00E-01
18	5.00E-01	2.00E-01
19	0.	3.00E-01
20	1.00E-01	2.99E-01
21	2.01E-01	2.99E-01
22	3.01E-01	2.99E-01
23	4.00E-01	2.99E-01
24	5.00E-01	3.00E-01
25	0.	4.00E-01
26	1.01E-01	3.98E-01
27	2.01E-01	3.98E-01
28	3.01E-01	3.98E-01
29	4.01E-01	3.99E-01
30	5.00E-01	4.00E-01
31	0.	5.00E-01
32	1.01E-01	4.97E-01
33	2.02E-01	4.96E-01
34	3.02E-01	4.96E-01
35	4.01E-01	4.97E-01
36	5.00E-01	5.00E-01
37	0.	6.00E-01
38	1.03E-01	5.95E-01
39	2.04E-01	5.92E-01
40	3.04E-01	5.92E-01
41	4.02E-01	5.95E-01
42	5.00E-01	6.00E-01
43	0.	7.00E-01
44	1.05E-01	6.90E-01
45	2.08E-01	6.85E-01
46	3.07E-01	6.85E-01
47	4.04E-01	6.91E-01
48	5.00E-01	7.00E-01
49	0.	8.00E-01
50	1.11E-01	7.81E-01
51	2.14E-01	7.73E-01
52	3.12E-01	7.73E-01
53	4.07E-01	7.83E-01
54	5.00E-01	8.00E-01
55	0.	9.00E-01
56	1.25E-01	8.62E-01

TABLE F-2 (Continued)

57	2.27E-01	8.51E-01
58	3.20E-01	8.53E-01
59	4.10E-01	8.67E-01
60	5.00E-01	9.00E-01
61	7.65E-02	9.15E-01
62	1.63E-01	9.16E-01
63	2.47E-01	9.16E-01
64	3.31E-01	9.21E-01
65	4.15E-01	9.32E-01
66	5.00E-01	9.50E-01
67	1.41E-01	9.59E-01
68	2.01E-01	9.71E-01
69	2.69E-01	9.77E-01
70	3.42E-01	9.82E-01
71	4.18E-01	9.90E-01
72	5.00E-01	1.00E+00
73	1.85E-01	1.02E+00
74	2.31E-01	1.03E+00
75	2.87E-01	1.04E+00
76	3.49E-01	1.04E+00
77	4.17E-01	1.05E+00
78	5.00E-01	1.05E+00
79	2.00E-01	1.10E+00
80	2.50E-01	1.10E+00
81	3.00E-01	1.10E+00
82	3.50E-01	1.10E+00
83	4.00E-01	1.10E+00
84	5.00E-01	1.10E+00

TABLE F-2 (Continued)

ELEMENT INFORMATION

	NODE POINTS				MAT.
1	1	2	8	7	1
2	7	8	14	13	1
3	13	14	20	19	1
4	19	20	26	25	1
5	25	26	32	31	1
6	31	32	38	37	1
7	37	38	44	43	1
8	43	44	50	49	1
9	49	50	56	55	1
10	55	56	62	61	1
11	61	62	68	67	1
12	67	68	74	73	1
13	73	74	80	79	1
14	2	3	9	8	1
15	8	9	15	14	1
16	14	15	21	20	1
17	20	21	27	26	1
18	26	27	33	32	1
19	32	33	39	38	1
20	38	39	45	44	1
21	44	45	51	50	1
22	50	51	57	56	1
23	56	57	63	62	1
24	62	63	69	68	1
25	68	69	75	74	1
26	74	75	81	80	1
27	3	4	10	9	1
28	9	10	16	15	1
29	15	16	22	21	1
30	21	22	28	27	1
31	27	28	34	33	1
32	33	34	40	39	1
33	39	40	46	45	1
34	45	46	52	51	1
35	51	52	58	57	1
36	57	58	64	63	1
37	63	64	70	69	1
38	69	70	76	75	1
39	75	76	82	81	1
40	4	5	11	10	1
41	10	11	17	16	1
42	16	17	23	22	1
43	22	23	29	28	1
44	28	29	35	34	1
45	34	35	41	40	1
46	40	41	47	46	1
47	46	47	53	52	1
48	52	53	59	58	1
49	58	59	65	64	1
50	64	65	71	70	1
51	70	71	77	76	1
52	76	77	83	82	1
53	5	6	12	11	1
54	11	12	18	17	1
55	17	18	24	23	1

TABLE F-2 (Continued)

56	23	24	30	29	1
57	29	30	36	35	1
58	35	36	42	41	1
59	41	42	48	47	1
60	47	48	54	53	1
61	53	54	60	59	1
62	59	60	66	65	1
63	65	66	72	71	1
64	71	72	78	77	1
65	77	78	84	83	1

ELEMENT	AREA
1	.99946116E-02
2	.99997529E-02
3	.10006206E-01
4	.10017352E-01
5	.10039095E-01
6	.10002951E-01
7	.10175468E-01
8	.10361695E-01
9	.10080361E-01
10	.47086167E-02
11	.32292632E-02
12	.29417102E-02
13	.33589966E-02
14	.99792164E-02
15	.99757942E-02
16	.99640098E-02
17	.99393873E-02
18	.98917419E-02
19	.97994875E-02
20	.96143060E-02
21	.92178631E-02
22	.82760845E-02
23	.57229496E-02
24	.43456555E-02
25	.37146934E-02
26	.33994390E-02
27	.99717558E-02
28	.99612468E-02
29	.99360127E-02
30	.98861000E-02
31	.97911791E-02
32	.96121788E-02
33	.92747557E-02
34	.86446317E-02
35	.75221713E-02
36	.58311385E-02
37	.46831439E-02
38	.39760624E-02
39	.33631843E-02
40	.99751925E-02
41	.99616453E-02
42	.99331120E-02
43	.98780428E-02
44	.97752086E-02
45	.95851553E-02
46	.92371998E-02
47	.86062680E-02
48	.75045325E-02

TABLE F-2 (Continued)

49	.56855855E-02
50	.47155407E-02
51	.41161365E-02
52	.33551020E-02
53	.99800396E-02
54	.99767687E-02
55	.99557191E-02
56	.99166813E-02
57	.98449921E-02
58	.97158476E-02
59	.94864708E-02
60	.90849918E-02
61	.83814069E-02
62	.49612133E-02
63	.84703695E-02
64	.43664522E-02
65	.48131834E-02

TABLE F-2 (Continued)

BOUNDARY CONDITIONS

BOUNDARY NODE								
1	U-R=	0.	0	U-Z=	1.00000E-03	0	ANG=	0.
2	U-R=	0.	0	U-Z=	1.00000E-03	0	ANG=	0.
3	U-R=	0.	0	U-Z=	1.00000E-03	0	ANG=	0.
4	U-R=	0.	0	U-Z=	1.00000E-03	0	ANG=	0.
5	U-R=	0.	0	U-Z=	1.00000E-03	0	ANG=	0.
6	U-R=	0.	0	U-Z=	1.00000E-03	0	ANG=	0.
79	P-R=	0.	0	U-Z=	0.	0	ANG=	0.
80	P-R=	0.	0	U-Z=	0.	0	ANG=	0.
81	P-R=	0.	0	U-Z=	0.	0	ANG=	0.
82	P-R=	0.	0	U-Z=	0.	0	ANG=	0.
83	P-R=	0.	0	U-Z=	0.	0	ANG=	0.
84	P-R=	0.	0	U-Z=	0.	0	ANG=	0.
7	U-R=	0.	0	P-Z=	0.	0	ANG=	0.
13	U-R=	0.	0	P-Z=	0.	0	ANG=	0.
19	U-R=	0.	0	P-Z=	0.	0	ANG=	0.
25	U-R=	0.	0	P-Z=	0.	0	ANG=	0.
31	U-R=	0.	0	P-Z=	0.	0	ANG=	0.
37	U-R=	0.	0	P-Z=	0.	0	ANG=	0.
43	U-R=	0.	0	P-Z=	0.	0	ANG=	0.
49	U-R=	0.	0	P-Z=	0.	0	ANG=	0.
55	U-R=	0.	0	P-Z=	0.	0	ANG=	0.

TABLE F-2 (Continued)

TIME= 0. PREC= 0. PREF= 1.000E+00 PRAG= 1.000E+00 0

NODE	DISPLACEMENT		
1	0.	1.00000E-03	0.
2	0.	1.00000E-03	0.
3	0.	1.00000E-03	0.
4	0.	1.00000E-03	0.
5	0.	1.00000E-03	0.
6	0.	1.00000E-03	0.
7	0.	9.35398E-04	0.
8	3.04193E-06	9.34795E-04	0.
9	8.57653E-06	9.32940E-04	0.
10	1.60916E-05	9.29692E-04	0.
11	2.81459E-05	9.26247E-04	0.
12	5.32025E-05	9.04821E-04	0.
13	0.	8.69164E-04	0.
14	7.10292E-06	8.67640E-04	0.
15	1.64672E-05	8.62623E-04	0.
16	2.99593E-05	8.55112E-04	0.
17	5.04322E-05	8.43004E-04	0.
18	7.25191E-05	8.27939E-04	0.
19	0.	8.02548E-04	0.
20	9.44201E-06	7.99773E-04	0.
21	2.14347E-05	7.90940E-04	0.
22	3.81946E-05	7.77312E-04	0.
23	5.93392E-05	7.61817E-04	0.
24	8.32429E-05	7.49969E-04	0.
25	0.	7.37459E-04	0.
26	1.02699E-05	7.33227E-04	0.
27	2.34444E-05	7.19481E-04	0.
28	4.11387E-05	6.99693E-04	0.
29	6.34819E-05	6.79374E-04	0.
30	8.84858E-05	6.66628E-04	0.
31	0.	6.76225E-04	0.
32	1.02233E-05	6.69976E-04	0.
33	2.40114E-05	6.49809E-04	0.
34	4.31188E-05	6.21870E-04	0.
35	6.69405E-05	5.93968E-04	0.
36	9.42108E-05	5.75513E-04	0.
37	0.	6.21495E-04	0.
38	1.01900E-05	6.11857E-04	0.
39	2.59101E-05	5.81823E-04	0.
40	4.84398E-05	5.42721E-04	0.
41	7.58084E-05	5.04569E-04	0.
42	1.06050E-04	4.75132E-04	0.
43	0.	5.76836E-04	0.
44	1.16842E-05	5.60407E-04	0.
45	3.22865E-05	5.13220E-04	0.
46	6.31552E-05	4.59731E-04	0.
47	9.63615E-05	4.11354E-04	0.
48	1.30715E-04	3.66450E-04	0.
49	0.	5.50082E-04	0.
50	1.69148E-05	5.14484E-04	0.
51	5.15980E-05	4.36871E-04	0.
52	9.24018E-05	3.72058E-04	0.
53	1.32820E-04	3.16562E-04	0.
54	1.72755E-04	2.55130E-04	0.
55	0.	5.58814E-04	0.
56	5.07598E-05	4.53819E-04	0.

TABLE F-2 (Continued)

57	8.96732E-05	3.51130E-04	0.
58	1.36266E-04	2.82479E-04	0.
59	1.80863E-04	2.26966E-04	0.
60	2.28837E-04	1.51608E-04	0.
61	7.62536E-05	4.89215E-04	0.
62	1.03447E-04	3.64711E-04	0.
63	1.43529E-04	2.58385E-04	0.
64	1.85981E-04	2.00543E-04	0.
65	2.23102E-04	1.58634E-04	0.
66	2.57704E-04	1.06903E-04	0.
67	1.51967E-04	3.76324E-04	0.
68	1.70928E-04	2.47109E-04	0.
69	2.02758E-04	1.64821E-04	0.
70	2.31508E-04	1.27644E-04	0.
71	2.57350E-04	1.01114E-04	0.
72	2.81939E-04	8.70452E-05	0.
73	2.12349E-04	2.10642E-04	0.
74	2.31739E-04	1.16719E-04	0.
75	2.49688E-04	7.90136E-05	0.
76	2.63460E-04	6.16597E-05	0.
77	2.79427E-04	5.01007E-05	0.
78	2.98776E-04	3.16973E-05	0.
79	2.33726E-04	0.	0.
80	2.61207E-04	0.	0.
81	2.69030E-04	0.	0.
82	2.75931E-04	0.	0.
83	2.84192E-04	0.	0.
84	3.04005E-04	0.	0.

ELEMENT STRESSES AND STRAINS

	SIGX	SIGZ	SIGY	SIGXY	EPX	EPZ	EPY	EPXY	DAMAGE
1	-5.8240E+03	0.	-2.1235E+04	1.6889E+02	1.8219E-05	2.7059E-04	-6.4960E-04	1.4637E-05	0.
2	-4.8230E+03	0.	-2.1478E+04	5.8188E+01	5.4013E-05	2.6301E-04	-6.6770E-04	5.0430E-06	0.
3	-3.9312E+03	0.	-2.1392E+04	-1.6350E+02	8.2879E-05	2.5323E-04	-6.7375E-04	-1.4170E-05	0.
4	-3.2977E+03	0.	-2.0802E+04	-4.4393E+02	9.8092E-05	2.4099E-04	-6.6041E-04	-3.8474E-05	0.
5	-2.8503E+03	0.	-1.9642E+04	-7.5879E+02	1.0141E-04	2.2492E-04	-6.2622E-04	-6.5761E-05	0.
6	-2.3443E+03	0.	-1.7815E+04	-1.1650E+03	1.0001E-04	2.0160E-04	-5.7040E-04	-1.0096E-04	0.
7	-1.3606E+03	0.	-1.5094E+04	-1.7789E+03	1.0559E-04	1.6455E-04	-4.8953E-04	-1.5417E-04	0.
8	7.7841E+02	0.	-1.0917E+04	-3.0673E+03	1.3512E-04	1.0139E-04	-3.7169E-04	-2.6584E-04	0.
9	8.3781E+03	0.	-4.5979E+03	-5.6499E+03	3.2525E-04	-3.7802E-05	-2.3704E-04	-4.8966E-04	0.
10	1.3929E+04	0.	-7.5236E+03	-2.1003E+03	5.3955E-04	-6.4058E-05	-3.9008E-04	-1.8203E-04	0.
11	1.0163E+03	0.	-1.6709E+04	-5.1354E+03	2.0097E-04	1.5693E-04	-5.6713E-04	-4.4507E-04	0.
12	-6.5087E+03	0.	-4.0095E+04	-1.1481E+04	1.8399E-04	4.6604E-04	-1.2714E-03	-9.9502E-04	0.
13	-5.4378E+03	0.	-6.4581E+04	-6.0432E+03	4.6455E-04	7.0018E-04	-2.0983E-03	-5.2375E-04	0.
14	-5.7412E+03	0.	-2.1607E+04	5.9518E+01	2.4701E-05	2.7348E-04	-6.6283E-04	5.1582E-05	0.
15	-4.4698E+03	0.	-2.2024E+04	2.4843E+02	7.1248E-05	2.6494E-04	-6.8944E-04	2.1531E-05	0.
16	-3.4255E+03	0.	-2.2064E+04	-4.1115E+02	1.0646E-04	2.5490E-04	-7.0121E-04	-3.5633E-05	0.
17	-2.7429E+03	0.	-2.1698E+04	-1.1964E+03	1.2555E-04	2.4441E-04	-6.9584E-04	-1.0369E-04	0.
18	-2.2494E+03	0.	-2.0904E+04	-2.0281E+03	1.3406E-04	2.3154E-04	-6.7431E-04	-1.7577E-04	0.
19	-1.5701E+03	0.	-1.9852E+04	-2.9558E+03	1.4618E-04	2.1422E-04	-6.4603E-04	-2.5617E-04	0.
20	-2.3128E+02	0.	-1.8757E+04	-4.2557E+03	1.7988E-04	1.8988E-04	-6.2293E-04	-3.6883E-04	0.
21	2.8194E+03	0.	-1.8314E+04	-6.1473E+03	2.7712E-04	1.5494E-04	-6.3864E-04	-5.3276E-04	0.
22	5.5348E+03	0.	-2.1207E+04	-8.5480E+03	3.9656E-04	1.5672E-04	-7.6226E-04	-5.6747E-04	0.
23	5.8621E+03	0.	-2.6767E+04	-5.8784E+03	4.6307E-04	2.0904E-04	-9.5084E-04	-5.0946E-04	0.
24	2.4703E+03	0.	-3.5433E+04	-3.6693E+03	4.3667E-04	3.2962E-04	-1.2058E-03	-3.1801E-04	0.

TABLE F-2 (Continued)

25	-3.0866E+03	0.	-4.3928E+04	-1.0944E+03	3.3636E-04	4.7011E-04	-1.4333E-03	-9.4847E-05	0.
26	-6.8115E+03	0.	-4.5394E+04	3.7767E+02	2.2689E-04	5.2206E-04	-1.4450E-03	3.2731E-05	0.
27	-5.5732E+03	0.	-2.2335E+04	1.2394E+03	3.7575E-05	2.7908E-04	-6.8876E-04	1.0741E-04	0.
28	-3.7294E+03	0.	-2.2935E+04	6.3753E+02	1.0504E-04	2.6664E-04	-7.2721E-04	5.5253E-05	0.
29	-2.4491E+03	0.	-2.3291E+04	-4.5790E+02	1.5127E-04	2.5740E-04	-7.5187E-04	-3.9685E-05	0.
30	-1.7661E+03	0.	-2.3118E+04	-1.6493E+03	1.7231E-04	2.4884E-04	-7.5292E-04	-1.4294E-04	0.
31	-1.3509E+03	0.	-2.2915E+04	-2.6248E+03	1.8412E-04	2.4266E-04	-7.5033E-04	-2.2748E-04	0.
32	-6.1690E+02	0.	-2.2912E+04	-3.4826E+03	2.0856E-04	2.3529E-04	-7.5758E-04	-3.0182E-04	0.
33	9.7252E+02	0.	-2.3590E+04	-4.1612E+03	2.6832E-04	2.2618E-04	-7.9607E-04	-3.6063E-04	0.
34	3.1408E+03	0.	-2.5834E+04	-3.9818E+03	3.6303E-04	2.2693E-04	-8.9253E-04	-3.4509E-04	0.
35	4.7730E+03	0.	-2.9205E+04	-2.5847E+03	4.5115E-04	2.4432E-04	-1.0212E-03	-2.2401E-04	0.
36	4.3622E+03	0.	-3.3274E+04	-8.1158E+01	4.7815E-04	2.8912E-04	-1.1528E-03	-7.0337E-06	0.
37	1.3685E+03	0.	-3.6229E+04	2.5201E+03	4.0791E-04	3.4861E-04	-1.2213E-03	2.1841E-04	0.
38	-2.6984E+03	0.	-3.6699E+04	3.1434E+03	2.7704E-04	3.9397E-04	-1.1963E-03	2.7243E-04	0.
39	-5.5333E+03	0.	-3.6183E+04	1.4315E+03	1.7739E-04	4.1716E-04	-1.1508E-03	1.2407E-04	0.
40	-5.1565E+03	0.	-2.3205E+04	2.3631E+03	6.0165E-05	2.8361E-04	-7.2193E-04	2.0480E-04	0.
41	-2.4732E+03	0.	-2.4487E+04	1.2086E+03	1.6242E-04	2.6960E-04	-7.9149E-04	1.0475E-04	0.
42	-1.0390E+03	0.	-2.4273E+04	-5.7167E+02	2.0809E-04	2.5312E-04	-7.9871E-04	-4.9545E-05	0.
43	-8.0355E+02	0.	-2.4447E+04	-1.6068E+03	2.1768E-04	2.5250E-04	-8.0686E-04	-1.3925E-04	0.
44	-5.4817E+02	0.	-2.4998E+04	-2.3717E+03	2.3171E-04	2.5547E-04	-8.2780E-04	-2.0555E-04	0.
45	-6.4805E+01	0.	-2.5949E+04	-2.8124E+03	2.5733E-04	2.6013E-04	-8.6430E-04	-2.4374E-04	0.
46	8.3915E+02	0.	-2.7396E+04	-2.5754E+03	3.0193E-04	2.6557E-04	-9.2159E-04	-2.2320E-04	0.
47	1.9544E+03	0.	-2.9188E+04	-1.3372E+03	3.5702E-04	2.7233E-04	-9.9247E-04	-1.1559E-04	0.
48	2.4647E+03	0.	-3.1060E+04	7.5508E+02	3.9275E-04	2.8595E-04	-1.0600E-03	6.5440E-05	0.
49	1.6924E+03	0.	-3.2014E+04	2.8214E+03	3.7655E-04	3.0321E-04	-1.0841E-03	2.4452E-04	0.
50	9.2256E+01	0.	-3.1664E+04	3.7591E+03	3.1971E-04	3.1572E-04	-1.0564E-03	3.2578E-04	0.
51	-1.6798E+03	0.	-3.0084E+04	3.1960E+03	2.5285E-04	3.2564E-04	-1.0127E-03	2.7698E-04	0.
52	-3.2607E+03	0.	-3.0827E+04	1.3317E+03	1.9958E-04	3.4087E-04	-9.9495E-04	1.1541E-04	0.
53	-4.2408E+03	0.	-2.6633E+04	3.4687E+03	1.2497E-04	3.0874E-04	-8.4536E-04	3.0062E-04	0.
54	-1.6717E+02	0.	-2.4095E+04	3.2110E+02	2.3538E-04	2.4262E-04	-8.0149E-04	2.7829E-05	0.
55	-3.0467E+02	0.	-2.4008E+04	-3.6812E+02	2.2993E-04	2.4313E-04	-7.9723E-04	-3.1904E-05	0.
56	-1.3435E+02	0.	-2.4988E+04	-7.7876E+02	2.4541E-04	2.5123E-04	-8.3160E-04	-6.7492E-05	0.
57	-1.0733E+02	0.	-2.6662E+04	-1.0727E+03	2.6304E-04	2.6769E-04	-8.8766E-04	-9.2964E-05	0.
58	2.5768E+01	0.	-2.8760E+04	-1.1835E+03	2.8846E-04	2.8734E-04	-9.5893E-04	-1.0257E-04	0.
59	2.5341E+02	0.	-3.0783E+04	-9.1619E+02	3.1628E-04	3.0529E-04	-1.0286E-03	-7.9403E-05	0.
60	4.9789E+02	0.	-3.1880E+04	-8.8746E+01	3.3540E-04	3.1382E-04	-1.0676E-03	-7.6913E-06	0.
61	4.9471E+02	0.	-3.1023E+04	1.1174E+03	3.2672E-04	3.0528E-04	-1.0390E-03	9.6838E-05	0.
62	1.6600E+02	0.	-2.8910E+04	1.8716E+03	2.9463E-04	2.8744E-04	-9.6532E-04	1.6221E-04	0.
63	-7.8348E+01	0.	-2.6734E+04	1.9436E+03	2.6472E-04	2.6812E-04	-8.9034E-04	1.6845E-04	0.
64	-4.4736E+02	0.	-2.4816E+04	1.4777E+03	2.3325E-04	2.5264E-04	-8.2274E-04	1.2807E-04	0.
65	-9.1388E+02	0.	-2.4099E+04	5.6850E+02	2.1053E-04	2.5013E-04	-7.9416E-04	4.9270E-05	0.

THE VOLUME CHANGE IS -.17453434E-03

TABLE F-3

INPUT FOR EXAMPLE 2 OF THE FINITE ELEMENT COMPUTER CODE

```
AEROJET PROPELLANT 5 ELEMENT AXISYMMETRIC CHECK CASE
[1]
    1    3     110.0
    1    3     99.25    600000.0    0.00006                                    0    5
   0.2955       -40.0     5.0789       0.0    1.97796       40.0        0.0       77.0
  -5.63827      140.0
  -1.8285    -0.92495        40.0       -1.0    7.1938     113.04       200.0      -1.0
                             200.0       -1.0
                                          77.0       1.0        1.0        1.0        1.0
      1.0          1.0-0.0604433 0.0883460
    200.0     42.430          1.0        1.0
[2]
    1    2
                               0.135      0.135
[3]
    1      0.025
    2      0.055
    3      0.075
    4      0.100
    5      0.125
[4]
    1        1.0        0.0
    6        2.0        0.0     1        1.0
    7        1.0        1.0
   12        2.0        1.0     1        1.0
[5]
    1    2    0    7    1    4    1
[7]
    2                                                          6    1
    0                                                         10    1
    1    1 1          1.0     1
    7    1 1          1.0
[9]
```

F-54

[ ] - The block enclosing the number was added to indicate the applicable input block. The actual card merely contains the number punched in Column 1.

TABLE F-4

OUTPUT FOR EXAMPLE 2 OF THE FINITE ELEMENT COMPUTER CODE

```
          AEROJET PROPELLANT  5 ELEMENT AXISYMMETRIC CHECK CASE


       AXISYMMETRIC ANALYSIS


  REF. TEMP.= 1.10E+02              0    0   1.000E+00   1.000E+01   1.000E-02   5.000E-02

  PROPERTIES FOR MAT    1
  EQIB. SHEAR MODULUS=    9.92500E+01
  BULK MODULUS=    6.00000E+05
  COEFF. OF EXPANSION=    6.00000E-05
  R BODY FORCE=    0.
  Z BODY FORCE=    0.

  TABULATION OF TIME-TEMPERATURE SHIFT FUNCTIONS

      POINT     TEMPERATURE     SHIFT FACTOR

        1         -40.000      .82955E+01
        2           0.000      .50789E+01
        3          40.000      .19780E+01
        4          77.000      0.
        5         140.000      -.56383E+01

  NONLINEAR VISCOELASTIC PROPERTIES
    -1.829E+00  -9.250E-01   8.000E+01  -1.000E+00   7.194E+00   1.130E+02   2.000E+02  -1.000E+00   0.
     0.          2.000E+02  -1.000E+00   0.          0.          0.          0.          0.          0.
     0.          7.700E+01   1.000E+00   1.000E+00   1.000E+00   1.000E+00   1.000E+00   1.000E+00  -6.044E-02
     8.835E-02   0.          0.          0.          0.          2.000E+02   4.243E+01   1.000E+00   1.000E+00

  FUNCTION  1                VALUE          TIME
                               0.            0.
                             1.350E-01     1.350E-01

      TIME STEP INFORMATION

       STEP          TIME          SPACING RATIO

         1         .25000E-01          0.
         2         .55000E-01          0.
         3         .75000E-01          0.
         4         .10000E+00          0.
         5         .12500E+00          0.
```

TABLE F-4 (Continued)

*****GEOMETRY*****

NODAL POINT	R-Z COORDINATES	
1	1.00E+00	0.
2	1.20E+00	0.
3	1.40E+00	0.
4	1.60E+00	0.
5	1.80E+00	0.
6	2.00E+00	0.
7	1.00E+00	1.00E+00
8	1.20E+00	1.00E+00
9	1.40E+00	1.00E+00
10	1.60E+00	1.00E+00
11	1.80E+00	1.00E+00
12	2.00E+00	1.00E+00

TABLE F-4 (Continued)

ELEMENT INFORMATION

	NODE POINTS				MAT.
1	1	2	8	7	1
2	2	3	9	8	1
3	3	4	10	9	1
4	4	5	11	10	1
5	5	6	12	11	1

ELEMENT	AREA
1	.20000000E+00
2	.20000000E+00
3	.20000000E+00
4	.20000000E+00
5	.20000000E+00

TABLE F-4 (Continued)

BOUNDARY CONDITIONS

BOUNDARY NODE								
2	P-R=	0.	0	P-Z=	0.	0	ANG=	0.
3	P-R=	0.	0	P-Z=	0.	0	ANG=	0.
4	P-R=	0.	0	P-Z=	0.	0	ANG=	0.
5	P-R=	0.	0	P-Z=	0.	0	ANG=	0.
6	P-R=	0.	0	P-Z=	0.	0	ANG=	0.
8	P-R=	0.	0	P-Z=	0.	0	ANG=	0.
9	P-R=	0.	0	P-Z=	0.	0	ANG=	0.
10	P-R=	0.	0	P-Z=	0.	0	ANG=	0.
1	U-R=	1.000000E+00	1	U-Z=	0.	0	ANG=	0.
7	U-R=	1.000000E+00	1	P-Z=	0.	0	ANG=	0.

TABLE F-4 (Continued)

TIME= 2.50000E-02 PRBC= 0. PRBF= 1.000E+00 PRAG= 1.000E+00 13

NODE	DISPLACEMENT		
1	2.50000E-02	3.10822E-03	1.10000E+02
2	2.17003E-02	3.24543E-03	1.10000E+02
3	1.94636E-02	3.26266E-03	1.10000E+02
4	1.78748E-02	3.17898E-03	1.10000E+02
5	1.66866E-02	3.02953E-03	1.10000E+02
6	1.57860E-02	3.01744E-03	1.10000E+02
7	2.50000E-02	-1.10659E-03	1.10000E+02
8	2.17003E-02	-1.18380E-03	1.10000E+02
9	1.94636E-02	-1.20103E-03	1.10000E+02
10	1.78748E-02	-1.11735E-03	1.10000E+02
11	1.66866E-02	-9.67901E-04	1.10000E+02
12	1.57860E-02	-9.55814E-04	1.10000E+02

ELEMENT STRESSES AND STRAINS

	SIGR	SIGTH	SIGZ	SIGRZ	EPR	EPTH	EPZ	EPRZ	DAMAGE
1	-8.2488E+00	1.7463E+01	3.0738E-02	3.8686E-11	-1.6499E-02	2.1227E-02	-4.3520E-03	1.1369E-13	0.
2	-4.5701E+00	1.3985E+01	5.7948E-02	1.9165E-11	-1.1183E-02	1.5832E-02	-4.4465E-03	2.2737E-13	0.
3	-2.2435E+00	1.1829E+01	2.1688E-01	5.0754E-11	-7.9444E-03	1.2446E-02	-4.3800E-03	1.7053E-13	0.
4	-9.4843E-01	5.6006E+00	-1.9665E-01	7.2631E-11	-5.9409E-03	1.0165E-02	-4.1469E-03	3.4106E-13	0.
5	-2.7077E-01	5.2065E+00	-5.3820E-02	7.2404E-11	-4.5031E-03	8.5454E-03	-3.9853E-03	3.4106E-13	0.

THE VOLUME CHANGE IS .50354533E-05

TABLE F-4 (Continued)

TIME= 5.50000E-02 PRHC= 0. PRHF= 0. PRAQ= 0. 17

NODE	DISPLACEMENT		
1	5.50000E-02	6.74936E-03	1.10000E+02
2	4.75390E-02	6.99422E-03	1.10000E+02
3	4.23980E-02	7.17731E-03	1.10000E+02
4	3.87467E-02	7.29207E-03	1.10000E+02
5	3.60881E-02	7.39410E-03	1.10000E+02
6	3.41236E-02	7.33863E-03	1.10000E+02
7	5.50000E-02	-4.98605E-04	1.10000E+02
8	4.75390E-02	-7.43469E-04	1.10000E+02
9	4.23980E-02	-9.26597E-04	1.10000E+02
10	3.87467E-02	-1.04131E-03	1.10000E+02
11	3.60881E-02	-1.05335E-03	1.10000E+02
12	3.41236E-02	-1.06807E-03	1.10000E+02

ELEMENT STRESSES AND STRAINS

	SIGR	SIGTH	SIGZ	SIGRZ	EPR	EPTH	EPZ	EPRZ	DAMAGE
1	-1.7905E+01	3.2117E+01	-1.3270E-01	6.0419E-13	-3.7305E-02	4.6609E-02	-7.4928E-03	0.	0.
2	-1.0712E+01	2.5845E+01	7.1120E-02	9.6338E-11	-2.5705E-02	3.4591E-02	-7.9208E-03	5.1159E-13	0.
3	-6.1294E+00	2.1609E+01	1.6824E-02	9.6190E-11	-1.8256E-02	2.7048E-02	-8.2186E-03	3.4106E-13	0.
4	-3.0456E+00	1.8701E+01	2.0767E-03	-3.3595E-11	-1.3293E-02	2.2010E-02	-8.3454E-03	-1.1369E-13	0.
5	-8.6726E-01	1.6638E+01	1.7585E-02	1.4164E-10	-9.8226E-03	1.8477E-02	-8.3922E-03	4.5475E-13	0.

THE VOLUME CHANGE IS .52541345E-03

TABLE F-4 (Continued)

TIME= 7.50000E-02 PRBC= 0. PRBF= 0. PRAG= 0. 7

NODE	DISPLACEMENT		
1	7.50000E-02	8.78652E-03	1.10000E+02
2	6.49019E-02	9.17737E-03	1.10000E+02
3	5.79111E-02	9.51378E-03	1.10000E+02
4	5.29400E-02	9.71465E-03	1.10000E+02
5	4.93204E-02	9.76964E-03	1.10000E+02
6	4.66463E-02	9.82411E-03	1.10000E+02
7	7.50000E-02	-5.95132E-04	1.10000E+02
8	6.49019E-02	-9.85980E-04	1.10000E+02
9	5.79111E-02	-1.32239E-03	1.10000E+02
10	5.29400E-02	-1.52323E-03	1.10000E+02
11	4.93204E-02	-1.57825E-03	1.10000E+02
12	4.66463E-02	-1.63271E-03	1.10000E+02

ELEMENT STRESSES AND STRAINS

	SIGR	SIGTH	SIGZ	SIGRZ	EPR	EPTH	EPZ	EPRZ	DAMAGE
1	-2.3131E+01	4.0704E+01	-3.2505E-01	9.6991E-12	-5.0490E-02	6.3592E-02	-9.7725E-03	-4.5475E-13	0.
2	-1.3906E+01	3.3243E+01	1.2361E-01	6.3377E-11	-3.4954E-02	4.7236E-02	-1.0500E-02	-1.1369E-13	0.
3	-7.9802E+00	2.8005E+01	6.5985E-02	9.9828E-11	-2.4856E-02	3.6950E-02	-1.1037E-02	-2.2737E-13	0.
4	-3.9714E+00	2.4350E+01	2.9143E-02	-9.4779E-11	-1.8098E-02	3.0077E-02	-1.1293E-02	-5.6843E-13	0.
5	-1.1315E+00	2.1723E+01	3.3004E-02	8.7905E-11	-1.3370E-02	2.5254E-02	-1.1402E-02	1.1369E-13	0.

THE VOLUME CHANGE IS .12720500E-02

TABLE F-4 (Continued)

TIME= 1.00000E-01 PRBC= 0. PRBF= 0. PRAG= 0. 10

NODE	DISPLACEMENT		
1	1.00000E-01	1.18990E-02	1.10000E+02
2	8.66671E-02	1.25081E-02	1.10000E+02
3	7.73832E-02	1.30890E-02	1.10000E+02
4	7.07708E-02	1.34302E-02	1.10000E+02
5	6.59547E-02	1.35552E-02	1.10000E+02
6	6.23956E-02	1.36396E-02	1.10000E+02
7	1.00000E-01	1.65119E-04	1.10000E+02
8	8.66671E-02	-4.43991E-04	1.10000E+02
9	7.73832E-02	-1.02572E-03	1.10000E+02
10	7.07708E-02	-1.36608E-03	1.10000E+02
11	6.59547E-02	-1.49112E-03	1.10000E+02
12	6.23956E-02	-1.57549E-03	1.10000E+02

ELEMENT STRESSES AND STRAINS

	SIGR	SIGTH	SIGZ	SIGRZ	EPR	EPTH	EPZ	EPRZ	DAMAGE
1	-2.9194E+01	5.0455E+01	-6.3700E-01	-3.2021E-11	-6.6665E-02	8.4849E-02	-1.2343E-02	-1.1369E-13	0.
2	-1.7641E+01	4.1779E+01	2.0227E-01	6.1550E-11	-4.6419E-02	6.3096E-02	-1.3534E-02	0.	0.
3	-1.0154E+01	3.5471E+01	1.4313E-01	1.3118E-10	-3.3062E-02	4.9385E-02	-1.4456E-02	1.1369E-13	0.
4	-5.0614E+00	3.0980E+01	7.3059E-02	-1.9292E-10	-2.4081E-02	4.0213E-02	-1.4921E-02	-3.4106E-13	0.
5	-1.4430E+00	2.7720E+01	6.4049E-02	8.6086E-11	-1.7798E-02	3.3776E-02	-1.5131E-02	0.	0.

THE VOLUME CHANGE IS .25305619E-02

TABLE F-4 (Continued)

TIME= 1.25000E-01 PRBC= 0. PRBF= 0. PRAQ= 0. 5

NODE	DISPLACEMENT		
1	1.25000E-01	1.48900E-02	1.10000E+02
2	1.08494E-01	1.57579E-02	1.10000E+02
3	9.69360E-02	1.66465E-02	1.10000E+02
4	8.86912E-02	1.71642E-02	1.10000E+02
5	8.26837E-02	1.73786E-02	1.10000E+02
6	7.82418E-02	1.74984E-02	1.10000E+02
7	1.25000E-01	1.16965E-03	1.10000E+02
8	1.08494E-01	3.01747E-04	1.10000E+02
9	9.69360E-02	-5.86841E-04	1.10000E+02
10	8.86912E-02	-1.10456E-03	1.10000E+02
11	8.26837E-02	-1.31893E-03	1.10000E+02
12	7.82418E-02	-1.43922E-03	1.10000E+02

ELEMENT STRESSES AND STRAINS

	SIGR	SIGTH	SIGZ	SIGRZ	EPR	EPTH	EPZ	EPRZ	DAMAGE
1	-3.4831E+01	5.9041E+01	-1.0240E+00	-4.9243E-11	-8.2530E-02	1.0613E-01	-1.4588E-02	3.9790E-13	0.
2	-2.1153E+01	4.9628E+01	2.9140E-01	1.9158E-10	-5.7790E-02	7.9012E-02	-1.6385E-02	4.5475E-13	0.
3	-1.2210E+01	4.2462E+01	2.3743E-01	7.9819E-11	-4.1224E-02	6.1876E-02	-1.7751E-02	3.4106E-13	0.
4	-6.0972E+00	3.7252E+01	1.2919E-01	-2.2562E-10	-3.0037E-02	5.0404E-02	-1.8483E-02	-1.0800E-12	0.
5	-1.7397E+00	3.3432E+01	1.0803E-01	2.9145E-12	-2.2209E-02	4.2349E-02	-1.8818E-02	2.2737E-13	0.

THE VOLUME CHANGE IS .41899664E-02

TABLE F-5

INPUT FOR EXAMPLE 3 OF THE FINITE ELEMENT COMPUTER CODE

```
MINUTEMAN   MOTOR    CHECK OF NEW PROGRAM
[2]
1  27
60.0          0.0          55.0          4.0          55.0          8.0          60.0          14.0
73.0          16.0         73.0          24.0         95.0          28.0         95.0          32.0
73.0          34.0         73.0          42.0         67.0          46.0         90.0          48.0
90.0          58.0         76.0          60.0         125.0         69.0         125.0         73.0
85.0          74.0         85.0          80.0         125.0         89.0         125.0         90.0
70.0          98.0         95.0          100.0        95.0          108.0        80.0          116.0
55.0          120.0        55.0          120.0        100.0         139.0
2  23
60.0          0.0          55.0          4.0          55.0          8.0          60.0          14.0
73.0          16.0         73.0          24.0         95.0          28.0         95.0          32.0
73.0          34.0         73.0          42.0         67.0          46.0         90.0          48.0
90.0          58.0         76.0          60.0         85.0          74.0         85.0          88.0
70.0          98.0         95.0          100.0        95.0          108.0        80.0          116.0
55.0          120.0        55.0          120.0        100.0         139.0
[3]
10        4.0         1.0
20        8.0         1.0
30        14.0        1.0
40        16.0        1.0
50        20.0        1.0
60        28.0        1.0
70        32.0        1.0
80        34.0        1.0
90        42.0        1.0
100       46.0        1.0
110       48.0        1.0
120       58.0        1.0
130       68.0        1.0
140       69.0        1.0
150       73.0        1.0
160       74.0        1.0
170       88.0        1.0
180       89.0        1.0
190       90.0        1.0
200       98.0        1.0
210       100.0       1.0
220       108.0       1.0
230       116.0       1.0
240       120.0       1.0
250       128.0       1.0
260       139.0       1.0
[4]
1         9.60        1.0
51        25.86       1.0       2         1.0
2         9.60        2.0
52        25.86       2.0       2         1.0
53        25.89       1.0
54        25.89       2.0
55        25.84       1.0
56        25.84       2.0
57        25.94       1.0
58        25.94       2.0
59        26.00       1.0
60        26.00       2.0
61        26.05       1.0
62        26.05       2.0
63        26.09       1.0
64        26.09       2.0
```

☐ - The block enclosing the number was added to indicate the applicable input block. The actual card merely contains the number punched in Column 1.

TABLE F-5 (Continued)

```
 2    1    3    4    1   24    2
52   51   53   54    2
54   53   55   56    3
56   55   57   58    4    1    2
60   59   61   62    5    1    2
[5]
 5    4    0    0         60.0
      1 0.0175833 0.0175833          0.273     0.064
      2 0.0089583 0.0089583          0.457     0.034
      3 0.0105833 0.0105833          0.340     0.044
      4     0.267     0.267          0.230    0.0738
      5  0.003333  0.003333          0.470    0.0176
 1    1         1.0    1
 2    1         1.0    1
63    1         1.0    2
64    1         1.0    2
20   13
[9]
```

☐ - The block enclosing the number was added to indicate the applicable input block. The actual card merely contains the number punched in Column 1.

TABLE F-6

OUTPUT FOR EXAMPLE 3 OF THE FINITE ELEMENT COMPUTER CODE

MINUTEMAN MOTOR CHECK OF NEW PROGRAM

FUNCTION 1	VALUE	TIME
	6.000E+01	0.
	5.500E+01	4.000E+00
	5.500E+01	8.000E+00
	6.000E+01	1.400E+01
	7.300E+01	1.600E+01
	7.300E+01	2.400E+01
	9.500E+01	2.800E+01
	9.500E+01	3.200E+01
	7.300E+01	3.400E+01
	7.300E+01	4.200E+01
	6.700E+01	4.600E+01
	9.000E+01	4.800E+01
	9.000E+01	5.800E+01
	7.600E+01	6.800E+01
	1.250E+02	6.900E+01
	1.250E+02	7.300E+01
	8.500E+01	7.400E+01
	8.500E+01	8.800E+01
	1.250E+02	8.900E+01
	1.250E+02	9.000E+01
	7.000E+01	9.800E+01
	9.500E+01	1.000E+02
	9.500E+01	1.080E+02
	8.000E+01	1.160E+02
	5.500E+01	1.200E+02
	5.500E+01	1.280E+02
	1.000E+02	1.390E+02

FUNCTION 2	VALUE	TIME
	6.000E+01	0.
	5.500E+01	4.000E+00
	5.500E+01	8.000E+00
	6.000E+01	1.400E+01
	7.300E+01	1.600E+01
	7.300E+01	2.400E+01
	9.500E+01	2.800E+01
	9.500E+01	3.200E+01
	7.300E+01	3.400E+01
	7.300E+01	4.200E+01
	6.700E+01	4.600E+01
	9.000E+01	4.800E+01
	9.000E+01	5.800E+01
	7.600E+01	6.800E+01
	8.500E+01	7.400E+01
	8.500E+01	8.800E+01
	7.000E+01	9.800E+01
	9.500E+01	1.000E+02
	9.500E+01	1.080E+02
	8.000E+01	1.160E+02
	5.500E+01	1.200E+02
	5.500E+01	1.280E+02
	1.000E+02	1.390E+02

TIME STEP INFORMATION

TABLE F-6 (Continued)

STEP	TIME	SPACING RATIO
10	.40000E+01	.10000E+01
20	.80000E+01	.10000E+01
30	.14000E+02	.10000E+01
40	.16000E+02	.10000E+01
50	.24000E+02	.10000E+01
60	.28000E+02	.10000E+01
70	.32000E+02	.10000E+01
80	.34000E+02	.10000E+01
90	.42000E+02	.10000E+01
100	.46000E+02	.10000E+01
110	.48000E+02	.10000E+01
120	.58000E+02	.10000E+01
130	.68000E+02	.10000E+01
140	.69000E+02	.10000E+01
150	.73000E+02	.10000E+01
160	.74000E+02	.10000E+01
170	.88000E+02	.10000E+01
180	.89000E+02	.10000E+01
190	.90000E+02	.10000E+01
200	.98000E+02	.10000E+01
210	.10000E+03	.10000E+01
220	.10800E+03	.10000E+01
230	.11600E+03	.10000E+01
240	.12000E+03	.10000E+01
250	.12800E+03	.10000E+01
260	.13900E+03	.10000E+01

TABLE F-6 (Continued)

*****GEOMETRY*****

NODAL POINT	R-Z COORDINATES	
1	9.60E+00	1.00E+00
2	9.60E+00	2.00E+00
3	1.02E+01	1.00E+00
4	1.02E+01	2.00E+00
5	1.09E+01	1.00E+00
6	1.09E+01	2.00E+00
7	1.15E+01	1.00E+00
8	1.15E+01	[illegible]0E+00
9	1.22E+01	1.00E+00
10	1.22E+01	2.00E+00
11	1.28E+01	1.00E+00
12	1.28E+01	2.00E+0
13	1.35E+01	1.00E+00
14	1.35E+01	2.00E+00
15	1.41E+01	1.00E+00
16	1.41E+01	2.00E+00
17	1.47E+01	1.00E+00
18	1.47E+01	2.00E+00
19	1.54E+01	1.00E+00
20	1.54E+01	2.00E+00
21	1.60E+01	1.00E+00
22	1.60E+01	2.00E+00
23	1.67E+01	1.00E+00
24	1.67E+01	2.00E+00
25	1.73E+01	1.00E+00
26	1.73E+01	2.00E+00
27	1.80E+01	1.00E+00
28	1.80E+01	2.00E+00
29	1.86E+01	1.00E+00
30	1.86E+01	2.00E+00
31	1.92E+01	1.00E+00
32	1.92E+01	2.00E+00
33	1.99E+01	1.00E+00
34	1.99E+01	2.00E+00
35	2.05E+01	1.00E+00
36	2.05E+01	2.00E+00
37	2.12E+01	1.00E+00
38	2.12E+01	2.00E+00
39	2.18E+01	1.00E+00
40	2.18E+01	2.00E+00
41	2.24E+01	1.00E+00
42	2.24E+01	2.00E+00
43	2.31E+01	1.00E+00
44	2.31E+01	2.00E+00
45	2.37E+01	1.00E+00
46	2.37E+01	2.00E+00
47	2.44E+01	1.00E+00
48	2.44E+01	2.00E+00
49	2.50E+01	1.00E+00
50	2.50E+01	2.00E+00
51	2.57E+01	1.00E+00
52	2.57E+01	2.00E+00
53	2.57E+01	1.00E+00
54	2.57E+01	2.00E+00
55	2.58E+01	1.00E+00
56	2.58E+01	2.00E+00

TABLE F-6 (Continued)

57	2.59E+01	1.00E+00
58	2.59E+01	2.00E+00
59	2.60E+01	1.00E+00
60	2.60E+01	2.00E+00
61	2.61E+01	1.00E+00
62	2.61E+01	2.00E+00
63	2.61E+01	1.00E+00
64	2.61E+01	2.00E+00

TABLE F-6 (Continued)

ELEMENT INFORMATION

	NODE POINTS				MAT.
1	4	2	1	3	1
2	6	4	3	5	1
3	8	6	5	7	1
4	10	8	7	9	1
5	12	10	9	11	1
6	14	12	11	13	1
7	16	14	13	15	1
8	18	16	15	17	1
9	20	18	17	19	1
10	22	20	19	21	1
11	24	22	21	23	1
12	26	24	23	25	1
13	28	26	25	27	1
14	30	28	27	29	1
15	32	30	29	31	1
16	34	32	31	33	1
17	36	34	33	35	1
18	38	36	35	37	1
19	40	38	37	39	1
20	42	40	39	41	1
21	44	42	41	43	1
22	46	44	43	45	1
23	48	46	45	47	1
24	50	48	47	49	1
25	52	50	49	51	1
26	54	52	51	53	2
27	56	54	53	55	3
28	58	56	55	57	4
29	60	58	57	59	4
30	62	60	59	61	5
31	64	62	61	63	5

ELEMENT	AREA
1	.64240000E+00
2	.64240000E+00
3	.64240000E+00
4	.64240000E+00
5	.64240000E+00
6	.64240000E+00
7	.64240000E+00
8	.64240000E+00
9	.64240000E+00
10	.64240000E+00
11	.64240000E+00
12	.64240000E+00
13	.64240000E+00
14	.64240000E+00
15	.64240000E+00
16	.64240000E+00
17	.64240000E+00
18	.64240000E+00
19	.64240000E+00
20	.64240000E+00
21	.64240000E+00
22	.64240000E+00

TABLE F-6 (Continued)

23	.64240000E+00
24	.64240000E+00
25	.64240000E+00
26	.30000000E-01
27	.15000000E+00
28	.10000000E+00
29	.60000000E-01
30	.50000000E-01
31	.40000000E-01

TABLE F-6 (Continued)

TRANSIENT HEAT TRANSFER CONTROL INFORMATION

NUMBER OF MATERIALS WITH SPECIFIED THERMAL PROPERTIES ... 5
NUMBER OF NODAL POINT BOUNDARY CONDITIONS 4
NUMBER OF CONVECTION BOUNDARY CONDITIONS 0

AXISYMMETRIC ANALYSIS

TABLE F-6 (Continued)

MATERIAL TABLE

MATERIAL	RCOND	ZCOND	RZCOND	SPECIFIC HEAT	DENSITY	HEAT/UNIT VOL.
1	1.75833E-02	1.75833E-02	0.	2.73000E-01	6.40000E-02	0.
2	8.95830E-03	8.95830E-03	0.	4.57000E-01	3.40000E-02	0.
3	1.05833E-02	1.05833E-02	0.	3.40000E-01	4.40000E-02	0.
4	2.67000E-01	2.67000E-01	0.	2.30000E-01	7.38000E-02	0.
5	3.33300E-03	3.33300E-03	0.	4.70000E-01	1.76000E-02	0.

TABLE F-6 (Continued)

NODAL POINT BOUNDARY CONDITIONS

NODE	TYPE	AMPLITUDE	FUNCTION
1	1	1.000	1
2	1	1.000	1
63	1	1.000	2
64	1	1.000	2

ELEMENT TEMPERATURE PRINT CONTROL

OUTPUT INTERVAL	PRINT OPERATIONS
20	13

TABLE F-6 (Continued)

SOLUTION TO THE TRANSIENT HEAT CONDUCTION PROBLEM

TIME=	.80000E+01										
1	.550000E+02	2	.550000E+02	3	.558708E+02	4	.558708E+02	5	.566638E+02		.566638E+02
7	.573663E+02	8	.573663E+02	9	.579698E+02	10	.579698E+02	11	.584731E+02		.584731E+02
13	.588795E+02	14	.588795E+02	15	.591970E+02	16	.591970E+02	17	.594365E+02	18	.594365E+02
19	.596098E+02	20	.596098E+02	21	.597285E+02	22	.597285E+02	23	.598023E+02	24	.598023E+02
25	.598385E+02	26	.598385E+02	27	.598410E+02	28	.598410E+02	29	.598106E+02	30	.598106E+02
31	.597449E+02	32	.597449E+02	33	.596385E+02	34	.596385E+02	35	.594836E+02	36	.594836E+02
37	.592715E+02	38	.592715E+02	39	.589934E+02	40	.589934E+02	41	.586419E+02	42	.586419E+02
43	.582134E+02	44	.582134E+02	45	.577088E+02	46	.577088E+02	47	.571350E+02	48	.571350E+02
49	.565054E+02	50	.565054E+02	51	.558382E+02	52	.558382E+02	53	.557761E+02	54	.557761E+02
55	.555133E+02	56	.555133E+02	57	.555063E+02	58	.555063E+02	59	.555022E+02	60	.555022E+02
61	.552232E+02	62	.552232E+02	63	.550000E+02	64	.550000E+02				
TIME=	.16000E+02										
1	.730000E+02	2	.730000E+02	3	.669501E+02	4	.669501E+02	5	.631875E+02	6	.631875E+02
7	.609861E+02	8	.609861E+02	9	.597890E+02	10	.597890E+02	11	.591987E+02	12	.591987E+02
13	.589508E+02	14	.589508E+02	15	.588816E+02	16	.588816E+02	17	.588961E+02	18	.588961E+02
19	.589410E+02	20	.589410E+02	21	.589873E+02	22	.589873E+02	23	.590192E+02	24	.590192E+02
25	.590280E+02	26	.590280E+02	27	.590104E+02	28	.590104E+02	29	.589665E+02	30	.589665E+02
31	.589002E+02	32	.589002E+02	33	.588193E+02	34	.588193E+02	35	.587364E+02	36	.587364E+02
37	.586718E+02	38	.586718E+02	39	.586593E+02	40	.586593E+02	41	.587561E+02	42	.587561E+02
43	.590586E+02	44	.590586E+02	45	.597227E+02	46	.597227E+02	47	.609839E+02	48	.609839E+02
49	.631714E+02	50	.631718E+02	51	.667084E+02	52	.667084E+02	53	.671121E+02	54	.671121E+02
55	.689122E+02	56	.689122E+02	57	.689635E+02	58	.689635E+02	59	.689959E+02	60	.689959E+02
61	.712131E+02	62	.712131E+02	63	.730000E+02	64	.730000E+02				
TIME=	.28000E+02										
1	.950000E+02	2	.950000E+02	3	.858642E+02	4	.858642E+02	5	.790525E+02	6	.790525E+02
7	.740284E+02	8	.740284E+02	9	.703490E+02	10	.703490E+02	11	.676666E+02	12	.676666E+02
13	.657121E+02	14	.657121E+02	15	.642887E+02	16	.642887E+02	17	.632564E+02	18	.632564E+02
19	.625204E+02	20	.625204E+02	21	.620192E+02	22	.620192E+02	23	.617143E+02	24	.617143E+02
25	.615832E+02	26	.615832E+02	27	.616137E+02	28	.616137E+02	29	.618011E+02	30	.618011E+02
31	.621474E+02	32	.621474E+02	33	.626619E+02	34	.626619E+02	35	.633642E+02	36	.633642E+02
37	.642890E+02	38	.642890E+02	39	.654919E+02	40	.654919E+02	41	.670566E+02	42	.670566E+02
43	.691018E+02	44	.691018E+02	45	.717863E+02	46	.717863E+02	47	.753122E+02	48	.753122E+02
49	.799224E+02	50	.799224E+02	51	.858913E+02	52	.858913E+02	53	.865130E+02	54	.865130E+02
55	.892243E+02	56	.892243E+02	57	.892992E+02	58	.892992E+02	59	.893455E+02	60	.893455E+02
61	.924805E+02	62	.924805E+02	63	.950000E+02	64	.950000E+02				
TIME=	.34000E+02										
1	.730000E+02	2	.730000E+02	3	.777822E+02	4	.777822E+02	5	.791655E+02	6	.791655E+02
7	.784496E+02	8	.784496E+02	9	.766167E+02	10	.766167E+02	11	.743475E+02	12	.743475E+02
13	.720694E+02	14	.720694E+02	15	.700193E+02	16	.700193E+02	17	.683073E+02	18	.683073E+02
19	.669695E+02	20	.669695E+02	21	.660049E+02	22	.660049E+02	23	.653983E+02	24	.653983E+02
25	.651326E+02	26	.651326E+02	27	.651952E+02	28	.651952E+02	29	.655796E+02	30	.655796E+02
31	.662856E+02	32	.662856E+02	33	.673170E+02	34	.673170E+02	35	.686776E+02	36	.686776E+02
37	.703626E+02	38	.703626E+02	39	.723446E+02	40	.723446E+02	41	.745501E+02	42	.745501E+02
43	.768263E+02	44	.768263E+02	45	.788982E+02	46	.788982E+02	47	.803285E+02	48	.803285E+02
49	.804885E+02	50	.804885E+02	51	.785619E+02	52	.785619E+02	53	.782561E+02	54	.782561E+02
55	.768080E+02	56	.768080E+02	57	.767633E+02	58	.767633E+02	59	.767338E+02	60	.767338E+02
61	.746712E+02	62	.746712E+02	63	.730000E+02	64	.730000E+02				
TIME=	.46000E+02										
1	.670000E+02	2	.670000E+02	3	.685889E+02	4	.685889E+02	5	.696084E+02	6	.696084E+02
7	.702078E+02	8	.702078E+02	9	.705108E+02	10	.705108E+02	11	.706166E+02	12	.706166E+02

TABLE F-6 (Continued)

13	.706030E+02	14	.706030E+02	15	.705287E+02	16	.705287E+02	17	.704363E+02	18	.704363E+02
19	.703559E+02	20	.703559E+02	21	.703068E+02	22	.703068E+02	23	.703006E+02	24	.703006E+02
25	.703422E+02	26	.703422E+02	27	.704315E+02	28	.704315E+02	29	.705641E+02	30	.705641E+02
31	.707314E+02	32	.707314E+02	33	.709211E+02	34	.709211E+02	35	.711170E+02	36	.711170E+02
37	.712979E+02	38	.712979E+02	39	.714371E+02	40	.714371E+02	41	.715009E+02	42	.715009E+02
43	.714471E+02	44	.714471E+02	45	.712245E+02	46	.712245E+02	47	.707713E+02	48	.707713E+02
49	.700178E+02	50	.700178E+02	51	.688836E+02	52	.688836E+02	53	.687591E+02	54	.687591E+02
55	.682106E+02	56	.682106E+02	57	.681953E+02	58	.681953E+02	59	.681856E+02	60	.681856E+02
61	.675301E+02	62	.675301E+02	63	.670000E+02	64	.670000E+02				
TIME=	.58000E+02										
1	.900000E+02	2	.900000E+02	3	.873482E+02	4	.873482E+02	5	.849438E+02	6	.849438E+02
7	.827012E+02	8	.827012E+02	9	.807232E+02	10	.807232E+02	11	.789750E+02	12	.789750E+02
13	.774672E+02	14	.774672E+02	15	.762023E+02	16	.762023E+02	17	.751752E+02	18	.751752E+02
19	.743789E+02	20	.743789E+02	21	.738058E+02	22	.738058E+02	23	.734482E+02	24	.734482E+02
25	.732989E+02	26	.732989E+02	27	.733522E+02	28	.733522E+02	29	.736037E+02	30	.736037E+02
31	.740506E+02	32	.740506E+02	33	.746906E+02	34	.746906E+02	35	.755209E+02	36	.755209E+02
37	.765373E+02	38	.765373E+02	39	.777326E+02	40	.777326E+02	41	.790962E+02	42	.790962E+02
43	.806131E+02	44	.806131E+02	45	.822595E+02	46	.822595E+02	47	.840060E+02	48	.840060E+02
49	.858400E+02	50	.858400E+02	51	.877059E+02	52	.877059E+02	53	.878716E+02	54	.878716E+02
55	.885707E+02	56	.885707E+02	57	.885895E+02	58	.885895E+02	59	.886010E+02	60	.886010E+02
61	.893754E+02	62	.893754E+02	63	.900000E+02	64	.900000E+02				
TIME=	.69000E+02										
1	.125000E+03	2	.125000E+03	3	.983207E+02	4	.983207E+02	5	.856846E+02	6	.856846E+02
7	.806124E+02	8	.806124E+02	9	.789526E+02	10	.789526E+02	11	.785048E+02	12	.785048E+02
13	.783442E+02	14	.783442E+02	15	.781940E+02	16	.781940E+02	17	.780228E+02	18	.780228E+02
19	.778598E+02	20	.778598E+02	21	.777359E+02	22	.777359E+02	23	.776728E+02	24	.776728E+02
25	.776831E+02	26	.776831E+02	27	.777709E+02	28	.777709E+02	29	.779324E+02	30	.779324E+02
31	.781563E+02	32	.781563E+02	33	.784238E+02	34	.784238E+02	35	.787093E+02	36	.787093E+02
37	.789804E+02	38	.789804E+02	39	.791984E+02	40	.791984E+02	41	.793196E+02	42	.793196E+02
43	.792997E+02	44	.792997E+02	45	.791054E+02	46	.791054E+02	47	.787355E+02	48	.787355E+02
49	.782502E+02	50	.782502E+02	51	.777957E+02	52	.777957E+02	53	.777626E+02	54	.777626E+02
55	.776365E+02	56	.776365E+02	57	.776338E+02	58	.776338E+02	59	.776325E+02	60	.776325E+02
61	.775556E+02	62	.775556E+02	63	.775000E+02	64	.775000E+02				
TIME=	.74000E+02										
1	.850000E+02	2	.850000E+02	3	.990981E+02	4	.990981E+02	5	.102361E+03	6	.102361E+03
7	.100166E+03	8	.100166E+03	9	.959733E+02	10	.959733E+02	11	.916213E+02	12	.916213E+02
13	.878699E+02	14	.878699E+02	15	.849084E+02	16	.849084E+02	17	.826912E+02	18	.826912E+02
19	.811009E+02	20	.811009E+02	21	.800096E+02	22	.800096E+02	23	.792987E+02	24	.792987E+02
25	.788663E+02	26	.788663E+02	27	.786298E+02	28	.786298E+02	29	.785254E+02	30	.785254E+02
31	.785074E+02	32	.785074E+02	33	.785454E+02	34	.785454E+02	35	.786228E+02	36	.786228E+02
37	.787357E+02	38	.787357E+02	39	.788927E+02	40	.788927E+02	41	.791153E+02	42	.791153E+02
43	.794380E+02	44	.794380E+02	45	.799095E+02	46	.799095E+02	47	.805908E+02	48	.805908E+02
49	.815552E+02	50	.815552E+02	51	.828847E+02	52	.828847E+02	53	.830267E+02	54	.830267E+02
55	.836496E+02	56	.836496E+02	57	.836669E+02	58	.836669E+02	59	.836777E+02	60	.836777E+02
61	.844093E+02	62	.844093E+02	63	.850000E+02	64	.850000E+02				
TIME=	.89000E+02										
1	.125000E+03	2	.125000E+03	3	.102311E+03	4	.102311E+03	5	.912163E+02	6	.912163E+02
7	.864656E+02	8	.864656E+02	9	.846728E+02	10	.846728E+02	11	.840152E+02	12	.840152E+02
13	.836970E+02	14	.836970E+02	15	.834497E+02	16	.834497E+02	17	.832111E+02	18	.832111E+02
19	.829779E+02	20	.829779E+02	21	.827575E+02	22	.827575E+02	23	.825582E+02	24	.825582E+02
25	.823886E+02	26	.823886E+02	27	.822564E+02	28	.822564E+02	29	.821689E+02	30	.821689E+02
31	.821317E+02	32	.821317E+02	33	.821490E+02	34	.821490E+02	35	.822231E+02	36	.822231E+02
37	.823543E+02	38	.823543E+02	39	.825408E+02	40	.825408E+02	41	.827786E+02	42	.827786E+02
43	.830593E+02	44	.830593E+02	45	.833649E+02	46	.833649E+02	47	.836577E+02	48	.836577E+02
49	.838657E+02	50	.838657E+02	51	.838712E+02	52	.838712E+02	53	.838571E+02	54	.838571E+02
55	.837789E+02	56	.837789E+02	57	.837760E+02	58	.837760E+02	59	.837739E+02	60	.837739E+02

TABLE F-6 (Continued)

61	.836230E+02	62	.836230E+02	63	.835000E+02	64	.835000E+02				
TIME=	.98000E+02										
1	.700000E+02	2	.700000E+02	3	.780249E+02	4	.780249E+02	5	.833540E+02	6	.833540E+02
7	.665997E+02	8	.865997E+02	9	.883377E+02	10	.883377E+02	11	.889930E+02	12	.889930E+02
13	.889282E+02	14	.889282E+02	15	.884200E+02	16	.884200E+02	17	.876742E+02	18	.876742E+02
19	.868378E+02	20	.868378E+02	21	.860081E+02	22	.860081E+02	23	.852425E+02	24	.852425E+02
25	.845681E+02	26	.845681E+02	27	.839891E+02	28	.839891E+02	29	.834937E+02	30	.834937E+02
31	.830587E+02	32	.830587E+02	33	.826532E+02	34	.826532E+02	35	.822407E+02	36	.822407E+02
37	.817810E+02	38	.817810E+02	39	.812302E+02	40	.812302E+02	41	.805413E+02	42	.805413E+02
43	.796642E+02	44	.796642E+02	45	.785462E+02	46	.785462E+02	47	.771319E+02	48	.771319E+02
49	.753641E+02	50	.753641E+02	51	.731843E+02	52	.731843E+02	53	.729630E+02	54	.729630E+02
55	.720044E+02	56	.720044E+02	57	.719782E+02	58	.719782E+02	59	.719621E+02	60	.719621E+02
61	.708738E+02	62	.708738E+02	63	.700000E+02	64	.700000E+02				
TIME=	.10800E+03										
1	.950000E+02	2	.950000E+0.	3	.935568E+02	4	.935568E+02	5	.922467E+02	6	.922467E+02
7	.910113E+02	8	.910113E+0.	9	.899145E+02	10	.899145E+02	11	.889193E+02	12	.889193E+02
13	.880331E+02	14	.880331E+02	15	.872499E+02	16	.872499E+02	17	.865611E+02	18	.865611E+02
19	.859604E+02	20	.859604E+02	21	.854433E+02	22	.854433E+02	23	.850086E+02	24	.850086E+02
25	.846595E+02	26	.846595E+02	27	.844038E+02	28	.844038E+02	29	.842542E+02	30	.842542E+02
31	.842271E+02	32	.842271E+02	33	.843411E+02	34	.843411E+02	35	.846152E+02	36	.846152E+02
37	.850660E+02	38	.850660E+02	39	.857050E+02	40	.857050E+02	41	.865371E+02	42	.865371E+02
43	.875586E+02	44	.875586E+02	45	.887547E+02	46	.887547E+02	47	.900949E+02	48	.900949E+02
49	.915569E+02	50	.915569E+02	51	.930945E+02	52	.930945E+02	53	.932321E+02	54	.932321E+02
55	.938125E+02	56	.938125E+02	57	.938281E+02	58	.938281E+02	59	.938376E+02	60	.938376E+02
61	.944796E+02	62	.944796E+02	63	.950000E+02	64	.950000E+02				
TIME=	.12000E+03										
1	.550000E+02	2	.550000E+02	3	.646594E+02	4	.646594E+02	5	.717054E+02	6	.717054E+02
7	.767327E+02	8	.767327E+02	9	.802375E+02	10	.802375E+02	11	.826178E+02	12	.826178E+02
13	.841907E+02	14	.841907E+02	15	.851975E+02	16	.851975E+02	17	.858194E+02	18	.858194E+02
19	.861872E+02	20	.861872E+02	21	.863923E+02	22	.863923E+02	23	.864963E+02	24	.864963E+02
25	.865373E+02	26	.865373E+02	27	.865348E+02	28	.865348E+02	29	.864928E+02	30	.864928E+02
31	.864006E+02	32	.864006E+02	33	.862322E+02	34	.862322E+02	35	.859435E+02	36	.859435E+02
37	.854695E+02	38	.854695E+02	39	.847184E+02	40	.847184E+02	41	.835673E+02	42	.835673E+02
43	.818562E+02	44	.818562E+02	45	.793854E+02	46	.793854E+02	47	.759147E+02	48	.759147E+02
49	.711642E+02	50	.711642E+02	51	.648303E+02	52	.648303E+02	53	.641635E+02	54	.641635E+02
55	.612469E+02	56	.612469E+02	57	.611660E+02	58	.611660E+02	59	.611159E+02	60	.611159E+02
61	.577211E+02	62	.577211E+02	63	.550000E+02	64	.550000E+02				
TIME=	.13900E+03										
1	.100000E+03	2	.100000E+03	3	.929116E+02	4	.929116E+02	5	.876030E+02	6	.876030E+02
7	.837611E+02	8	.837611E+02	9	.810327E+02	10	.810327E+02	11	.791756E+02	12	.791756E+02
13	.779641E+02	14	.779641E+02	15	.772137E+02	16	.772137E+02	17	.767743E+02	18	.767743E+02
19	.765269E+02	20	.765269E+02	21	.763807E+02	22	.763807E+02	23	.762709E+02	24	.762709E+02
25	.761569E+02	26	.761569E+02	27	.760209E+02	28	.760209E+02	29	.758662E+02	30	.758662E+02
31	.757164E+02	32	.757164E+02	33	.756147E+02	34	.756147E+02	35	.756230E+02	36	.756230E+02
37	.758211E+02	38	.758211E+02	39	.763059E+02	40	.763059E+02	41	.771901E+02	42	.771901E+02
43	.786011E+02	44	.786011E+02	45	.806796E+02	46	.806796E+02	47	.835769E+02	48	.835769E+02
49	.874438E+02	50	.874438E+02	51	.924487E+02	52	.924487E+02	53	.929701E+02	54	.929701E+02
55	.952396E+02	56	.952396E+02	57	.953018E+02	58	.953018E+02	59	.953401E+02	60	.953401E+02
61	.979254E+02	62	.979254E+02	63	.100000E+03	64	.100000E+03				

REFERENCES FOR APPENDIX F

F-1. Farris, R. J., and Schapery, R. A., "Development of A Solid Rocket Propellant Nonlinear Constitutive Theory", Report No. AFRPL-TR-73-50, June 1973.